ANALYSIS OF SKEW-CURVED CONCRETE BOX GIRDER BRIDGES

Thesis submitted to

FACULTY OF ENGINEERING AND TECHNOLOGY

in partial fulfillment of the requirements for the degree of

MASTER OF CIVIL ENGINEERING

&

Specialization in

STRUCTURAL ENGINEERING

Prepared By

KOUSHIK DATTA

ROLL NO: 001710402015

EXAMINATION ROLL NO: M4CIV19019

REGN NO: 140642 of 2017-18

Under the Guidance of

PROF. DR. DIPANKAR CHAKRAVORTY

CIVIL ENGINEERING DEPARTMENT
JADAVPUR UNIVERSITY
KOLKATA – 700032

MAY 2019

FACULTY OF ENGINEERING & TECHNOLOGY

DEPARTMENT OF CIVIL ENGINEERING

JADAVPUR UNIVERSITY

Kolkata, India

……

CERTIFICATE OF APPROVAL

This is to certify that the thesis entitled "**Analysis of Skew-Curved Concrete Box Girder Bridges**" is being submitted by **Sri Koushik Datta** in partial fulfillment of the requirements for the award of the Master degree in Civil Engineering from Jadavpur University and it is delightfully declared that it is a record of bonafide research work carried out by him under my supervision in the year of 2018-2019.

This is ensured that the outcomes of the present research work have not been submitted to any other university or institution for the award of any degree or diploma.

Supervisor
(Dr. Dipankar Chakravorty)
Professor
Civil Engineering Department
Jadavpur University, Kolkata

Head of the Department
(Dr. Dipankar Chakravorty)
Professor
Civil Engineering Department
Jadavpur University, Kolkata

Dean, FET
(Dr. Chiranjib Bhattacharjee)
Jadavpur University,
Kolkata

CERTIFICATE

The foregoing thesis is hereby approved as a creditable study of an engineering subject carried out and presented in a manner satisfactory to warrant its acceptance as a pre-requisite to the Degree of Master in Civil Engineering for which it has been submitted. It is understood that by this approval the undersigned do not necessarily endorse or approve any statement made, opinion expressed or conclusion drawn therein, but approve the thesis only for the purpose for which it is submitted.

Final Examination for
Evaluation of Thesis

1. _____

2. _____

3. _____

(Signatures of Examiners)

DECLARATION

I, Koushik Datta, Master of Engineering in Civil Engineering (Structure Engineering), Jadavpur University, Faculty of Engineering and Technology, hereby declare that the work being presented in the thesis work titled, "**Analysis of Skew-Curved Concrete Box Girder Bridges**", is an authentic record of work that has been carried out in the Department of Civil Engineering, Jadavpur University, Kolkata under the guidance of Prof. Dipankar Chakravorty. The work contained in this thesis has not yet been submitted in parts or full to any other university or institute or professional body for award of any degree or diploma or any fellowship.

Place: Kolkata

Date:

_____

Koushik Datta

Roll No.: 001710402015

Registration no.: 140642 of 2017-18

Examinations roll no. M4CIV19019

ACKNOWLEDGEMENT

The author owes his most sincere thanks and profound gratitude for the indispensable advice and inspiration rendered by the supervisor, Prof. Dr. Dipankar Chakravorty at each phase of the research work. At the same time the author would also like to take the opportunity to express his gratefulness for the valuable suggestions and continuous guidance of Prof. Dr. Arup Guha Niyogi, Ex-Head of the Civil Engineering department of Jadavpur University, especially for permitting him to carry out the research work under the guidance of Prof. Dr. Dipankar Chakravorty.

The author would also like to take this opportunity to express his gratefulness to all the respected teachers of Structural Engineering department of Jadavpur University for their valuable suggestions, to all the laboratory staffs of Structural Engineering department of Jadavpur University for their continuous support and to all the beloved classmates for their continuous inspiration to pursue this thesis work. The author is also deeply thankful to the civil engineering departmental library as well as to the central library of the Jadavpur University.

The author would also like to thank the management of M/S C.E. Testing Co. Pvt. Ltd. For supporting him and allowing him to pursue this post graduation program and all his beloved colleagues for their constant effort to manage the inconvenience caused by the author's absence.

It would not have been possible for the author to pursue the research work without the constant effort, sacrifices and encouragement of his family from the very first day of his student life till date.

The author is thankful to all those, whose efforts either directly or indirectly have contributed well during the course of this thesis work.

Date:

Place: Jadavpur University, Kolkata

Signature of the Candidate:

CONTENTS

LIST OF FIGURES

LIST OF TABLES

LIST OF NOTATIONS

The following notations are used in the text of the thesis. The symbols which are not listed in the following are explained where they are used for the first time.

a	Shell section material angle
ang	Shell element coordinate angle
a1, a2	Coefficient of thermal expansion
e1, e2, e3	Moduli of elasticity
g12, g13, g23	Shear modulus
j_1, j_2, j_3, j_4	Joint no of area element
m	Mass density for computing element mass
th	Membrane thickness
thb	Plate bending thickness
w	Weight density for computing self weight
u12, u13, u23	Poisson's Ratio
B	Soffit width/ Bottom width of box girder cross section
C	Response coefficient
C_{Rec}	Recommended response coefficient
F_{ij}	Membrane direct force (i=j; i,j= 1,2,3)
F_{ij}	Membrane shear force (i≠j; i,j= 1,2,3)
I_{xx}	Moment of inertia about horizontal axes
M_{ij}	Membrane bending moment (i=j; i,j= 1,2,3)
M_{ij}	Membrane torsion (i≠j; i,j= 1,2,3)
N	Number of cell in box girder section
R	Radius of curvature of box girder in plan
V_{13}, V_{23}	Plate transverse shear force
Y_b	Height of neutral axis from bottom most fiber
Y_t	Depth of neutral axis from top most fiber

Z_b	Sectional modulus with respect to bottom most fiber
Z_t	Sectional modulus with respect to top most fiber
α	Central angle, represents the curvature in plan
θ	Skew angle, represents the skewness of supports
σ_{ij}	Membrane direct stress (i=j; i,j= 1,2,3)
σ_{ij}	Membrane shear stress (i≠j; i,j= 1,2,3)

ABSTRACT:

With the growing economy and rapid urbanization, the traffic demand in highways in India has increased manifold over the last few decades. In order to ensure smooth flow of traffic, numerous new bridges and flyovers are being constructed. In present bridge engineering scenario, the use of box-girders has proven to be a very efficient structural solution due to its high tensional rigidity, serviceability, economy, aesthetics and the ability to efficiently distribute the eccentric vehicular live load among the webs of the box-girder. Multi-Cell box girders are generally adopted for the multi-lane bridges in order to limit the local deformations in the top slab of box. The curvilinear nature of box girder bridges along with their complex deformation patterns and stress fields have led designers to adopt approximate and conservative methods for their analyses and design. Recent literature on straight, skewed and curved box girder bridges has dealt with analytical formulations to better understand the behavior of these complex structural systems. Responses of concrete box girder bridge, subjected to skewness and curvature, termed as skew-curved bridge cannot be found out by simply superimposing the skewness and curvature effect. The analyses of such thin walled structures become more complex when it is subjected to eccentric vehicular live load causing additional torsion and warping effect. During present study, an attempt has been made to predict the primary bridge response of simply supported skew-curve concrete box girder bridge through an exhaustive parametric study using SAP 2000 software. The skew angle has been varied from 0° to 45° at an interval of 15°, while the central angle varied from 0° to 36° at an interval of 12°. Total 80 number of 3D model for 30m and 35m span with single and double cell having 5m and 6m soffit width has been prepared and analyzed for dead load and Class 70R wheeled load as per IRC-6:2017. Conclusion has been identified via parametric study for bending moment, torsion, shear force, joint reaction and deflection. Response coefficient for each of the bridge response has been proposed based on the response of the primary straight model and compared between 30m and 35m span.

Chapter-1: Introduction

1.1 Background and Motivation

1.1.1 General:

A **Bridge** is a structure providing passage over an obstacle without closing the way beneath. The required passage may be for roadway, railway, pipeline or canal. The obstacle may be due to stream, valley, roadway, railway, pipeline etc. A bridge is termed as an **Overbridge** when it carries the traffic or pipeline over a communication system and **Viaduct** when is constructed over a busy locality to carry the vehicular traffic over the area keeping the activities the area below the viaduct uninterrupted. Bridges are generally constructed in various shapes, sizes and with different materials depending upon their purpose and site requirement with sufficiently designed members.

1.1.2 Development of bridge engineering:

The history of the development of bridge is closely associated with the history of human civilization. The art of bridge building is, therefore, attracted the attention of the engineers and builders from the beginning of the civilization. It may be well presumed that the idea of building a bridge across an obstacle e.g. channels or stream has been developed by observing natural phenomenon e.g. tree trunk fallen across a water course accidentally or a piece of stone in the form of a arch forming a small opening caused by erosion of soft soil underneath. It may also be well presumed that inhabitants of those old days were, generally, encouraged by those natural phenomenon and built bridges over small water courses by placing a piece of log or tieing a bunch of long creeper with the trees situated on either side of the stream. The former was the predecessor of girder type bridge and the later was the forbearer of the suspension bridge. Though these are example of primitive nature, but there is no doubt that these were the beginning of the science of bridge construction which has been upgraded to present state through continuous effort and desire of human to build longer and stronger bridges by advancing in technology and bridge building materials. ***Flow chart*** **below shows the advancement in bridge engineering from the primitive days.**

Ancient Bridges

700 AD Asia

Clapper Bridge

Natural Bridges made of tree trunks/stones

Great Stone Bridge in China

Shallow Bridge, Arch Action

Roman Arch Bridge

Arch Action, Natural Cement

100 BC Romans

Development in science and technology, e.g. Strength of Materials, Mathematical Theories, Development of Metallurgy

1300 AD *Renaissance*

1800 AD

1900 AD

2000 AD

Coalbrookdale bridge, England

First Cast-Iron Bridge

Truss bridge

Improvement of Structural Mechanics

Prestressed concrete, Cable stayed bridge

Britania Tubular Bridge

Wrought-Iron Bridge

1850 AD

Suspension Bridge

Steel suspenders

1920 AD

The earliest bridge on record is the bridge over the Nile, built by Menes, the king of Egypt about 2650 BC. Five centuries later, another bridge was built by Queen Semiramino of Babylon across the river Euphrates. A number of arch bridges were built by Mesopotamians, the Egyptians and the Chinese up to 600 AD. The Romans were considered as best bridge builders as they knew use of Pozzolana in masonry structures and they constructed large arch bridges in systematic manner. But, their deficient knowledge in scour, made the foundations weaker and damage caused by collapse of foundation in course of time.

In middle age, number of bridges has been constructed in Europe e.g. over Thames in London (1209), over Arno in Florence (1177 and 1569), over Grand Canal in Venice (1591). Different bridge architecture and other functional requirement e.g. defense towers, statue, shops are the key features of these bridges.

The modern bridge engineering practice has been started in 18th century, when bridge builders leant the use of cast iron. Many arch bridges have been constructed with cast iron at that time and, then, cast iron has been replaced by wrought iron. Wrought iron was also replaced by steel when Bessemier process of steel making was introduced. First, Iron Bridge has been constructed over the Severn, Coalbrookdale (1779). First steel bridge has been built is Eads Bridge, Missouri, in 1874. With the introduction of steel as construction material and development in engineering technology, suspension bridge, cantilever bridge and truss bridge have been built for longer span. But, many of these bridge collapsed sue to lack of knowledge for safeguarding the bridges against sway due to vibration and dynamic loading.

Advancement of bridge engineering has been taken place in 19th century due to production of alloy steel and cement, manufacture of heavy load lifting equipment and construction machinery, advancement in construction methodology and engineering design.

Reinforced concrete bridges gained popularity in the 20th century due to their versatility in construction, economy and ease of maintenance. These bridges can be casted at site in any shape and form to meet the architectural requirement. Again, locally

available material e.g. coarse aggregate and fine aggregate can be utilized eliminating high carriage cost. Reinforced concrete bridges have been further improved in prestressed concrete bridge.

Now a days, extra dosed bridge, cable stayed bridge are being used as long span bridges, where the deck is being made of reinforced concrete/prestressed concrete.

The chart below shows the brief history of bridge engineering:

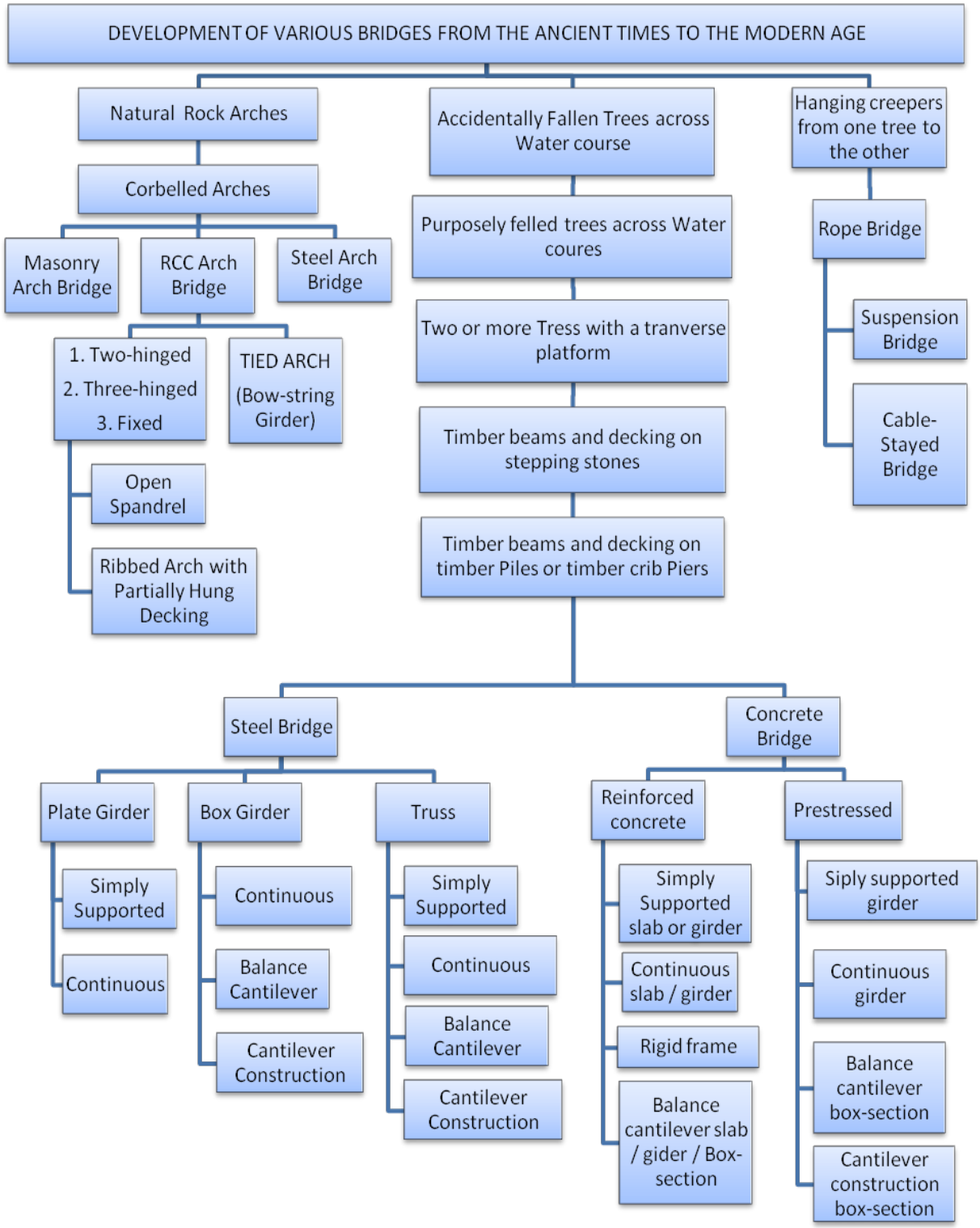

Figure 1: History of Bridges

1.1.3 Motivation:

The evolution of bridge engineering from ancient time to present age is a continuous process and is a result of human desire to use more and more improved methods and materials in order to build cheaper, finer and stronger bridges of lasting quality. Now a day, with the growing economy and rapid urbanization, the traffic demand in highways has been increased manifold. This lead to planning of complicated interchanges. Again, space constraint has lead to oblique crossing of obstacles. These lead to introduction of skew and curved span bridges. As those bridges are not very simple to analyze and has a very complex load transfer mechanism, systematic research is required to understand the behavior of these bridges.

1.2 Classification of Bridges:

Bridges may be classified from various consideration e.g. life span, functionality, span length, span arrangement. Structural arrangement, materials, loads carrying capacity etc. A brief classification is presented below.

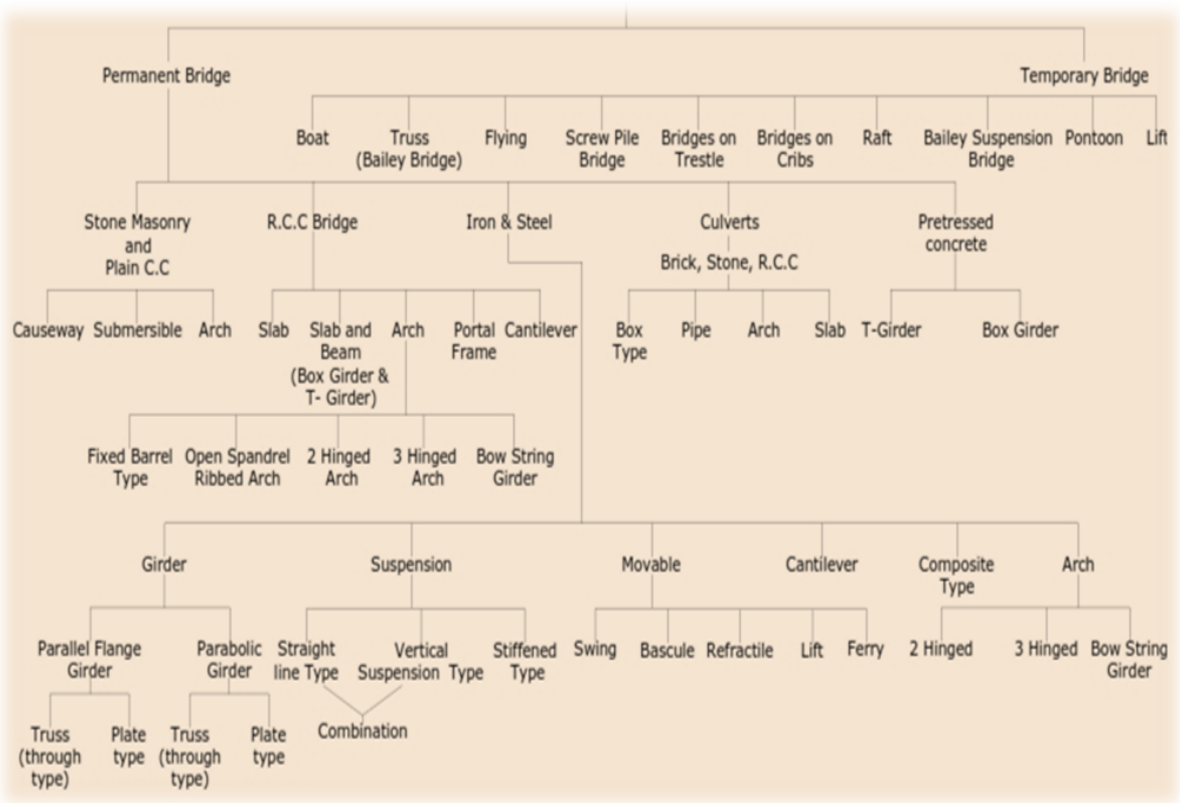

Figure 1: Classification of Bridges

1.3 Introduction to Concrete Box Girder Bridges:

With rapid growth in technology, the conventional bridge has been replaced by innovative cost effective structural system such as T-Beam Girder System and Box Girder Bridge System. Box girder bridges are generally consists of two or more longitudinal girders connected with deck slab at top and soffit slab at bottom. In spite of difficult design procedure and complex form work requirement, box girders, have gained wide acceptance for medium long span bridges due to their structural efficiency, better stability, serviceability, economy of construction and aesthetic appearance. Great in built torsional resistance in box girders helps in more even distribution of live loads though the loading may be eccentric.

Another advantage of box girder may be achieved, as it allows increasing in moment of resistance by increasing soffit/deck thickness, as the case may be, instead of increasing girder depth. One can suitably increase the compression area by increasing

deck/soffit thickness for positive/negative moment. This will lead to increase in moment of resistance.

The type of box Girder Bridge may be of various types depending on the material properties e.g. RC Box Girder, PSC Box Girder, Steel-Concrete composite box girder etc. Depending on the width of the bridge, box girder may be of single cell or multi-cell bridge.

1.4 Introduction to Skew/Curved Bridges:

Horizontally curved bridge are more required than straight bridge at complicated interchanges or stream crossing where geometric restrictions and limited site space constraints make extremely difficult for adoption of standard straight superstructure.

There is also a growing demand for skewed bridges to meet needs for complex intersections and the problems with space constraint in urban areas arise. Skewed bridges are useful when roadway alignment changes are not feasible or economical due to the topography of the site and also at particular areas where environmental impact is an issue. If a road alignment crosses a river or other obstruction at an inclination different from 90°, a skew crossing may be necessary.

1.5 Analysis Methods:

Concrete box-girders are constructed with thin webs and flanges in order to reduce self-weight and these sections are referred to as thin-walled or deformable sections. The structural response of the thin-walled box-girder bridge subjected to eccentric live load are different from that observed for the thick-walled section, due to its significant distortion and out-of-plane warping deformations. The usual assumption made in the elementary beam theory (plane sections remain plane after deformation) is no longer valid due to the out of plane axial deformations. In addition to that enormous shear flow is transmitted from vertical webs to the horizontal flanges, which causes in-plane shear deformation in flanges and results in an unpredicted extra longitudinal displacement at the web-flange junction, in box section. Consequently, the central portion of the flange lags behind that of the web-slab junction and this phenomenon is known as the shear lag effect. Thus, the overall structural response of the thin-walled box girder bridges becomes complex since it comprises of distortion, warping, and shear lag, in addition to usual flexure (both longitudinal and transverse

directions), shear and torsional actions. The analysis and design of a skew-curved box girder bridge are much more complicated than those for a right bridge.

The review of the literature shows that, for the simplified elastic analysis of straight box girder bridges, longitudinal bending, transverse bending, torsion, shear, warping and distortional actions are decoupled and global response of bridge is obtained by superimposing the effect of all these actions. However, to obtain the overall structural response without decoupling these structural actions researchers has suggested following methods, such as:

- Orthotropic plate theory
- Grillage analogy method
- Folded plate method
- Approximate analysis by membrane equations coupled with plane frame theory
- Finite difference method
- Finite strip method
- Finite element method

In the present study, skew and curved RC Box Girder Bridge has been considered. Determination of overall structural response of skew curved box Girder Bridge is much more critical than its straight counterpart. The critical geometry of skew-curved bridge leads to change in critical load path and increase in torsional effect due to eccentric live load. In order to capture the total structural response, SAP 2000 software will be used. Generally, SAP 2000 uses finite element method to analyze the model.

1.6 Present Study and its Importance:

A close look in the course of development of box girder bridges both in industrial practice as well as research clearly brings out the fact that though several analytical as well as experimental results are available for skew and curved box girder bridges, but very few analyses has been reported considering combined skew and curvature effect. Hence in the present thesis, the reported literature on box girder bridges is examined meticulously to identify the broad areas that should be studied in details. The pin pointed precise scope which this thesis is going to encompass is clearly identified there from. SAP 2000

software has been used as analysis tool to study the individual as well as combined effect of skewness and curvature on reinforced concrete box girder bridges. Different practical parametric variations are taken up for the present study and the results obtained are studied meticulously from engineering standpoint to extract conclusions of practical engineering significance.

Chapter-2: Bridge Geometry

2.0 General:

The geometric layout of the highway bridges and urban highway interchanges often requires the use of curved bridges for smooth and comfortable traffic transition. Generally, geometric restrictions and limited site space constraints lead to the requirement of curved bridges.

There is also a growing demand for skewed bridges to meet needs for complex intersections and the problems with space constraint in urban areas arise. Skewed bridges are useful when roadway alignment changes are not feasible or economical due to the topography of the site and also at particular areas where environmental impact is an issue. If a road alignment crosses a river or other obstruction at an inclination different from 90°, a skew crossing may be necessary.

However, sometimes due to highway alignment layout and site restrictions, it becomes necessary to provide skewed supports for the curved bridges and these bridges are referred to as skew-curved bridges. In addition to overcoming these geometrical constrain, construction of skew-curved box-girder bridges is becoming increasingly popular for economic and aesthetic reasons.

2.1 Curvature in Bridges:

When the axis of the bridge girder system is having a curvature in plan, the bridge is called curved bridge. Curvature of a particular span is measured by central angle. Curvature of a girder may be achieved either by a single curve or joining small straight beam elements.

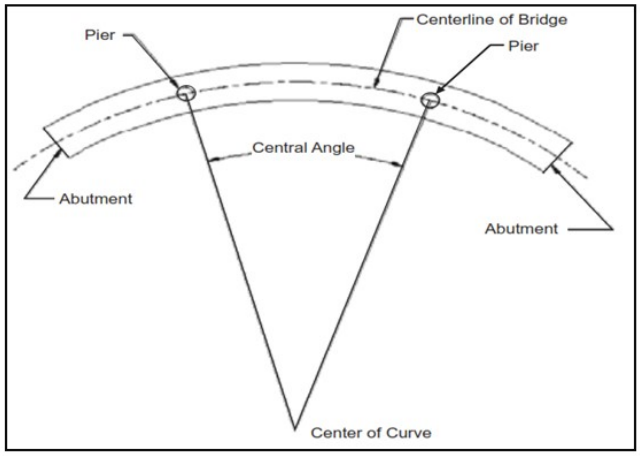

Central Angle

The central angle of a total span and with segmental bridge is illustrated in Left hand side diagram and Figure 2.

The analysis method for bridges curved in plan varies a lot based on the length

of the bridge and radius of curvature. In case of the horizontally curved bridges, significant torsional moments are developed and due to the coupling of torsional and longitudinal moments, the structural response of the curved bridges becomes more complex. To deal with such complexities, several international codal provisions have been developed. These codes also stipulate the circumstances under which a curved bridge can be analyzed as an equivalent straight bridge.

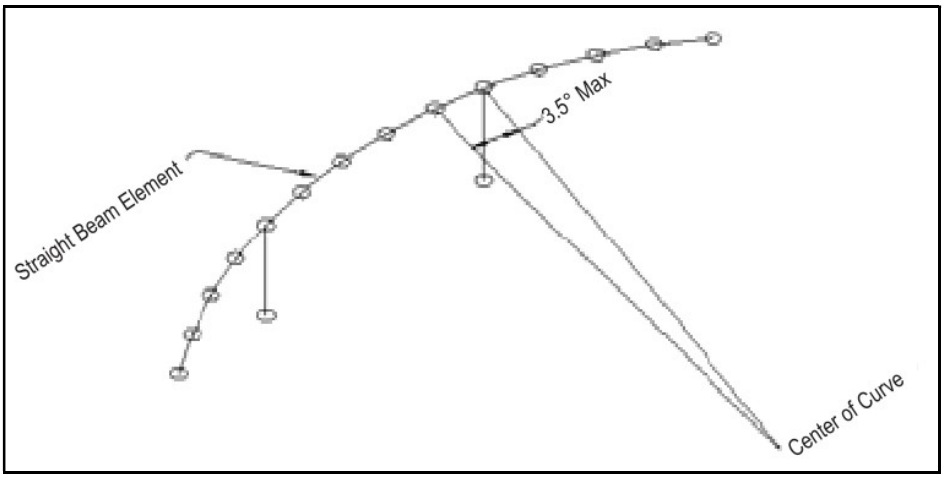

Figure 2: Central Angle with straight beam element

AASTHO LRFD Bridge design specification-2012 has come out with a recommendation as *Horizontally curved segmental concrete box girder superstructures, whose central angle within one span is between 12 degrees and 34 degrees may be analyzed as a single-spine beam comprised of straight segments provided no segment has a central angle greater than 3.5 degrees as shown in Figure-2. For integral substructures, an appropriate three-dimensional model of the structure shall be used. Redistribution of forces due to the time-dependant properties of concrete shall be accounted for*.

2.2 Skewness in Bridges:

A bridge, built obliquely between abutments/piers is called as Skew Bridge. The angle between the normal to the center line of the bridge and the center line of the abutment(s) or the angle between direction of traffic with the normal to the abutment(s) is known as Skew Angle. A clockwise rotation of the bridge abutment normal with respect to the traffic direction is denoted as positive skew ($\theta 1$ and $\theta 2$) while a

counter-clockwise rotation represents negative skew (θ3 and θ4) as shown in figure below.

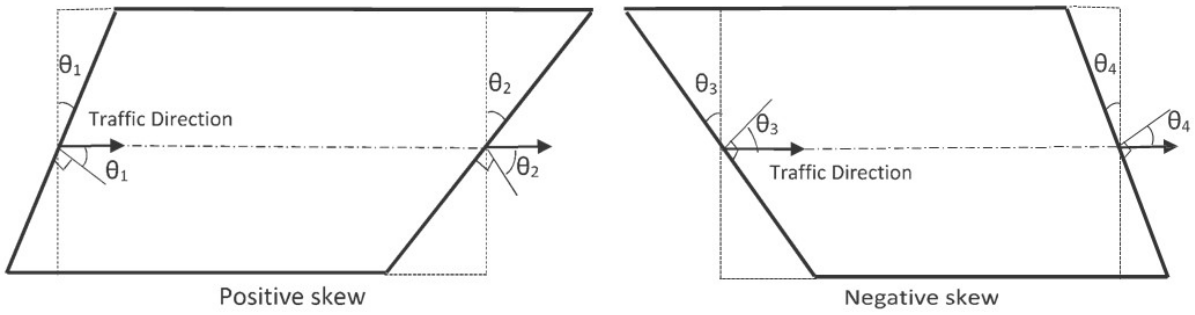

Figure 3: Types of skew deck

The load path (Force transfer mechanism), in straight bridges, is found along the direction of span, while in skew bridges load tends to take the shortest path along the obtuse corners. Due to change in load transfer mechanism, higher reactions are developed at obtuse corner while lower reactions are observed at acute corners. Moreover, due to skewness in the bridges, additional torsional and transverse moments are developed; though, the longitudinal moments are reduced. It is well documented in the literature that the bridges with small skew angles (< 15–20°) may be analyzed and designed similar to the straight bridges with little/no modifications. But, the structural behavior of the bridges with large skewness substantially differs from the straight bridges.

2.3 Skew-Curved Bridges:

On the other hand, the skew-curved bridge geometry, even within individual specified safe limits of skewness and curvature (12° for curvature and 20° for skew), cannot be analyzed and designed similar to their straight counterpart due to the coupling of curvature and skewness, and needs a robust analytical technique for analysis and design. Various possible geometries of skew-curved bridge are shown below.

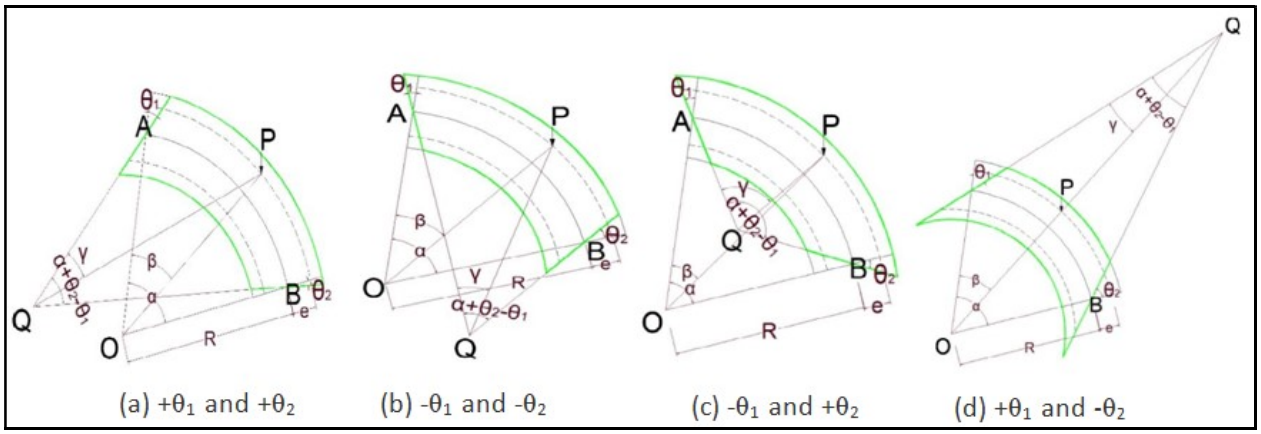

Figure 4: Various Skew Curved Geometries

The various points of Figure 4 are described as follows:

A, B: Center point of abutments.

O: Center of the curvature.

Q: Intersection point of abutment centre line.

P: Point of application of live load

Several analytical studies have been undertaken in past to understand the structural response of curved, skew and skew-curved box girder bridges using different methods of analysis.

Chapter-3: Literature Review

3.0 General:

Since the inception of research on skew bridges in 1948 (Newmark), it was well established that skew bridges are more vulnerable as the force experienced by them gets significantly altered as compared to their straight counter parts. Research on curved bridge also started from middle of second half of twentieth century. Due to lack of experimental and computational advancements, in initial years, response of skew/curved bridges could not be predicted clearly. With the inception of computer and advancement in computational techniques, the researchers predicted the response of skew/curved bridges. However, those were mainly on slab/culvert type structures. During the last 4-5 decades research has been advanced in this particular field of civil engineering. The available literature and research works from 1970s has been studied and presented in this chapter.

3.1 Skew Bridges:

Generally, it is observed that highly skewed bridges tend to attract more torsion, thus making the design more complicated, on the other hand the relieving fact is that as the skew angle increases, generally the longitudinal moment on the whole bridge reduces, thus providing the balancing effect. In the skewed bridges the load path follows the shortest route thus as a result the obtuse corner reactions are found noticeably large as compared to acute corner reactions, while the acute corners get the possibility of uplift also. Moreover, the obtuse corners are found to attract more negative (hogging) moments. Also, the transverse bending moments are found to be constantly increasing with increase in skewness.

Many researchers have proven above mentioned responses via various experimental, numerical and analytical studies, their works in case of skewed box girder bridges can be summarized as follows:

3.1.1 Rakshit KS, Design and Construction of Highway Bridges:

Though this book does not deals with Concrete box girder bridges in particular, following important recommendations has been made:

- The behavior of skew bridge differs widely from that of normal bridge and, therefore, special attention is required for design of skew bridge. There is always a doubt regarding load path for the skew bridges or the direction of span of the slab. It is believed that the load will be transferred in proportion of rigidity i.e. if the superstructure section remains same, the load will follow the shortest path.
- It has been observed that the reactions at supports for skew bridges are different, as the same is more at obtuse angle corners and less at acute angle corners. The increase in reaction at obtuse angle corner varies from 0 to 50% of the average reaction for skew angle of 0 to 20° and 50% to 90% for skew angle of 20° to 50°. For skew angle more than 90% the reaction at obtuse angle corner becomes almost double and the acute angle corners becomes zero pressure point. Figure 5 may be referred.

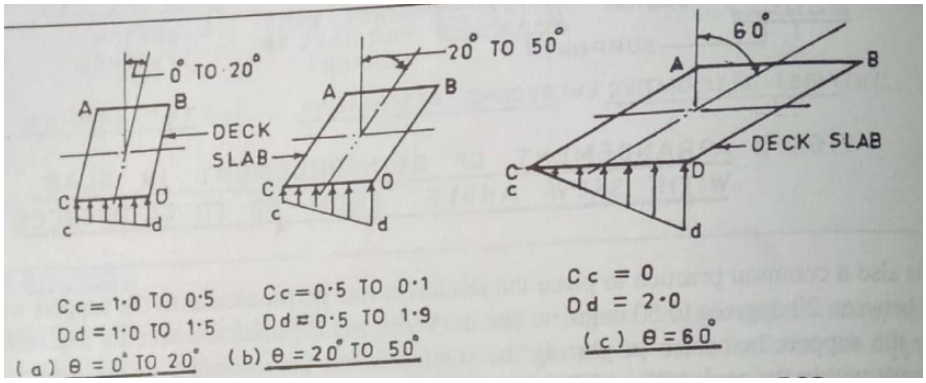

Figure 5: Variation of reaction in skew deck

- It has also been revealed that the longer diagonals connecting the acute angle corners has a tendency to elongate possibly because of load transfer mechanism. Hence it causes creep along the longer diagonal and thus results tensile stress along the longer diagonal. The section shall be sufficiently designed to cater this tensile stress. Following Figure may be referred.

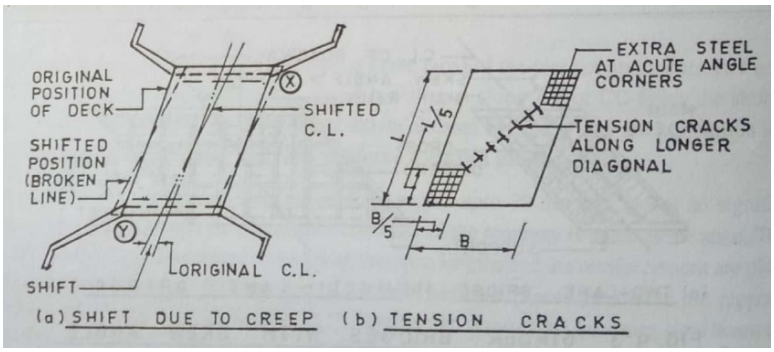

Figure 6: Creep effect

- Diaphragms must be provided at closer spacing for better redistribution of moment/torsion causing from skewness effect.
- The bearing shall be so aligned that the movement of superstructure due to temperature variation shall be allowed with obstruction.

3.1.2 Sisodiya RG, Cheung YK, Ghali A, "Finite Element Analysis of Skew, Curved Box-Girder Bridge", Publication of Kajima institute of Construction Technology, Japan, Vol. 30, pp. 191-199, 1970.

Sisodiya and his colleagues carried out experiment on simply supported two-span continuous single cell box-girder bridge model of aluminum alloy, having curvature in plan and was supported on skewed supports. The bridge model considered was having span 41 in (1.04 m), width 8 in (0.2 m) and depth 1.2 in (0.03 m) and was subjected to a concentrated load placed at mid span of the inner web. They found the following:

- They compared various responses, e.g. vertical deflection, tangential strains and maximum stresses present in webs at mid span, obtained with finite element results and experimental findings.
- In finite element analysis, effect of aspect ratios chosen (1:1, 1:2, 1:4) for rectangular element was investigated. Results showed that there was not much difference between the 2-D finite element results using rectangular elements with aspect ratio 1:1 and the results obtained from beam theory using shear deformation.

3.1.3 Brown TG, Ghali A, "Semi-Analytic Solution of Skew Box Girder Bridges", Proc. Of Institution of Civil Engineers Part 2, Vol. 59, No. 3, pp. 487-500, 1975

Brown and Ghali (1975) presented a semi-analytical procedure to analyze simply supported skew box-girder bridge using finite strip method and compared their results with the results obtained by finite element analysis. They considered three examples: two were four-cell rectangular sections and one single cell trapezoidal section. The four-cell box- girder models were previously experimentally tested by Godden and Aslam (1971) and were having skew angle 30° and 45° and span 29.66 in (0.753 m) and 35.5 in (0.902 m) respectively. All the girders were idealized as a combination of parallelogram shape strips, connected along nodal lines. They found the following:

- They compared the outcomes for deflection, longitudinal bending stresses and the transverse bending moments for different skew cases.
- The deflections were noted at 11 locations and it was found that deflection has been reduced by about 45% with the increase of skew angle from 30° to 45°.
- The longitudinal bending stresses and the transverse bending moments were found in good agreement with the results obtained via finite strip method, finite element method and experimental study.

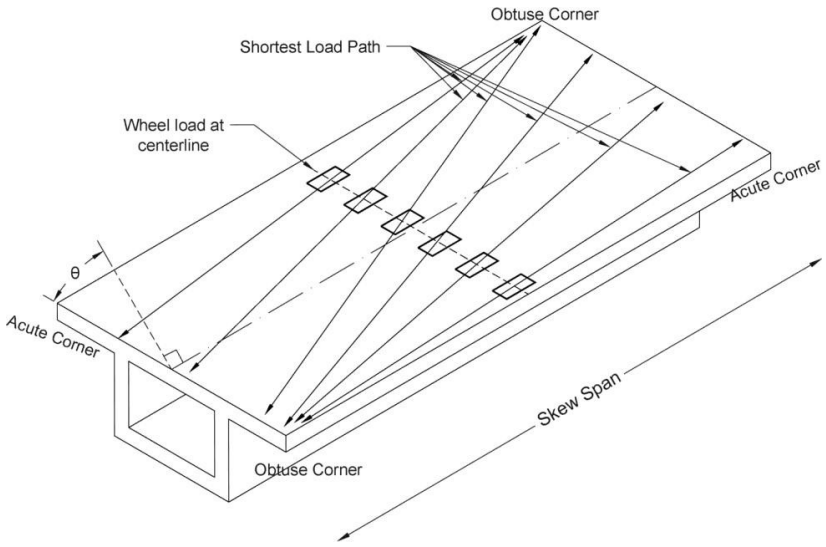

Figure 7: Wheel load distribution path in skew bridge

3.1.4 Mark R. Wallace (1976), Studies of Skewed Concrete Box Girder Bridge by, Division of Structures, California Department of Transportation

Researchers of University of California has developed one finite element program CELL, to study and analyzed number of mathematical models to assess the effect of varying superstructure geometry, number of cells, skew angle, types of loading and depth of superstructure. Those results were also verified through experiments with "Aluminum Models". They found the following:

- Aspect ratio and skew angles are the main parameters affecting the bending behavior of the structure.
- Span length and skewness are the significant parameters affecting the shear behavior of the structure.
- Deal load moment will reduce in skew bridges.
- Dead load deflection will reduce in skew girders. The difference of displacement in the exterior girders will again depend on the aspect ratio and skewness.

3.1.5 Bouwkamp JG, Scordelis AC, Wasti ST, "Failure Study of a Skew Box Girder Bridge Model", IABSE Congress Report, Vol. 11, pp. 855-860, 1980.

Bouwkamp and his associates (1980) performed an experimental study to investigate the effect of skewness on a multi-cell two span continuous box girder bridge. They tested a 1:2.82 scale model of a 61 m long two-lane, four cell box girder bridge located at California with 45° skew bent central support. The bridge model was subjected to concentrated loads at mid length of each span and the loads were gradually increased up to collapse of bridge. Based on the study conducted it was observed that

- Obtuse corners attract high reactions as well as significant end moments and torsional moments, which reflected the tendency of the skew-bridge to span across the shortest load path between the supports.
- It was suggested that the vertical reaction, bending moment and torsional moment may be represented by an eccentric resultant concentrated load.
- They compared the results of right and skewed geometries and concluded that mid-span and support moments (positive as well as negative moments) reduce for the live load as well as dead load case, due to the skewness.

- It was also observed that experimental model sustained ultimate loading of dead load plus 4.5 times live load before failure e. Such rising of collapse load was explained due to transfer of support failure zone as a consequence of skewness present in the bridge.

3.1.6 Scordelis AC, Bouwkamp JG, Wasti ST, Seible F, "Ultimate Strength of Skew RC Box Girder Bridge", Journal of the Structural Division ASCE, Vol. 108, No. 1, pp. 105-121 and pp. 89-104, 1982

Scordelis and colleagues (1972, 1982) conducted an experimental study on a 45° skew reinforced concrete bridge model to check the adequacy of analytical design methods in terms of deflection, reaction, strain and moments generated in the bridge. They proposed the following:

- Total moment in right mid-span section of simply supported 45° skew bridge would be 0.07WL (W being the weight and L being the total length of the bridge) which was 56% lesser than the simply supported right bridge case (0.125 WL), thus they recommended to use of less number of longitudinal steel bars in the section.
- Further, they investigated the typical California continuous box-girder bridge tested by Bowkamp and results were taken for 4 load cases: dead loads, working stress loads, Overloads and failure loads. Based on the results it was predicted that skewness effect was dependent upon Skew angle, span to width ratio, position of applied loads and support conditions.
- Above behavior was explained in terms of attraction of negative moments at obtuse end side due to presence of skewness. They also recommended that in skew bridges transverse moment is not uniformly distributed thus use of load distribution factor as per right bridge approximation should be avoided.

3.1.7 Wasti ST, Scordelis AC, "Comparative Structural Behavior of Straight, Curved and Skew Reinforced Concrete Box Girder Bridge Models". Analysis and Design of Bridges Springer Netherlands, Vol. 74, pp. 191-211, 1984.

Wasti and colleagues (1984) conducted an experimental study on three large scale models of two span, four cell, reinforced concrete box-girder bridge, which were subjected to dead load, working loads, overloads and failure load to compare various

structural responses e.g. reactions, deflections and moments of right, skewed and curved bridges. The models were same in cross-sectional dimensions but different in plan i.e., one was right, other was skewed and third was curved. The dimensions of models were 72 ft (21 m) long along the longitudinal centre line, 12 ft (3.7 m) wide and 1.71 ft (0.52 m) deep. The skew bridge was having skew angle of 45° and the radius of curvature of curved bridge was 100 ft (30.48 m).

- It was observed that the skew bridge showed significant amount of changes in the vertical reactions depending on the transverse positioning of the load. When the acute side of span was loaded, the adjacent end reaction was smaller than that of the corresponding right and curved bridge cases.
- When the loads shifted from the acute to the obtuse side of the skew span, the reaction increased drastically than that of the right and curved bridge models.
- The mid-span deflection and longitudinal bending moments in the skew bridge were even found dependent upon the transverse location of the load on the top deck.
- It was also shown that higher deflections and moments were developed, when the loads were placed on the acute side of the span, while lower moments and deflections were observed when the loads were placed on the obtuse side of the span.
- It was demonstrated that in the case of the skew bridge only, end moments and torsional moments were produced for all load cases considered, which led to conclusion that its behavior was most complex out of the three geometries considered.

3.1.8 Paavola J, "A Finite Element Technique for Thin-Walled Girders", Computers & Structures, Vol. 44, No. 1, pp. 159-175, 1992.

Paavola (1992) developed a numerical model based on Vlasov's theory to analyze the thin walled box-girder and coded a computer program in FORTRAN. This study had been carried out for a continuous skewed concrete box-girder bridge of 80.0 m, width 6.0 m and depth 3.0 m. The bridge was simply supported at the ends and at the mid-span it was resting on a skew support line. The skew angle was varied from 0° to 60°. The bridge was stiffened by diaphragms which restrained distortion at ends and at skew support line. The bridge was loaded symmetrically by two line loads above the webs having value of 100 kN/m.

- He studied the effect of skewed support line on the deflection and stresses.

- It was shown that, as the angle of skew increases maximum deflection tends to decrease throughout the span, while axial stresses were not found much affected.

3.1.9 Shushkewich KW. (July-1998), Approximate Analysis of Concrete Box Girder Bridges, ASCE, Journal of Bridge Engineering, Vol.114, No.7, Pg. 1644-1657

Kenneth W. Shushkewich performed approximate analysis of Concrete Box Girder Bridges. He suggested that the actual three dimensional behavior of a box girder bridges as predicted by a folded plate, finite strip or finite element analysis can be approximated by using some simple membrane equations in conjunction with plane frame analysis. This is a useful method since virtually all structural engineers have access to a plane frame computer program. The researcher considers the following points for explanations: the webs may be inclined or vertical; Self-weight, uniform load, and load over the webs may be considered with respect to transverse flexure; both symmetrical (flexural) and anti-symmetrical (Torsional) loads may be considered with respect to longitudinal shear and torsion. This paper is particularly useful in the design of single cell precast concrete segmental box girder bridges without considering the effect shear lag and warping torsion.

- The author represents the three examples of box girder bridges with different load cases and concluded that the results of a folded plate analysis which is considered to be exact can be approximated very closely by using some simple membrane equation in conjunction with a plane frame analysis.

3.1.10 Jun-Tao K, Jun-Jie Z, Guo-Ding W, Qin-Han F, Rui D, "A New Method on Resolving the Rotation in the Plane of Skew Bridges", Wuhan University Journal of Natural Sciences, Vol. 10, No. 6, pp. 1081-1084, 2005.

In 2005, Jun-Tao and his associates (2005) carried out the analysis of a slant- leg, rigid frame continuous prestressed concrete box-girder bridge having a skewness of 60°. The bridge did not have any abutment and the objective was to study the lateral horizontal displacement and rotation of bridge at supports.

- They identified three main forces which are responsible to developed in-plane displacements and rotation in skew bridge namely: longitudinal forces due to braking

and seismic effects, lateral forces due to wind and seismic effect, and forces due to temperature variation, concrete shrinkage, creep, and prestressing force.

- They concluded that slant-leg rigid frame bridges without abutments have advantage over other bridge sections as the former have more horizontal stiffness

3.1.11 Ashebo DB, Chan TH, Yu L, "Evaluation of Dynamic Loads on a Skew Box Girder Continuous Bridge Part I: Field Test and Model Analysis" Engineering Structures Vol. 29, No. 6, pp. 1052-1063, 2007.

Ashebo and his colleagues (2007) evaluated the effect of skewness on longitudinal bending moment in an existing skew continuous box-girder bridge. They tested the Tsing Yi south twin-cell box-girder bridge which was continuous over three spans having first and last span as 23 m long while middle span was 27 m long. The carriageway width was 10.58m and the bridge was having a 27° angle of skew. As a preliminary result of the study they observed:

- As higher skew angles were applied in finite element modeling of the bridge maximum span bending moment decreased, such decrease was swifter in cases when skew angles were increase more than 30°.

3.1.12 Grace NF, Patki KD, Soliman EM, Hanson JQ, "Flexural Behavior of Side -By-Side Box-Beam Bridges: A Comparative Study", PCI Journal, Vol. 56, No. 3, pp. 94-112, 2011.

Grace and colleagues (2011) constructed, instrumented, and tested two 30° skew precast, prestressed concrete four cell half-scale box-girder bridge models which were reinforced with carbon-fiber-composite cable [CFCC] and conventional steel strands respectively, to study their structural responses. Model bridges were 31 ft (9.5 m) long, 18 in. (0.46 m) wide and 11 in. (0.280 m) deep. The reinforced concrete bridge model was designed to be under-reinforced while CFCC-reinforced bridge model was designed to be over-reinforced. The bridge models were tested in two stages, namely un-cracked deck slab and cracked deck slab stage.

- This investigation compared flexural behavior of above mentioned bridges in terms of the load-deflection response, load versus strain response, ultimate strength, failure mode and energy ratios.

- They also considered transverse post-tensioning (TPT) with TPT diaphragms, to check the excessive cracking in the longitudinal direction of the deck.
- The cracking load of the CFCC bridge model was found 25% higher as compared to conventional RC bridge model.
- The ultimate load of the CFCC bridge model was found 17% higher when compared to conventional RC bridge model.
- It was noted that CFCC model suffered a compressive failure due to crushing of concrete while the normal model had a tensile failure due to reinforcement yielding.
- Both the models demonstrated approximately same deflection at ultimate load capacity.

3.1.13 Hodson DJ, Barr PJ, Halling MW, "Live-Load Analysis of Post tensioned Box-Girder Bridges", Journal of Bridge Engineering ASCE, Vol. 17, No. 4, pp. 644-651, 2011 and "Live Load Test and Finite Element Analysis of a Box Girder Bridge for the Long Term Bridge Performance Program", MS Dissertation in Utah State University, 2011.

Hodson and associates (2011) performed live load and dynamic load tests on 12° skew, five span, prestressed concrete box-girder bridge which was consisting of four-cells. Also they carried out a finite element analysis to compare the analytical results with the test data to calibrated finite element results. This calibrated FE model was then employed to determine load distribution factors and theoretical load ratings of the bridge.

- Results from the study indicated that the distribution factors taken from AASHTO LRFD specifications were 29% to 46% conservative as compared to those obtained from the finite element model for an interior girder while for exterior girder they were 2% to 9% un-conservative.

Further, Hodson and his colleagues (2011) conducted static live-load tests on cast-in-place 8° skew, prestressed concrete bridge, consisting of four box-girders which were continuous over two equal spans each measuring 39.35 m and having 12.8 m width. In total, they conducted sixteen quasi-static live-load tests along five different load paths to estimate flexural live load distribution factor experimentally. Further, using the eight

noded solid elements (CSI, 2009) maximum distribution factor for the one, two, and three loaded lanes were also obtained. To investigate the effect of span length, girder spacing and overhang on load distribution, the span length of the bridge model was varied from 18.3 m to 73.2 m, girder spacing was varied from 2.1 m to 4 m and overhang was varied from 0.3 m to 1.2 m. Further, for vast parametric study, they varied the skew angle from 0° to 60°.

- AASHTO LRFD distribution factors were found significantly higher than FEM results for the interior girders, however, for the exterior girder, when the parapets were included in the analysis, the AASHTO LRFD distribution factors were found somewhat un-conservative.
- Consequently, they concluded that the presence of parapets severely affects distribution factor values.
- Also, the study indicated that diaphragms did not have much effect on the moment distribution factors, as with or without diaphragms distribution factors changed only by 1%.
- Results suggested that a decrease take place in moment distribution factors when span length in increased, while the increase in girder spacing resulted an increase in the distribution factors, but at the same time increase in deck overhang distance did not considerably affected the interior girder, but it raised the distribution factor of exterior girder.
- Change in deck thickness also failed to affect any distribution factors.
- They concluded that distribution factors tend to decrease for both girders when the skew angle reaches 15° and higher and at the same time the ratio of AASHTO to FEM distribution factors decreased for interior girder while it increased for exterior girder.

3.1.14 Mohseni Iman, Rashid A. Khalim, (2011) ,"Transverse load distribution of skew cast-in-place concrete multicell box - girder bridges subjected to traffic condition", Department of Civil Engineering, University Kebangsaan Malaysia (National University of Malaysia)

Iman Mohseni, A. Khalim Rashid has performed extensive analysis to investigate the maximum deflection, tensile and compressive stress distribution factor of concrete

continuous skewed multi cell box girder bridges. A parametric study is performed on 240 prototype bridges to determine effective parameters on live load distribution factor of bridges. The parameters investigated included: skew angle, span length, number of box and number of lane. Using a statistical approach several empirical equations are deduced to determine maximum distribution factor of stress and deflection of skewed MCB bridges subjected to the AASHTO LRFD truck loads. They recommended the following:

- The three–dimensional finite element modeling by SAP 2000 is appropriate for evaluating the behavior of skewed bridges.
- For straight bridges, the maximum tensile stress occurs in the mid-span of longitudinal direction, however, it is provided at the cross section along a line passing among the mid-span of each lane in skewed multi cell box-girder bridges.
- The bridge span length, skew angle, number of boxes and number of lane loadings are the most crucial parameters that affect stress and deflection distributions factor of these types of bridges.
- The simplified empirical equations were deduced for distribution factor of tensile stress, negative stress and deflection of the skewed multi cell box-girder bridges.
- The effect of skew angle on positive stress distribution factor was negligible.
- There is a good agreement between finite element analysis, non-orthogonal grillage method and proposed equations. It was discovered that grillage analysis can be used to determine bridge responses.

3.1.15 Reddy P, Karuna S, "Comparative study on normal and skew bridge of PSC box girder", International Journal of Research in Engineering and Technology", Vol-04, Issue-06, June-2015.

Reddy P, Karuna S (2015) carried out finite element based software analysis of skewed PSC box girder bridges. A single span, two span and three span, two lane PSC box girder is considered in the present study. The different bridge spans considered are 30m 60m and 90 m and skew angle is varied from 0° to 50° at 10° interval. Beam depth of 1.5m and width of 0.3m is provided. The bridge deck is analyzed for Dead load, Live load i.e., IRC class 70R considered from table 2 of IRC 6:2000 and Temperature load effect. Comparison of critical structural response of above class is analyzed for the models. A

total of 18 slab deck models generated and analyzed using SAP2000 ver. 14. Findings are as follows:

- Deflection decreases with increase in skew angle in two or three span skew slab whereas in case of single span deflection increases with increase in skew angle. This shows that the effect of skewness on deflection in single span skew deck slabs as the stiffness of slab is less.
- Bending moment has reduced with increase in skew angle under dead load in single, two and three spans deck. But under moving load there is slight reduction in bending moment up to 20° and then increased for 30° and further reduced for 40° skew angle only on single span deck.
- When compared with all the three spans, the magnitude of bending moment has reduced its maximum value in single span deck.
- The magnitude of shear force has slightly reduced with increase in skew angle under dead load in two and three span deck, it was observed that the magnitude had increased under moving load.
- In single span, the shear force remained same in all the models (skewed bridge) compared with normal bridge under dead load but there is increase in shear force with increase in skew angle under moving load.

3.1.16 Gupta T, Kumar M, "Structural Response of Concrete Skew Box-Girder Bridges-A State-of-the-Art Review", International Journal of Bridge Engineering (IJBE), Vol. 5, No. 1, (2017), pp. 37-59

Gupta and Kumar have reviewed the available literature and available codal provisions. They made the following recommendation about the flexural behavior of skewed concrete box girder under dead and live loads:

- Bridges with skew angle lower than 20° are simple enough to design by few modifications in right bridge guidelines; however, for bridges with high skew angle a careful in-depth analysis is needed.
- Width to span ratio play a major role in deciding the extent to which skew angle will affect the response of the bridge. Very long bridges tend to negate the skew

effect but in short bridges high skew angle can generate a variety of extra forces which must be accounted in while designing.

- Although the presence of orthogonal diaphragms is proved to be most advantageous in skew box-girder bridges, as they reduce structural actions to great extent still, due to construction difficulties they might be omitted in some cases
- Live load distribution factors in multi-cell skew box-girder bridges predicted by some of the codal provisions are found either way over-conservative or sometime risky also, especially in skew box-girder bridges. Efforts have been made by various researchers to distribute the live load among spines/webs of multi-spine/cell box-girder in a simplistic way to facilitate the manual design of girders.
- Although a good amount of research work has already been done to understand the behavior of skew box-girder bridges, however, still there are no exclusive guidelines available for selecting the optimum cross-section dimensions for different skew angle.

3.2 Curved and Skew-Curved Bridges:

In horizontally curved bridges, significant torsional moments are developed and due to the coupling of torsional and longitudinal moments, the structural response of the curved bridges becomes more complex. Several international codal provisions are available to deal with such complexities. These codes also stipulate the circumstances under which a curved bridge can be analyzed as an equivalent straight bridge. Canadian Highway Bridge Design Code, AASHTO-LRFD Bridge Design specifications, and the AASHTO specifications for horizontally curved Bridges recommends that curved bridges can be treated as straight bridges with curvature angle up to 12°. In contrast, the skew-curved bridge geometry, even within individual recommended safe limits of skewness and curvature (12° for curvature and 15° for skew), cannot be analyzed and designed similar to their straight counterpart due to the coupling of curvature and skewness. Skew-Curved bridge needs a robust analytical technique for analysis and design. Several analytical studies have been undertaken in past to understand the

structural response of curved and skew-curved box girder bridges using different methods of analysis.

3.2.1 Rakshit KS, Design and Construction of Highway Bridges:

Though this book does not deals with Concrete box girder bridges in particular, following important recommendations has been made:

- The axis of bridge deck is not a straight line and changes the direction at every point and hence, the pier or abutment caps supporting the superstructure are not parallel to each other though these are normal to bridge axis. Hence, it requires a careful consideration in respect of fixing the axis of metallic bearings whether it is rocker, roller, hinged or sliding. The orientation of metallic bearings shall be such that the direction of translation of bearing shall coincide with the direction of movement of bridge deck. As the axis of curved bridges changes at every point and pier caps are not parallel to each other the bearing should be placed either at right angle to the bridge axis at that particular point or at right angle parallel to pier cap axis. It should be ensured that the free movement of deck due to temperature variation must be allowed through free bearing without obstruction. The direction of movement of curved bridge deck at the free end can be found theoretically from the figure below (Figure-8).

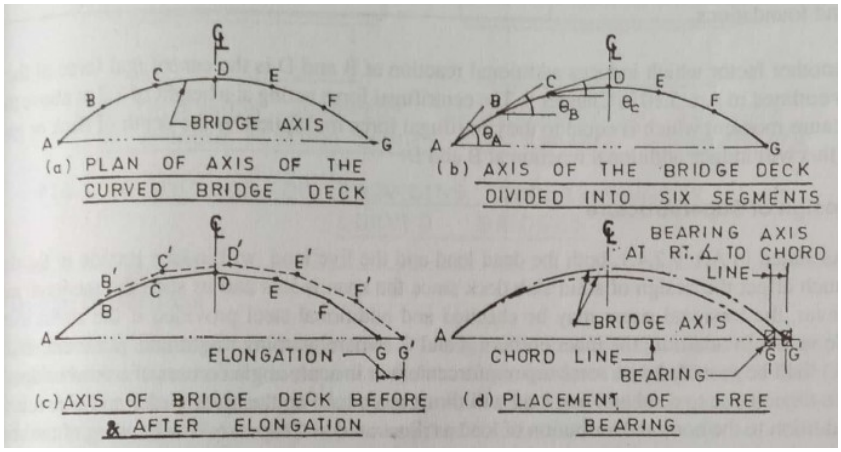

Figure 8: Layout of free bearing

- Both the dead load and live load (especially when eccentric outwards) produce torsion in the superstructure. Centrifugal force due to curvature will also cause

additional torsion in the bridge deck. This total Torsional moment will increase if the span is more.

- The torsional moment due to deal load and live load thrust will cause additional reaction in outer girder and reduces the reaction in inner girder. In addition, there is possibility of warping at the inner corners. So, all these factors must be considered during design and detailing work.
- To prevent the overturning of the moving vehicles due to centrifugal force super-elevation must be provided as per standards. This can be achieved either by varying web height or varying the pedestal height.

3.2.2 LRFD Bridge Design Specification12th Edition

Being the most authentic guideline/standards available for the design of Curved and Skew bridges, it recommends the following.

- The moments, shears, and other force effects required to proportion the superstructure components shall be based on a rational analysis of the entire superstructure. Analysis of sections with no axis of symmetry should consider the relative locations of the center of gravity and the shear center. The substructure shall also be considered in the case of integral abutments, piers, or bents. The entire superstructure, including bearings, shall be considered as an integral structural unit. Boundary conditions shall represent the articulations provided by the bearings and/or integral connections used in the design. Analyses may be based on elastic small deflection theory, unless more rigorous approaches are deemed necessary.
- Analyses shall consider bearing orientation and restraint of bearings afforded by the substructure. These load effects shall be considered in designing bearings, cross-frames, diaphragms, bracing, and the deck. Distortion of the cross-section need not be considered in the structural analysis. Centrifugal force effects shall be considered.
- Where transverse distortion of a superstructure is small in comparison with longitudinal deformation, the former does not significantly affect load distribution;

hence, an equivalent beam idealization is appropriate. The relative transverse distortion is a function of the ratio between structural width and height, the latter, in turn, depending on the length. Hence, the limits of such idealization are determined in terms of the width-to effective length ratio.

- Plan-Aspect Ratio: If the span length of superstructure with torsionally stiff closed cross-sections exceeds 2.5 times its width, the superstructure may be idealized as a single-spine beam. The following dimensional definitions shall be used to apply this criterion:
    - Width— the core width of a monolithic deck or the average distance between the outside faces of exterior webs.
    - Length for rectangular simply supported bridges—the distance between deck joints.
    - Length for continuous and/or skewed bridges—the length of the longest side of the rectangle that can be drawn within the plan view of the width of the smallest span, as defined herein.
- The length-to-width restriction specified above does not apply to cast-in place multi-cell concrete box girder bridges.
- Simultaneous torsion, moment, shear, and reaction forces and the attendant stresses are to be super imposed as appropriate. The equivalent beam idealization does not alleviate the need to investigate warping effects in steel structures. In all equivalent beam idealizations, the eccentricity of loads should be taken with respect to the center line of the equivalent beam. Asymmetrical sections need to consider the relative location of the shear center and center of gravity.
- Horizontally curved concrete box girders may be designed with straight segments, for central angles up to12 degrees within one span, unless concerns about other force effects dictate otherwise. Horizontally curved non segmental concrete box girder bridge superstructures may be analyzed and designed for global force effects as single-spine beams with straight segments for central angles up to 34 degrees within one span, unless concerns about local force effects dictate otherwise. The location of the centerline of such a beam shall be taken at the

center of gravity of the cross-section and the eccentricity of dead loads shall be established by volumetric consideration.

3.2.3 Sennah Khaled M., Kennedy John B., "State-of-The-Art in Design of Curved Box-Girder Bridges", May-June, 2001, Journal of Bridge Engineering

The researchers studied available analytical as well as the experimental work on box girder bridges. They found that the research in this field has been developed from 1970s. They recommend the following:

- The current North American codes as well as the published literature do not provide the design engineer with adequate information on the behavior of the un-shored straight and curved box-girder bridges during the construction phase. Further research work is required using 3D finite-element analysis to investigate the behavior of straight and curved box girders at this phase and avoid possible failure.
- The study of load distribution in curved box-girder bridges due to dead load and truck loads was not covered for all cross-section configurations, span continuity, and different support conditions.
- Simple expressions for the load carrying capacity or for the ultimate load distribution in straight and curved box girder bridges are still required since the published literature on this subject is not yet conclusive.

3.2.4 Sarode Asish B, Vesmawala G.R, "Torsional Behavior and Constancy of Curved Box Girder Superstructures", TARCE - Vol.1, No.2, July-December, 2012

In this paper, the numerous finite element models of single cell box girder superstructure are analyzed, using LUSAS software, for different parameters such as span length, radius of horizontal curve of box girder and loadings. The bending moments, shear and torsional moments are compared. Also the feasibility and stability of the curved box girder of various span length and radius considering support reactions are discussed. Authors concluded the following:

- There is no significant variation of bending moment and shear force for different radii in same span i.e. with different central angle.
- Torsional moment increases with decrease in radius and this effect is almost nullified when the radius is 400m or more.
- The authors have found out a limit in terms of radius to mark the instability against overturning moment.

3.2.5 Miner L, Zokaie T, Fell Ben, "Effect of Curved Alignment and Skewed Support on Bridge Response"

Extensive analytical study has been made on single span 4-cell Foot Bridge with varying skewness and curvature effect. The authors concluded the following:

- Aspect ratio and support stiffness (bearing pad stiffness) influences the skew effect and curvature effect.
- Spine model analysis with codal modification (AASTHO) may not yield conservative responses in skewed or curved bridges when the aspect ratio is high.

3.2.6 Raj B, Jivani D, "Parametric Study on Effect of Curvature and Skew on Box Type Bridge", May 2016, IJSDR, Volume 1, Issue 5

Bhalani Raj, Dipak Jivani has developed few analytical model of curved and skewed single cell RC box girder superstructure and compared various responses viz. time period, bending moment, shear force and deflection due to dead load, SIDL and live load (IRC-Class-70R). This analysis has been done in SAP 2000 software.

3.2.7 Gupta Tanmoy, Kumar Manoj, "Flexural response of skew-curved concrete box-girder bridges", ELSEVIER, Engineering Structures 163 (2018), pp- 358–372

Researchers have carried out 3D finite element based parametric study to understand the behavior of combined skewness and curvature effect on single cell concrete box girder bridge. They have considered the Han-Jiang bridge at Shayang located in Wuhan, China with actual dimensions has been considered as root geometry. The span, width and depth of the bridge are 27.4m, 10.8m and 2.96m respectively. They have used CSI Bridge as analysis software. Findings are as follows:

- Based on the 3D FEA results, it has been demonstrated that, in general, an increase in the degree of curvature (α) the magnitude of absolute maximum moment in outer girder of the non-skew box- girder bridge enhances up to 45.2% and 23.7% under the DL and LL conditions, respectively. On the other hand, an increase in skewness causes a reduction in absolute maximum moment in most of the cases. An inclusion of 50° skewness in 48° curved bridge reduced the rise in absolute maximum outer girder moment from 45.2% to 28% and from 23.7% to 14% for DL and LL respectively. Thus, for the bridges considered in this study, it has been observed that inclusion of skewness becomes advantageous in highly curved ($\alpha \geq 36°$) geometrical layouts to control the flexure in the box girder bridges.
- The study has been extended to investigate the influence of skewness and curvature on the location of the critical section for moment and the associated critical position of live load. Since it is difficult to define the position of a point on skew-curved bridge deck using conventional coordinate systems, a new skew-curve coordinate sys- tem has been developed to define critical positions more systematically.
- It has been perceived that for curved bridges up to 12° curvature, one can rely on elementary bending theory to find out critical section and live load position for maximum moment with reasonable accuracy.
- With the introduction of skewness in curved bridges, critical section for maximum moment as well as the positions of live load developing maximum moment have been found to move towards right-hand support irrespective of curvature present in the bridge. In case of 48° curved bridge having 50° skewness associated with it, the critical section and the live load position have been found to shift by 37% and 28% in terms of angular distance in the framework of the new skew-curve coordinate system.

3.3 Critical Discussion:

A close review of literature shows that the researchers are working on various responses of skew, curved and skew-curved concrete box girder bridges. It has also been reported

that various experimental study on scale model has also been undertaken in addition with analytical study.

Generally, concrete box girders sections are comprised with thin webs and flanges in order to reduce self weight and these sections are referred to as thin-walled or deformable sections. It is well established that, the structural response of the thin-walled box girder bridge becomes complex due to out of plane deformations and enormous shear flow between the vertical webs and horizontal flanges. The former is the responsible for distortion and warping while the later is responsible for shear lag of central portion in the flanges and in plane shear deformation. The usual assumption of elementary beam theory remains invalid due to the out-of plane deformation. Thus, the overall structural response of the thin-walled box girder bridges becomes complex as it comprises of distortion, warping, and shear lag, in addition to usual flexure action in two horizontal orthogonal direction, shear and torsion.

Concrete box girders are becoming increasingly popular in Skew, curved and skew-curved bridges, due to their pleasing aesthetics, better economy and other functional advantages, at congested interchanges. This type of structures is also being used to allow the flexibility of highway alignment in rural area also. Change in geometry of box girder bridges leads to more complexity in overall structural response.

Overall structural response of box girder bridges can be obtained by various analysis procedure, e.g.- orthotropic plate theory, grillage analysis or folded plate method. This is also seen that membrane equation in conjunction with some plane frame analysis provides the results, which are in good agreement with the results of classical analysis. But, as technology advanced, approximate methods such as finite difference, finite strip or finite element method has been introduced to find out the structural responses of box girder bridges. Now a days, researchers are using finite element based software packages e.g. SAP2000, CSIBridge etc to reduce the analysis time.

An examination of research papers and codal provisions of various countries reveals that analysis of straight box girder bridge has enjoyed the focus of the researchers the most. Though some experimental as well as the analytical study has been carried out

by the researchers separately, very few research work is available for skew-curved box girder bridge. As Skew, Curved, Skew-curved box girder bridges are the solution for complicated urban interchange and to overpass any obstruction on an alignment with space constraint, response of these types of structures are to be investigated in future also to develop a guideline to design and construct these structures.

Chapter-4: Scope of the Present Study

4.0 General:

A study of the literatures that exists on research of concrete box girder bridge on different geometry, is presented in the last chapter with emphasis on the developments, that took place in the last thirty to forty years. With the knowledge collected from the literature review and keeping in view the voids in the volume of accumulated literature as indicated in the critical discussion, the actual scope of the present study is outlined in this chapter.

4.1 Present Scope:

From the discussion presented in Chapter-3, it has been seen that substantial research, both analytical and experimental, has been carried out to understand the structural behavior of curved and skewed box-girder bridges individually. But very little research has been carried out for skew-curved bridges. It has also been seen that the recommendation of national and international codes are also not enough to capture the structural response of skew, curved or skew-curved box girder bridge.

Concrete box girder sections are becoming popular due to their pleasing aesthetics and other functional advantages. As the webs of the box girders are connected by both the top slab (top flange) and soffit slab (bottom flange), the cross section allows to reduce the slab thickness and number of webs leading to less self weight and thus provides greater strength per unit area of concrete. The box girder sections are also torsionally stiff and thus capable of carrying eccentric live loads and also most suitable for skew, curved and skew-curved bridges. Less width requirement at soffit of the box girder bridge allows the infrastructure engineer more flexibility in planning urban infrastructure. Now a days, concrete box girder bridges are being extensively used in urban infrastructures (flyovers, via ducts and metros) and to overpass any obstacle (stream, infrastructure or pipe line), in certain stretches having space constraint, at rural area also.

From the literature review presented at Chapter-3, it may be concluded that in order to obtain the realistic response of skew, curved and skew curved bridges, a sophisticated analytical technique such as finite element method or finite element based software packages e.g. SAP 2000, CSI Bridge, Midas Civil should be used. These software packages are very useful for bridge girder analysis as these allow accommodating the complex geometry due to curvature and skewness and ensuring to obtain reasonably accurate response by capturing the interaction of all the structural actions along with the effect of curvature and skewness. Moreover, the analysis and design of skew-curved concrete box girder bridge is still not explicitly adopted by the design engineers and thus needs further investigations.

An analytical parametric study of concrete box girder bridge has been taken up under this thesis and formulation of the same has been presented in Chapter-5. SAP2000 software has been used to prepare and analyze the models of concrete box girder bridges. Determination of absolute maximum bending moment is required, in addition to other effects such as torsional moments and shear forces, for design of the bridges. The aim of this thesis is to determine the various structural responses e.g. moment shear, support reactions, torsions and deflections of straight, skewed, curved and skew-curved concrete box girder bridges caused by dead load and live loads(vehicular load) and to develop a parametric study thereby. The parametric study has been carried out for 30m and 35m span 12m wide concrete box girder bridge. Number of cell and bottom width has also been varied in addition to different skew angle and curvature to carry out the parametric study. The results are presented and discussed in detail and important conclusions are identified.

Chapter-5: Modeling and Analysis

5.0 General:

Based on the scope of the work, a concrete box girder bridge has been modeled using SAP 2000 software, which can effectively be utilized to determine the various structural responses and carry out the parametric study thereby under dead load and live load (vehicular load).

5.1 Concrete box girder modeling in SAP 2000:

The box girder model has been developed in SAP 2000 using the bridge wizard to enable three dimensional finite element analysis. Concrete box girder with vertical webs has been chosen form available bridge modules. The bridge layout line, cross sections, bearings, abutment properties, diaphragm properties has been modified/ assigned properly. The material has been used as M35 concrete. Bridge lanes are defined with respect to layout lines. Vehicular live loads has been selected from the SAP library and multiplied with proper impact factor.

Box girders are comprised of top slab, soffit slab and vertical girders considered as top flange, bottom flange and webs respectively. All together box girder sections are considered as thin walled member and thus discretized as area object model of maximum discretized span as 3.0m along deck and maximum sub-mesh size of 1.2m. The area object in SAP is basically a shell element capable to simulate membrane, plate or shell behavior in two/three dimensional structures. Depending upon complexities in geometry the number of discretized area element in a particular model has been varied from 132 to 780.

5.2 Shell Element in SAP 2000 in connection with bridge modeling:

The Shell element is a type of area object that is used to model membrane, plate, and shell behavior in planar and three-dimensional structures. The shell material may be homogeneous or layered through the thickness. Material nonlinearity can be considered

when using the layered shell. But, in present study homogenous shell has been considered.

The homogeneous shell combines independent membrane and plate behavior. These behaviors become coupled if the element is warped (non planar.) The membrane behavior uses an isoparametric formulation that includes translational in- plane stiffness components and a "drilling" rotational stiffness component in the direction normal to the plane of the element. In-plane displacements are quadratic. Plate-bending behavior includes two-way, out-of-plane, plate rotational stiffness components and a translational stiffness component in the direction normal to the plane of the element. We can choose a thin-plate (Kirchhoff) formulation that neglects transverse shearing deformation, or a thick-plate (Mindlin/Reissner) formulation which includes the effects of transverse shearing deformation. Out-of-plane displacements are cubic.

For each homogeneous Shell element in the structure, we can choose to model pure-membrane, pure-plate, or full-shell behavior. It is generally recommended to use the full shell behavior unless the entire structure is planar and is adequately restrained.

In present study, full shell behavior in combination with membrane and plate behavior has been used. Thin shell (Kirchoff) formulation has been used to neglect the transverse shear as the thickness to span ratio of flanges and the webs are near $1/10^{th}$.

A four-point numerical integration formulation is used for the Shell stiffness. Stresses and internal forces and moments, in the element local coordinate system, are evaluated at the 2-by-2 Gauss integration points and extrapolated to the joints of the element. An approximate error in the element stresses or internal forces can be estimated from the difference in values calculated from different elements attached to a common joint. This will give an indication of the accuracy of a given finite element approximation and can then be used as the basis for the selection of a new and more accurate finite element mesh.

Each Shell element may have either of the following shapes, as shown in Figure 9 and 10. Four noded quadrilateral element is defined as , defined by the four joints j1, j2, j3, and j4, whereas three noded triangular, defined by the three joints j1, j2, and j3.

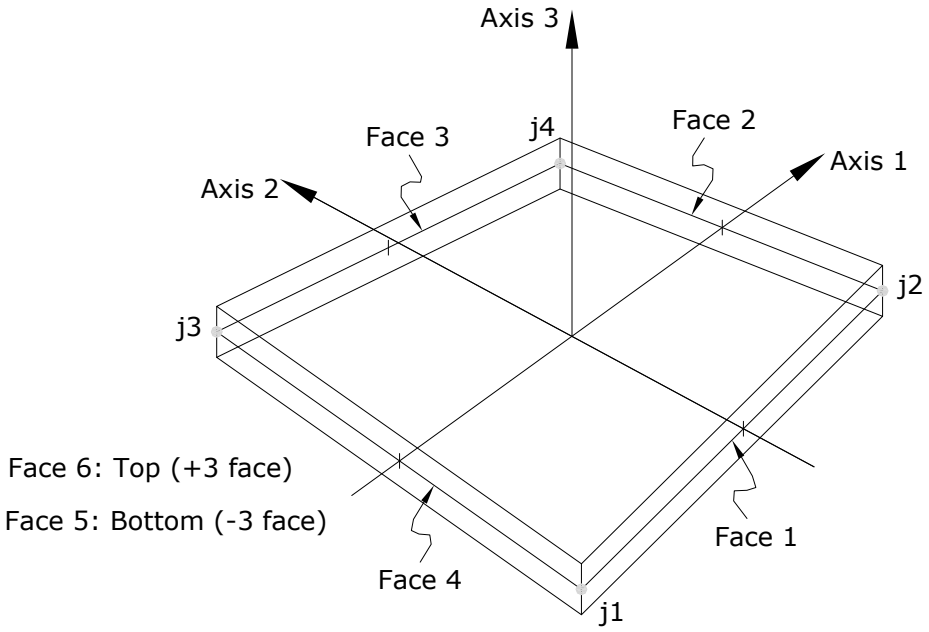

Figure 9: Four noded quadrilateral shell element

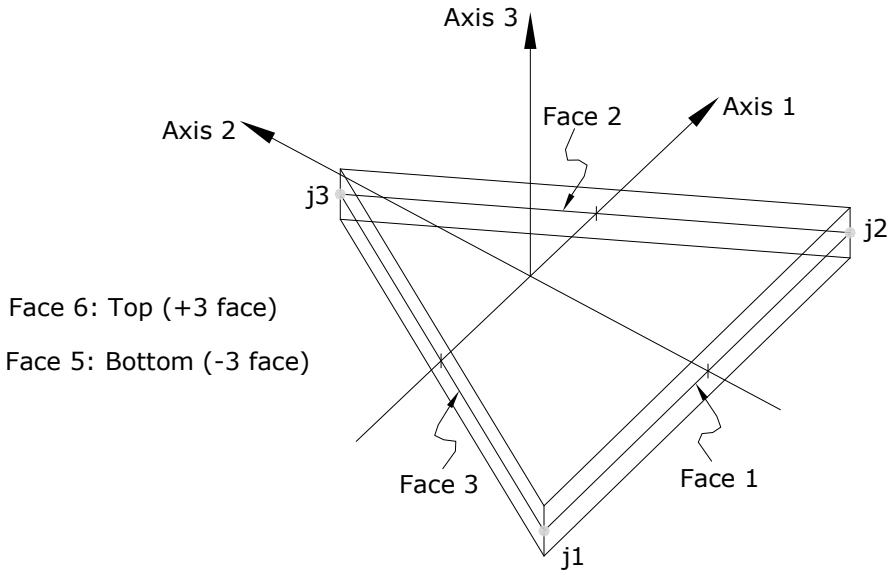

Figure 10: Three noded triangular shell element

The quadrilateral formulation is the more accurate of the two. The triangular element is only recommended for locations where the stresses do not change rapidly. The use of large triangular elements is not recommended where in-plane (membrane) bending is significant. In this study four noded element has been considered.

The Shell element always activates all six degrees of freedom at each of its connected joints. When the element is used as a pure membrane, it is to be ensured that restraints or other supports are provided to the degrees of freedom for normal translation and bending rotations. When the element is used as a pure plate, we must ensure that restraints or other supports are provided to the degrees of freedom for in-plane translations and the rotation about the normal. The use of the full shell behavior (membrane plus plate) is recommended for all three-dimensional structures.

Each Shell element has its own element local coordinate system used to define material properties, loads and output. The axes of this local system are denoted 1, 2 and 3. The first two axes lie in the plane of the element with a specified orientation; the third axis is normal. It is important to establish the definition of the element local 1-2-3 coordinate system and its relationship to the global X-Y-Z coordinate system to simplify data input and interpretation of results. Both systems are right-handed coordinate systems. The element local coordinate system can be defined using the default orientation and the Shell element coordinate angle in a simplest way.

Local axis 3 is always normal to the plane of the Shell element. This axis, as follows the right hand rule, is directed toward out of the plane when the path j1-j2-j3-j4 appears counterclockwise. For quadrilateral elements, the element plane is defined by the vectors that connect the midpoints of the two pairs of opposite sides.

The default orientation of the local 1 and 2 axes is determined by the relationship between the local 3 axis and the global Z axis:

- The local 3-2 plane is taken to be vertical, i.e., parallel to the Z axis.

- The local 2 axis is taken to have an upward (+Z) sense unless the element is horizontal, in which case the local 2 axis is taken along the global +Y direction.

- The local 1 axis is horizontal, i.e., it lies in the X-Y plane.

- The element is considered to be horizontal if the sine of the angle between the local axis and the Z axis is less than 10-3.

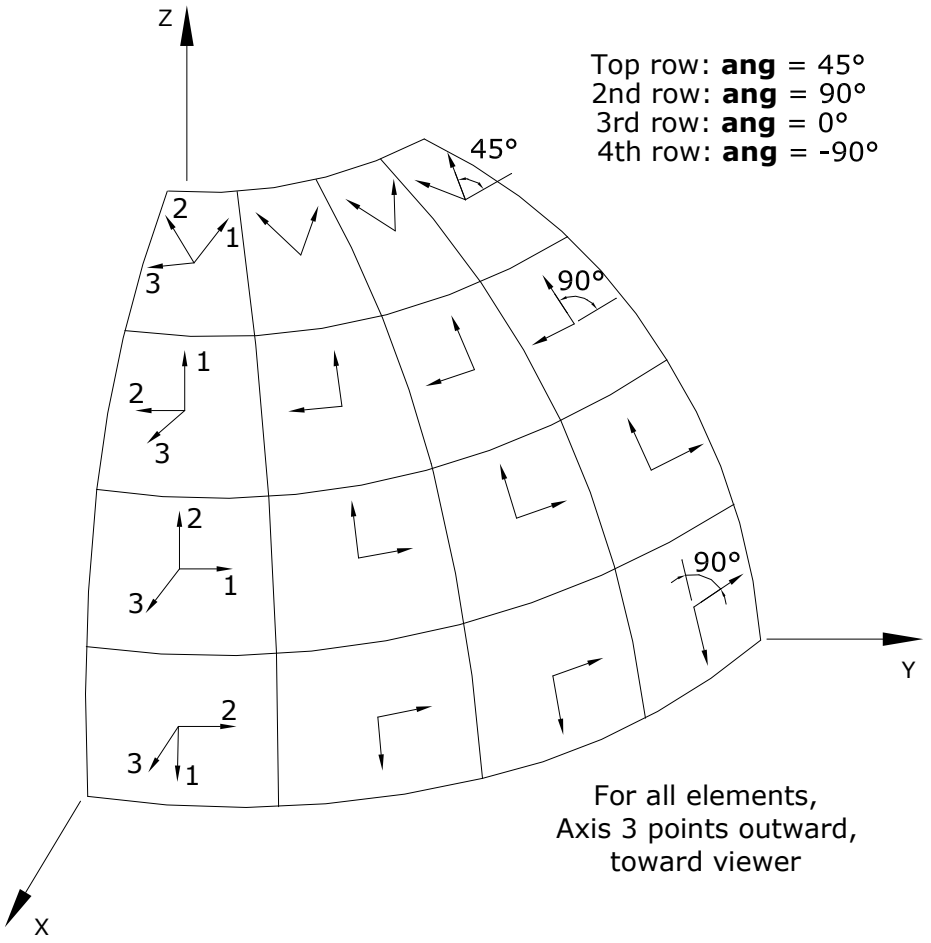

Figure 11: Area element coordinate angle with respect to default orientation

The Shell element coordinate angle, **ang**, is used to define element orientations that are different from the default orientation. It is the angle through which the local 1 and 2 axes are rotated about the positive local 3 axis from the default orientation. The rotation for a positive value of **ang** appears counterclockwise when the local+3 axis is

pointing toward viewer. For horizontal elements, **ang** is the angle between the local 2 axis and the horizontal +Y axis. Otherwise, **ang** is the angle between the local 2 axis and the vertical plane containing the local 3 axis. Figure 11may be referred.

The material properties for each Section are specified by reference to a previously defined Material. The material may be isotropic, uniaxial or orthotropic. The material properties used by the Shell Section are: the moduli of elasticity, e1, e2, and e3; the shear modulus, g12, g13, and g23; the Poisson's ratios, u12, u13, and u23; the coefficients of thermal expansion, a1 and a2; the mass density, m, for computing element mass and the weight density, w, for computing Self-Weight and Gravity Loads.

The properties e3, u13, and u23 are condensed out of the material matrix by assuming a state of plane stress in the element. The resulting, modified values of e1, e2, g12, and u12 are used to compute the membrane and plate-bending stiffness. The shear moduli, g13 and g23, are used to compute the transverse shearing stiffness if the thick-plate formulation is used. The coefficients of thermal expansion, a1 and a2, are used for membrane expansion and thermal bending strain.

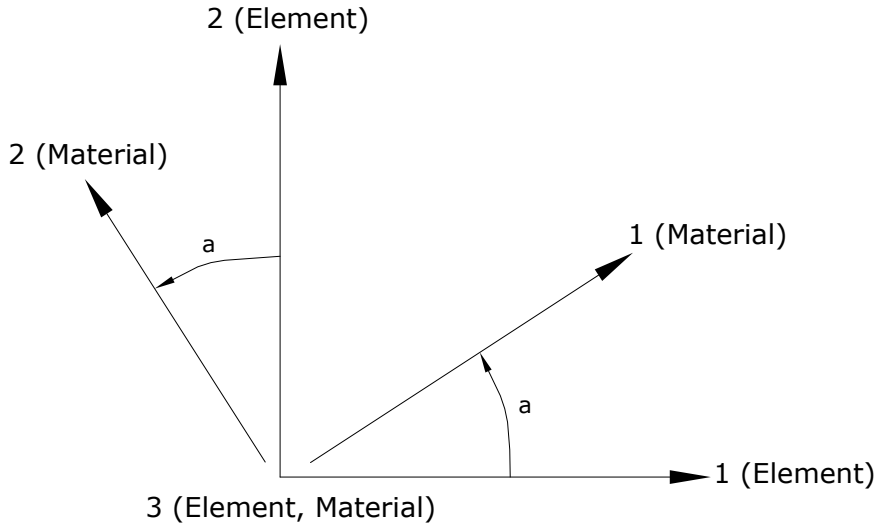

Figure 12: Shell section material angle

The material local coordinate system and the element (Shell Section) local coordinate system need not be the same. The local 3 directions always coincide for the

two systems, but the material 1 axis and the element 1 axis may differ by the angle a as shown in Figure 12. This angle has no effect for isotropic material properties since they are independent of orientation.

The Shell element internal forces (also called stress resultants) are the forces and moments that result from integrating the stresses over the element thickness. For a homogeneous shell, these internal forces and moments per unit in plane length are:

- Membrane direct forces:

$$F_{11} = \int_{-\frac{th}{2}}^{+\frac{th}{2}} \sigma_{11}\, dx_3 \qquad F_{22} = \int_{-\frac{th}{2}}^{+\frac{th}{2}} \sigma_{22}\, dx_3$$

- Membrane Shear force:

$$F_{12} = \int_{-\frac{th}{2}}^{+\frac{th}{2}} \sigma_{12}\, dx_3$$

- Plate bending moments:

$$M_{11} = \int_{-\frac{thb}{2}}^{+\frac{thb}{2}} x_3\sigma_{11}\, dx_3 \qquad M_{22} = \int_{-\frac{thb}{2}}^{+\frac{thb}{2}} x_3\sigma_{22}\, dx_3$$

- Plate twisting moments:

$$M_{12} = \int_{-\frac{thb}{2}}^{+\frac{thb}{2}} x_3\sigma_{12}\, dx_3$$

- Plate transverse shear fore:

$$V_{13} = \int_{-\frac{thb}{2}}^{+\frac{thb}{2}} \sigma_{13}\, dx_3 \qquad V_{23} = \int_{-\frac{thb}{2}}^{+\frac{thb}{2}} \sigma_{23}\, dx_3$$

Where x_3 represents the thickness coordinate measured from the mid-surface of the element, **th** is the membrane thickness, and **thb** is the plate-bending thickness.

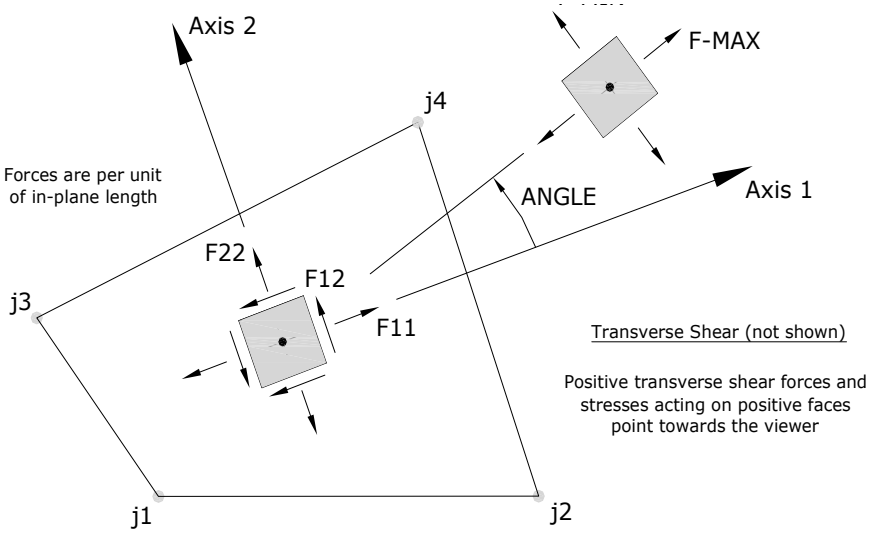

STRESSES AND MEMBRANE FORCES

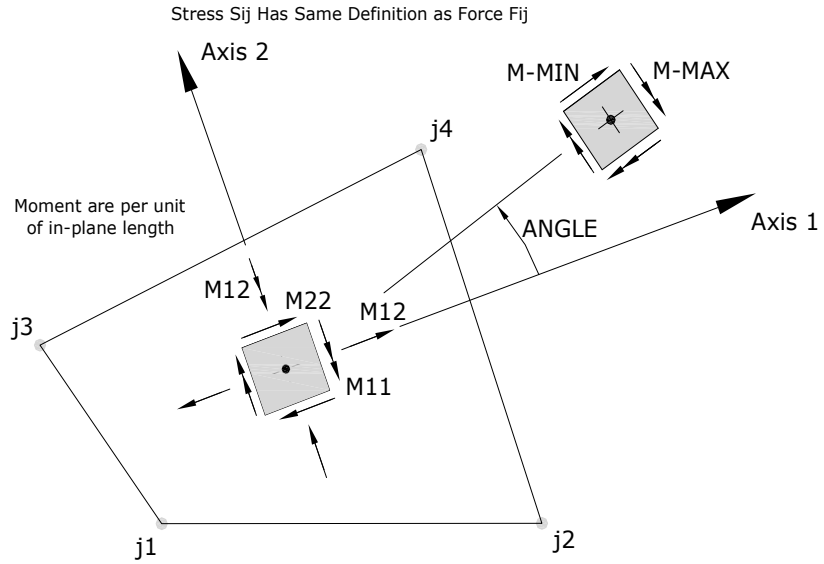

PLATE BENDING AND TWISTING MOMENTS

Figure 13: Shell element stress and internal forces and moments

The sign conventions for the stresses and internal forces are illustrated in Figure 13. Stresses acting on a positive face are oriented in the positive direction of the element local coordinate axes. Stresses acting on a negative face are oriented in the negative direction of the element local coordinate axes. A positive face is one whose outward normal (pointing away from element) is in the positive local 1 or 2 directions. Positive internal forces correspond to a state of positive stress that is constant through the thickness. Positive internal moments correspond to a state of stress that varies linearly through the thickness and is positive at the bottom. Thus for a homogeneous shell stresses are:

$$\sigma_{11} = \frac{F_{11}}{th} - \frac{12\,M_{11}}{thb^3}x_3 \qquad \sigma_{22} = \frac{F_{22}}{th} - \frac{12\,M_{22}}{thb^3}x_3$$

$$\sigma_{12} = \frac{F_{12}}{th} - \frac{12\,M_{12}}{thb^3}x_3 \qquad \sigma_{13} = \frac{V_{13}}{thb}$$

$$\sigma_{23} = \frac{V_{23}}{thb} \qquad \sigma_{33} = 0$$

The transverse shear stresses given here are average values. The actual shear stress distribution is parabolic, being zero at the top and bottom surfaces and taking a maximum or minimum value at the mid-surface of the element.

Principal values and the associated principal directions are available for Load Cases and Load Combinations that are single valued. The angle given is measured counterclockwise (when viewed from the top) from the local 1 axis to the direction of the maximum principal value.

5.3 Box girder cross section:

Simply supported concrete box girder bridge of 30m and 35m span has been modeled and analyzed. The roadway and carriageway width of the bridge has been kept as 9.5m and 10.5m respectively as per typical cross section of grade separated structure given in fig-7.11 of IRC:SP:73-2015. Four box girder sections have been considered: single

cell and double cell in combination with two types of soffit width 5m and 6m. Box girder sections are presented below:

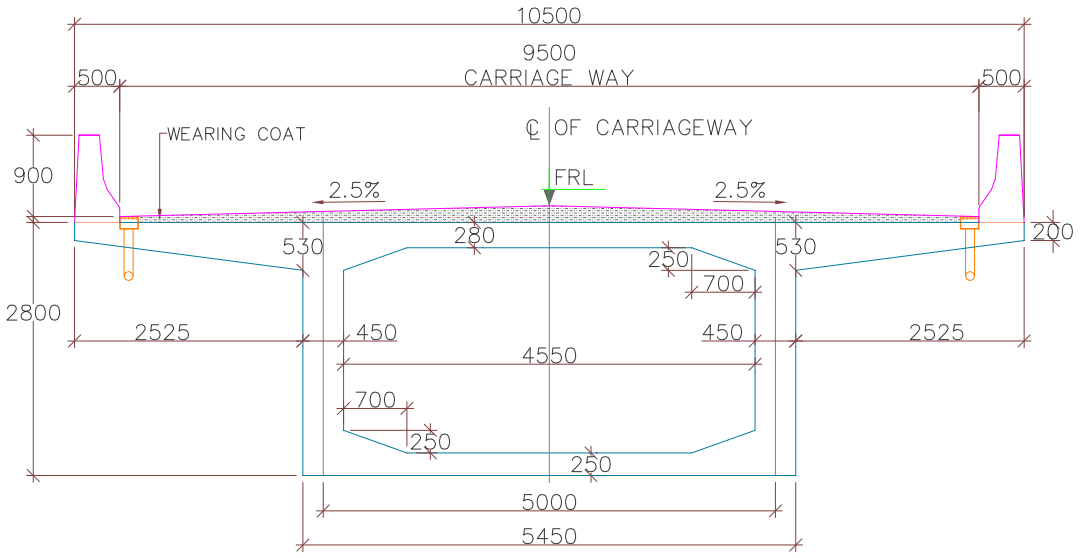

Figure 14: Cross section of box girder: Single cell, Soffit width 5.0m

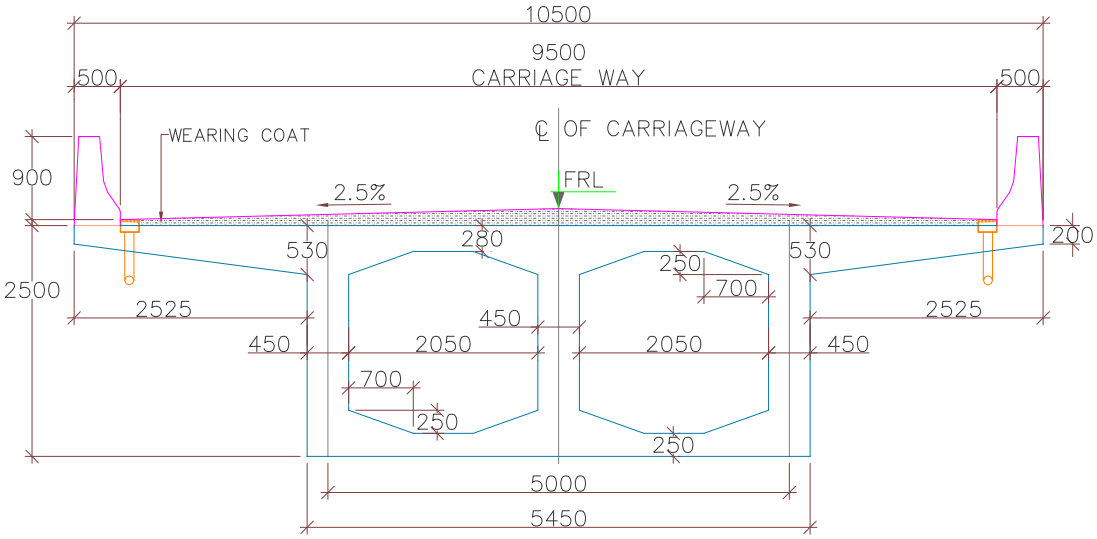

Figure 15: Cross section of box girder: Double cell, Soffit width 5.0m

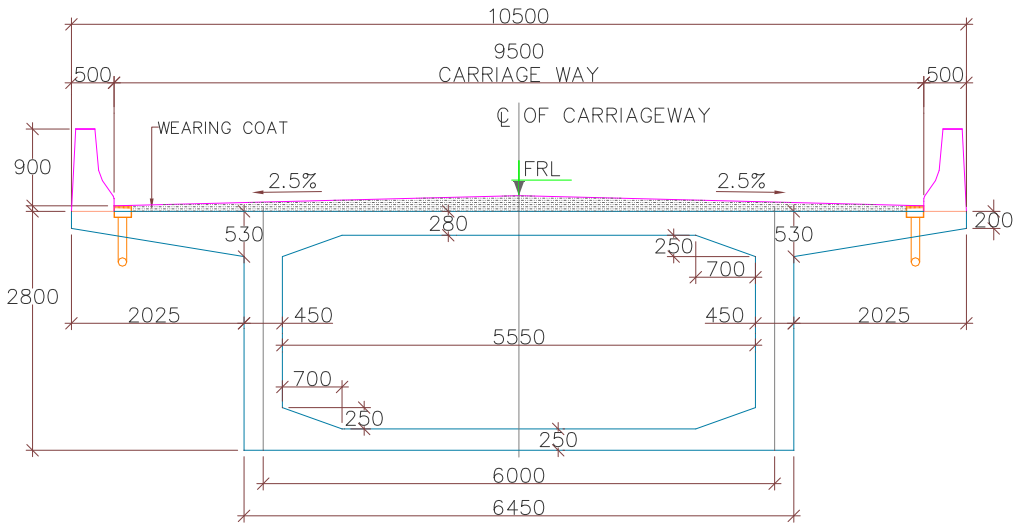

Figure 16: Cross section of box girder: Single cell, Soffit width 6.0m

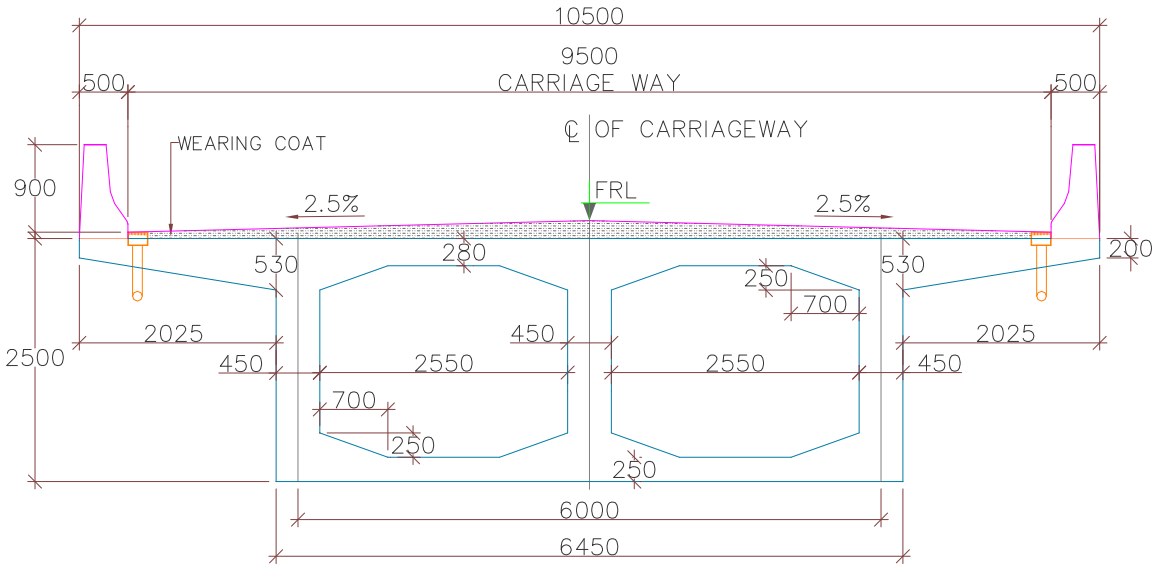

Figure 17: Cross section of box girder: Double cell, Soffit width 6.0m

A table with the cross sectional properties is presented below:

Table 1: Cross sectional properties of box girder

Soffit Width (m),(B)	Number of Cell (N)	Depth (m)	Area (m^2)	Y_b (m)	Y_t (m)	I_{xx}(m^4)	Z_b (m^3)	Z_t (m^3)
5	1	2.8	7.125	1.733	1.067	7.837	4.522	7.345
5	2	2.5	8.091	1.504	0.996	6.612	4.396	6.639
6	1	2.8	7.289	1.67	1.13	8.415	5.039	7.447
6	2	2.5	8.256	1.456	1.044	7.037	4.833	6.74

5.4 Parametric variation:

A set of four skew angles has been chosen from 0° to 45° with an interval of 15 ° (θ=0°, 15°, 30° and 45°) to study the skewness effect. Similarly, a set of four central angles from 0° to 36° with an interval of 12° (α=0°, 12°, 24° and 36°) has been chosen to study the curvature effect. Hence this parametric study includes four types of plan geometry variation: straight, skew, curved and skew-curved bridges. These four types of bridge models have been presented below.

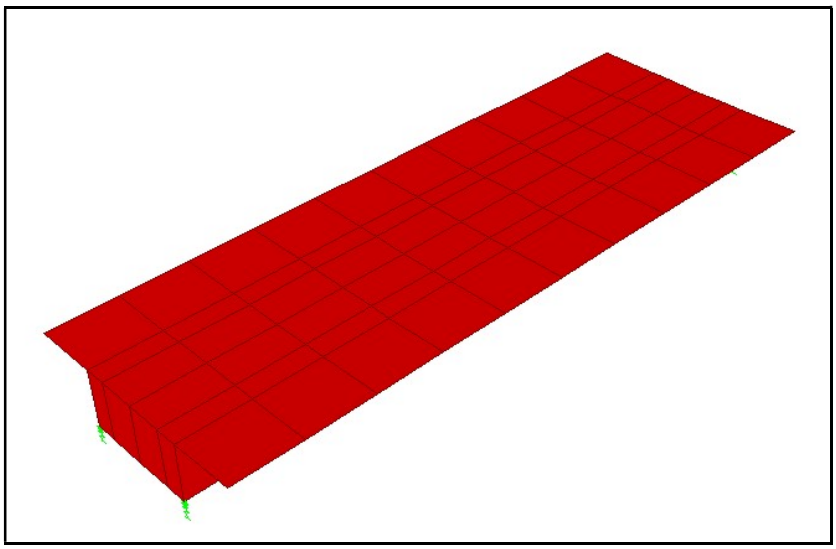

Figure 18: Straight bridge (θ=0°, α=0°)

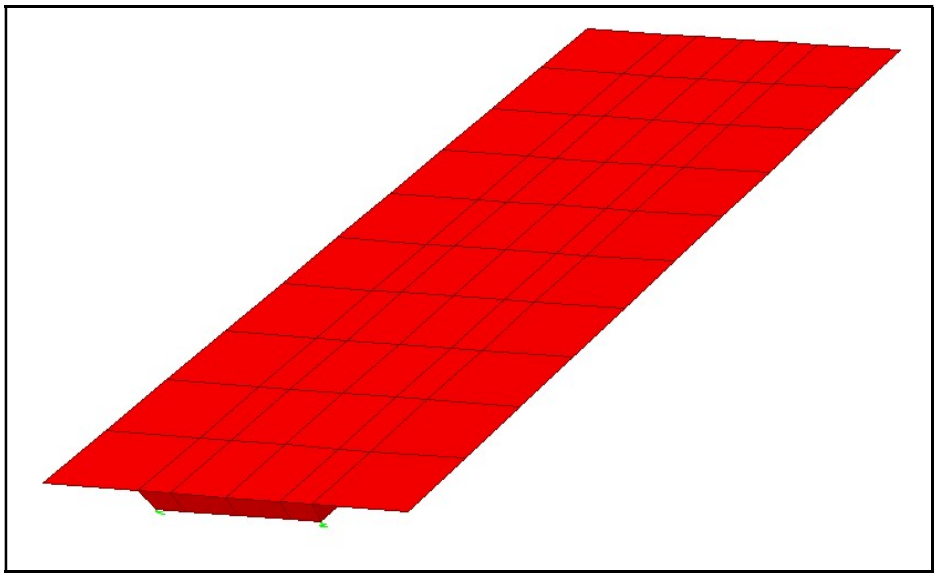

Figure 19: Skew bridge (θ=45°, α=0°)

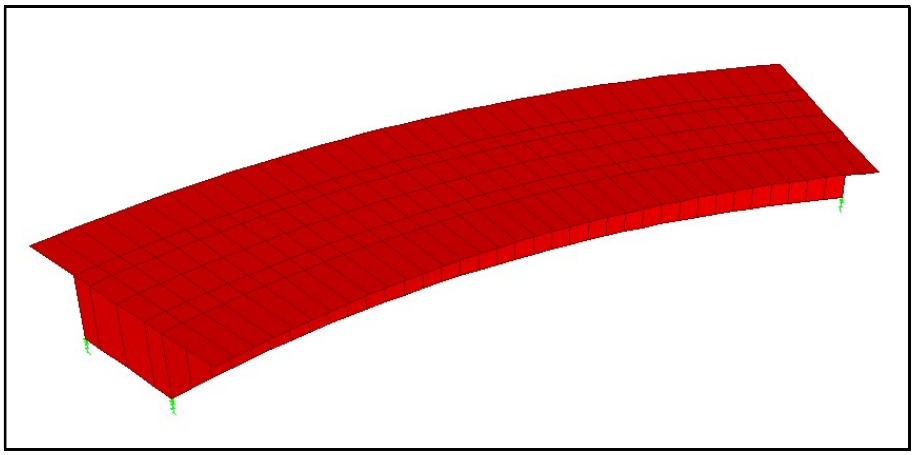

Figure 20: Curved bridge (θ=0°, α=36°)

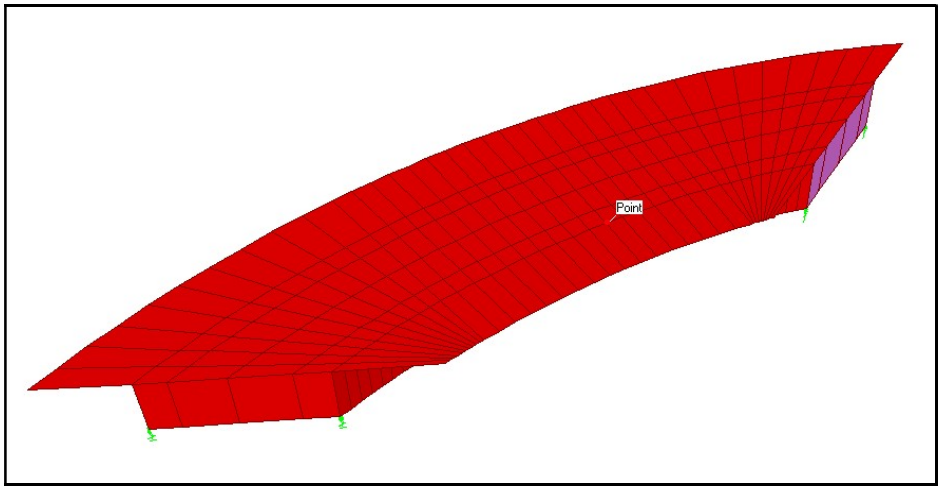

Figure 21: Skew-Curved bridge (θ=45°, α=36°)

A very important point to note here is, in case of skew-curved bridge the skewness of start abutment is θ=45° and the skewness of end abutment is θ=-45°.

Desired bridge responses (Bending moment, Torsion/Torsional Moment, Shear force, Joint Reactions and Deflection) and its variation have been studied for 30m span. A comparison also carried out for 35m span cross section with single cell and bottom width 5.0m.

5.5 Materials:

M35 concrete has been used for this analysis. The unit weight has been taken as 25kN/m^3. Elasticity modulus, Possion's ration and compressive strength have been taken as 29580 MPa, 0.2 and 35 MPa respectively.

5.6 Loads:

These box girder bridge models have been analyzed for dead loads and vehicular live loads. One type of vehicular live load has been considered in this analysis. As the carriageway width has been restricted to 9.5m, Class 70R wheeled single lane (Outer lane for curved/skew-curved bridge models) has been considered as per Table-6 of IRC-6:2017. Appropriate impact factor (1.100 for Class 70R) has been taken into account as per cl-208 of IRC-6:2017. The details of IRC Class 70R wheeled are presented below. The loads are in "ton" and the axle distances are in "m".

IRC Class 70R Wheeled Vehicle: IRC Class 70R wheeled vehicle weighs 100 ton. The longitudinal and transverse arrangement has been shown in figure 24 and 25. Class 70R wheeled vehicle has been placed on only one lane-Specifically on outer lane for curved bridges.

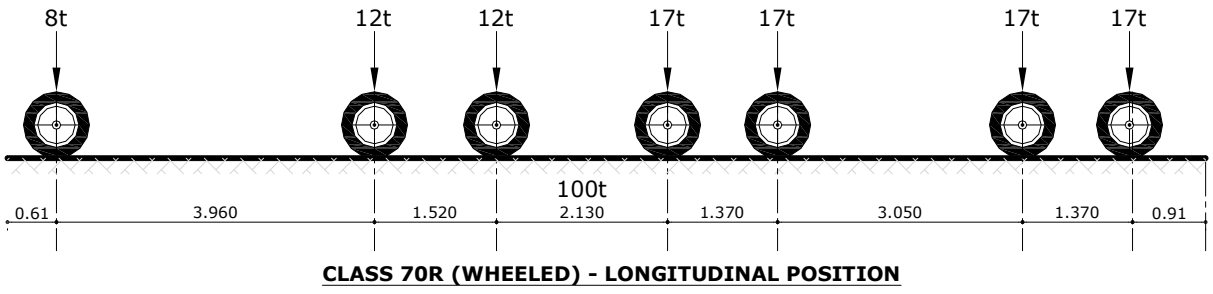

Figure 22: IRC Class 70R Wheeled-Longitudinal arrangement

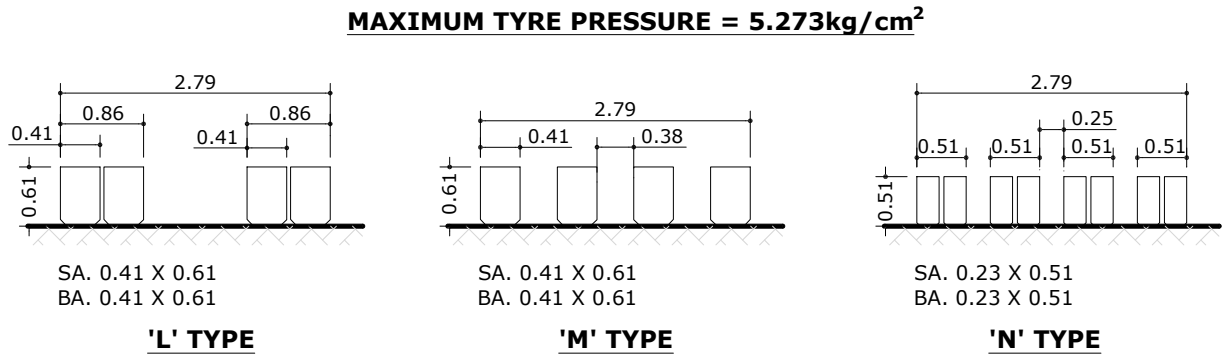

Figure 23: IRC Class 70R Wheeled-Transverse arrangement

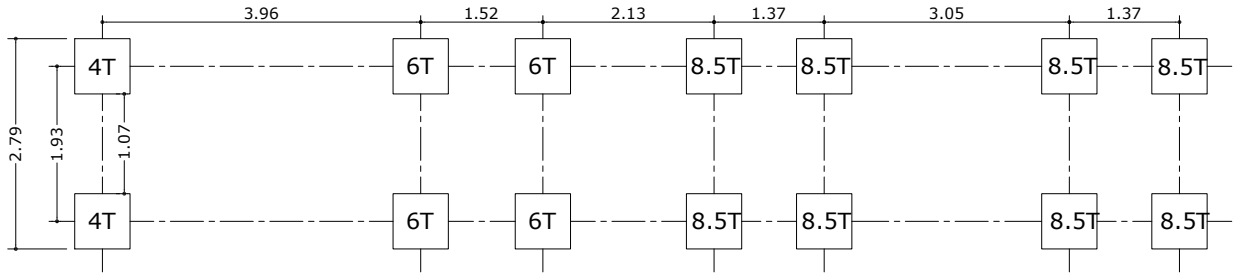

Figure 24: IRC Class 70R Wheeled load in Plan

Response or response envelops (limit of maximum and minimum response) for bending moment, hear force, torsion, deflection and bearing reaction due to dead load and vehicular live load has been obtained and compared.

5.7 Development of bridge models:

Considering different cross sections and the parametric variation, as stated above (paragraph 5.3 and 5.4 respectively), total 80 number models has been prepared to capture the variation of structural response in a simply supported 30m and 35m span concrete box girder bridge. The list of models is presented in the following table.

Table 2: Bridge models for 30m span

Sl No	Model ID	Span length (L) (m)	Radius (R) (m)	Central Angle (α°)	Skew Angle (θ°)	Bottom Width, (B) (m)	Number of Cell (N)	Cross sectional Area (m^2)
1	M-L30C0S0B5N1	30	infinity	0	0	5	1	7.125
2	M-L30C0S0B5N2	30	infinity	0	0	5	2	8.091

Sl No	Model ID	Span length (L) (m)	Radius (R) (m)	Central Angle (α°)	Skew Angle (θ°)	Bottom Width, (B) (m)	Number of Cell (N)	Cross sectional Area (m^2)
3	M-L30C0S0B6N1	30	infinity	0	0	6	1	7.289
4	M-L30C0S0B6N2	30	infinity	0	0	6	2	8.256
5	M-L30C0S15B5N1	30	infinity	0	15	5	1	7.125
6	M-L30C0S15B5N2	30	infinity	0	15	5	2	8.091
7	M-L30C0S15B6N1	30	infinity	0	15	6	1	7.289
8	M-L30C0S15B6N2	30	infinity	0	15	6	2	8.256
9	M-L30C0S30B5N1	30	infinity	0	30	5	1	7.125
10	M-L30C0S30B5N2	30	infinity	0	30	5	2	8.091
11	M-L30C0S30B6N1	30	infinity	0	30	6	1	7.289
12	M-L30C0S30B6N2	30	infinity	0	30	6	2	8.256
13	M-L30C0S45B5N1	30	infinity	0	45	5	1	7.125
14	M-L30C0S45B5N2	30	infinity	0	45	5	2	8.091
15	M-L30C0S45B6N1	30	infinity	0	45	6	1	7.289
16	M-L30C0S45B6N2	30	infinity	0	45	6	2	8.256
17	M-L30C12S0B5N1	30	143	12	0	5	1	7.125
18	M-L30C12S0B5N2	30	143	12	0	5	2	8.091
19	M-L30C12S0B6N1	30	143	12	0	6	1	7.289
20	M-L30C12S0B6N2	30	143	12	0	6	2	8.256
21	M-L30C12S15B5N1	30	143	12	15	5	1	7.125
22	M-L30C12S15B5N2	30	143	12	15	5	2	8.091
23	M-L30C12S15B6N1	30	143	12	15	6	1	7.289
24	M-L30C12S15B6N2	30	143	12	15	6	2	8.256
25	M-L30C12S30B5N1	30	143	12	30	5	1	7.125
26	M-L30C12S30B5N2	30	143	12	30	5	2	8.091
27	M-L30C12S30B6N1	30	143	12	30	6	1	7.289
28	M-L30C12S30B6N2	30	143	12	30	6	2	8.256
29	M-L30C12S45B5N1	30	143	12	45	5	1	7.125
30	M-L30C12S45B5N2	30	143	12	45	5	2	8.091
31	M-L30C12S45B6N1	30	143	12	45	6	1	7.289
32	M-L30C12S45B6N2	30	143	12	45	6	2	8.256
33	M-L30C24S0B5N1	30	72	24	0	5	1	7.125

Sl No	Model ID	Span length (L) (m)	Radius (R) (m)	Central Angle (α°)	Skew Angle (θ°)	Bottom Width, (B) (m)	Number of Cell (N)	Cross sectional Area (m^2)
34	M-L30C24S0B5N2	30	72	24	0	5	2	8.091
35	M-L30C24S0B6N1	30	72	24	0	6	1	7.289
36	M-L30C24S0B6N2	30	72	24	0	6	2	8.256
37	M-L30C24S15B5N1	30	72	24	15	5	1	7.125
38	M-L30C24S15B5N2	30	72	24	15	5	2	8.091
39	M-L30C24S15B6N1	30	72	24	15	6	1	7.289
40	M-L30C24S15B6N2	30	72	24	15	6	2	8.256
41	M-L30C24S30B5N1	30	72	24	30	5	1	7.125
42	M-L30C24S30B5N2	30	72	24	30	5	2	8.091
43	M-L30C24S30B6N1	30	72	24	30	6	1	7.289
44	M-L30C24S30B6N2	30	72	24	30	6	2	8.256
45	M-L30C24S45B5N1	30	72	24	45	5	1	7.125
46	M-L30C24S45B5N2	30	72	24	45	5	2	8.091
47	M-L30C24S45B6N1	30	72	24	45	6	1	7.289
48	M-L30C24S45B6N2	30	72	24	45	6	2	8.256
49	M-L30C36S0B5N1	30	48	36	0	5	1	7.125
50	M-L30C36S0B5N2	30	48	36	0	5	2	8.091
51	M-L30C36S0B6N1	30	48	36	0	6	1	7.289
52	M-L30C36S0B6N2	30	48	36	0	6	2	8.256
53	M-L30C36S15B5N1	30	48	36	15	5	1	7.125
54	M-L30C36S15B5N2	30	48	36	15	5	2	8.091
55	M-L30C36S15B6N1	30	48	36	15	6	1	7.289
56	M-L30C36S15B6N2	30	48	36	15	6	2	8.256
57	M-L30C36S30B5N1	30	48	36	30	5	1	7.125
58	M-L30C36S30B5N2	30	48	36	30	5	2	8.091
59	M-L30C36S30B6N1	30	48	36	30	6	1	7.289
60	M-L30C36S30B6N2	30	48	36	30	6	2	8.256
61	M-L30C36S45B5N1	30	48	36	45	5	1	7.125
62	M-L30C36S45B5N2	30	48	36	45	5	2	8.091
63	M-L30C36S45B6N1	30	48	36	45	6	1	7.289
64	M-L30C36S45B6N2	30	48	36	45	6	2	8.256

Sl No	Model ID	Span length (L) (m)	Radius (R) (m)	Central Angle (α°)	Skew Angle (θ°)	Bottom Width, (B) (m)	Number of Cell (N)	Cross sectional Area (m^2)
65	M-L35C0S0B5N1	35	infinity	0	0	5	1	7.125
66	M-L35C0S15B5N1	35	infinity	0	15	5	1	7.125
67	M-L35C0S30B5N1	35	infinity	0	30	5	1	7.125
68	M-L35C0S45B5N1	35	infinity	0	45	5	1	7.125
69	M-L35C12S0B5N1	35	167	12	0	5	1	7.125
70	M-L35C12S15B5N1	35	167	12	15	5	1	7.125
71	M-L35C12S30B5N1	35	167	12	30	5	1	7.125
72	M-L35C12S45B5N1	35	167	12	45	5	1	7.125
73	M-L35C24S0B5N1	35	84	24	0	5	1	7.125
74	M-L35C24S15B5N1	35	84	24	15	5	1	7.125
75	M-L35C24S30B5N1	35	84	24	30	5	1	7.125
76	M-L35C24S45B5N1	35	84	24	45	5	1	7.125
77	M-L35C36S0B5N1	35	56	36	0	5	1	7.125
78	M-L35C36S15B5N1	35	56	36	15	5	1	7.125
79	M-L35C36S30B5N1	35	56	36	30	5	1	7.125
80	M-L35C36S45B5N1	35	56	36	45	5	1	7.125

In the above list, following variables are used:

M: Bridge Model

L: Length of the bridge

C: Curvature, given by central angle in degrees

S: Skewness, given by skew angle in degrees

B: Soffit width, to introduce the aspect ratio parameter.

N: Number of cell.

Various bridge responses e.g. Bending moment, Shear force, Torsional Moment, deflection and bearing force (joint reaction) has been studied. Effect of parametric variation, e.g. skewness, curvature, aspect ratio and number of cell, on bridge responses will also be studied.

Chapter-6: Results and Discussions

6.0 General:

As stated in the previous chapter, an exhaustive 3D finite element based study for simply supported concrete box girder bridge has been carried out with SAP 2000 software. The objective is to find out the effect of curvature and skewness on various bridge responses. The bridge responses are studied for bridge object as a whole. For easy interpretation, models has been divided into four groups B5N1, B5N2, B6N1 and B6N2, where **B** stands for base width and **N** stands for number of cell. The results are presented below.

6.1 Effect of curvature and skewness:-Dead Load:

The effect on various bridge responses, i.e. bending moment diagram and absolute bending moment, torsional moment and its absolute value, shear force and its absolute value and joint reaction/bearing forces, for dead load due to curvature and skewness is studied and described below.

6.1.1 Effect on Bending Moment:

The basic bridge response, on which bridge engineers are interested, is the bending moment. The curvature and skewness in a box girder bridge not only affects the absolute value of bending moment but also the bending moment pattern. Effect on both the bending moment diagram and absolute bending moment due to curvature and skewness is presented below.

6.1.1.1 Variation of Bending Moment diagram due to skewness:

Effect on bending moment diagram for variation in skewness has been plotted and explained graphically for all the four groups as described above.

B5N1:

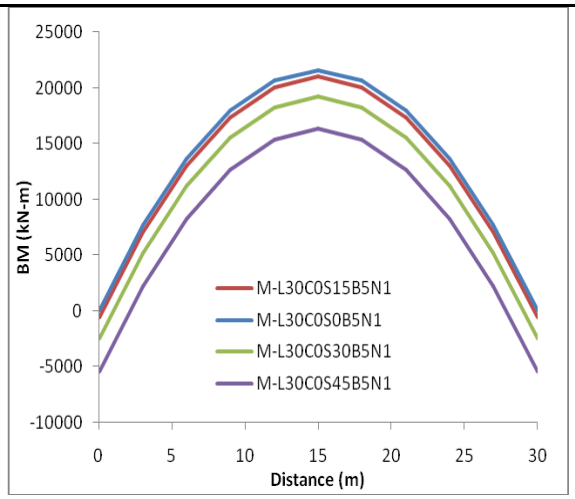

Plot- 1:B=5; N=1; α=0°

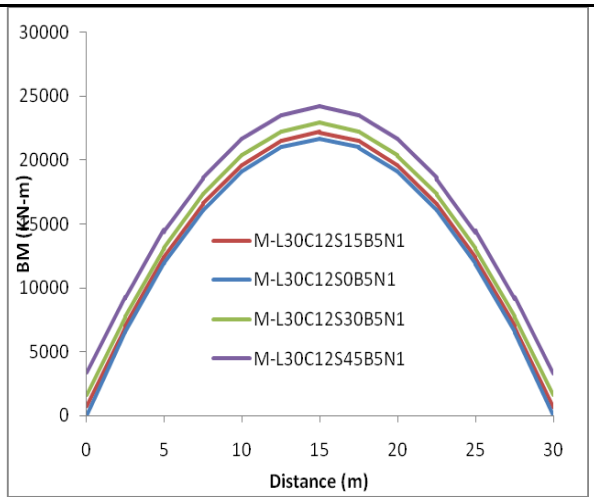

Plot- 2:B=5; N=1; α =12°

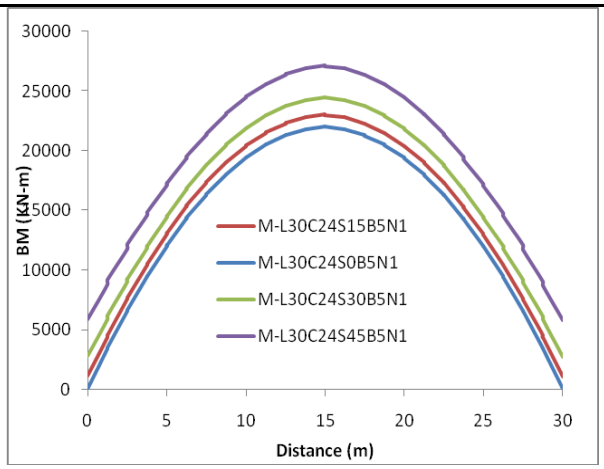

Plot- 3:B=5; N=1; α =24°

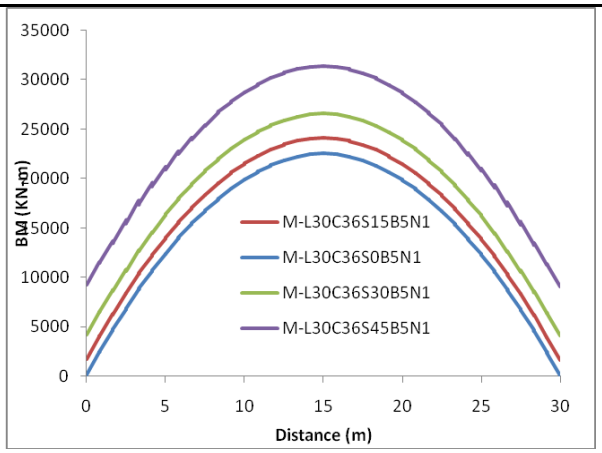

Plot- 4:B=5; N=1; α=36°

Discussion: The BM pattern remains almost same. The BM value (upto 24%) decreses with increase in skewness when the curvature is zero and hogging moment also increases with skewness. When curvature is introduced, the value of BM increases gradually with skewness . For α=36°, the BM value increases upto 39% .

B5N2:

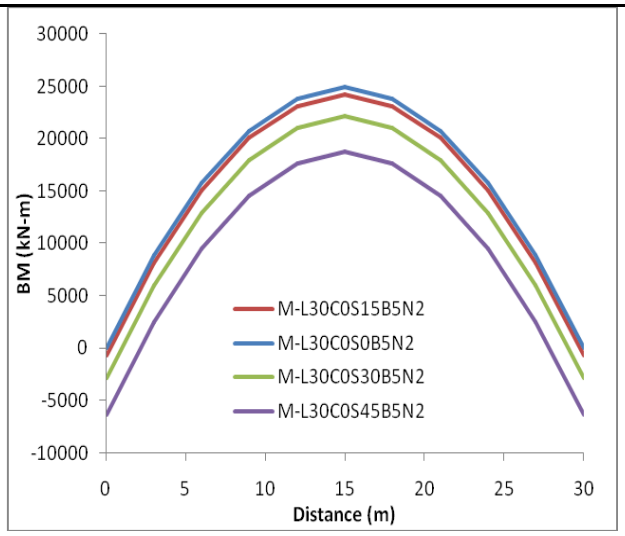

Plot- 5:B=5; N=2; α=0°

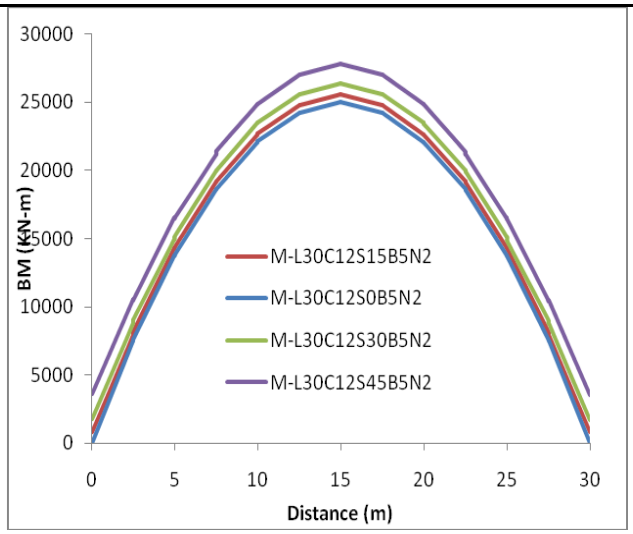

Plot- 6:B=5; N=2; α =12°

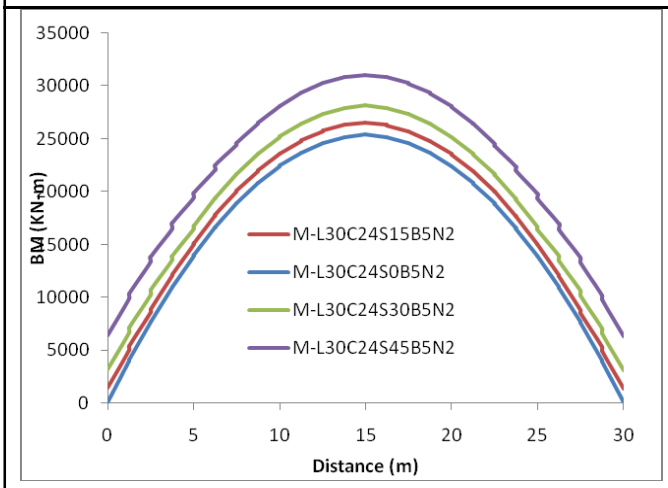

Plot- 7:B=5; N=2; α =24°

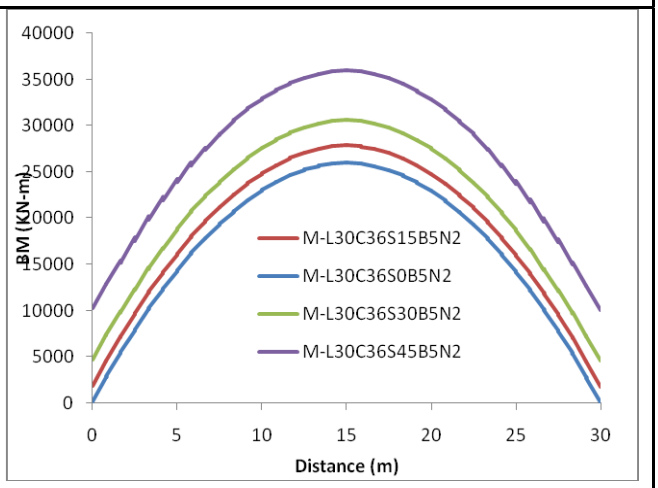

Plot- 8:B=5; N=2; α=36°

Discussion: The BM pattern remains almost same. The BM value (upto 25%) decreses with increase in skewness when the curvature is zero and hogging moment also increases with skewness. When curvature is introduced, the value of BM increases gradually with skewness . For α=36°, the BM value increases upto 38% .

B6N1:

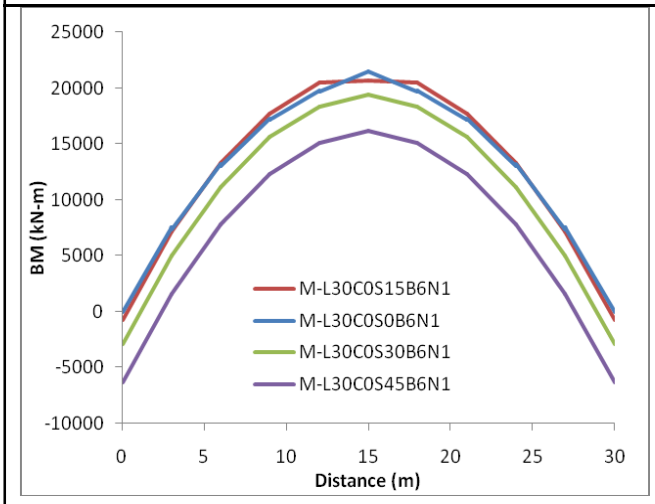

Plot- 9:B=6; N=1; α=0°

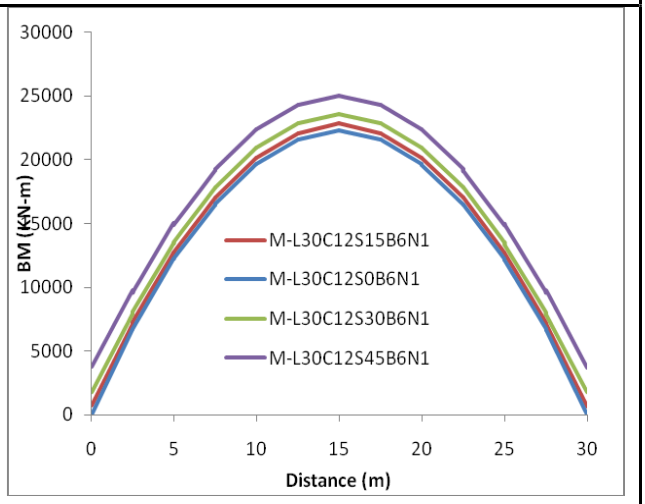

Plot- 10:B=6; N=1; α =12°

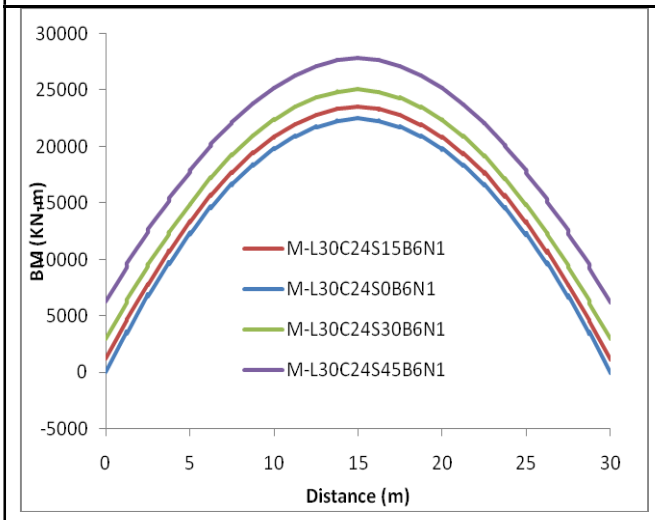

Plot- 11:B=6; N=1; α =24°

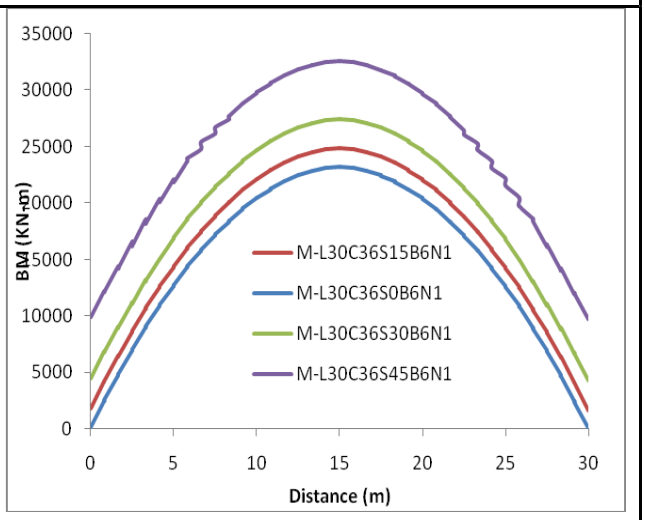

Plot- 12:B=5; N=1; α=36°

Discussion: The BM pattern remains almost same. The BM value (upto 25%) decreses with increase in skewness when the curvature is zero and hogging moment also increases with skewness. When curvature is introduced, the value of BM increases gradually with skewness . For α=36°, the BM value increases upto 40% .

B6N2:

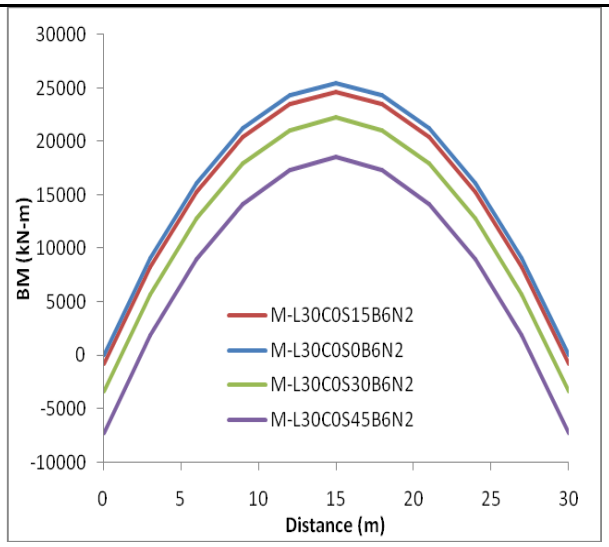

Plot- 13:B=6; N=2; α=0°

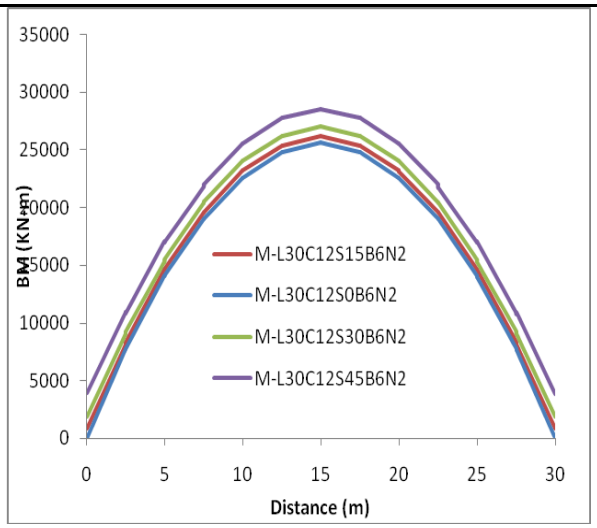

Plot- 14:B=6; N=2; α =12°

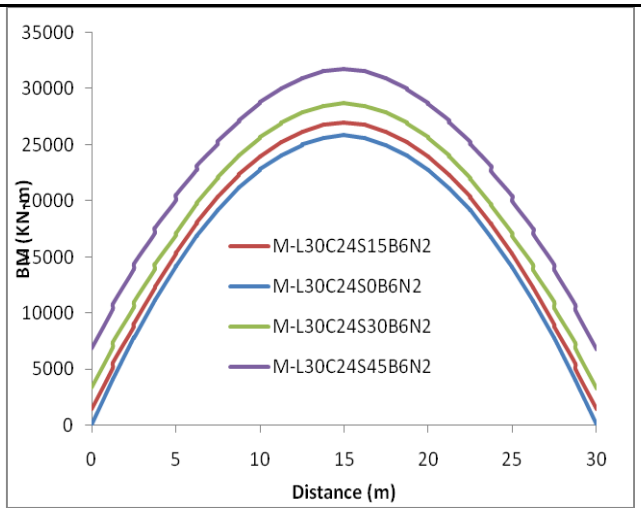

Plot- 15:B=6; N=2; α =24°

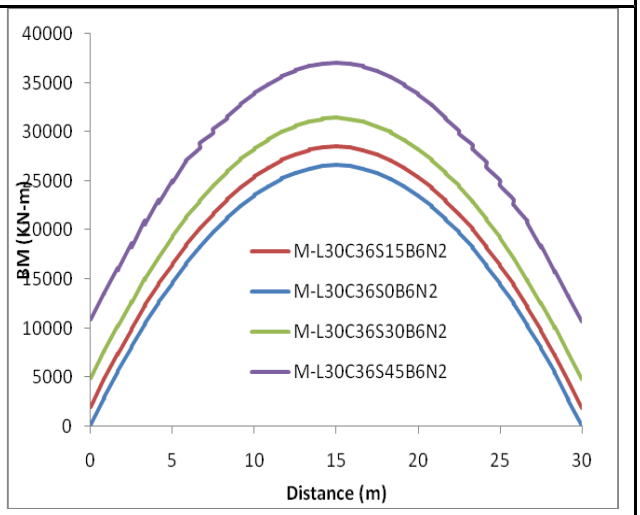

Plot- 16:B=6; N=2; α=36°

Discussion: The BM pattern remains almost same. The BM value (upto 27%) decreses with increase in skewness when the curvature is zero and hogging moment also increases with skewness. When curvature is introduced, the value of BM increases gradually with skewness . For α=36°, the BM value increases upto 39% .

6.1.1.2 Variation of Bending Moment diagram due to Curvature:

Effect on bending moment diagram for variation in curvature has been plotted and explained graphically for all the four groups as described above.

B5N1:

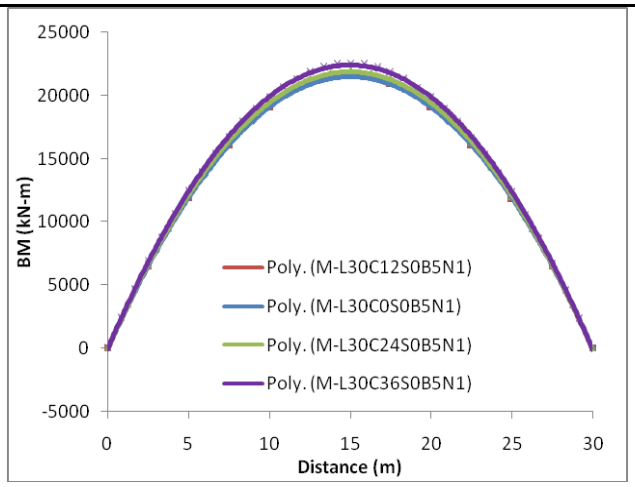

Plot- 17:B=5; N=1; θ=0°

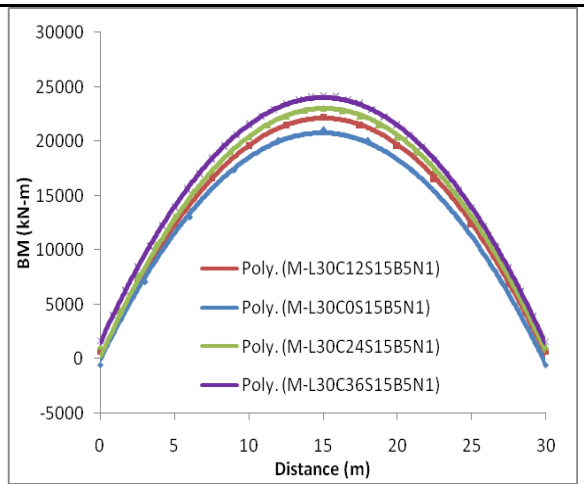

Plot- 18:B=5; N=1; θ =15°

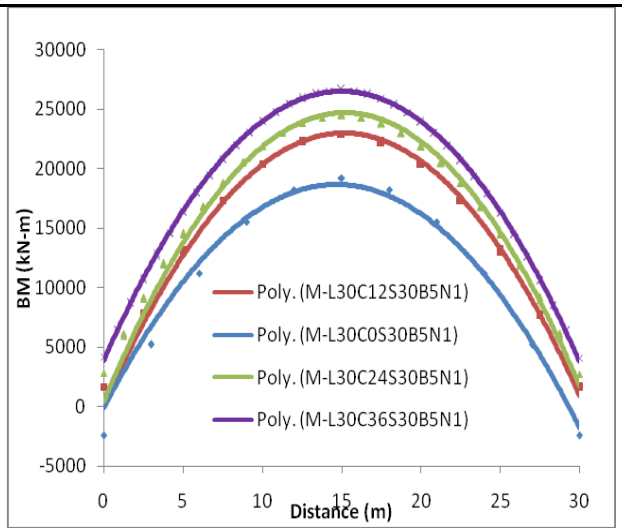

Plot- 19:B=5; N=1; θ =30°

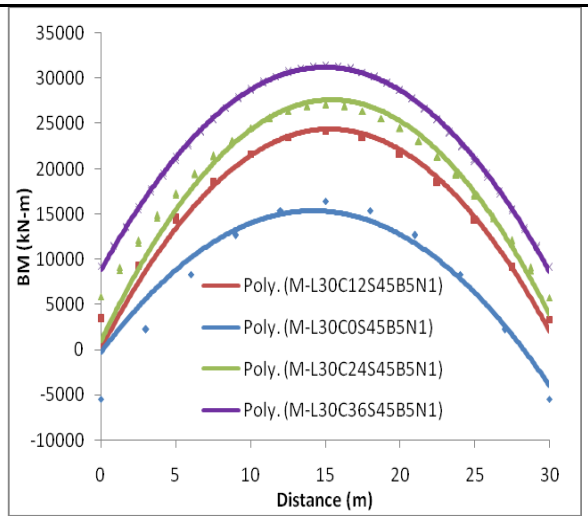

Plot- 20:B=5; N=1; θ=45°

Discussion: The BM pattern remains almost same. The BM value increases with increase in curvature. This increment is very minimum, 5%, when the skewness is zero. When skewness is introduced, the value of BM increases with curvature rapidly. For θ=45°, the BM increases upto 92% with curvature.

B5N2:

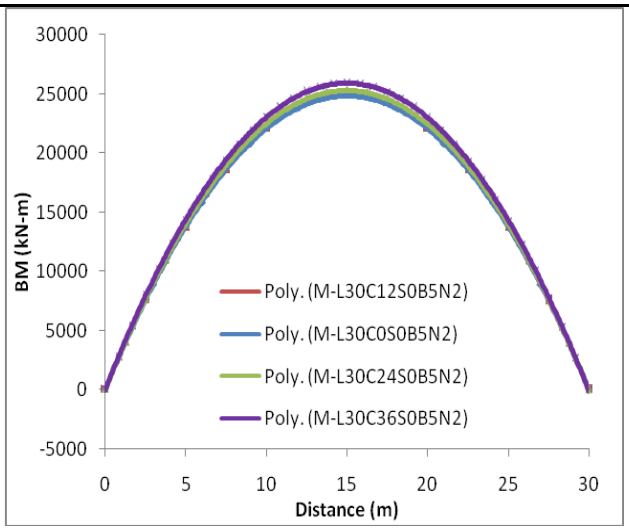

Plot- 21:B=5; N=2; θ=0°

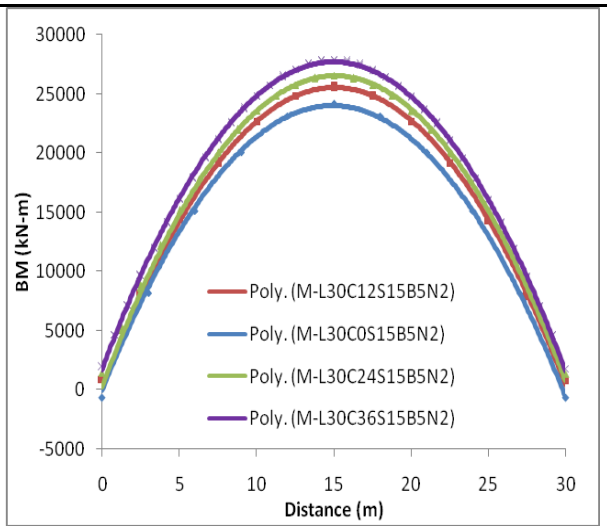

Plot- 22:B=5; N=2; θ =15°

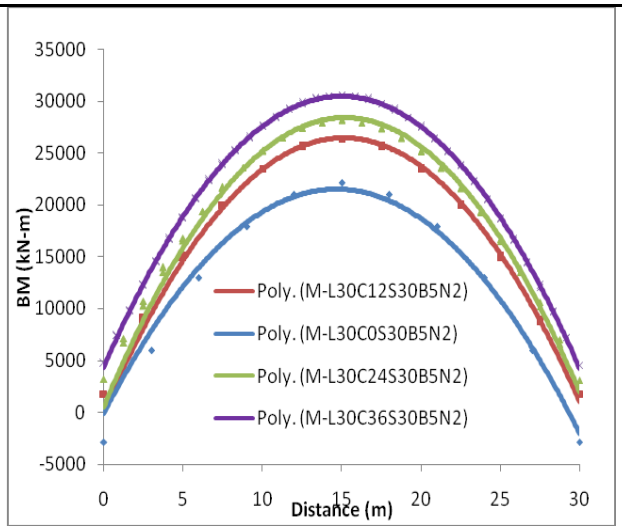

Plot- 23:B=5; N=2; θ =30°

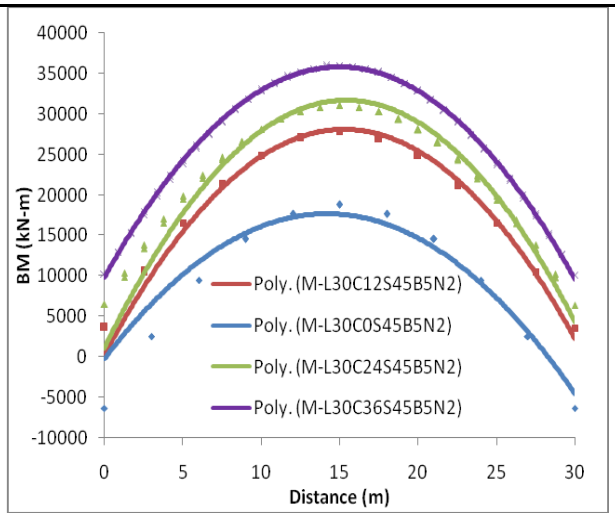

Plot- 24:B=5; N=2; θ=45°

Discussion: The BM pattern remains almost same. The BM value increases with increase in curvature. This increment is very minimum, 5%, when the skewness is zero. When skewness is introduced, the value of BM increases with curvature rapidly. For θ=45°, the BM increases upto 92% with curvature.

B6N1:

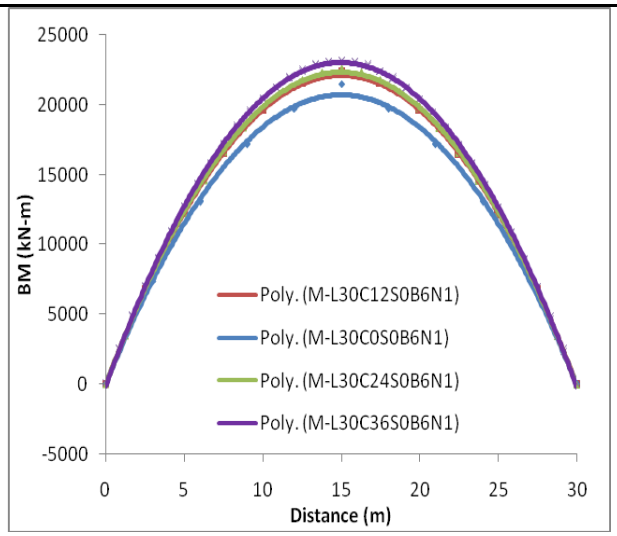

Plot- 25:B=6; N=1; θ=0°

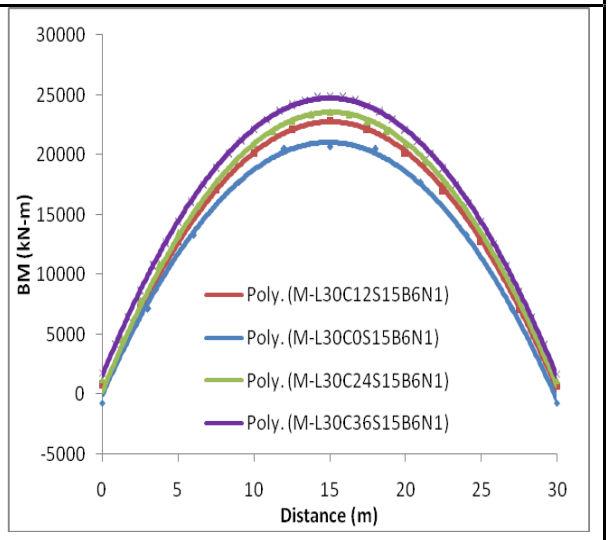

Plot- 26:B=6; N=1; θ =15°

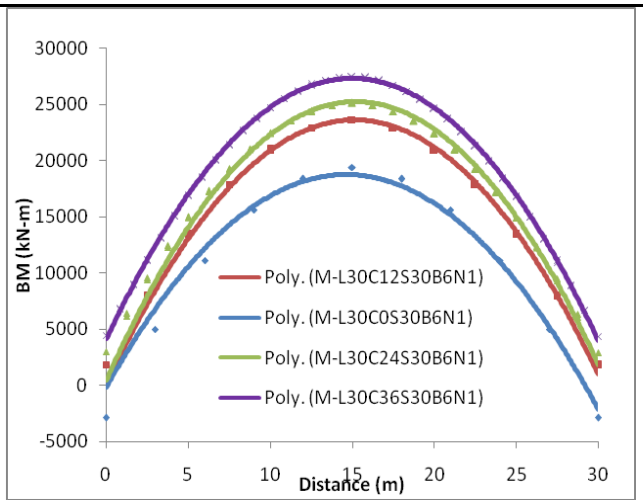

Plot- 27:B=6; N=1; θ =30°

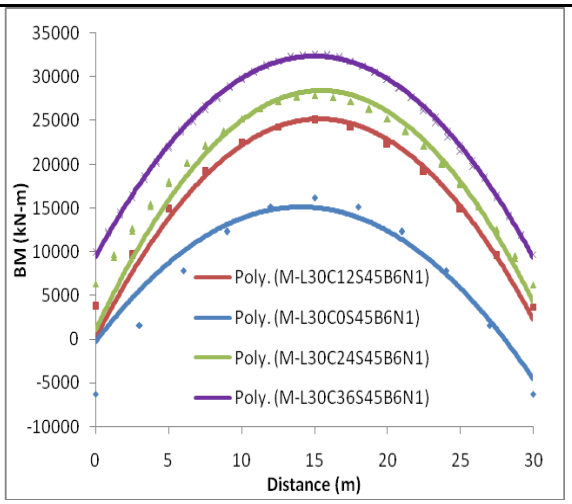

Plot- 28:B=6; N=1; θ=45°

Discussion: The BM pattern remains almost same. The BM value increases with increase in curvature. This increment is very minimum, 8%, when the skewness is zero. When skewness is introduced, the value of BM increases with curvature rapidly. For θ=45°, the BM increases upto 101% with curvature.

B6N2:

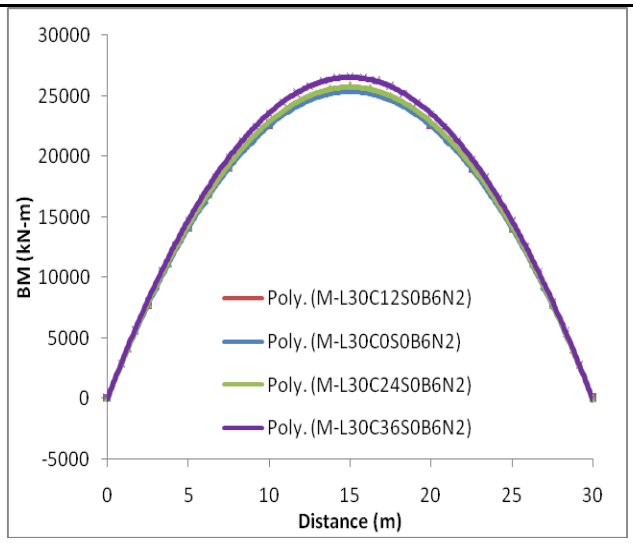

Plot- 29:B=6; N=2; θ=0°

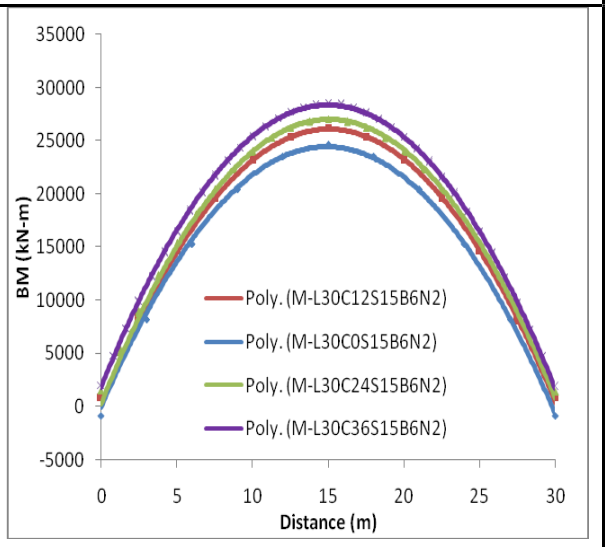

Plot- 30:B=6; N=2; θ =15°

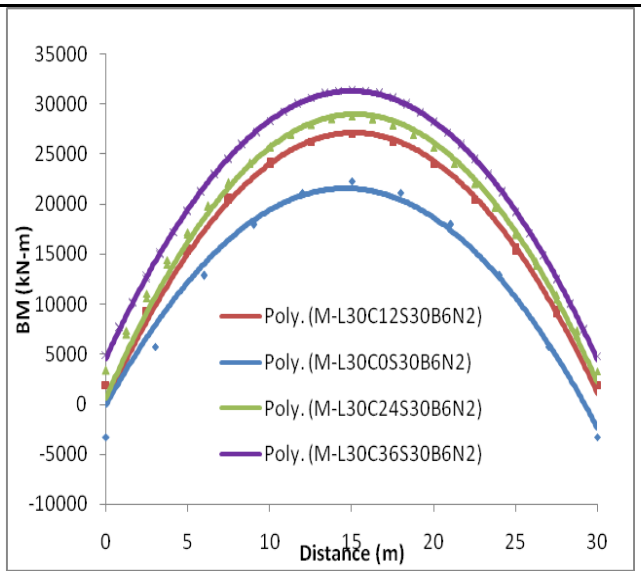

Plot- 31:B=6; N=2; θ =30°

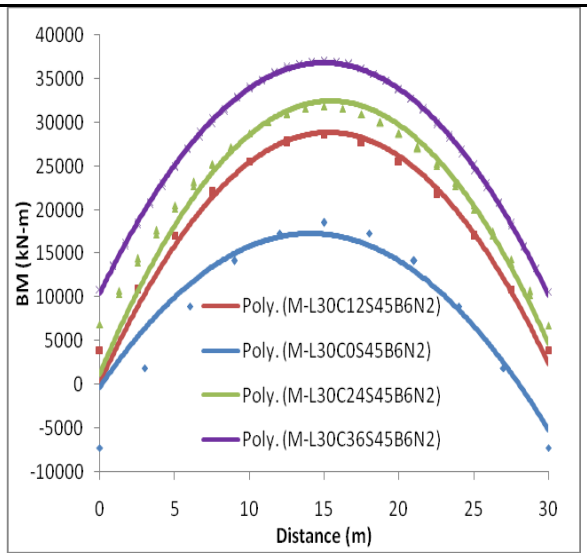

Plot- 32:B=6; N=2; θ=45°

Discussion: The BM pattern remains almost same. The BM value increases with increase in curvature. This increment is very minimum, 5%, when the skewness is zero. When skewness is introduced, the value of BM increases with curvature rapidly. For θ=45°, the BM increases upto 100% with curvature.

6.1.1.3 Variation of Maximum Bending Moment:

Variation of maximum bending moment has been compared as a ratio to the maximum bending moment of the straight bridge for all the four groups. The comparison has been presented below.

Table 3: Maximum DL Bending Moment for B5N1

Model ID	Span length (L in m)	Central Angle (α °)	Skew Angle (θ°)	Bottom Width, (B) (m)	Number of Cell (N)	Max. Bending Moment (KN-m)	As % of straight model	Remarks
M-L30C0S0B5N1	30	0	0	5	1	21587	100%	Decreases with Skewness
M-L30C0S15B5N1	30	0	15	5	1	20991	97%	
M-L30C0S30B5N1	30	0	30	5	1	19210	89%	
M-L30C0S45B5N1	30	0	45	5	1	16382	76%	
M-L30C12S0B5N1	30	12	0	5	1	21691	100%	Increases with Skewness and Curvature
M-L30C12S15B5N1	30	12	15	5	1	22188	103%	
M-L30C12S30B5N1	30	12	30	5	1	22920	106%	
M-L30C12S45B5N1	30	12	45	5	1	24221	112%	
M-L30C24S0B5N1	30	24	0	5	1	22014	102%	
M-L30C24S15B5N1	30	24	15	5	1	23023	107%	
M-L30C24S30B5N1	30	24	30	5	1	24484	113%	
M-L30C24S45B5N1	30	24	45	5	1	27121	126%	
M-L30C36S0B5N1	30	36	0	5	1	22569	105%	
M-L30C36S15B5N1	30	36	15	5	1	24188	112%	
M-L30C36S30B5N1	30	36	30	5	1	26635	123%	
M-L30C36S45B5N1	30	36	45	5	1	31447	146%	

Table 4: Maximum DL Bending Moment for B5N2

Model ID	Span length (L in m)	Central Angle (α °)	Skew Angle, (θ°)	Bottom Width, (B) (m)	Number of Cell (N)	Max. Bending Moment (KN-m)	As % of straight model	Remarks
M-L30C0S0B5N2	30	0	0	5	2	24908	100%	Decreases with Skewness
M-L30C0S15B5N2	30	0	15	5	2	24213	97%	
M-L30C0S30B5N2	30	0	30	5	2	22123	89%	
M-L30C0S0B5N2	30	0	45	5	2	18763	75%	

Model ID	Span length (L in m)	Central Angle (α °)	Skew Angle, (θ°)	Bottom Width, (B) (m)	Number of Cell (N)	Max. Bending Moment (KN-m)	As % of straight model	Remarks
M-L30C12S0B5N2	30	12	0	5	2	25028	100%	Increases with Skewness and Curvature
M-L30C12S15B5N2	30	12	15	5	2	25586	103%	
M-L30C12S30B5N2	30	12	30	5	2	26389	106%	
M-L30C12S45B5N2	30	12	45	5	2	27789	112%	
M-L30C24S0B5N2	30	24	0	5	2	25396	102%	
M-L30C24S15B5N2	30	24	15	5	2	26539	107%	
M-L30C24S30B5N2	30	24	30	5	2	28171	113%	
M-L30C24S45B5N2	30	24	45	5	2	31080	125%	
M-L30C36S0B5N2	30	36	0	5	2	26032	105%	
M-L30C36S15B5N2	30	36	15	5	2	27869	112%	
M-L30C36S30B5N2	30	36	30	5	2	30622	123%	
M-L30C36S45B5N2	30	36	45	5	2	35990	144%	

Table 5: Maximum DL Bending Moment for B6N1

Model ID	Span length (L in m)	Central Angle (α °)	Skew Angle, (θ°)	Bottom Width, (B) (m)	Number of Cell (N)	Max. Bending Moment (KN-m)	As % of straight model	Remarks
M-L30C0S0B6N1	30	0	0	6	1	21481	100%	Decreases with Skewness
M-L30C0S15B6N1	30	0	15	6	1	20688	96%	
M-L30C0S30B6N1	30	0	30	6	1	19392	90%	
M-L30C0S45B6N1	30	0	45	6	1	16209	75%	
M-L30C12S0B6N1	30	12	0	6	1	22306	104%	Increases with Skewness and Curvature
M-L30C12S15B6N1	30	12	15	6	1	22831	106%	
M-L30C12S30B6N1	30	12	30	6	1	23619	110%	
M-L30C12S45B6N1	30	12	45	6	1	25047	117%	

Model ID	Span length (L in m)	Central Angle (α °)	Skew Angle, (θ°)	Bottom Width, (B) (m)	Number of Cell (N)	Max. Bending Moment (KN-m)	As % of straight model	Remarks
M-L30C24S0B6N1	30	24	0	6	1	22535	105%	
M-L30C24S15B6N1	30	24	15	6	1	23576	110%	
M-L30C24S30B6N1	30	24	30	6	1	25106	117%	
M-L30C24S45B6N1	30	24	45	6	1	27910	130%	
M-L30C36S0B6N1	30	36	0	6	1	23218	108%	
M-L30C36S15B6N1	30	36	15	6	1	24909	116%	
M-L30C36S30B6N1	30	36	30	6	1	27489	128%	
M-L30C36S45B6N1	30	36	45	6	1	32606	152%	

Table 6: Maximum DL Bending Moment for B6N2

Model ID	Span length (L in m)	Central Angle (α °)	Skew Angle, (θ°)	Bottom Width, (B) (m)	Number of Cell (N)	Max. Bending Moment (KN-m)	As % of straight model	Remarks
M-L30C0S0B6N2	30	0	0	6	2	25502	100%	Decreases with Skewness
M-L30C0S15B6N2	30	0	15	6	2	24677	97%	
M-L30C0S30B6N2	30	0	30	6	2	22255	87%	
M-L30C0S45B6N2	30	0	45	6	2	18520	73%	
M-L30C12S0B6N2	30	12	0	6	2	25625	100%	Increases with Skewness and Curvature
M-L30C12S15B6N2	30	12	15	6	2	26210	103%	
M-L30C12S30B6N2	30	12	30	6	2	27066	106%	
M-L30C12S45B6N2	30	12	45	6	2	28584	112%	
M-L30C24S0B6N2	30	24	0	6	2	25860	101%	
M-L30C24S15B6N2	30	24	15	6	2	27039	106%	
M-L30C24S30B6N2	30	24	30	6	2	28742	113%	
M-L30C24S45B6N2	30	24	45	6	2	31814	125%	

Model ID	Span length (L in m)	Central Angle (α °)	Skew Angle, (θ°)	Bottom Width, (B) (m)	Number of Cell (N)	Max. Bending Moment (KN-m)	As % of straight model	Remarks
M-L30C36S0B6N2	30	36	0	6	2	26661	105%	
M-L30C36S15B6N2	30	36	15	6	2	28568	112%	
M-L30C36S30B6N2	30	36	30	6	2	31446	123%	
M-L30C36S45B6N2	30	36	45	6	2	37102	145%	

6.1.2 Effect on Torsional Moment:

Another important bridge response for curved, skew and skew-curved bridge is the torsional moment. The curvature and skewness in a box girder bridge affects both the absolute value of torsional moment but and the torsional moment pattern. Effect on both the torsional moment diagram and absolute torsional moment due to curvature and skewness is presented below.

6.1.2.1 Variation of Torsional Moment diagram due to skewness:

Effect on torsional moment diagram for variation in skewness has been plotted and explained graphically for all the four groups as described above.

B5N1:

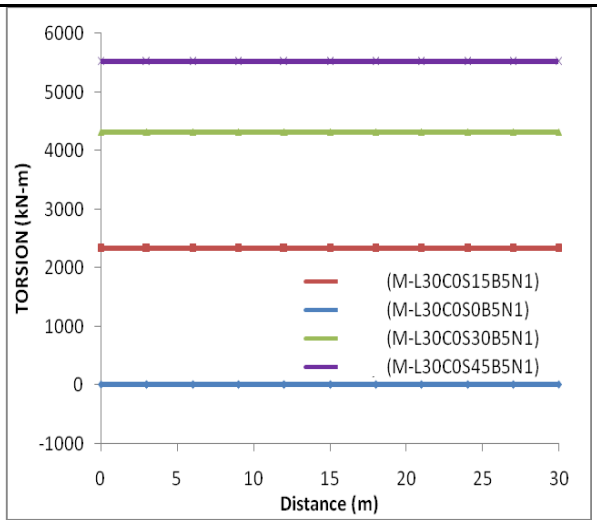

Plot- 1:B=5; N=1; α=0°

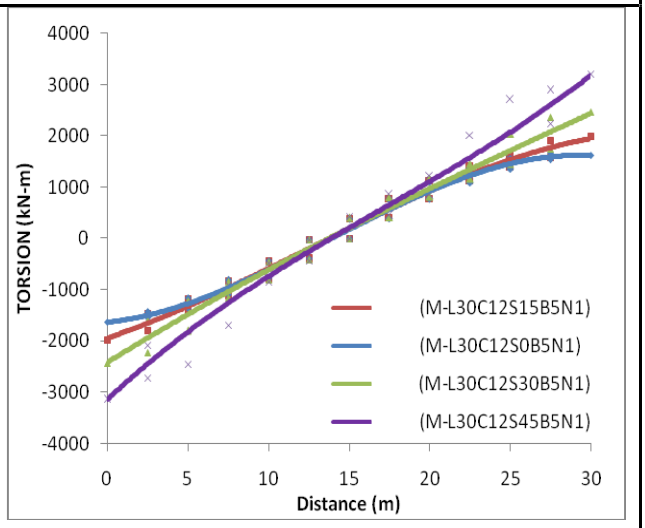

Plot- 2:B=5; N=1; α =12°

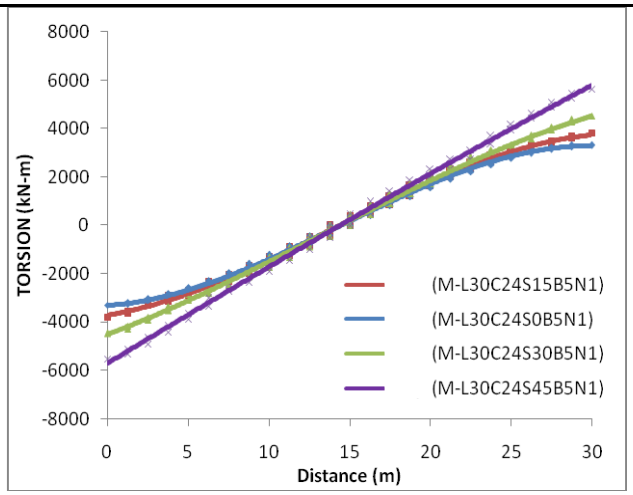

Plot- 3:B=5; N=1; α =24°

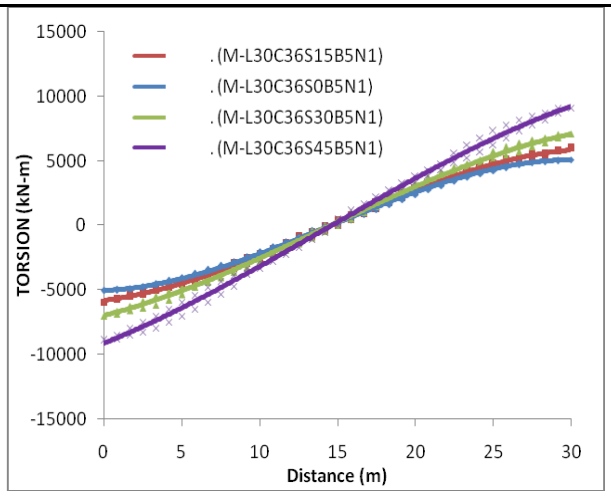

Plot- 4:B=5; N=1; α=36°

Discussion: Torsion is zero for the straight bridge model. It show a constant variation over the length, when skew angle increases and no curvature is introduced. When curvature is introduced, the torsion varies from negetive maximum value to positive maximum value at ends having a zero value near midspan. Both the positive and negetive maximum value increases with skewness. For a specifice curvature (say, α=36°), the value of torsion increases up to 79% with increase in skewness (θ=0° and 45°).

B5N2:

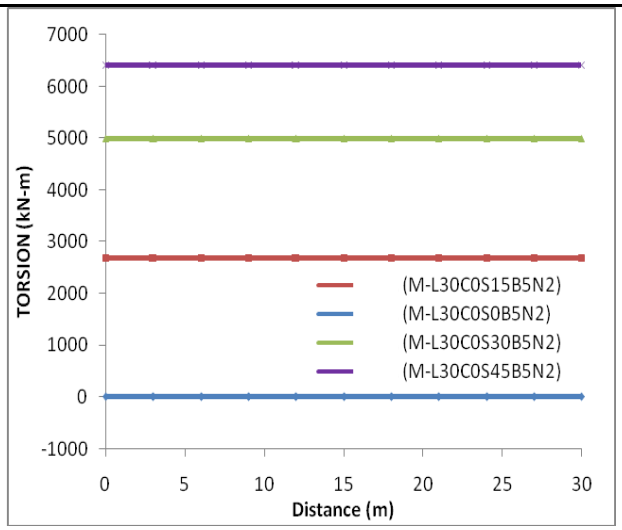

Plot- 5:B=5; N=2; α=0°

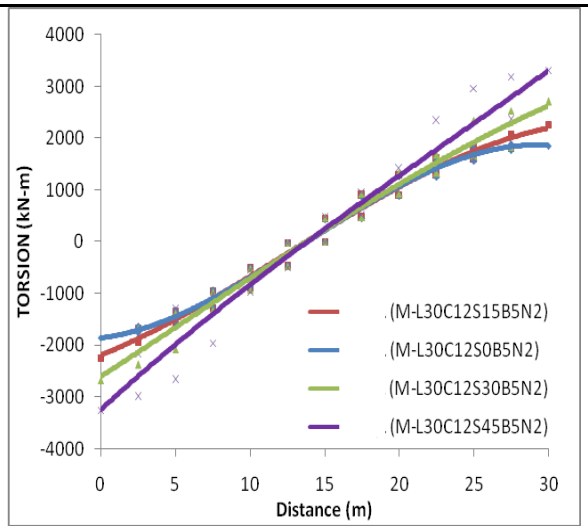

Plot- 6:B=5; N=2; α =12°

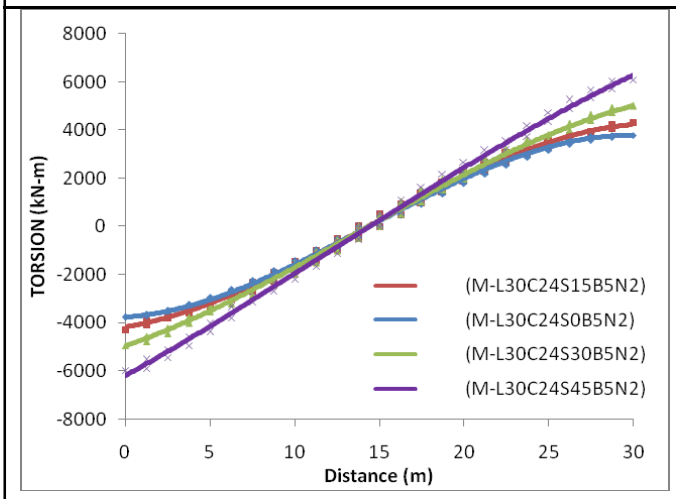

Plot- 7:B=5; N=2; α =24°

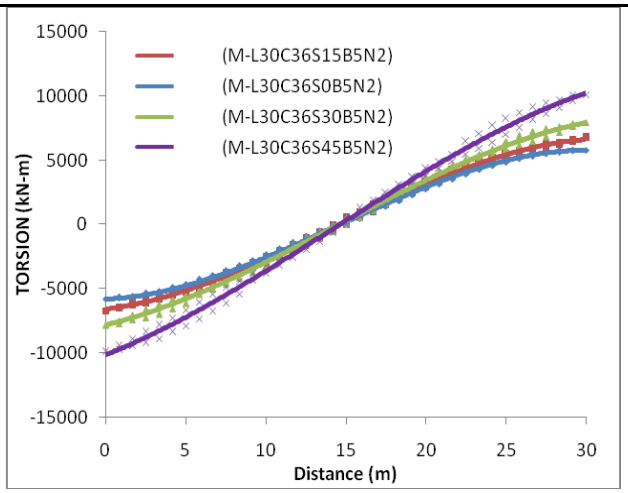

Plot- 8:B=5; N=2; α=36°

Discussion: Torsion is zero for the straight bridge model. It show a constant variation over the length, when skew angle increases and no curvature is introduced. When curvature is introduced, the torsion varies from negetive maximum value to positive maximum value at ends having a zero value near midspan. Both the positive and negetive maximum value increases with skewness. For a specifice curvature (say, α=36°), the value of torsion increases up to 74% with increase in skewness (θ=0° and 45°).

B6N1:

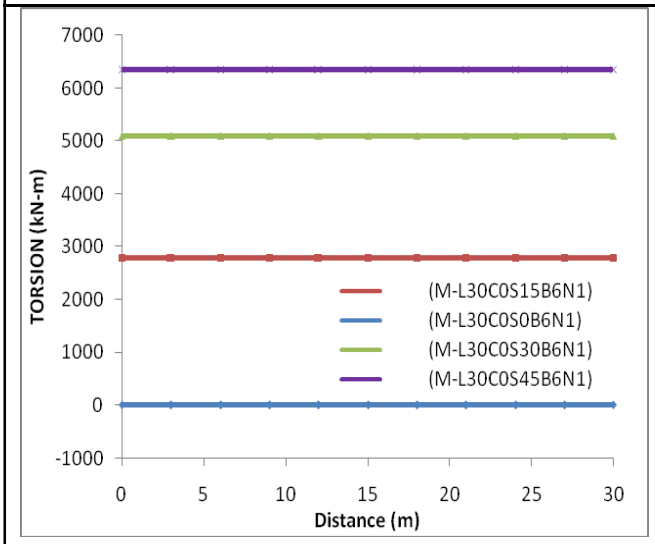

Plot- 9:B=6; N=1; α=0°

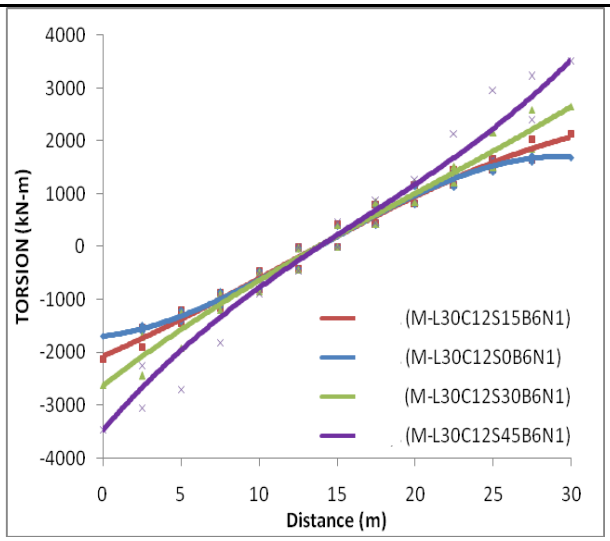

Plot- 10:B=6; N=1; α =12°

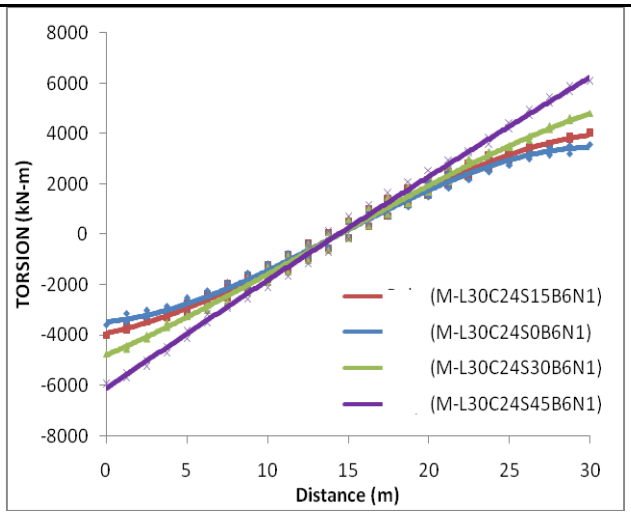

Plot- 11:B=6; N=1; α =24°

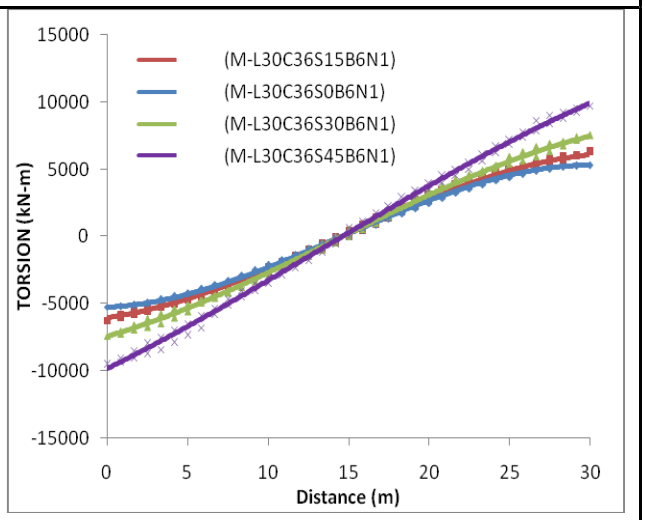

Plot- 12:B=6; N=1; α=36°

Discussion: Torsion is zero for the straight bridge model. It show a constant variation over the length, when skew angle increases and no curvature is introduced. When curvature is introduced, the torsion varies from negetive maximum value to positive maximum value at ends having a zero value near midspan. Both the positive and negetive maximum value increases with skewness. For a specifice curvature (say, α=36°), the value of torsion increases up to 84% with increase in skewness (θ=0° and 45°).

B6N2:

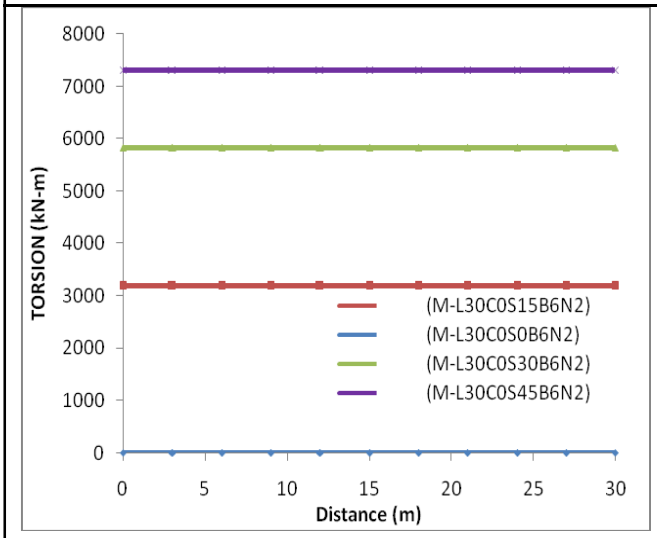

Plot- 13:B=6; N=2; α=0°

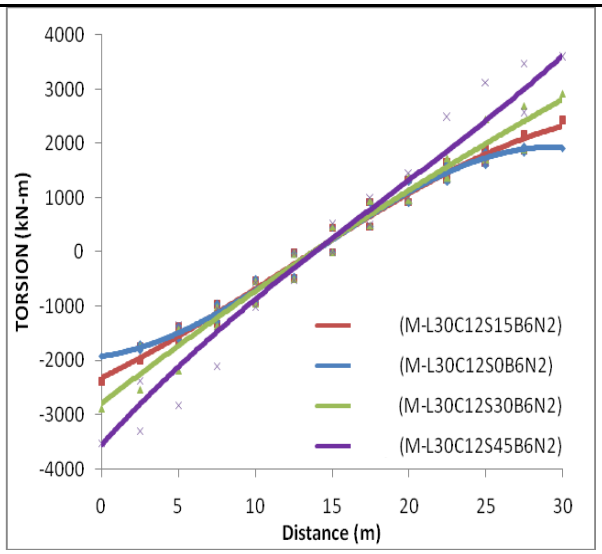

Plot- 14:B=6; N=2; α =12°

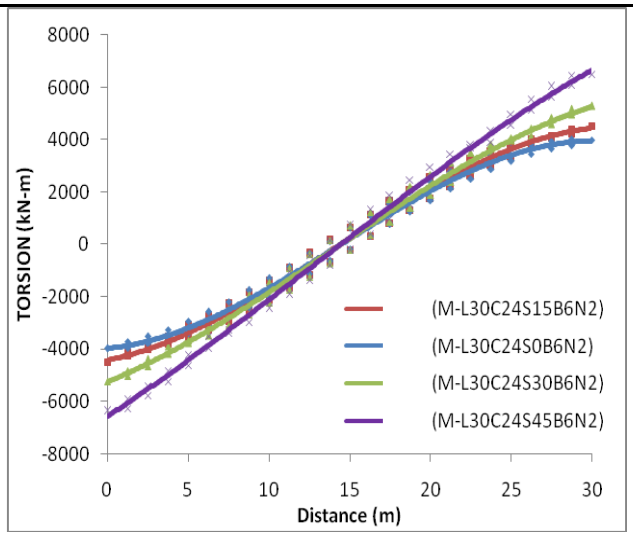

Plot- 15:B=6; N=2; α =24°

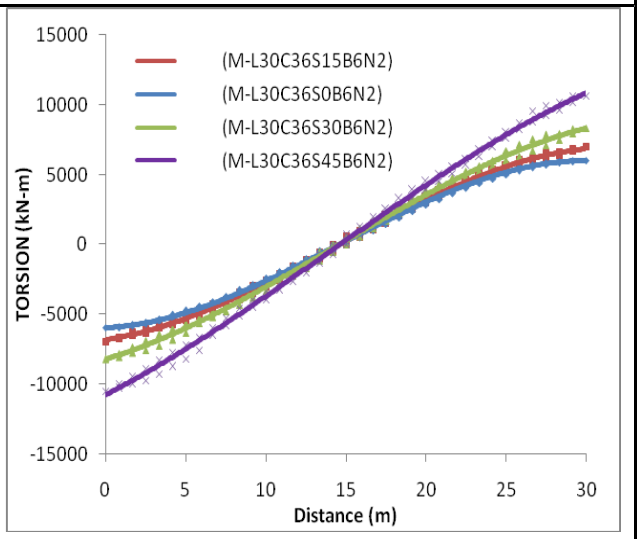

Plot- 16:B=6; N=2; α=36°

Discussion: Torsion is zero for the straight bridge model. It show a constant variation over the length, when skew angle increases and no curvature is introduced. When curvature is introduced, it varies from negetive maximum value to positive maximum value at ends having a zero value near midspan. Both the positive and negetive maximum value increases with skewness. For a specifice curvature (say, α=36°), the value of torsion increases up to 78% with increase in skewness (θ=0° and 45°).

6.1.2.2 Variation of Torsional Moment diagram due to Curvature:

Effect on torsional moment diagram for variation in curvature has been plotted and explained graphically for all the four groups as described above.

B5N1:

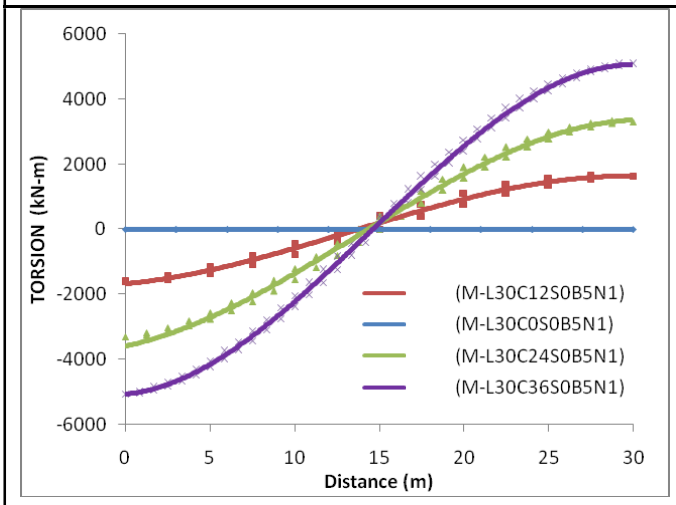

Plot- 17:B=5; N=1; θ=0°

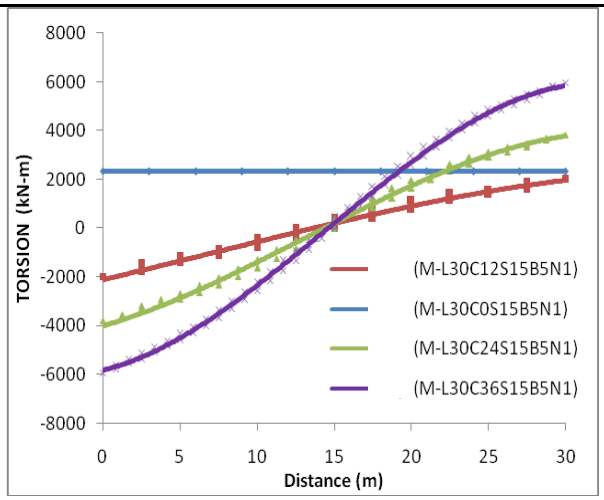

Plot- 18:B=5; N=1; θ =15°

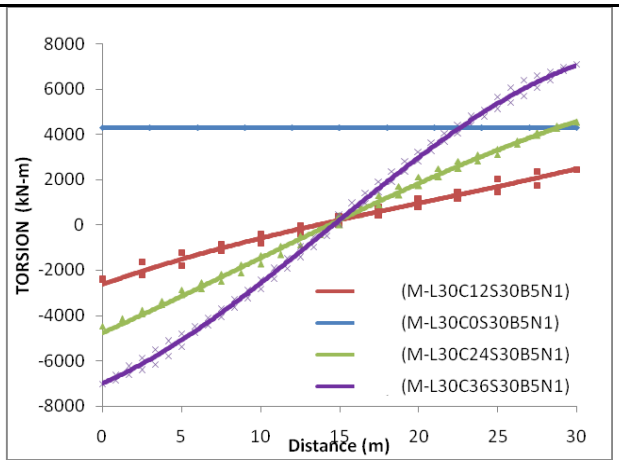

Plot- 19:B=5; N=1; θ =30°

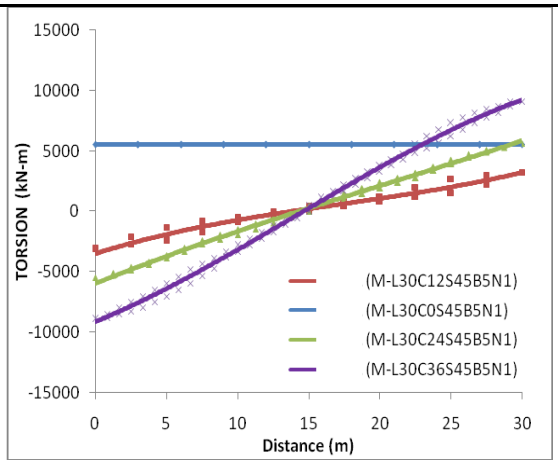

Plot- 20:B=5; N=1; θ=45°

Discussion: The torsional moment is zero, when there is neither curvature nor skewness and is constant when there is only skewness. When, curvature is introduced, torsional moment increases ath the ends with opposite sign and remains zero at midspan. When skewness is coupled with curvature, the magnitude of torsion increases further though the pattern remains almost similar. For aparticular skew angle (θ=45°), the torsional moment increases up to 65% due to increase in curvature (α=0° and 36°).

B5N2:

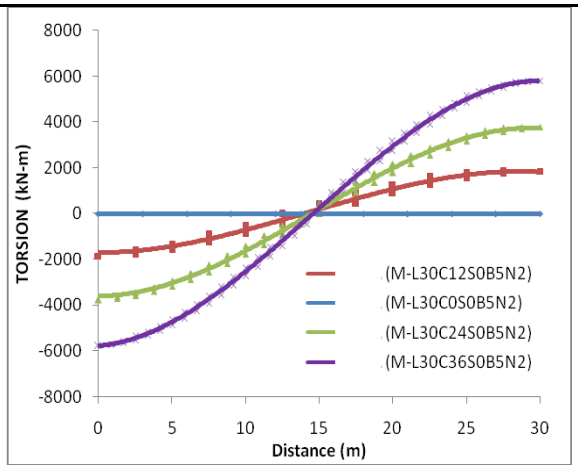

Plot- 21:B=5; N=2; θ=0°

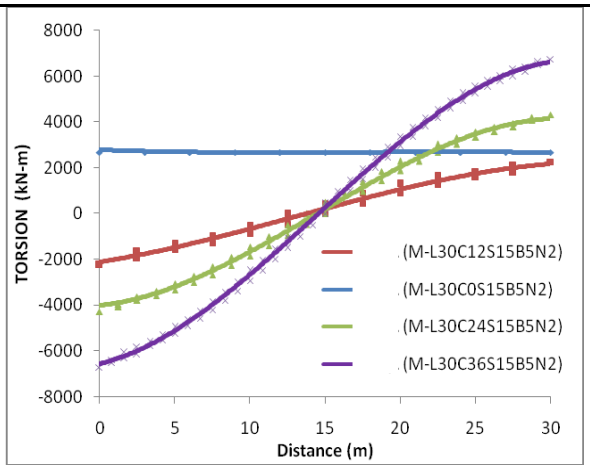

Plot- 22:B=5; N=2; θ =15°

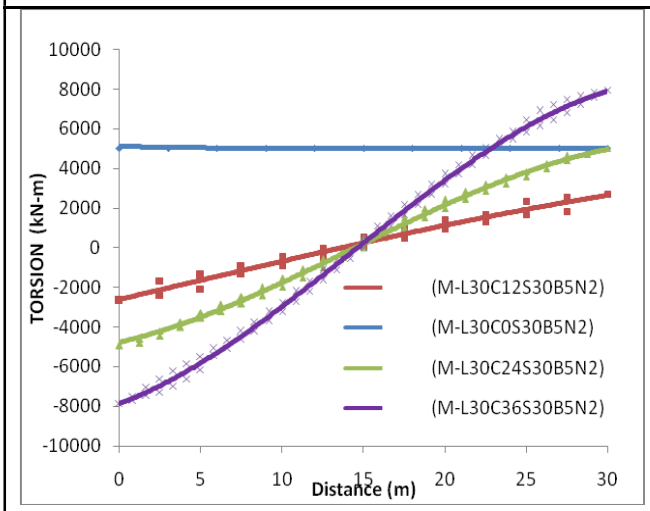

Plot- 23:B=5; N=2; θ =30°

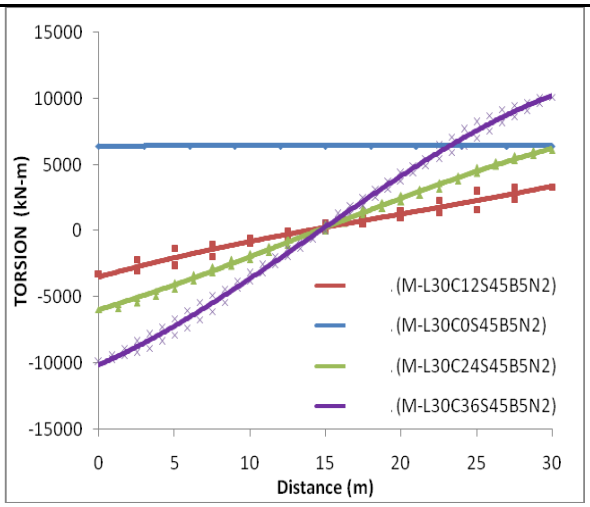

Plot- 24:B=5; N=2; θ=45°

Discussion: The torsional moment is zero, when there is neither curvature nor skewness and is constant when there is only skewness. When, curvature is introduced, torsional moment increases ath the ends with opposite sign and remains zero at midspan. When skewness is coupled with curvature, the magnitude of torsion increases further though the pattern remains almost similar. For aparticular skew angle (θ=45°), the torsional moment increases up to 57% due to increase in curvature (α=0° and 36°).

B6N1:

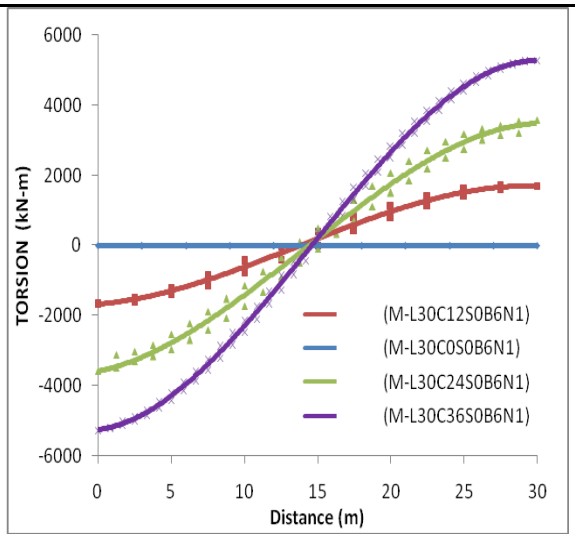

Plot- 25:B=6; N=1; θ=0°

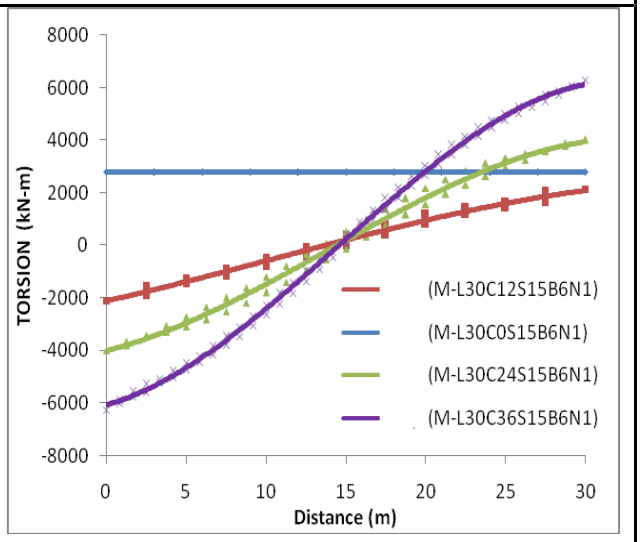

Plot- 26:B=6; N=1; θ =15°

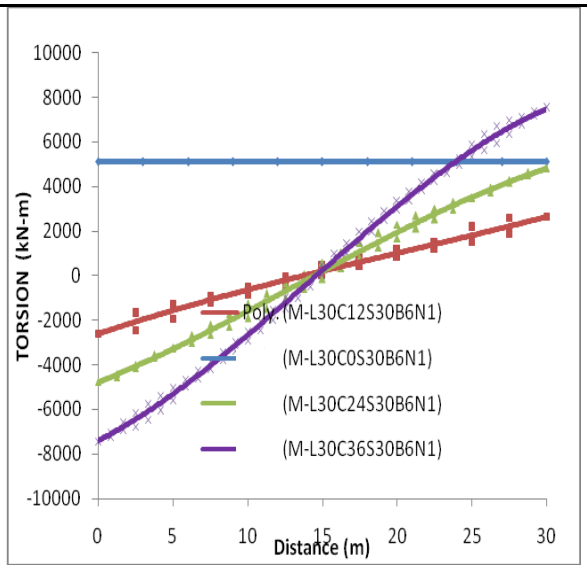

Plot- 27:B=6; N=1; θ =30°

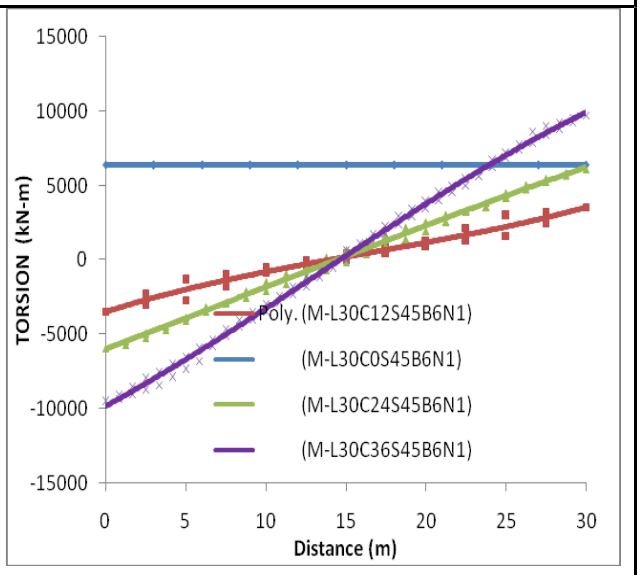

Plot- 28:B=6; N=1; θ=45°

Discussion: The torsional moment is zero, when there is neither curvature nor skewness and is constant when there is only skewness. When, curvature is introduced, torsional moment increases ath the ends with opposite sign and remains zero at midspan. When skewness is coupled with curvature, the magnitude of torsion increases further though the pattern remains almost similar. For aparticular skew angle (θ=45°), the torsional moment increases up to 53% due to increase in curvature (α=0° and 36°).

B6N2:

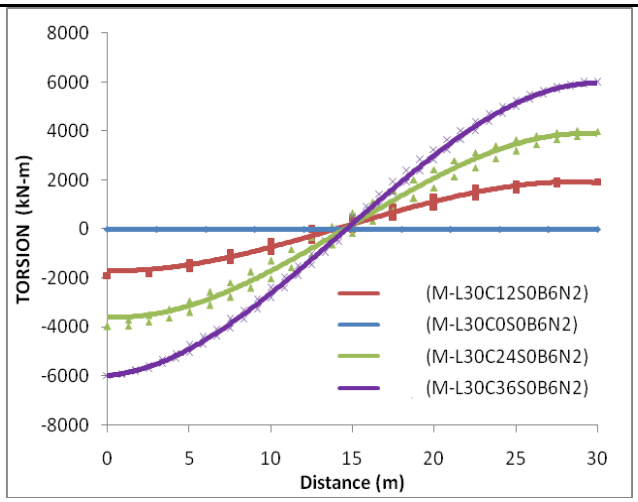

Plot- 29:B=6; N=2; θ=0°

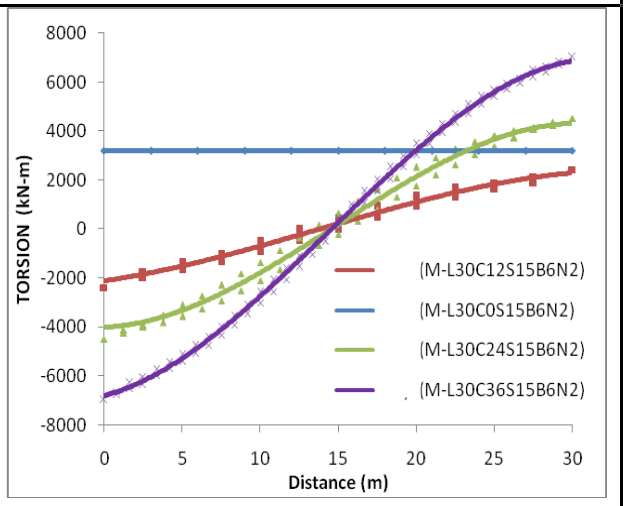

Plot- 30:B=6; N=2; θ =15°

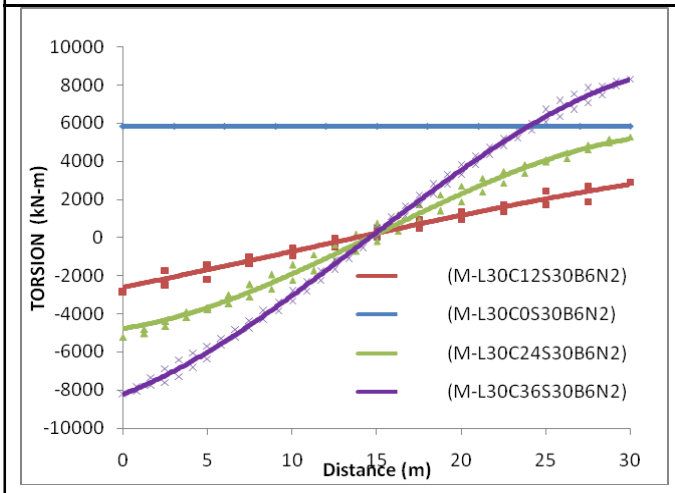

Plot- 31:B=6; N=2; θ =30°

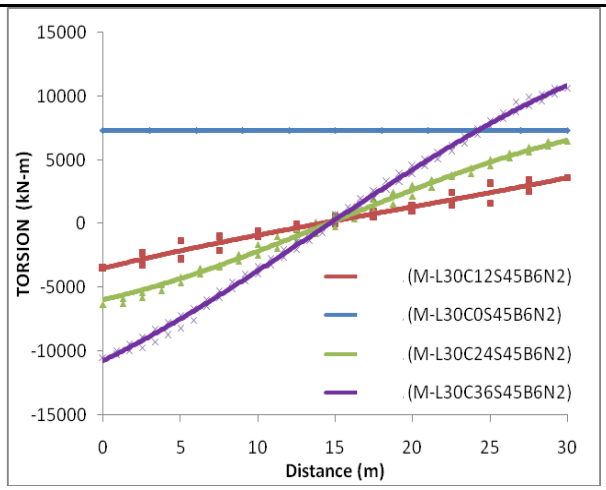

Plot- 32:B=6; N=2; θ=45°

Discussion: The torsional moment is zero, when there is neither curvature nor skewness and is constant when there is only skewness. When, curvature is introduced, torsional moment increases ath the ends with opposite sign and remains zero at midspan. When skewness is coupled with curvature, the magnitude of torsion increases further though the pattern remains almost similar. For aparticular skew angle (θ=45°), the torsional moment increases up to 46% due to increase in curvature (α=0° and 36°).

Another important discussion is that percentage increase in torsion with curvature reduces with increase in soffit width or increase in number of cell i.e. increase in transverse stiffness of the box girder.

6.1.2.3 Variation of Maximum Bending Moment:

Variation of maximum torsion has been compared as a ratio to the maximum torsion of the curved bridge (α=0°,12°,24° and 36°) for all the four groups. The comparison has been presented below.

Table 7: Maximum DL Torsion for B5N1

Model ID	Span length (L in m)	Central Angle (α °)	Skew Angle (θ°)	Bottom Width, (B) (m)	Number of Cell (N)	Max. Torsion (KN-m)	As % of curved model	Remarks
M-L30C0S0B5N1	30	0	0	5	1	0	-	Increases with Skewness
M-L30C0S15B5N1	30	0	15	5	1	2324	100%	
M-L30C0S30B5N1	30	0	30	5	1	4315	186%	
M-L30C0S45B5N1	30	0	45	5	1	5515	237%	
M-L30C12S0B5N1	30	12	0	5	1	1658	100%	Increases with Skewness and Curvature
M-L30C12S15B5N1	30	12	15	5	1	1990	120%	
M-L30C12S30B5N1	30	12	30	5	1	2461	148%	
M-L30C12S45B5N1	30	12	45	5	1	3205	193%	
M-L30C24S0B5N1	30	24	0	5	1	3313	100%	Increases with Skewness and Curvature
M-L30C24S15B5N1	30	24	15	5	1	3818	115%	
M-L30C24S30B5N1	30	24	30	5	1	4527	137%	
M-L30C24S45B5N1	30	24	45	5	1	5621	170%	
M-L30C36S0B5N1	30	36	0	5	1	5075	100%	Increases with Skewness and Curvature
M-L30C36S15B5N1	30	36	15	5	1	5979	118%	
M-L30C36S30B5N1	30	36	30	5	1	7091	140%	
M-L30C36S45B5N1	30	36	45	5	1	9099	179%	

Table 8: Maximum DL Torsion Moment for B5N2

Model ID	Span length (L in m)	Central Angle (α °)	Skew Angle (θ°)	Bottom Width, (B) (m)	Number of Cell (N)	Max. Torsion (KN-m)	As % of curved model	Remarks
M-L30C0S0B5N2	30	0	0	5	2	0	-	Increases with Skewness
M-L30C0S15B5N2	30	0	15	5	2	2682	100%	
M-L30C0S30B5N2	30	0	30	5	2	5001	186%	
M-L30C0S45B5N2	30	0	45	5	2	6420	239%	
M-L30C12S0B5N2	30	12	0	5	2	1897	100%	Increases with Skewness and Curvature
M-L30C12S15B5N2	30	12	15	5	2	2269	120%	
M-L30C12S30B5N2	30	12	30	5	2	2707	143%	
M-L30C12S45B5N2	30	12	45	5	2	3314	175%	
M-L30C24S0B5N2	30	24	0	5	2	3785	100%	Increases with Skewness and Curvature
M-L30C24S15B5N2	30	24	15	5	2	4320	114%	
M-L30C24S30B5N2	30	24	30	5	2	5001	132%	
M-L30C24S45B5N2	30	24	45	5	2	6077	161%	
M-L30C36S0B5N2	30	36	0	5	2	5792	100%	Increases with Skewness and Curvature
M-L30C36S15B5N2	30	36	15	5	2	6743	116%	
M-L30C36S30B5N2	30	36	30	5	2	7936	137%	
M-L30C36S45B5N2	30	36	45	5	2	10095	174%	

Table 9: Maximum DL Torsion for B6N1

Model ID	Span length (L in m)	Central Angle (α °)	Skew Angle (θ °)	Bottom Width, (B) (m)	Number of Cell (N)	Max. Torsion (KN-m)	As % of curved model	Remarks
M-L30C0S0B6N1	30	0	0	6	1	0	-	Increases with Skewness
M-L30C0S15B6N1	30	0	15	6	1	2794	100%	
M-L30C0S30B6N1	30	0	30	6	1	5098	182%	
M-L30C0S45B6N1	30	0	45	6	1	6361	228%	

Model ID	Span length (L in m)	Central Angle (α °)	Skew Angle (θ °)	Bottom Width, (B) (m)	Number of Cell (N)	Max. Torsion (KN-m)	As % of curved model	Remarks
M-L30C12S0B6N1	30	12	0	6	1	1721	100%	Increases with Skewness and Curvature
M-L30C12S15B6N1	30	12	15	6	1	2132	124%	
M-L30C12S30B6N1	30	12	30	6	1	2653	154%	
M-L30C12S45B6N1	30	12	45	6	1	3526	205%	
M-L30C24S0B6N1	30	24	0	6	1	3577	100%	Increases with Skewness and Curvature
M-L30C24S15B6N1	30	24	15	6	1	4013	112%	
M-L30C24S30B6N1	30	24	30	6	1	4800	134%	
M-L30C24S45B6N1	30	24	45	6	1	6065	170%	
M-L30C36S0B6N1	30	36	0	6	1	5279	100%	Increases with Skewness and Curvature
M-L30C36S15B6N1	30	36	15	6	1	6283	119%	
M-L30C36S30B6N1	30	36	30	6	1	7518	142%	
M-L30C36S45B6N1	30	36	45	6	1	9720	184%	

Table 10: Maximum DL Torsion for B6N2

Model ID	Span length (L in m)	Central Angle (α °)	Skew Angle (θ °)	Bottom Width, (B) (m)	Number of Cell (N)	Max. Torsion (KN-m)	As % of curved model	Remarks
M-L30C0S0B6N2	30	0	0	6	2	0	-	**Increases with Skewness**
M-L30C0S15B6N2	30	0	15	6	2	3183	100%	
M-L30C0S30B6N2	30	0	30	6	2	5837	183%	
M-L30C0S45B6N2	30	0	45	6	2	7310	230%	
M-L30C12S0B6N2	30	12	0	6	2	1957	100%	**Increases with Skewness and Curvature**
M-L30C12S15B6N2	30	12	15	6	2	2418	124%	
M-L30C12S30B6N2	30	12	30	6	2	2916	149%	
M-L30C12S45B6N2	30	12	45	6	2	3590	183%	

Model ID	Span length (L in m)	Central Angle (α °)	Skew Angle (θ °)	Bottom Width, (B) (m)	Number of Cell (N)	Max. Torsion (KN-m)	As % of curved model	Remarks
M-L30C24S0B6N2	30	24	0	6	2	4022	100%	**Increases with Skewness and Curvature**
M-L30C24S15B6N2	30	24	15	6	2	4514	112%	
M-L30C24S30B6N2	30	24	30	6	2	5285	131%	
M-L30C24S45B6N2	30	24	45	6	2	6489	161%	
M-L30C36S0B6N2	30	36	0	6	2	5985	100%	**Increases with Skewness and Curvature**
M-L30C36S15B6N2	30	36	15	6	2	7018	117%	
M-L30C36S30B6N2	30	36	30	6	2	8327	139%	
M-L30C36S45B6N2	30	36	45	6	2	10672	178%	

It has been seen that, when there is no curvature introduced the torsion varies almost 2.0 to 2.3 times for varying the skew angle (α=0°; θ=15°) to (α=0°; θ=45°). When the curvature is introduced and it is coupled with skewness, the torsional moment varies up to 1.65 to 1.85 times (α=12°; θ=0° to α=36°; θ=45°).

6.1.3 Effect on Shear Force:

Effect on both the shear force diagram and absolute shear force due to curvature and skewness is presented below.

6.1.3.1 Variation of Shear force diagram due to skewness:

Effect on shear diagram for variation in skewness has been plotted and explained graphically for all the four groups as described above.

B5N1:

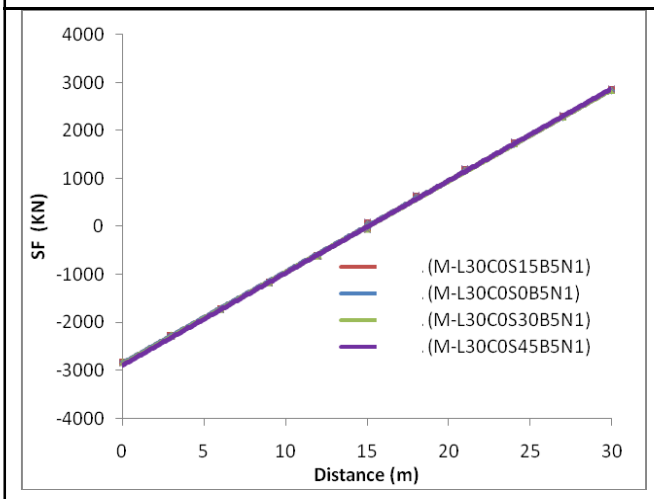

Plot- 1:B=5; N=1; α=0°

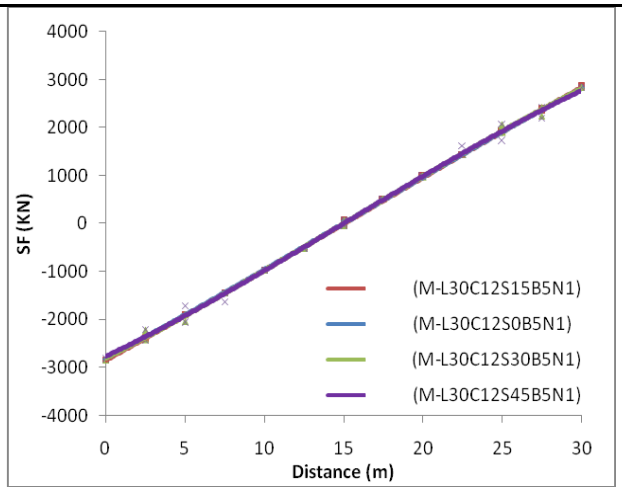

Plot- 2:B=5; N=1; α =12°

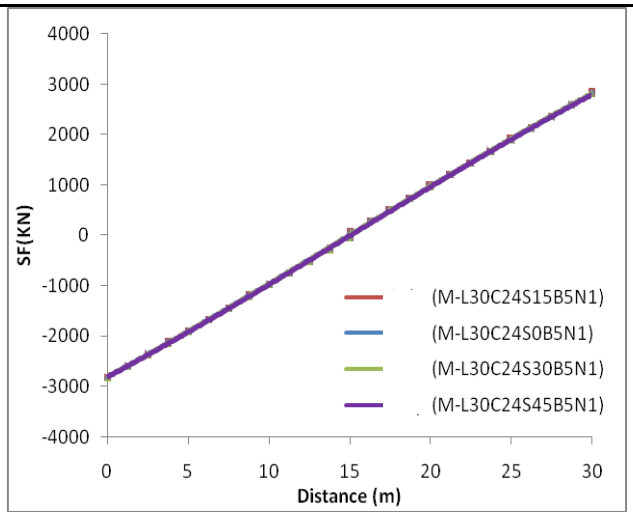

Plot- 3:B=5; N=1; α =24°

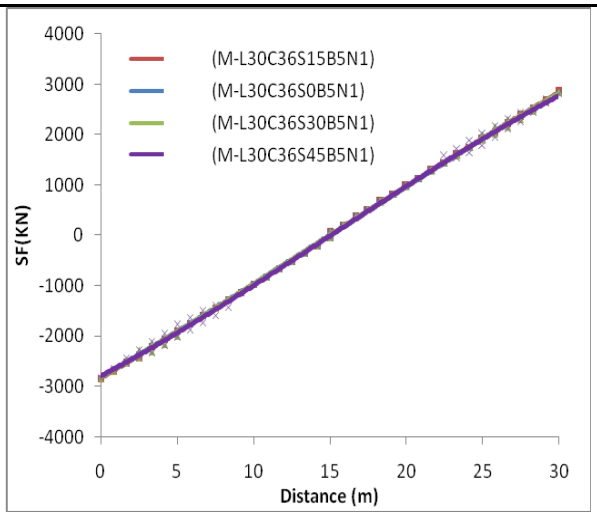

Plot- 4:B=5; N=1; α=36°

Discussion: Variation of shear force is almost same irrespective of curvature and skew. The maximum shear force also does not vary much. Variation of shear force due to curvature and skewness is within ±1%.

B5N2:

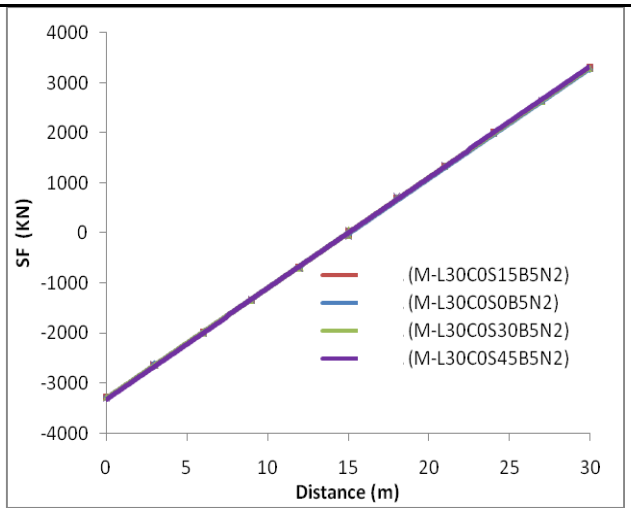

Plot- 5:B=5; N=2; α=0°

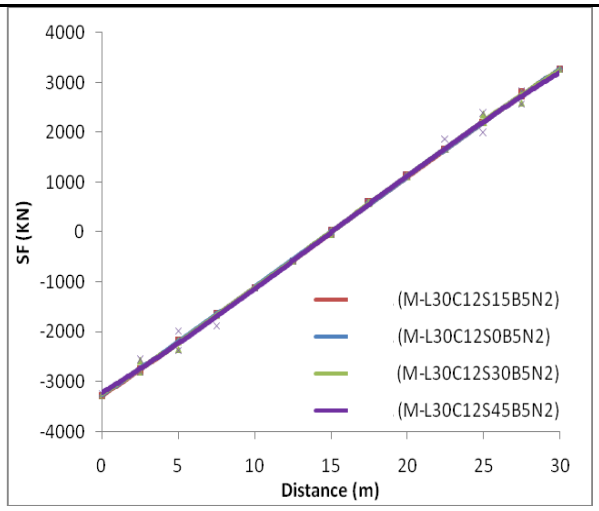

Plot- 6:B=5; N=2; α =12°

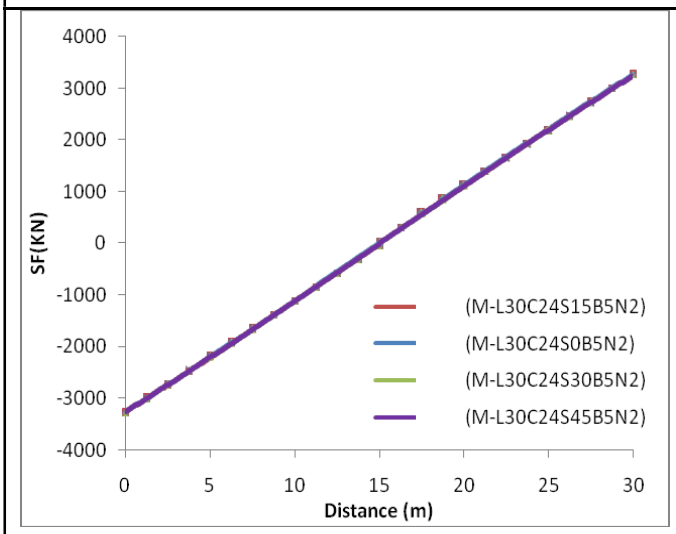

Plot- 7:B=5; N=2; α =24°

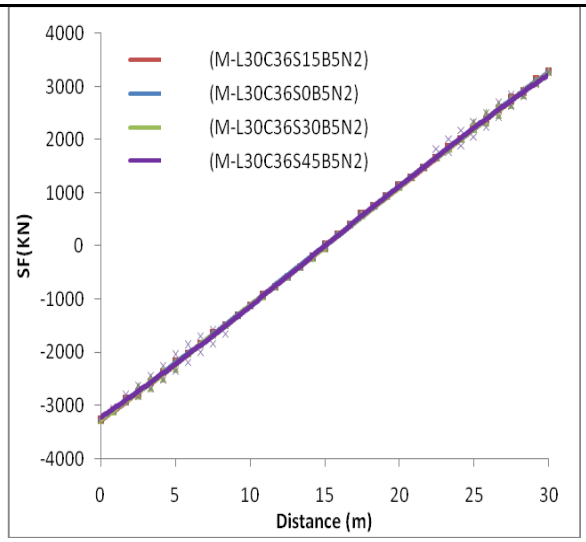

Plot- 8:B=5; N=2; α=36°

Discussion: Variation of shear force is almost same irrespective of curvature and skew. The maximum shear force also does not vary much. Variation of shear force due to curvature and skewness is within ±1%.

B6N1:

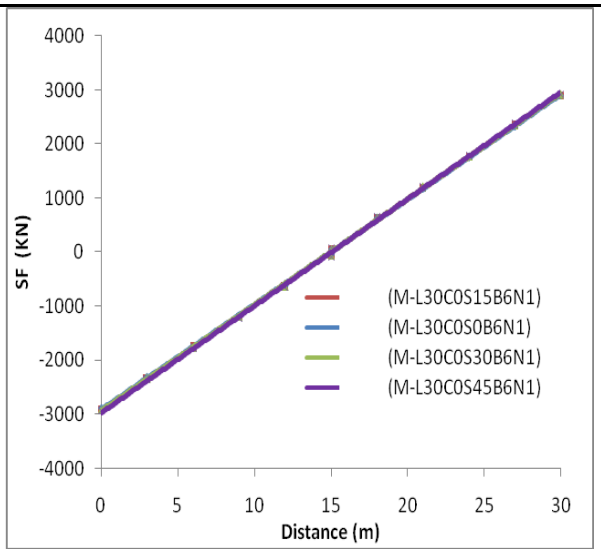

Plot- 9:B=6; N=1; α=0°

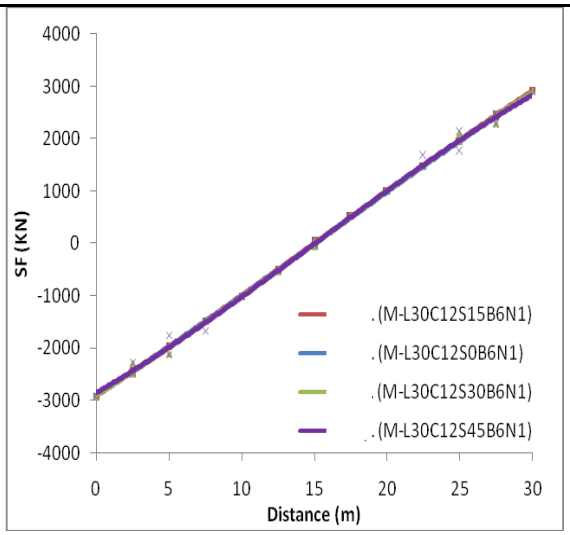

Plot- 10:B=6; N=1; α =12°

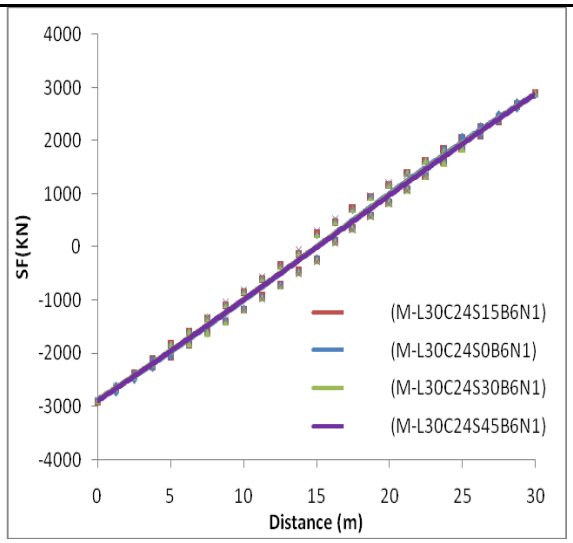

Plot- 11:B=6; N=1; α =24°

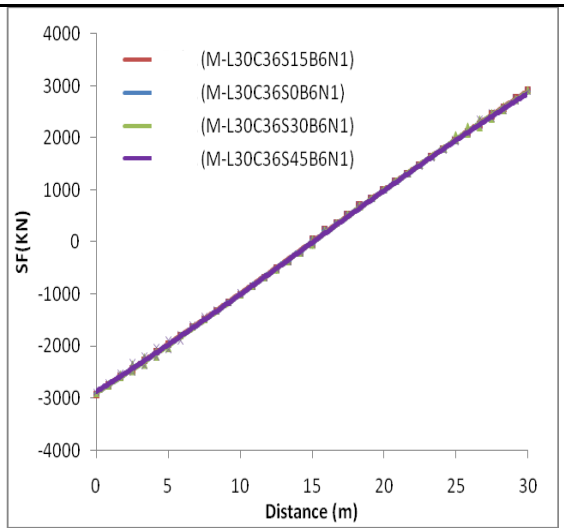

Plot- 12:B=6; N=1; α=36°

Discussion: Variation of shear force is almost same irrespective of curvature and skew. The maximum shear force also does not vary much. Variation of shear force due to curvature and skewness is within ±1%.

B6N2:

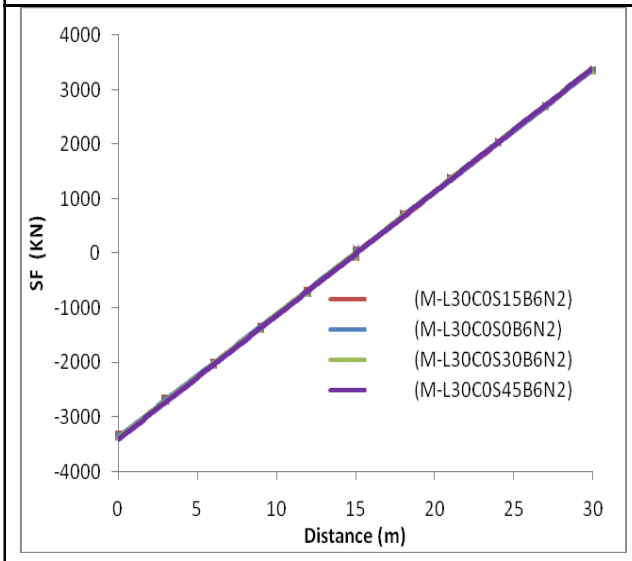

Plot- 13:B=6; N=2; α=0°

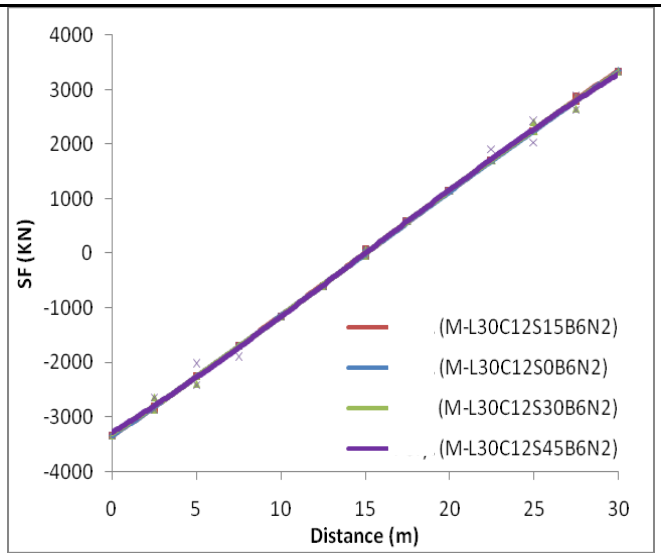

Plot- 14:B=6; N=2; α =12°

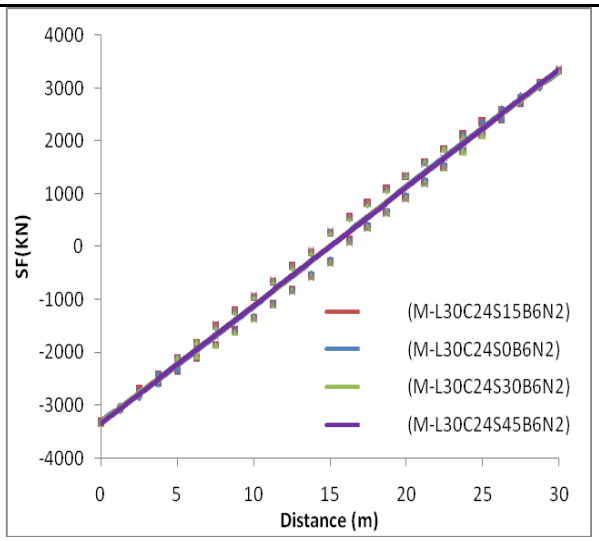

Plot- 15:B=6; N=2; α =24°

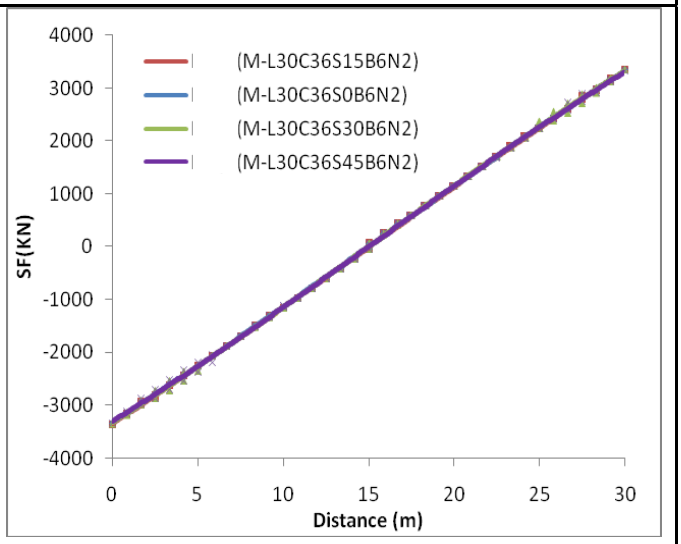

Plot- 16:B=6; N=2; α=36°

Discussion: Variation of shear force is almost same irrespective of curvature and skew. The maximum shear force also does not vary much. Variation of shear force due to curvature and skewness is within ±1%.

6.1.3.2 Variation of Shear force diagram due to Curvature:

Effect on shear force diagram for variation in curvature has been plotted and explained graphically for all the four groups as described above.

B5N1:

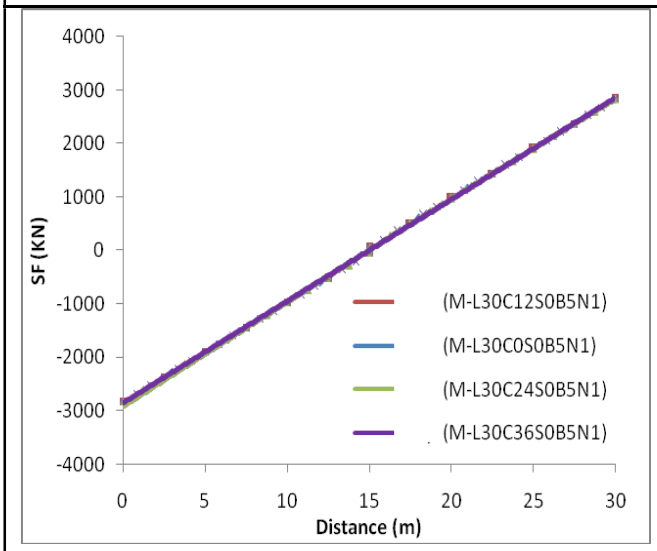

Plot- 17:B=5; N=1; θ=0°

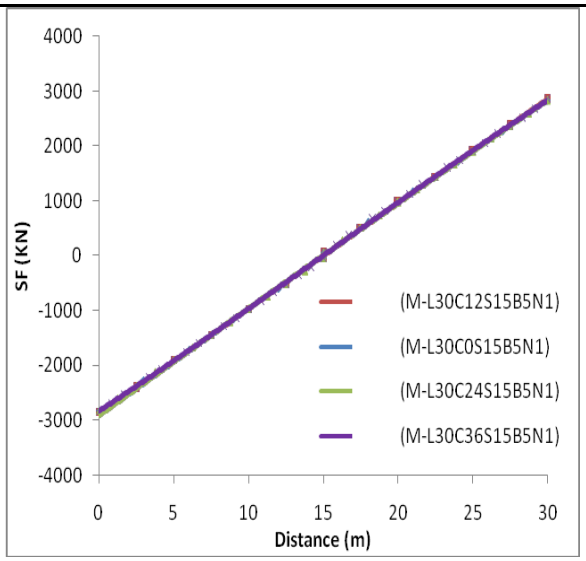

Plot- 18:B=5; N=1; θ =15°

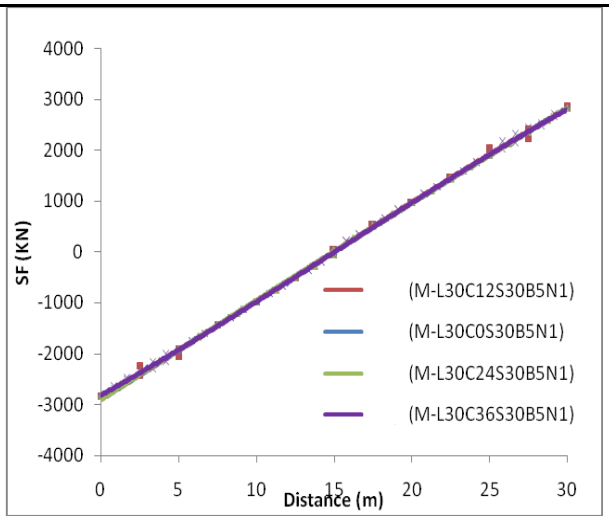

Plot- 19:B=5; N=1; θ =30°

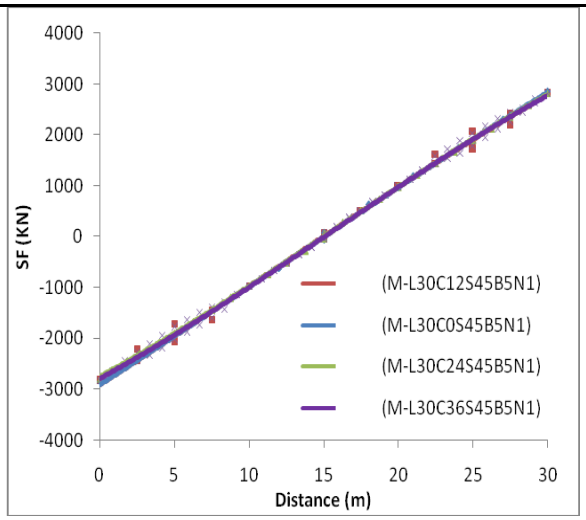

Plot- 20:B=5; N=1; θ=45°

Discussion: Variation of shear force is almost same irrespective of curvature and skew. The maximum shear force also does not vary much. Variation of shear force due to curvature and skewness is within ±1%.

B5N2:

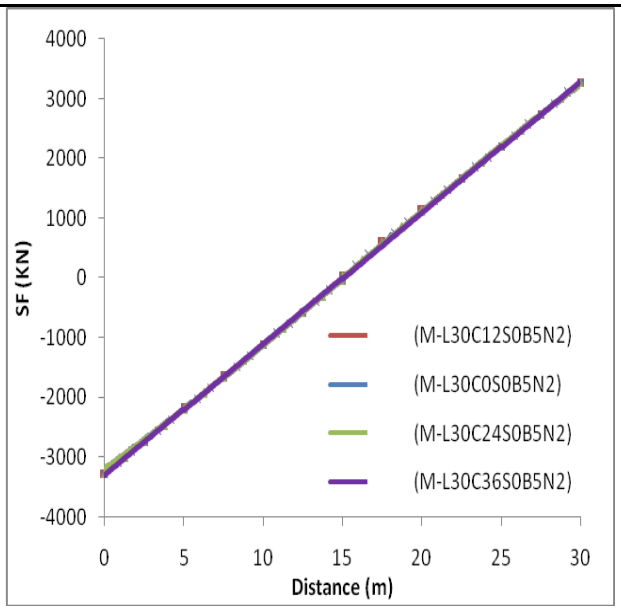

Plot- 21:B=5; N=2; θ=0°

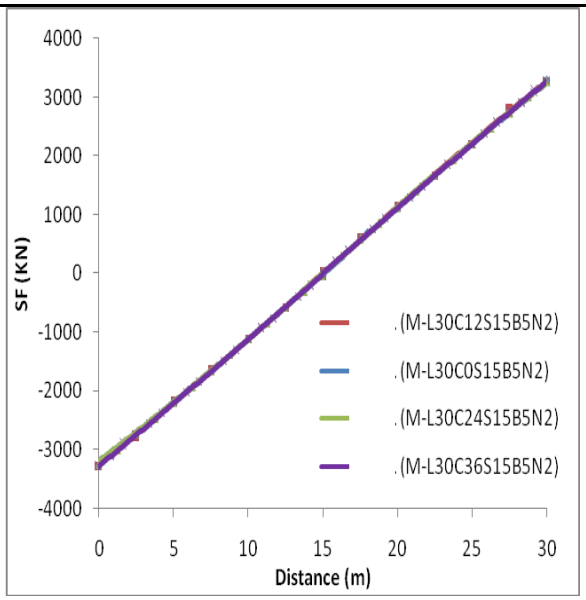

Plot- 22:B=5; N=2; θ =15°

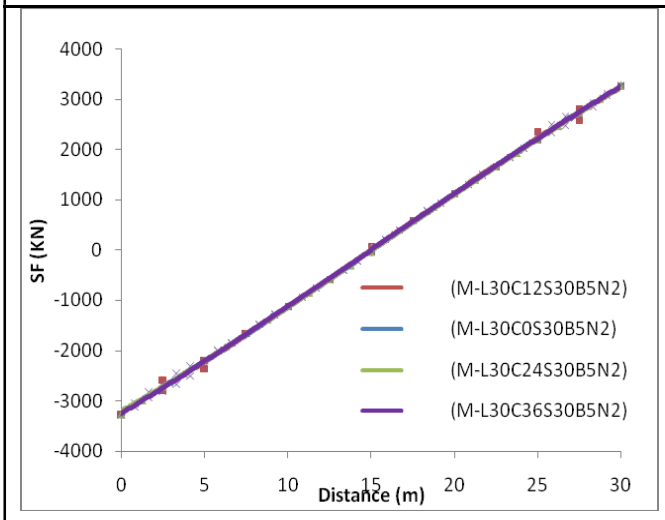

Plot- 23:B=5; N=2; θ =30°

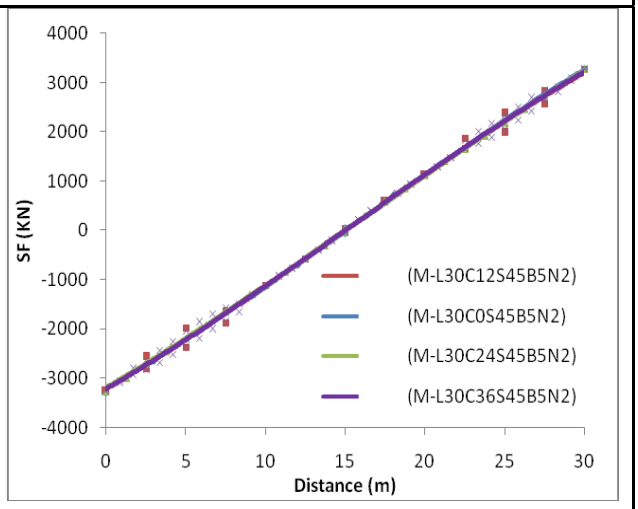

Plot- 24:B=5; N=2; θ=45°

Discussion: Variation of shear force is almost same irrespective of curvature and skew. The maximum shear force also does not vary much. Variation of shear force due to curvature and skewness is within ±1%.

B6N1:

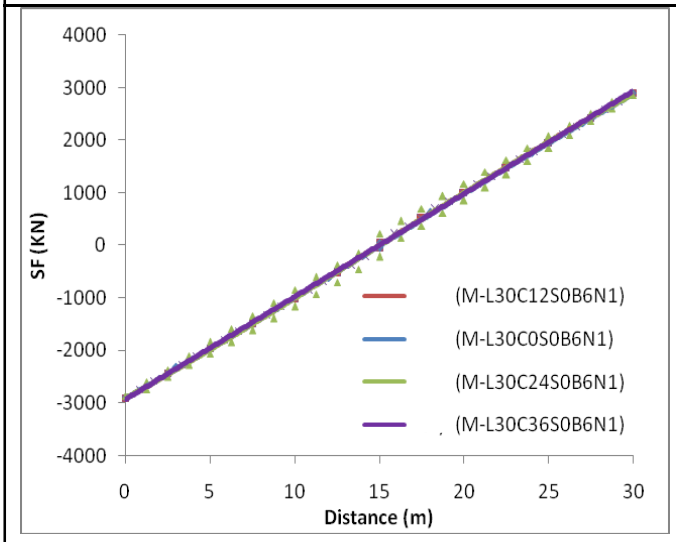

Plot- 25:B=6; N=1; θ=0°

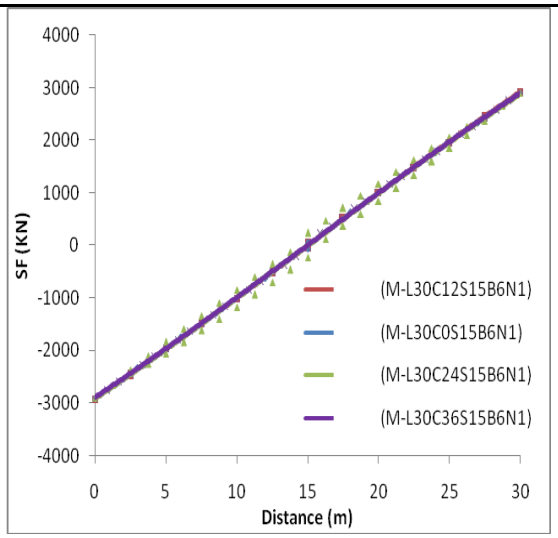

Plot- 26:B=6; N=1; θ =15°

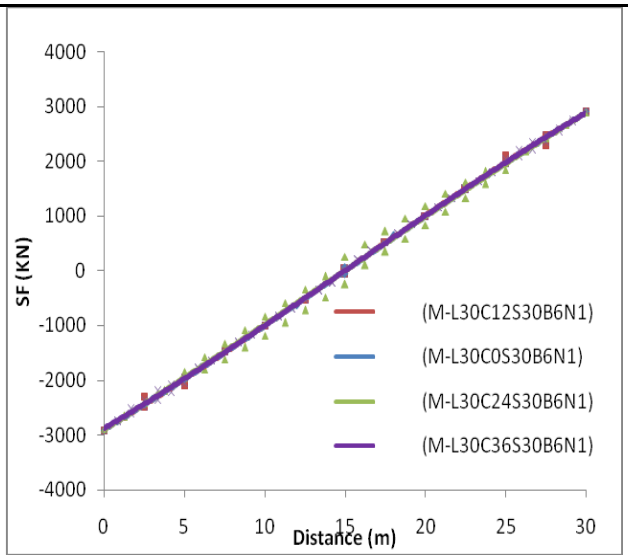

Plot- 27:B=6; N=1; θ =30°

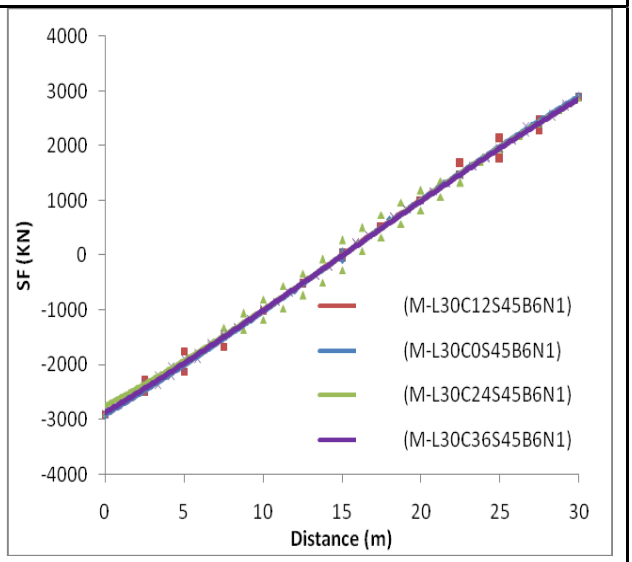

Plot- 28:B=6; N=1; θ=45°

Discussion: Variation of shear force is almost same irrespective of curvature and skew. The maximum shear force also does not vary much. Variation of shear force due to curvature and skewness is within ±1%.

B6N2:

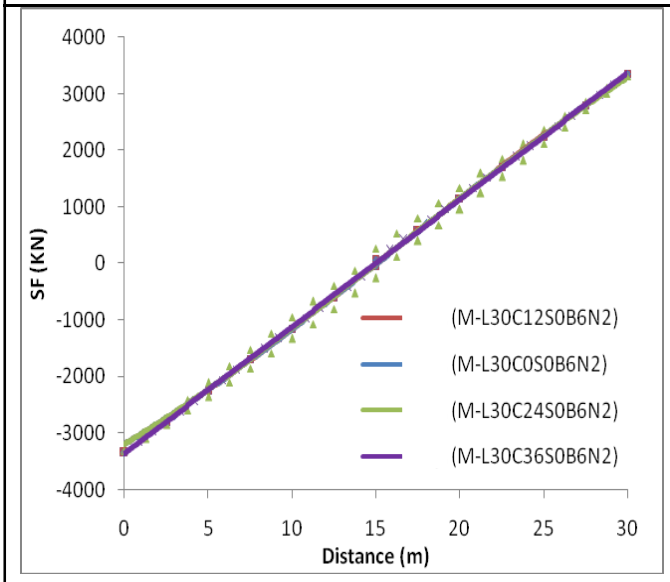

Plot- 29:B=6; N=2; θ=0°

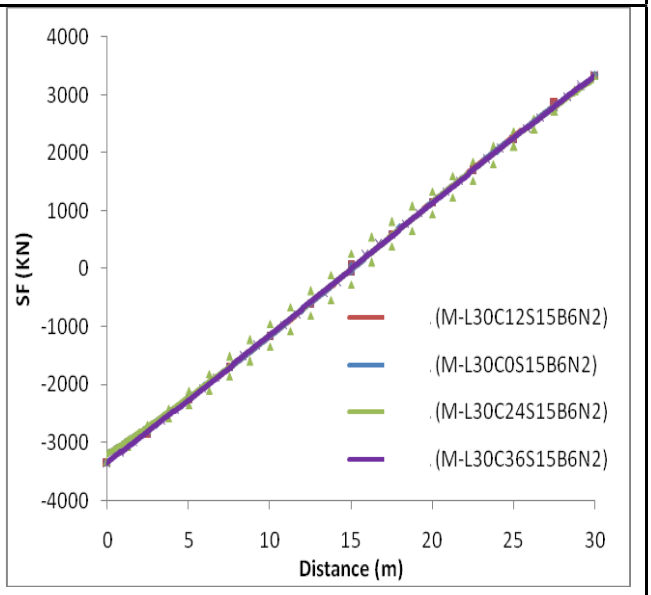

Plot- 30:B=6; N=2; θ =15°

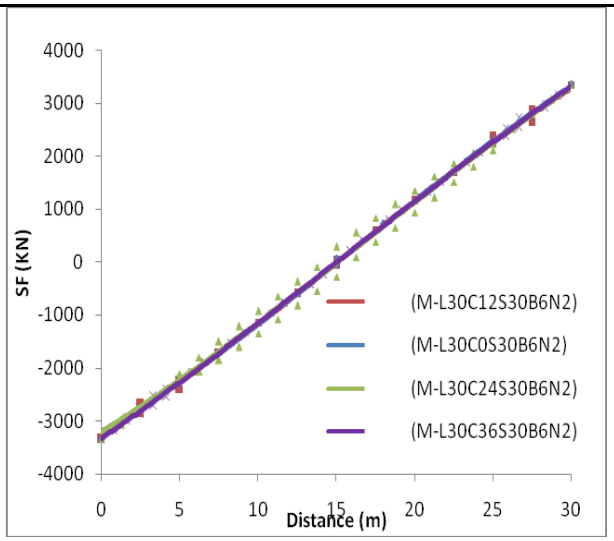

Plot- 31:B=6; N=2; θ =30°

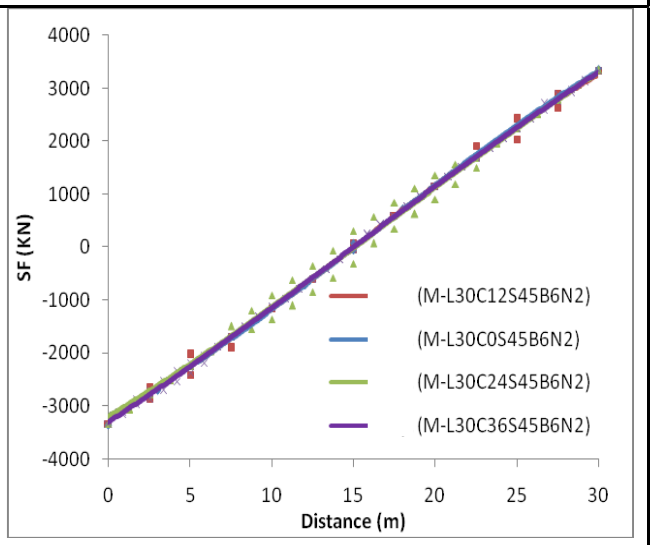

Plot- 32:B=6; N=2; θ=45°

Discussion: Variation of shear force is almost same irrespective of curvature and skew. The maximum shear force also does not vary much. Variation of shear force due to curvature and skewness is within ±1%.

6.1.3.3 Variation of Maximum Shear Force:

Variation of maximum shear force has been compared as a ratio to the maximum shear force of the straight bridge (α=0° and θ=0°) for all the four groups. The comparison has been presented below.

Table 11: Maximum DL Shear Force for B5N1

Model ID	Span length (L in m)	Central Angle (α °)	Skew Angle, (θ °)	Bottom Width, (B) (m)	Number of Cell (N)	Max. Shear Force (KN)	As % of straight model	Remarks
M-L30C0S0B5N1	30	0	0	5	1	2829	100%	Varies within ±1%
M-L30C0S15B5N1	30	0	15	5	1	2830	100%	
M-L30C0S30B5N1	30	0	30	5	1	2836	100%	
M-L30C0S45B5N1	30	0	45	5	1	2849	101%	
M-L30C12S0B5N1	30	12	0	5	1	2829	100%	
M-L30C12S15B5N1	30	12	15	5	1	2848	101%	
M-L30C12S30B5N1	30	12	30	5	1	2841	100%	
M-L30C12S45B5N1	30	12	45	5	1	2835	100%	
M-L30C24S0B5N1	30	24	0	5	1	2829	100%	
M-L30C24S15B5N1	30	24	15	5	1	2828	100%	
M-L30C24S30B5N1	30	24	30	5	1	2823	100%	
M-L30C24S45B5N1	30	24	45	5	1	2812	99%	
M-L30C36S0B5N1	30	36	0	5	1	2829	100%	
M-L30C36S15B5N1	30	36	15	5	1	2848	101%	
M-L30C36S30B5N1	30	36	30	5	1	2837	100%	
M-L30C36S45B5N1	30	36	45	5	1	2818	100%	

Table 12: Maximum DL Shear Force for B5N2

Model ID	Span length (L in m)	Central Angle (α °)	Skew Angle (θ °)	Bottom Width, (B) (m)	Number of Cell (N)	Max. Shear Force (KN)	As % of straight model	Remarks
M-L30C0S0B5N2	30	0	0	5	2	3278	100%	Varies within ±1%
M-L30C0S15B5N2	30	0	15	5	2	3279	100%	
M-L30C0S30B5N2	30	0	30	5	2	3284	100%	
M-L30C0S45B5N2	30	0	45	5	2	3295	100%	
M-L30C12S0B5N2	30	12	0	5	2	3278	100%	
M-L30C12S15B5N2	30	12	15	5	2	3271	100%	
M-L30C12S30B5N2	30	12	30	5	2	3269	100%	
M-L30C12S45B5N2	30	12	45	5	2	3269	100%	
M-L30C24S0B5N2	30	24	0	5	2	3278	100%	
M-L30C24S15B5N2	30	24	15	5	2	3263	100%	
M-L30C24S30B5N2	30	24	30	5	2	3274	100%	
M-L30C24S45B5N2	30	24	45	5	2	3274	100%	
M-L30C36S0B5N2	30	36	0	5	2	3278	100%	
M-L30C36S15B5N2	30	36	15	5	2	3291	100%	
M-L30C36S30B5N2	30	36	30	5	2	3279	100%	
M-L30C36S45B5N2	30	36	45	5	2	3261	99%	

Table 13: Maximum Shear DL Force for B6N1

Model ID	Span length (L in m)	Central Angle (α °)	Skew Angle (θ °)	Bottom Width, (B) (m)	Number of Cell (N)	Max. Shear Force (KN)	As % of straight model	Remarks
M-L30C0S0B6N1	30	0	0	6	1	2897	100%	**Varies within ±1%**
M-L30C0S15B6N1	30	0	15	6	1	2903	100%	
M-L30C0S30B6N1	30	0	30	6	1	2909	100%	
M-L30C0S45B6N1	30	0	45	6	1	2924	101%	
M-L30C12S0B6N1	30	12	0	6	1	2900	100%	

Model ID	Span length (L in m)	Central Angle (α °)	Skew Angle (θ °)	Bottom Width, (B) (m)	Number of Cell (N)	Max. Shear Force (KN)	As % of straight model	Remarks
M-L30C12S15B6N1	30	12	15	6	1	2920	101%	
M-L30C12S30B6N1	30	12	30	6	1	2915	101%	
M-L30C12S45B6N1	30	12	45	6	1	2907	100%	
M-L30C24S0B6N1	30	24	0	6	1	2861	99%	
M-L30C24S15B6N1	30	24	15	6	1	2900	100%	
M-L30C24S30B6N1	30	24	30	6	1	2894	100%	
M-L30C24S45B6N1	30	24	45	6	1	2881	99%	
M-L30C36S0B6N1	30	36	0	6	1	2900	100%	
M-L30C36S15B6N1	30	36	15	6	1	2920	101%	
M-L30C36S30B6N1	30	36	30	6	1	2912	101%	
M-L30C36S45B6N1	30	36	45	6	1	2893	100%	

Table 14: Maximum DL Shear Force for B6N2

Model ID	Span length (L in m)	Central Angle (α °)	Skew Angle (θ°)	Bottom Width, (B) (m)	Number of Cell (N)	Max. Shear Force (KN)	As % of straight model	Remarks
M-L30C0S0B6N2	30	0	0	6	2	3348	100%	Varies within ±1%
M-L30C0S15B6N2	30	0	15	6	2	3350	100%	
M-L30C0S30B6N2	30	0	30	6	2	3356	100%	
M-L30C0S45B6N2	30	0	45	6	2	3369	101%	
M-L30C12S0B6N2	30	12	0	6	2	3348	100%	
M-L30C12S15B6N2	30	12	15	6	2	3339	100%	
M-L30C12S30B6N2	30	12	30	6	2	3338	100%	
M-L30C12S45B6N2	30	12	45	6	2	3338	100%	
M-L30C24S0B6N2	30	24	0	6	2	3320	99%	
M-L30C24S15B6N2	30	24	15	6	2	3331	99%	
M-L30C24S30B6N2	30	24	30	6	2	3342	100%	

Model ID	Span length (L in m)	Central Angle (α °)	Skew Angle (θ°)	Bottom Width, (B) (m)	Number of Cell (N)	Max. Shear Force (KN)	As % of straight model	Remarks
M-L30C24S45B6N2	30	24	45	6	2	3341	100%	
M-L30C36S0B6N2	30	36	0	6	2	3348	100%	
M-L30C36S15B6N2	30	36	15	6	2	3360	100%	
M-L30C36S30B6N2	30	36	30	6	2	3351	100%	
M-L30C36S45B6N2	30	36	45	6	2	3334	100%	

So, for all the four groups, it is noticed that the shear force due to dead load has almost no impact with curvature and skewness.

6.1.4 Effect on Joint Reaction/Bearing Force:

Bearing is a very complex component of bridge, as it simulates the support condition and negotiates the movement of the bridge due to environmental force. More or less all bearings deteriorate with time. Hence, bearings were always been a major concern for bridge engineers. The scenario becomes worse when skewness or curvature is introduced in a bridge leading to unequal joint reaction. The variation of joint reaction due to curvature and skewness has been studied for all the four groups and presented below in tabular format. R is denoted for Joint Reaction.

Table 15: DL Joint Reaction B5N1

Model ID	Obtuse Corner			Central Joint			Acute Corner		
	R Max (KN)	As % of straight model	Remarks	R (KN)	As % of straight model	Remarks	R Min (KN)	As % of straight model	Remarks
M-L30C0S0B5N1	1462	100%	Increases with Skewness	NA	NA	NA	1462	100%	Decreases with Skewness
M-L30C0S15B5N1	1928	132%		NA	NA	NA	1001	68%	
M-L30C0S30B5N1	2334	160%		NA	NA	NA	612	42%	
M-L30C0S45B5N1	2592	177%		NA	NA	NA	391	27%	
M-L30C12S0B5N1	1787	122%	Increases with	NA	NA	NA	1137	78%	Decreases with

Model ID	Obtuse Corner			Central Joint			Acute Corner		
	R Max (KN)	As % of straight model	Remarks	R (KN)	As % of straight model	Remarks	R Min (KN)	As % of straight model	Remarks
M-L30C12S15B5N1	1869	128%	Skewness and Curvature	NA	NA	NA	1057	72%	Skewness and Curvature
M-L30C12S30B5N1	1974	135%		NA	NA	NA	963	66%	
M-L30C12S45B5N1	2132	146%		NA	NA	NA	823	56%	
M-L30C24S0B5N1	2123	145%		NA	NA	NA	801	55%	
M-L30C24S15B5N1	2238	153%		NA	NA	NA	689	47%	
M-L30C24S30B5N1	2395	164%		NA	NA	NA	541	37%	
M-L30C24S45B5N1	2648	181%		NA	NA	NA	303	21%	
M-L30C36S0B5N1	2477	169%		NA	NA	NA	447	31%	
M-L30C36S15B5N1	2652	181%		NA	NA	NA	275	19%	
M-L30C36S30B5N1	2903	199%		NA	NA	NA	32	2%	
M-L30C36S45B5N1	3347	229%		NA	NA	NA	-402	-28%	

Table 16: DL Joint Reaction B5N2

Model ID	Obtuse Corner			Central Joint			Acute Corner		
	R Max (KN)	As % of straight model	Remarks	R (KN)	As % of straight model	Remarks	R Min (KN)	As % of straight model	Remarks
M-L30C0S0B5N2	1080	100%	Increases with Skewness	1204	100%	Decreases with Skewness	1080	100%	Decreases with Skewness
M-L30C0S15B5N2	1641	152%		1157	96%		570	53%	
M-L30C0S30B5N2	2180	202%		1020	85%		182	17%	
M-L30C0S45B5N2	2575	238%		827	69%		13	1%	
M-L30C12S0B5N2	1444	134%	Increases with Skewness and Curvature	1215	101%	Increases with Skewness and Curvature	703	65%	Decreases with Skewness and Curvature
M-L30C12S15B5N2	1507	140%		1250	104%		607	56%	
M-L30C12S30B5N2	1531	142%		1404	117%		439	41%	
M-L30C12S45B5N2	1491	138%		1775	147%		123	11%	

Model ID	Obtuse Corner			Central Joint			Acute Corner		
	R Max (KN)	As % of straight model	Remarks	R (KN)	As % of straight model	Remarks	R Min (KN)	As % of straight model	Remarks
M-L30C24S0B5N2	1819	168%		1232	102%		311	29%	
M-L30C24S15B5N2	1894	175%		1318	109%		154	14%	
M-L30C24S30B5N2	1933	179%		1548	129%		-109	-10%	
M-L30C24S45B5N2	1902	176%		2081	173%		-598	-55%	
M-L30C36S0B5N2	2227	206%		1225	102%		-90	-8%	
M-L30C36S15B5N2	2351	218%		1345	112%		-332	-31%	
M-L30C36S30B5N2	2449	227%		1661	138%		-739	-68%	
M-L30C36S45B5N2	2496	231%		2426	201%		-1541	-143%	

Table 17: DL Joint Reaction B6N1

Model ID	Obtuse Corner			Central Joint			Acute Corner		
	R Max (KN)	As % of straight model	Remarks	R (KN)	As % of straight model	Remarks	R Min (KN)	As % of straight model	Remarks
M-L30C0S0B6N1	1507	100%		NA	NA	NA	1507	100%	
M-L30C0S15B6N1	1975	131%	Increases with Skewness	NA	NA	NA	1045	69%	Decreases with Skewness
M-L30C0S30B6N1	2369	157%		NA	NA	NA	673	45%	
M-L30C0S45B6N1	2600	172%		NA	NA	NA	486	32%	
M-L30C12S0B6N1	1789	119%		NA	NA	NA	1226	81%	
M-L30C12S15B6N1	1870	124%		NA	NA	NA	1148	76%	
M-L30C12S30B6N1	1974	131%	Increases with Skewness and Curvature	NA	NA	NA	1056	70%	Decreases with Skewness and Curvature
M-L30C12S45B6N1	2132	141%		NA	NA	NA	921	61%	
M-L30C24S0B6N1	2080	138%		NA	NA	NA	934	62%	
M-L30C24S15B6N1	2190	145%		NA	NA	NA	828	55%	
M-L30C24S30B6N1	2340	155%		NA	NA	NA	688	46%	

Model ID	Obtuse Corner			Central Joint			Acute Corner		
	R Max (KN)	As % of straight model	Remarks	R (KN)	As % of straight model	Remarks	R Min (KN)	As % of straight model	Remarks
M-L30C24S45B6N1	2585	172%		NA	NA	NA	462	31%	
M-L30C36S0B6N1	2387	158%		NA	NA	NA	627	42%	
M-L30C36S15B6N1	2549	169%		NA	NA	NA	469	31%	
M-L30C36S30B6N1	2783	185%		NA	NA	NA	245	16%	
M-L30C36S45B6N1	3199	212%		NA	NA	NA	-158	-10%	

Table 18: DL Joint Reaction B6N2

Model ID	Obtuse Corner			Central Joint			Acute Corner		
	R Max (KN)	As % of straight model	Remarks	R (KN)	As % of straight model	Remarks	R Min (KN)	As % of straight model	Remarks
M-L30C0S0B6N2	1112	100%	Increases with Skewness	1226	100%	Decreases with Skewness	1112	100%	Decreases with Skewness
M-L30C0S15B6N2	1669	150%		1176	96%		610	55%	
M-L30C0S30B6N2	2189	197%		1039	85%		246	22%	
M-L30C0S45B6N2	2534	228%		875	71%		103	9%	
M-L30C12S0B6N2	1425	128%	Increases with Skewness and Curvature	1237	101%	Increases with Skewness and Curvature	787	71%	Decreases with Skewness and Curvature
M-L30C12S15B6N2	1477	133%		1291	105%		684	62%	
M-L30C12S30B6N2	1479	133%		1484	121%		500	45%	
M-L30C12S45B6N2	1403	126%		1924	157%		156	14%	
M-L30C24S0B6N2	1758	158%		1233	101%		459	41%	
M-L30C24S15B6N2	1807	163%		1355	111%		291	26%	
M-L30C24S30B6N2	1817	163%		1628	133%		18	2%	
M-L30C24S45B6N2	1738	156%		2229	182%		-490	-44%	
M-L30C36S0B6N2	2096	188%		1252	102%		101	9%	
M-L30C36S15B6N2	2191	197%		1399	114%		-138	-12%	
M-L30C36S30B6N2	2243	202%		1764	144%		-547	-49%	
M-L30C36S45B6N2	2211	199%		2602	212%		-1343	-121%	

Discussion: It is observed that the vertical reaction becomes unequal with introduction of curvature and skewness. When no curvature is introduced, increase/decrease of the vertical reaction is 72% (B6N1) to (B5N1) 75% for a single cell structure. But, for double cell structure the increase in reaction due to skewness only is observed as 138% (B5N2) and 128% (B6N2) and decrease in reaction is observed as 99% (B5N2) to (B6N2) 91% for single cell models. When, curvature is introduced, the difference in reactions increases further causes uplift at one acute corner and 2 to 2.4 time reactions at adjacent obtuse corner.

The reaction at central joints also decreased with skewness up to 30% and increases further when curvature is introduced.

6.1.5 Effect on Maximum Deflection:

For the same structure, deflection shows a variation when skewness and curvature is introduced. Maximum deflection near mid span has been considered. The study is presented below in tabular format.

Table 19: DL Deflection for B5N1

Model ID	Span length (L in m)	Central Angle (α °)	Skew Angle, (θ °)	Bottom Width, (B) (m)	Number of Cell (N)	Deflection (mm)	As % of straight model	Remarks
M-L30C0S0B5N1	30	0	0	5	1	9.6	100%	Decreases with Skewness
M-L30C0S15B5N1	30	0	15	5	1	9.3	97%	
M-L30C0S30B5N1	30	0	30	5	1	8.4	88%	
M-L30C0S45B5N1	30	0	45	5	1	6.9	72%	
M-L30C12S0B5N1	30	12	0	5	1	9.8	102%	Increases with curvature and Skewness.
M-L30C12S15B5N1	30	12	15	5	1	10.3	107%	
M-L30C12S30B5N1	30	12	30	5	1	11.0	115%	
M-L30C12S45B5N1	30	12	45	5	1	12.5	130%	
M-L30C24S0B5N1	30	24	0	5	1	10.4	108%	
M-L30C24S15B5N1	30	24	15	5	1	11.4	119%	
M-L30C24S30B5N1	30	24	30	5	1	13.1	136%	

Model ID	Span length (L in m)	Central Angle (α °)	Skew Angle, (θ °)	Bottom Width, (B) (m)	Number of Cell (N)	Deflection (mm)	As % of straight model	Remarks
M-L30C24S45B5N1	30	24	45	5	1	16.5	172%	
M-L30C36S0B5N1	30	36	0	5	1	11.3	118%	
M-L30C36S15B5N1	30	36	15	5	1	13.1	136%	
M-L30C36S30B5N1	30	36	30	5	1	16.3	170%	
M-L30C36S45B5N1	30	36	45	5	1	23.7	247%	

Table 20: DL Deflection for B5N2

Model ID	Span length (L in m)	Central Angle (α °)	Skew Angle, (θ °)	Bottom Width, (B) (m)	Number of Cell (N)	Deflection (mm)	As % of straight model	Remarks
M-L30C0S0B5N2	30	0	0	5	2	12.1	100%	Decreases with Skewness
M-L30C0S15B5N2	30	0	15	5	2	11.7	97%	
M-L30C0S30B5N2	30	0	30	5	2	10.5	87%	
M-L30C0S45B5N2	30	0	45	5	2	8.4	69%	
M-L30C12S0B5N2	30	12	0	5	2	12.9	107%	Increases with curvature and Skewness.
M-L30C12S15B5N2	30	12	15	5	2	14.5	120%	
M-L30C12S30B5N2	30	12	30	5	2	16.8	139%	
M-L30C12S45B5N2	30	12	45	5	2	20.7	171%	
M-L30C24S0B5N2	30	24	0	5	2	14.2	117%	
M-L30C24S15B5N2	30	24	15	5	2	16.8	139%	
M-L30C24S30B5N2	30	24	30	5	2	20.6	170%	
M-L30C24S45B5N2	30	24	45	5	2	28.2	233%	
M-L30C36S0B5N2	30	36	0	5	2	16.0	132%	
M-L30C36S15B5N2	30	36	15	5	2	19.9	164%	
M-L30C36S30B5N2	30	36	30	5	2	26.4	218%	
M-L30C36S45B5N2	30	36	45	5	2	41.4	342%	

Table 21: DL Deflection for B6N1

Model ID	Span length (L in m)	Central Angle (α °)	Skew Angle, (θ °)	Bottom Width, (B) (m)	Number of Cell (N)	Deflection (mm)	As % of straight model	Remarks
M-L30C0S0B6N1	30	0	0	6	1	9.01	100%	Decreases with Skewness
M-L30C0S15B6N1	30	0	15	6	1	9.27	103%	
M-L30C0S30B6N1	30	0	30	6	1	8.35	93%	
M-L30C0S45B6N1	30	0	45	6	1	6.6	73%	
M-L30C12S0B6N1	30	12	0	6	1	9.5	105%	Increases with curvature and Skewness.
M-L30C12S15B6N1	30	12	15	6	1	10	111%	
M-L30C12S30B6N1	30	12	30	6	1	10.8	120%	
M-L30C12S45B6N1	30	12	45	6	1	12.3	137%	
M-L30C24S0B6N1	30	24	0	6	1	9.9	110%	
M-L30C24S15B6N1	30	24	15	6	1	10.9	121%	
M-L30C24S30B6N1	30	24	30	6	1	12.6	140%	
M-L30C24S45B6N1	30	24	45	6	1	16.1	179%	
M-L30C36S0B6N1	30	36	0	6	1	10.8	120%	
M-L30C36S15B6N1	30	36	15	6	1	12.6	140%	
M-L30C36S30B6N1	30	36	30	6	1	15.7	174%	
M-L30C36S45B6N1	30	36	45	6	1	23.0	255%	

Table 22: DL Deflection for B6N2

Model ID	Span length (L in m)	Central Angle (α °)	Skew Angle, (θ °)	Bottom Width, (B) (m)	Number of Cell (N)	Deflection (mm)	As % of straight model	Remarks
M-L30C0S0B6N2	30	0	0	6	2	11.8	100%	Decreases with Skewness
M-L30C0S15B6N2	30	0	15	6	2	11.2	95%	
M-L30C0S30B6N2	30	0	30	6	2	9.9	84%	
M-L30C0S45B6N2	30	0	45	6	2	7.7	65%	

Model ID	Span length (L in m)	Central Angle (α °)	Skew Angle, (θ °)	Bottom Width, (B) (m)	Number of Cell (N)	Deflection (mm)	As % of straight model	Remarks
M-L30C12S0B6N2	30	12	0	6	2	12.5	106%	Increases with curvature and Skewness.
M-L30C12S15B6N2	30	12	15	6	2	14.3	121%	
M-L30C12S30B6N2	30	12	30	6	2	16.8	142%	
M-L30C12S45B6N2	30	12	45	6	2	21.1	179%	
M-L30C24S0B6N2	30	24	0	6	2	13.7	116%	
M-L30C24S15B6N2	30	24	15	6	2	16.4	139%	
M-L30C24S30B6N2	30	24	30	6	2	20.5	174%	
M-L30C24S45B6N2	30	24	45	6	2	28.6	242%	
M-L30C36S0B6N2	30	36	0	6	2	15.5	131%	
M-L30C36S15B6N2	30	36	15	6	2	19.6	166%	
M-L30C36S30B6N2	30	36	30	6	2	26.3	223%	
M-L30C36S45B6N2	30	36	45	6	2	42.0	356%	

Discussion: Generally, deflection shows almost a same variation with BM when the bridge is skew, curve or skew curved. It is found that, deflection reduces with skewness for skew bridges (Up to 25%). When Curvature comes into picture, deflection increases. For Skew-curved bridges the deflection increases 2.5 times for single cell bridges and 3.5 times for double cell bridges.

6.2 Effect of curvature and skewness:-Class 70R Wheel Load:

The effect on various bridge responses, i.e. bending moment diagram and absolute bending moment, torsional moment and its absolute value, shear force and its absolute value and joint reaction/bearing forces, for Class 70R vehicular live load due to curvature and skewness is studied and described below.

6.2.1 Effect on Bending Moment:

The basic bridge response, on which bridge engineers are interested, is the bending moment. The curvature and skewness in a box girder bridge not only affects the absolute

value of bending moment but also the bending moment pattern. Maximum/minimum envelope has been obtained from analysis. However, maximum envelope has been considered for study, as maximum envelopes give the governing response. Effect on both the bending moment diagram and absolute bending moment due to curvature and skewness is presented below.

6.2.1.1 Variation of Bending Moment diagram due to skewness:

Effect on bending moment diagram for variation in skewness has been plotted and explained graphically for all the four groups as described above.

B5N1:

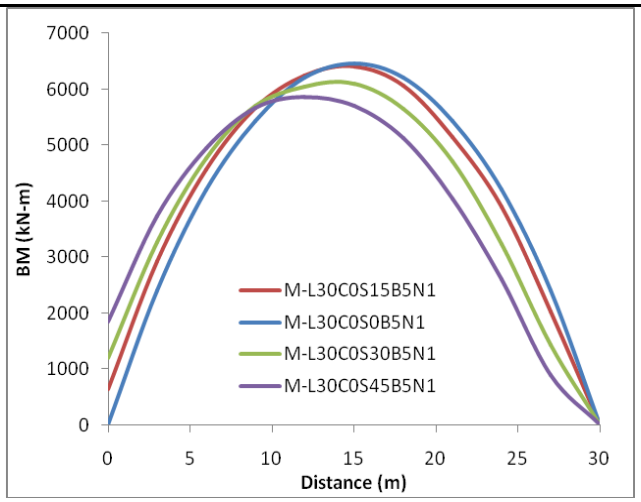

Plot- 5:B=5; N=1; α=0°

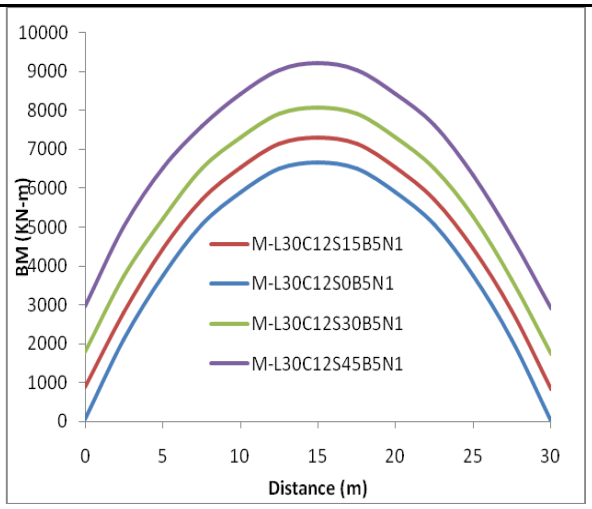

Plot- 6:B=5; N=1; α =12°

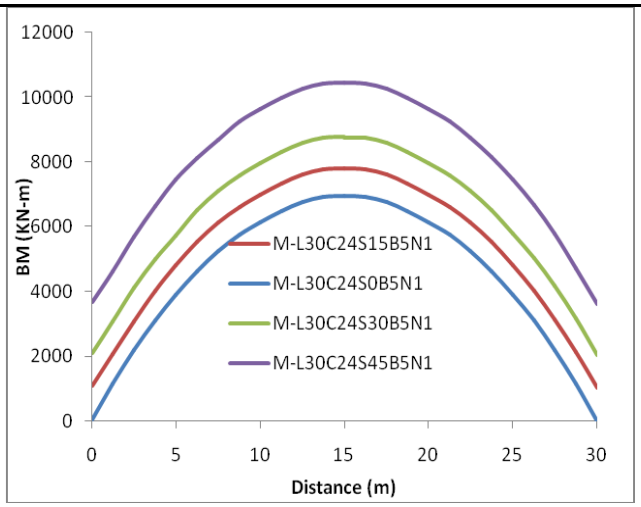

Plot- 7:B=5; N=1; α =24°

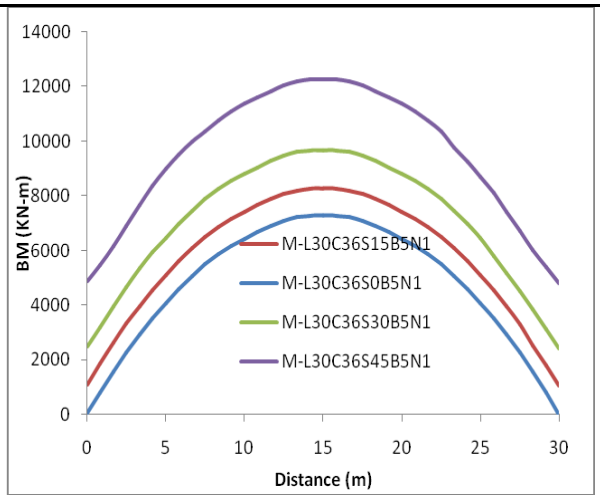

Plot- 8:B=5; N=1; α=36°

Discussion: The critical section of the BM diagram towards LHS for skew bridge (α=0°). For 45 °skew bridge, the critical section shifts almost 33%. The BM value (upto 9%) decreses with increase in skewness when the curvature is zero. When curvature is introduced, the value of BM increases gradually with skewness . For α=36°, the BM value increases upto 68% .

B5N2:

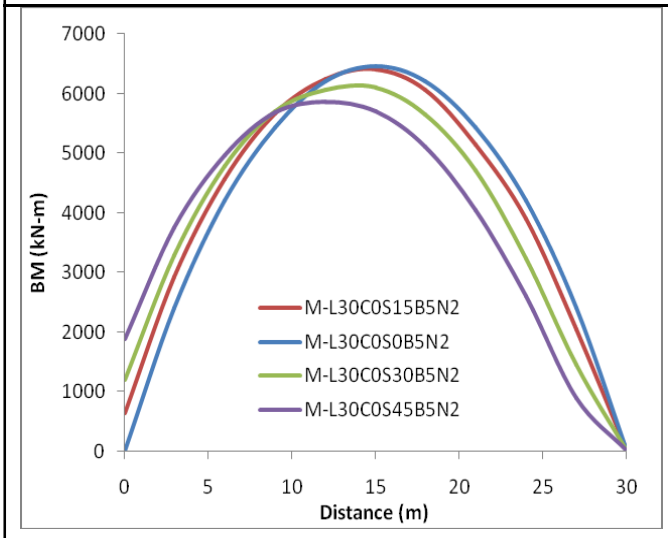

Plot- 5:B=5; N=2; α=0°

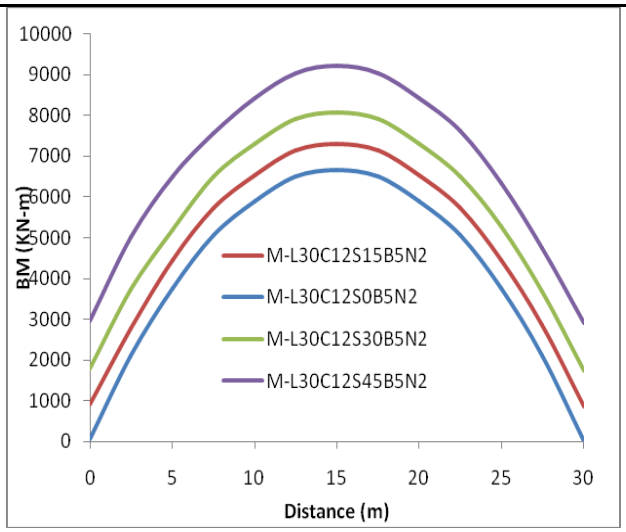

Plot- 6:B=5; N=2; α =12°

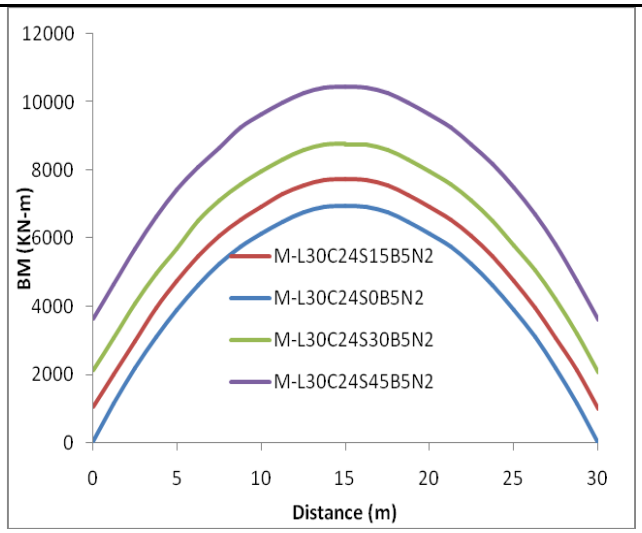

Plot- 7:B=5; N=2; α =24°

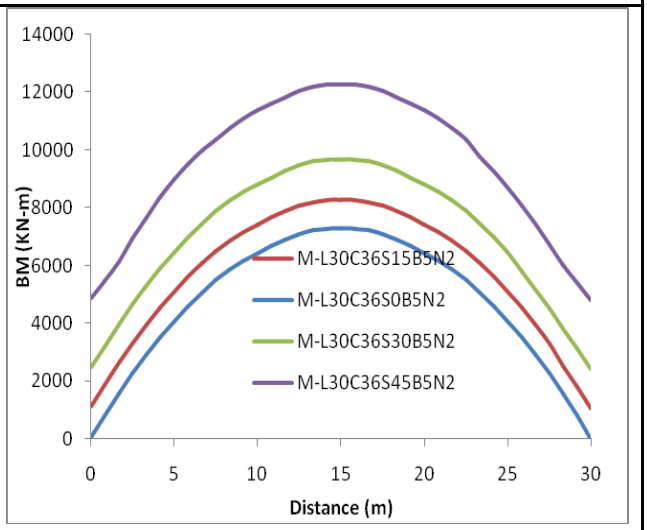

Plot- 8:B=5; N=2; α=36°

Discussion: The critical section of the BM diagram towards LHS for skew bridge (α=0°). For 45 °skew bridge, the critical section shifts almost 33%. The BM value (upto 9%) decreses with increase in skewness when the curvature is zero. When curvature is introduced, the value of BM increases gradually with skewness . For α=36°, the BM value increases upto 68% .

B6N1:

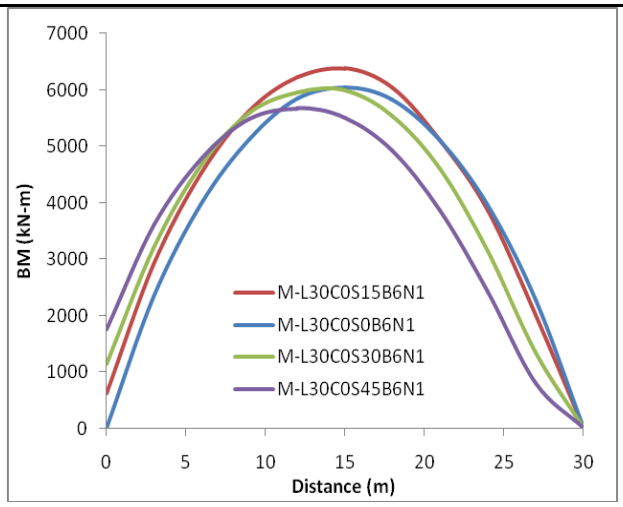

Plot- 9:B=6; N=1; α=0°

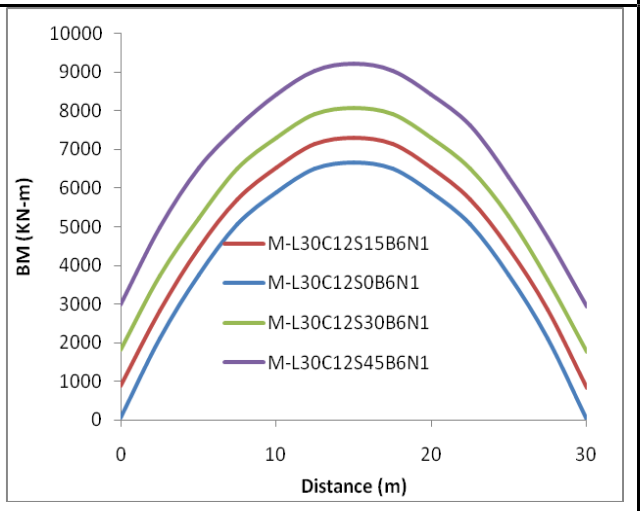

Plot- 10:B=6; N=1; α =12°

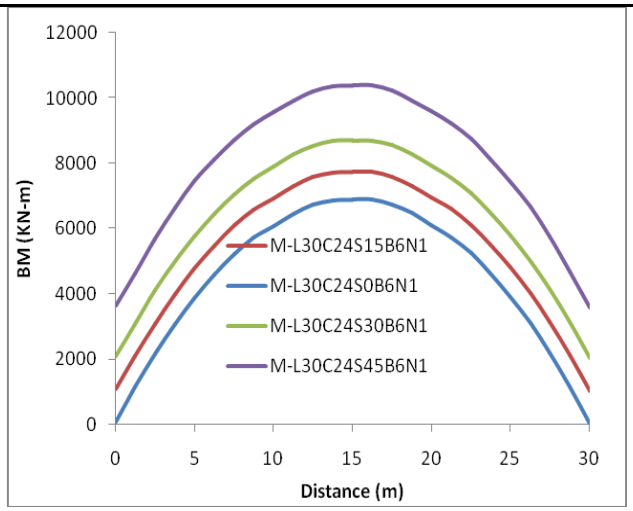

Plot- 11:B=6; N=1; α =24°

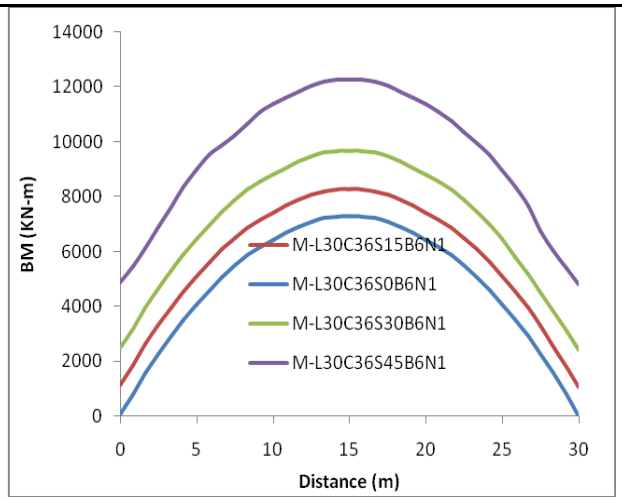

Plot- 12:B=5; N=1; α=36°

Discussion: The critical section of the BM diagram towards LHS for skew bridge (α=0°). For 45 °skew bridge, the critical section shifts almost 33%. The BM value (upto 6%) decreses with increase in skewness when the curvature is zero. When curvature is introduced, the value of BM increases gradually with skewness . For α=36°, the BM value increases upto 68% .

B6N2:

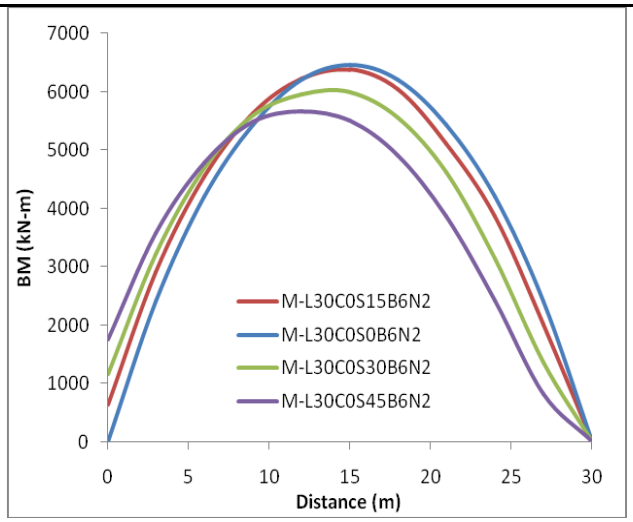

Plot- 13:B=6; N=2; α=0°

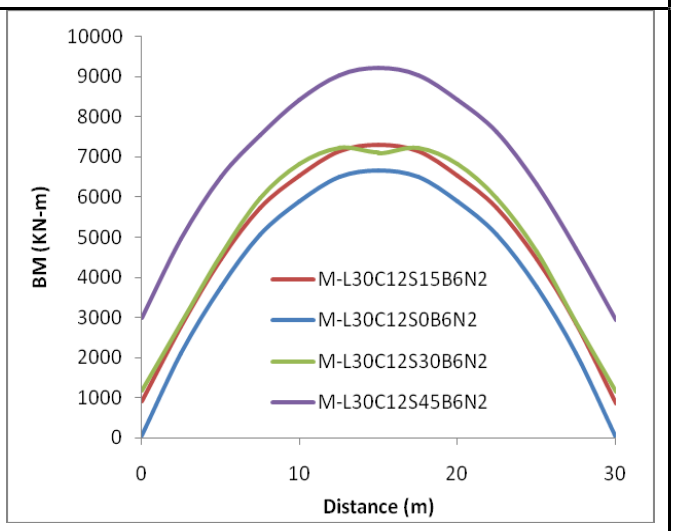

Plot- 14:B=6; N=2; α =12°

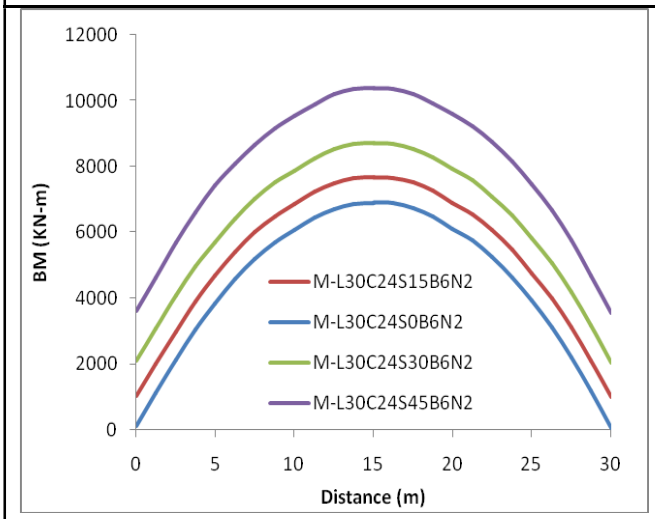

Plot- 15:B=6; N=2; α =24°

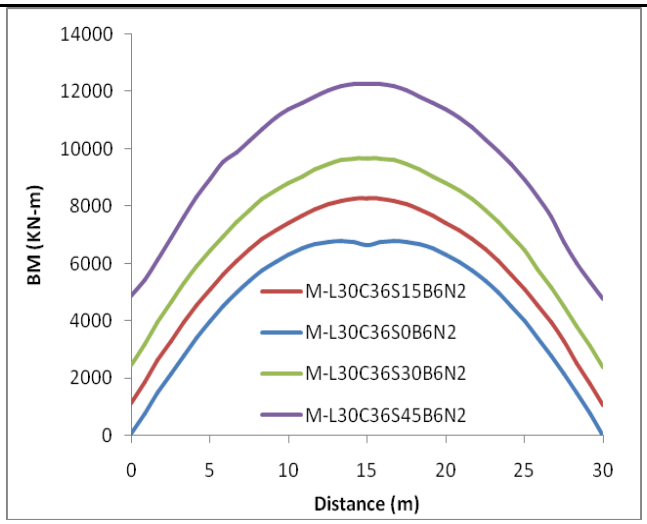

Plot- 16:B=6; N=2; α=36°

Discussion: The critical section of the BM diagram towards LHS for skew bridge (α=0°). For 45 °skew bridge, the critical section shifts almost 33%. The BM value (upto 12%) decreses with increase in skewness when the curvature is zero. When curvature is introduced, the value of BM increases gradually with skewness . For α=36°, the BM value increases upto 68% .

It has been seen that the critical section 33% from LHS. This is also possible to obtain that shifting 33% towards RHS via modeling the bridge with opposite end. Hence, when for purely skew box girder bridges, the critical section shifts ±33%.

6.2.1.2 Variation of Bending Moment diagram due to Curvature:

Effect on bending moment diagram for variation in curvature has been plotted and explained graphically for all the four groups as described above.

B5N1:

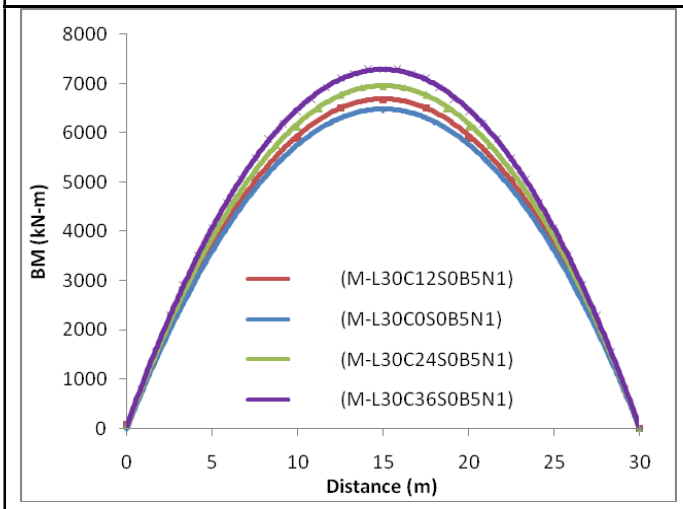

Plot- 17:B=5; N=1; θ=0°

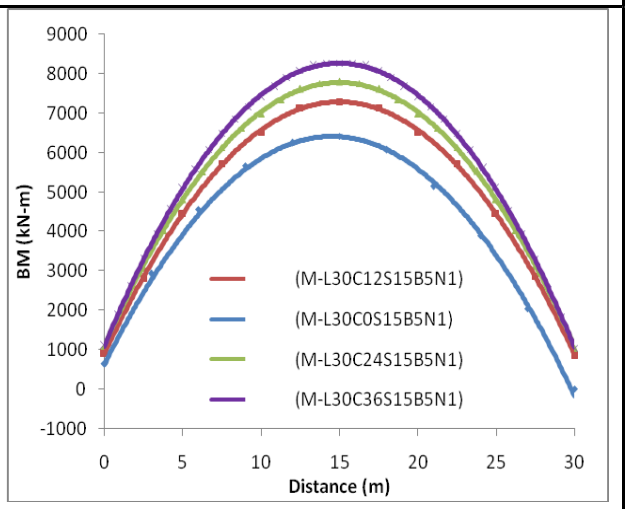

Plot- 18:B=5; N=1; θ =15°

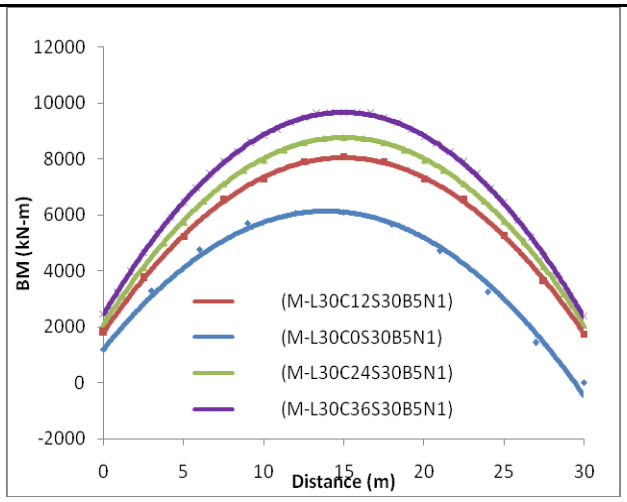

Plot- 19:B=5; N=1; θ =30°

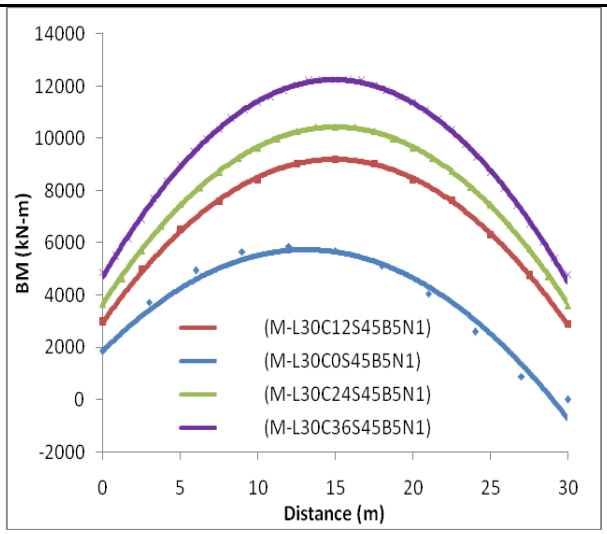

Plot- 20:B=5; N=1; θ=45°

Discussion: The BM pattern remains almost same, except the shfting of critical section for purely skew bridges. The BM value increases with increase in curvature. This increment is 13%, when the skewness is zero. When skewness is introduced, the value of BM increases with curvature rapidly. For θ=45°, the BM increases upto 109% with curvature.

B5N2:

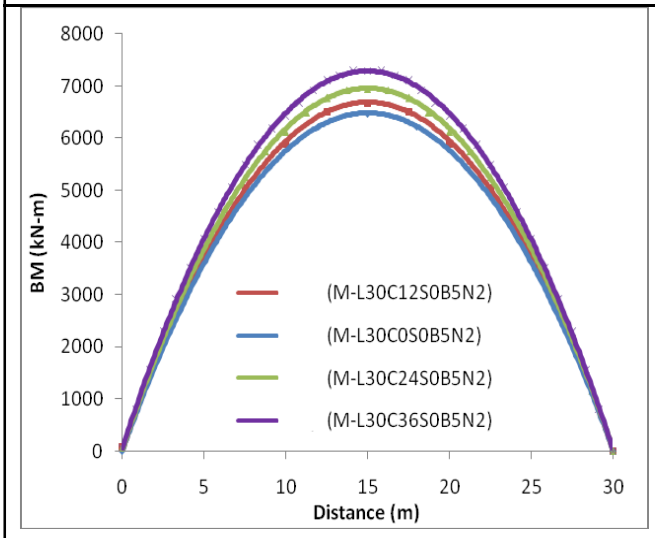

Plot- 21:B=5; N=2; θ=0°

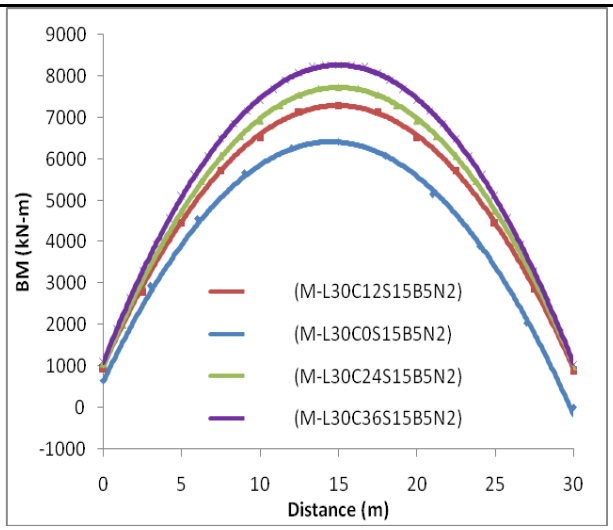

Plot- 22:B=5; N=2; θ =15°

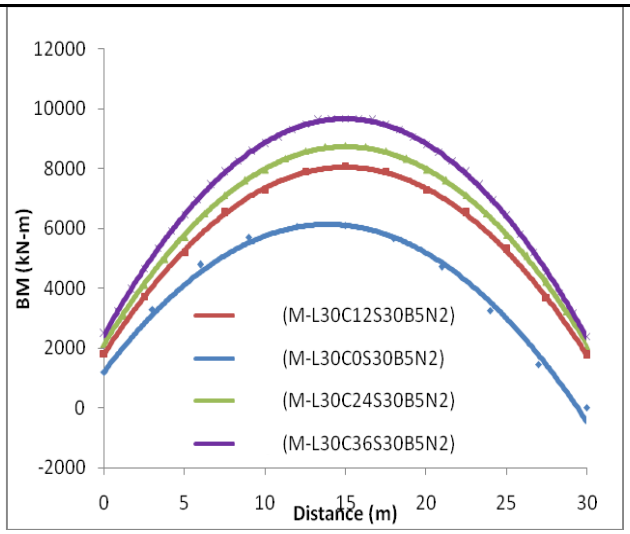

Plot- 23:B=5; N=2; θ =30°

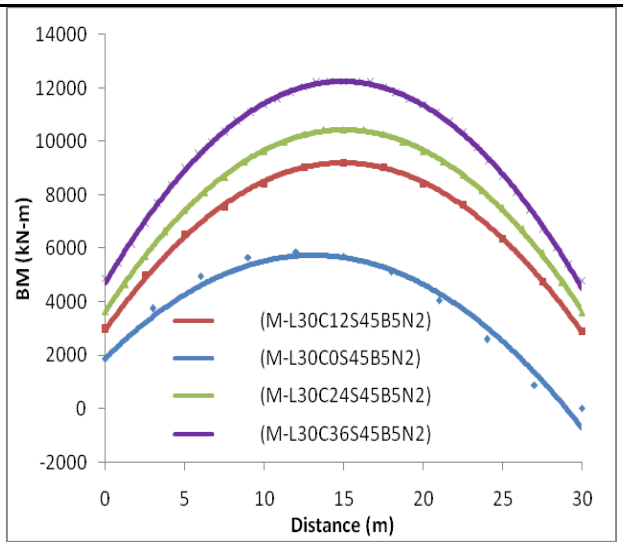

Plot- 24:B=5; N=2; θ=45°

Discussion: The BM pattern remains almost same, except the shfting of critical section for purely skew bridges. The BM value increases with increase in curvature. This increment is 13%, when the skewness is zero. When skewness is introduced, the value of BM increases with curvature rapidly. For θ=45°, the BM increases upto 109% with curvature.

B6N1:

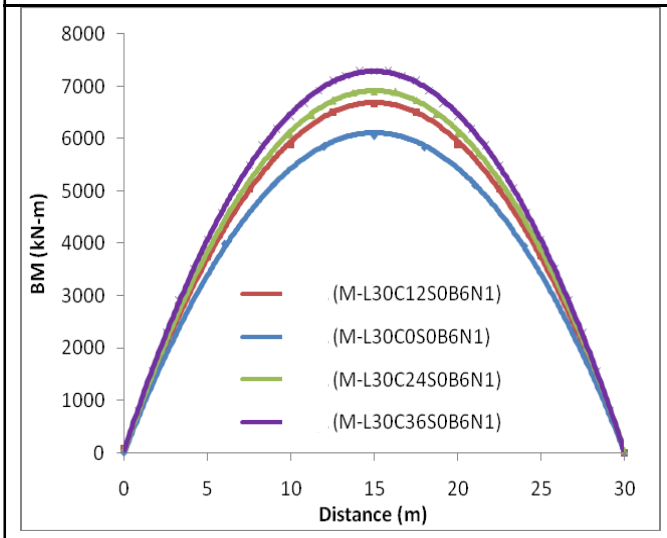

Plot- 25:B=6; N=1; θ=0°

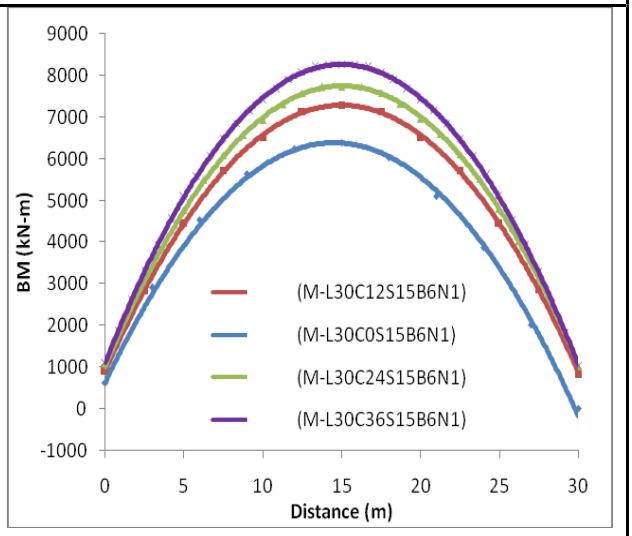

Plot- 26:B=6; N=1; θ =15°

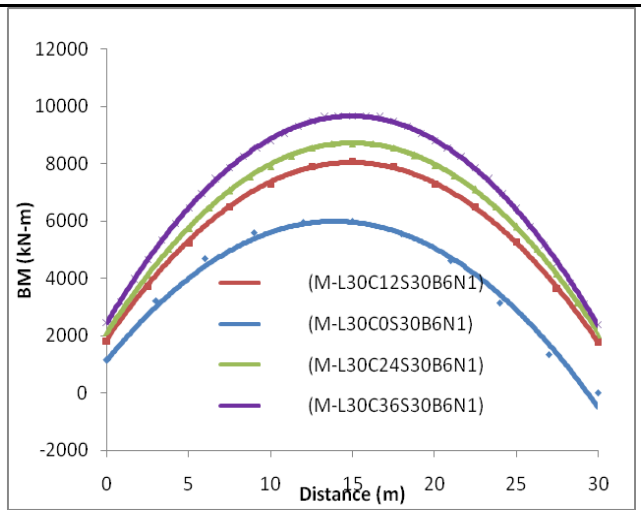

Plot- 27:B=6; N=1; θ =30°

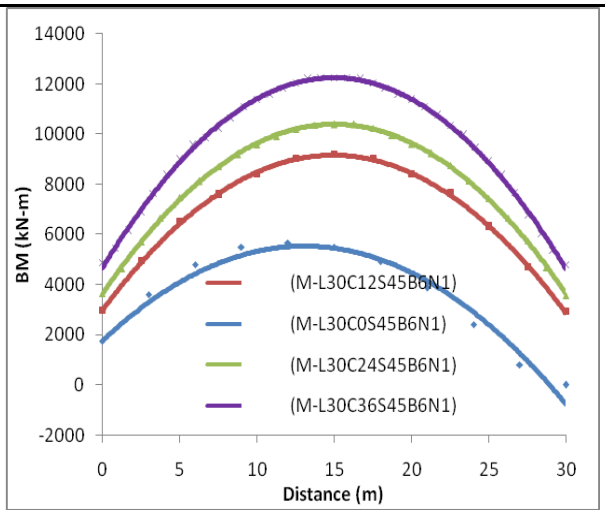

Plot- 28:B=6; N=1; θ=45°

Discussion: The BM pattern remains almost same, except the shfting of critical section for purely skew bridges. The BM value increases with increase in curvature. This increment is 20%, when the skewness is zero. When skewness is introduced, the value of BM increases with curvature rapidly. For θ=45°, the BM increases upto 117% with curvature.

B6N2:

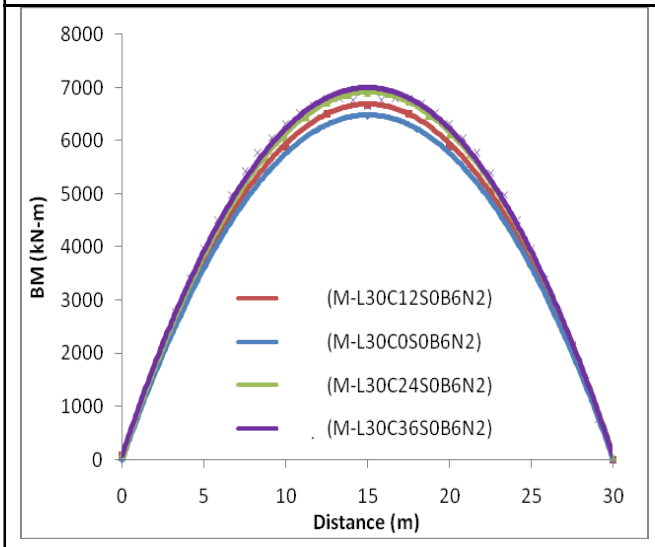

Plot- 29:B=6; N=2; θ=0°

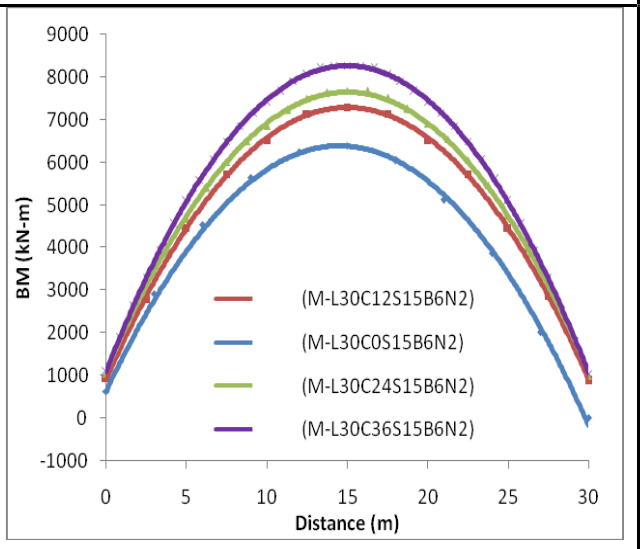

Plot- 30:B=6; N=2; θ =15°

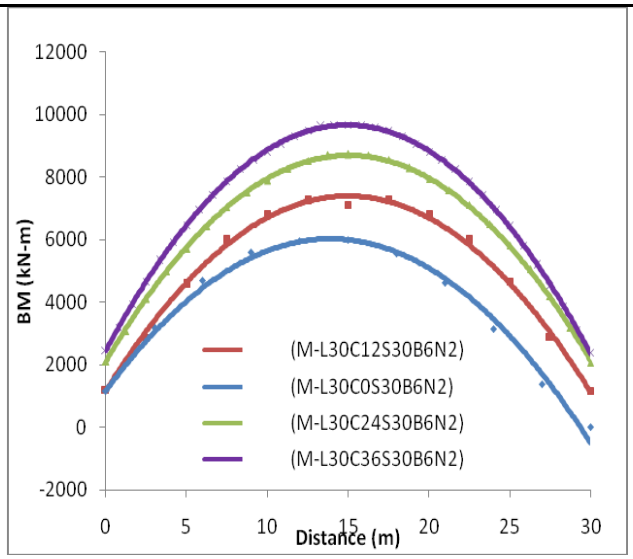

Plot- 31:B=6; N=2; θ =30°

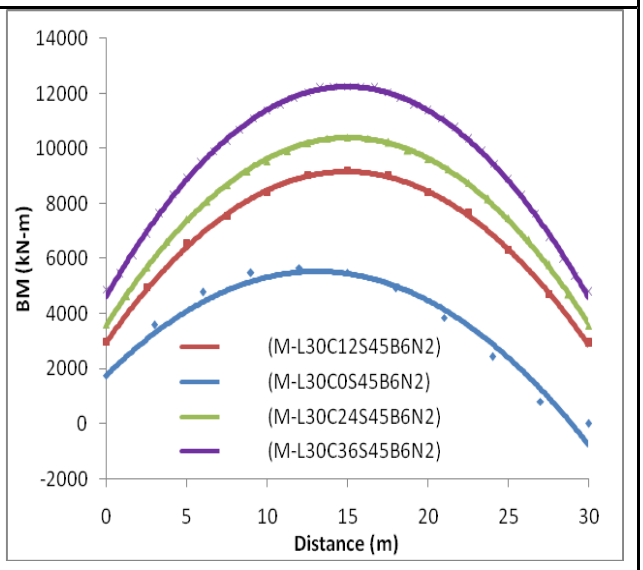

Plot- 32:B=6; N=2; θ=45°

Discussion: The BM pattern remains almost same, except the shfting of critical section for purely skew bridges. The BM value increases with increase in curvature. This increment is 20%, when the skewness is zero. When skewness is introduced, the value of BM increases with curvature rapidly. For θ=45°, the BM increases upto 117% with curvature.

6.2.1.3 Variation of Maximum Bending Moment:

Variation of maximum bending moment has been compared as a ratio to the maximum bending moment of the straight bridge for all the four groups. The comparison has been presented below.

Table 23: Maximum LL Bending Moment for B5N1

Model ID	Span length (L in m)	Central Angle (α °)	Skew Angle (θ °)	Bottom Width, (B) (m)	Number of Cell (N)	Max. Bending Moment (KN-m)	As % of straight model	Remarks
M-L30C0S0B5N1	30	0	0	5	1	6466	100%	Decreases with Skewness
M-L30C0S15B5N1	30	0	15	5	1	6409	99%	
M-L30C0S30B5N1	30	0	30	5	1	6097	94%	
M-L30C0S45B5N1	30	0	45	5	1	5866	91%	
M-L30C12S0B5N1	30	12	0	5	1	6674	103%	Increases with Skewness and Curvature
M-L30C12S15B5N1	30	12	15	5	1	7300	113%	
M-L30C12S30B5N1	30	12	30	5	1	8069	125%	
M-L30C12S45B5N1	30	12	45	5	1	9210	142%	
M-L30C24S0B5N1	30	24	0	5	1	6946	107%	
M-L30C24S15B5N1	30	24	15	5	1	7790	120%	
M-L30C24S30B5N1	30	24	30	5	1	8765	136%	
M-L30C24S45B5N1	30	24	45	5	1	10456	162%	
M-L30C36S0B5N1	30	36	0	5	1	7287	113%	
M-L30C36S15B5N1	30	36	15	5	1	8273	128%	
M-L30C36S30B5N1	30	36	30	5	1	9675	150%	
M-L30C36S45B5N1	30	36	45	5	1	12265	190%	

Table 24: Maximum LL Bending Moment for B5N2

Model ID	Span length (L in m)	Central Angle (α °)	Skew Angle, (θ°)	Bottom Width, (B) (m)	Number of Cell (N)	Max. Bending Moment (KN-m)	As % of straight model	Remarks
M-L30C0S0B5N2	30	0	0	5	2	6467	100%	Decreases with Skewness
M-L30C0S15B5N2	30	0	15	5	2	6412	99%	
M-L30C0S30B5N2	30	0	30	5	2	6101	94%	
M-L30C0S0B5N2	30	0	45	5	2	5866	91%	

Model ID	Span length (L in m)	Central Angle (α °)	Skew Angle, (θ°)	Bottom Width, (B) (m)	Number of Cell (N)	Max. Bending Moment (KN-m)	As % of straight model	Remarks
M-L30C12S0B5N2	30	12	0	5	2	6675	103%	Increases with Skewness and Curvature
M-L30C12S15B5N2	30	12	15	5	2	7300	113%	
M-L30C12S30B5N2	30	12	30	5	2	8069	125%	
M-L30C12S45B5N2	30	12	45	5	2	9210	142%	
M-L30C24S0B5N2	30	24	0	5	2	6947	107%	
M-L30C24S15B5N2	30	24	15	5	2	7732	120%	
M-L30C24S30B5N2	30	24	30	5	2	8766	136%	
M-L30C24S45B5N2	30	24	45	5	2	10457	162%	
M-L30C36S0B5N2	30	36	0	5	2	7287	113%	
M-L30C36S15B5N2	30	36	15	5	2	8274	128%	
M-L30C36S30B5N2	30	36	30	5	2	9676	150%	
M-L30C36S45B5N2	30	36	45	5	2	12266	190%	

Table 25: Maximum LL Bending Moment for B6N1

Model ID	Span length (L in m)	Central Angle (α °)	Skew Angle, (θ °)	Bottom Width, (B) (m)	Number of Cell (N)	Max. Bending Moment (KN-m)	As % of straight model	Remarks
M-L30C0S0B6N1	30	0	0	6	1	6047	100%	Decreases with Skewness
M-L30C0S15B6N1	30	0	15	6	1	6380	106%	
M-L30C0S30B6N1	30	0	30	6	1	5991	99%	
M-L30C0S45B6N1	30	0	45	6	1	5673	94%	
M-L30C12S0B6N1	30	12	0	6	1	6674	110%	Increases with Skewness and Curvature
M-L30C12S15B6N1	30	12	15	6	1	7300	121%	
M-L30C12S30B6N1	30	12	30	6	1	8069	133%	
M-L30C12S45B6N1	30	12	45	6	1	9210	152%	
M-L30C24S0B6N1	30	24	0	6	1	6895	114%	
M-L30C24S15B6N1	30	24	15	6	1	7735	128%	
M-L30C24S30B6N1	30	24	30	6	1	8707	144%	
M-L30C24S45B6N1	30	24	45	6	1	10389	172%	

Model ID	Span length (L in m)	Central Angle (α °)	Skew Angle, (θ °)	Bottom Width, (B) (m)	Number of Cell (N)	Max. Bending Moment (KN-m)	As % of straight model	Remarks
M-L30C36S0B6N1	30	36	0	6	1	7287	120%	
M-L30C36S15B6N1	30	36	15	6	1	8273	137%	
M-L30C36S30B6N1	30	36	30	6	1	9675	160%	
M-L30C36S45B6N1	30	36	45	6	1	12265	203%	

Table 26: Maximum LL Bending Moment for B6N2

Model ID	Span length (L in m)	Central Angle (α °)	Skew Angle, θ (°)	Bottom Width, (B) (m)	Number of Cell (N)	Max. Bending Moment (KN-m)	As % of straight model	Remarks
M-L30C0S0B6N2	30	0	0	6	2	6467	100%	Decreases with Skewness
M-L30C0S15B6N2	30	0	15	6	2	6384	99%	
M-L30C0S30B6N2	30	0	30	6	2	6000	93%	
M-L30C0S45B6N2	30	0	45	6	2	5664	88%	
M-L30C12S0B6N2	30	12	0	6	2	6675	103%	Increases with Skewness and Curvature
M-L30C12S15B6N2	30	12	15	6	2	7300	113%	
M-L30C12S30B6N2	30	12	30	6	2	8069	125%	
M-L30C12S45B6N2	30	12	45	6	2	9210	142%	
M-L30C24S0B6N2	30	24	0	6	2	6901	107%	
M-L30C24S15B6N2	30	24	15	6	2	7683	119%	
M-L30C24S30B6N2	30	24	30	6	2	8711	135%	
M-L30C24S45B6N2	30	24	45	6	2	10394	161%	
M-L30C36S0B6N2	30	36	0	6	2	7287	113%	
M-L30C36S15B6N2	30	36	15	6	2	8274	128%	
M-L30C36S30B6N2	30	36	30	6	2	9676	150%	
M-L30C36S45B6N2	30	36	45	6	2	12266	190%	

6.2.1.4 Variation of Maximum Bending Moment with "B" and "N":

Variation of Maximum Bending Moment with aspect ratio and number of cells has been presented below in bar chart.

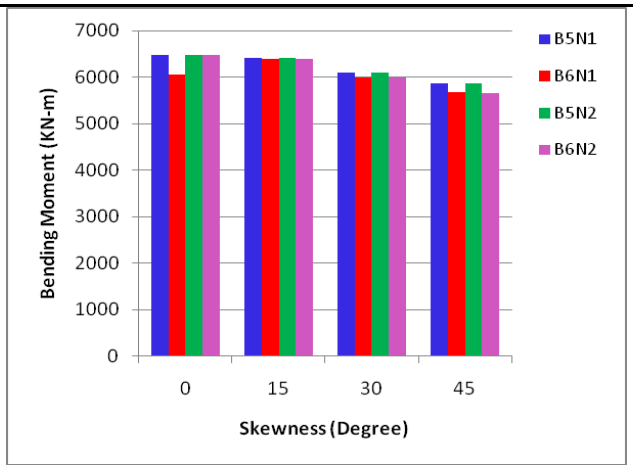

Plot- 1:α=0°

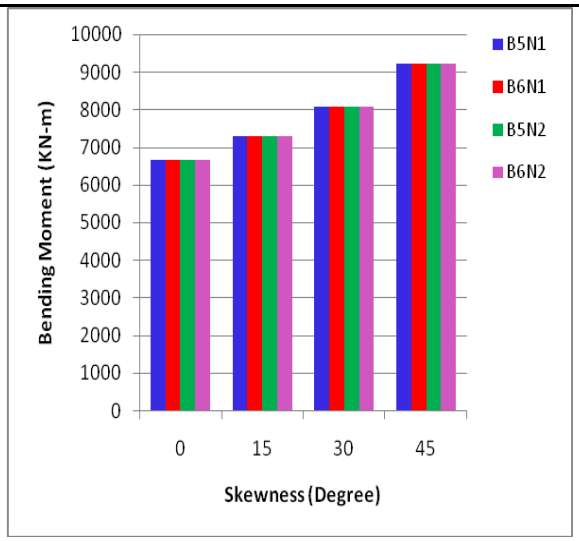

Plot- 2: α=12°

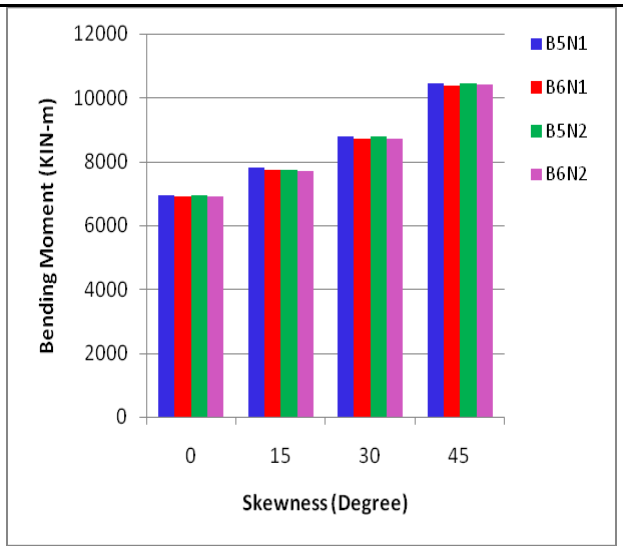

Plot- 3: α=24°

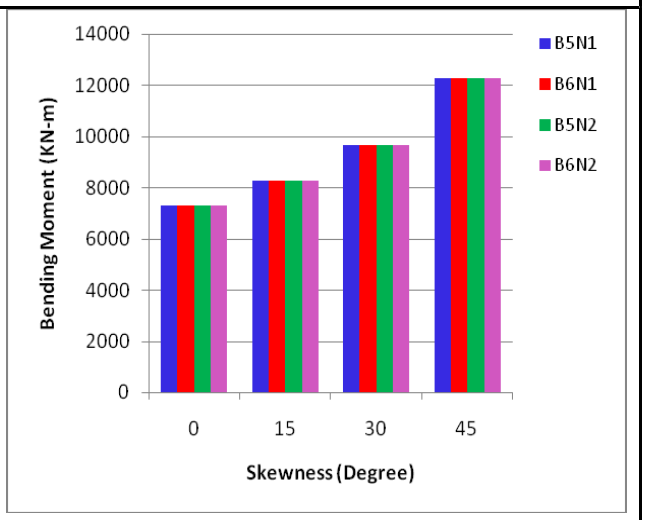

Plot- 4: α=36°

Discussion: It is seen that maximum BM differs slightly, when no curvature is introduced. But, it shows almost same response when curvature is introduced. However, the value decreases with increase in skewness for purely skew bridges but increases with both curvature and skewness for skew-curved bridges.

6.2.2 Effect on Torsional Moment:

Another important bridge response for curved, skew and skew-curved bridge is the torsional moment. The curvature and skewness in a box girder bridge affects both the absolute value of torsional moment but and the torsional moment pattern. An important point to note that the bridge is symmetrical with respect to torsional rigidity, any of the maximum/minimum envelopes for torsion will correctly represent the torsional moment pattern. Hence, maximum torsional moment has been considered in this study. Minimum envelope is the anti-symmetric of the maximum envelope. Effect on both the torsional moment diagram and absolute torsional moment due to curvature and skewness is presented below.

6.2.2.1 Variation of Torsional Moment diagram due to skewness:

Effect on torsional moment diagram for variation in skewness has been plotted and explained graphically for all the four groups as described above.

B5N1:

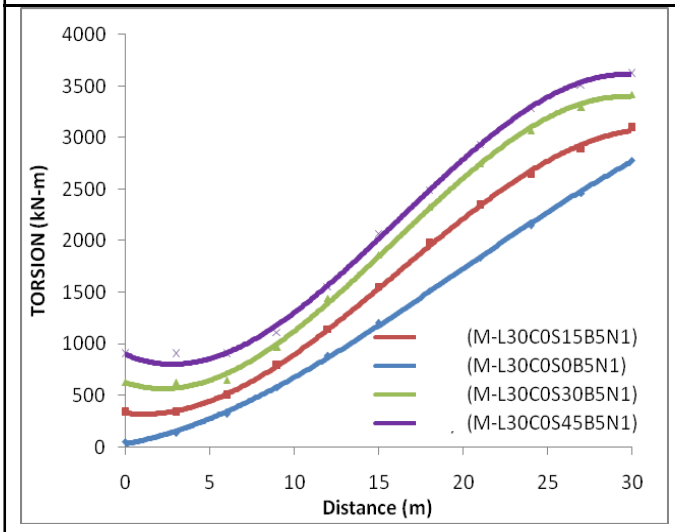

Plot- 1:B=5; N=1; α=0°

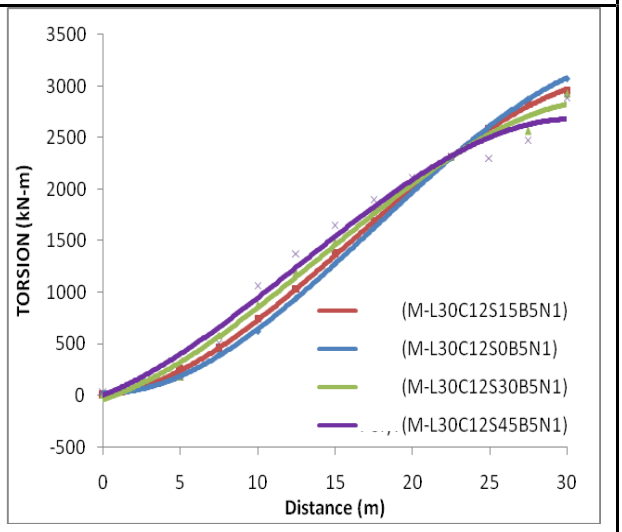

Plot- 2:B=5; N=1; α =12°

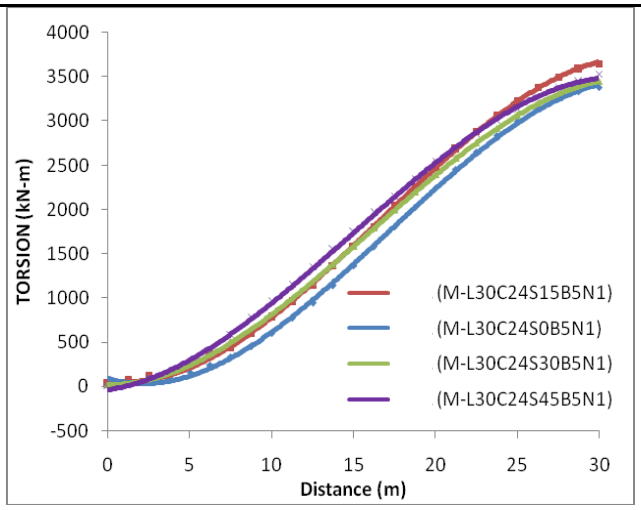

Plot- 3:B=5; N=1; α =24°

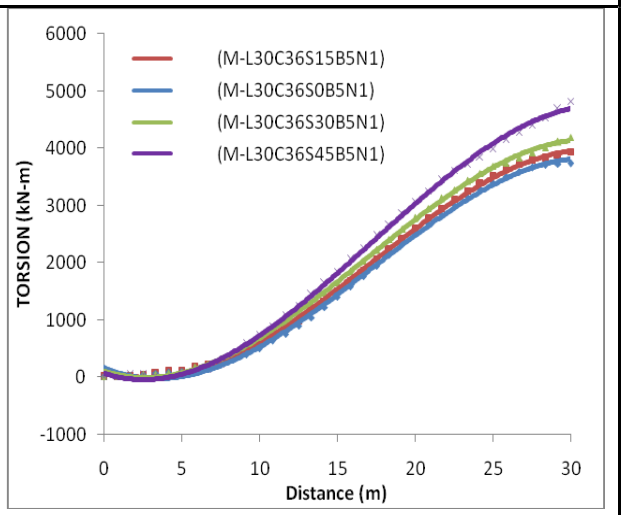

Plot- 4:B=5; N=1; α=36°

Discussion: Above plots shows that unlike dead load case torsional moment has been obtained for straight model also due to eccentricity of vehicular live load. This torsional moment increases further with skewness for skew bridges. But, when curvature is introduced, though the pattern changes. For α=12°, maximum torsion occurs at θ=0°; for α=24°, maximum torsion occurs at θ=15° and for α=36°, maximum torsion occurs at θ=45°.

B5N2:

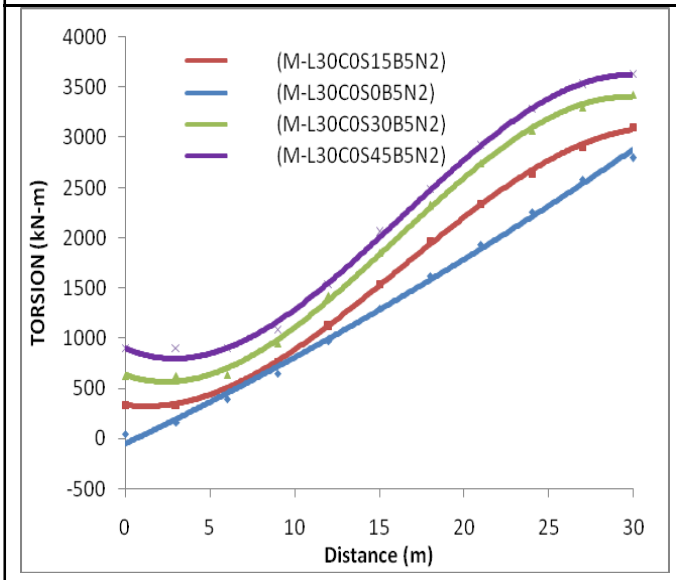

Plot- 5:B=5; N=2; α=0°

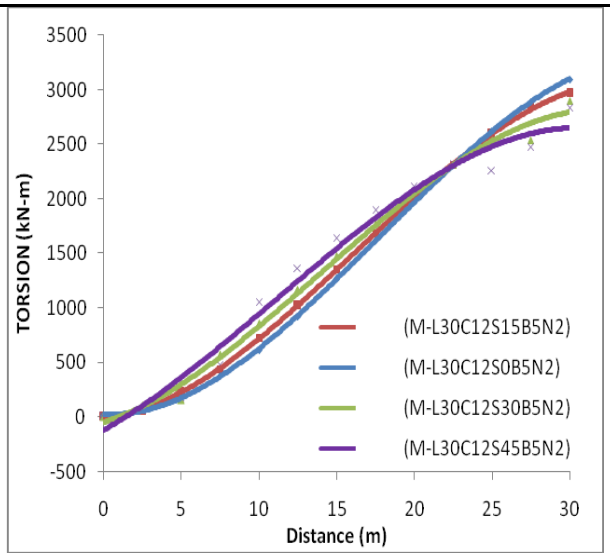

Plot- 6:B=5; N=2; α =12°

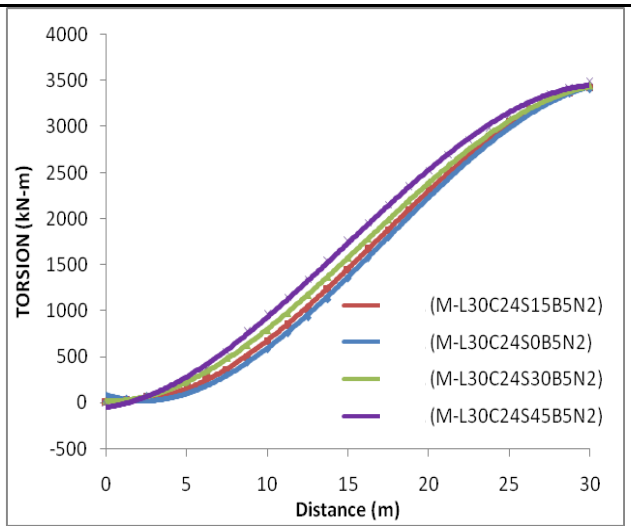

Plot- 7:B=5; N=2; α =24°

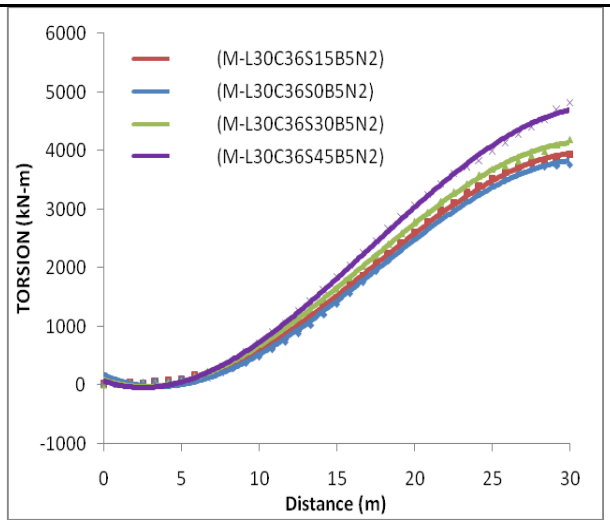

Plot- 8:B=5; N=2; α=36°

Discussion: Above plots shows that unlike dead load case torsional moment has been obtained for straight model also due to eccentricity of vehicular live load. This torsional moment increases further with skewness for skew bridges. But, when curvature is introduced, though the pattern changes. For α=12°, maximum torsion occurs at θ=0°; for α=24°, maximum torsion occurs at θ=45° and for α=36°, maximum torsion occurs at θ=45°.

B6N1:

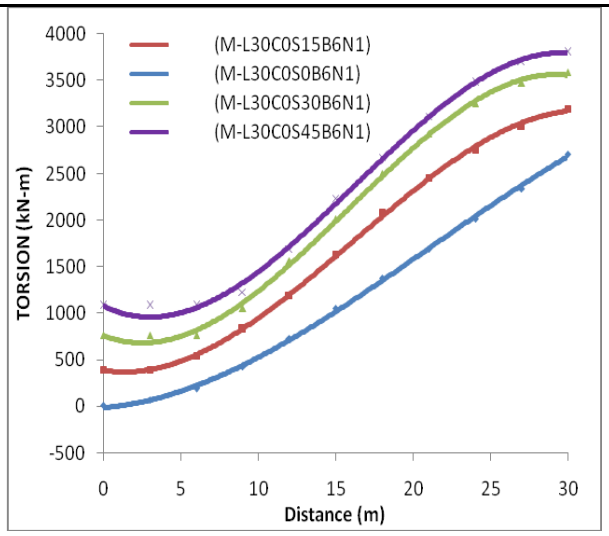

Plot- 9:B=6; N=1; α=0°

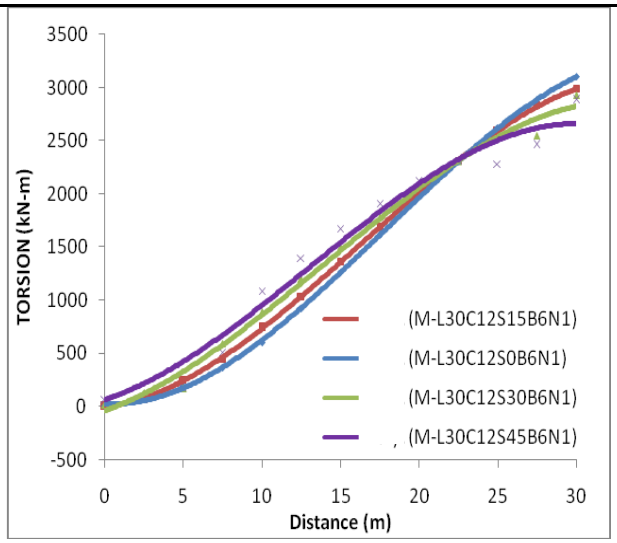

Plot- 10:B=6; N=1; α =12°

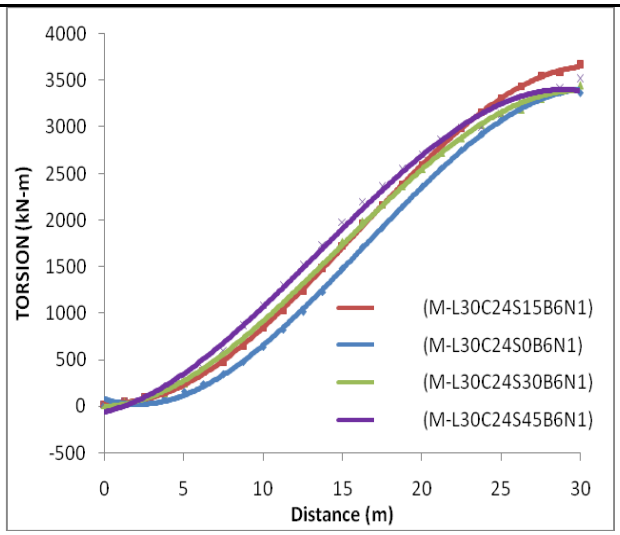

Plot- 11:B=6; N=1; α =24°

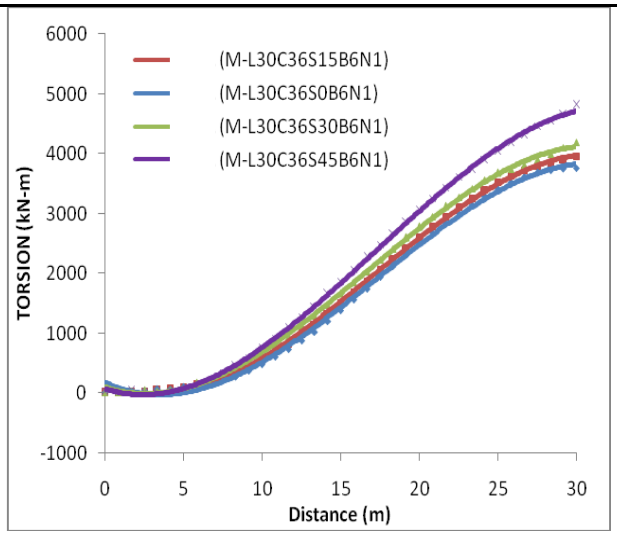

Plot- 12:B=6; N=1; α=36°

Discussion: Above plots shows that unlike dead load case torsional moment has been obtained for straight model also due to eccentricity of vehicular live load. This torsional moment increases further with skewness for skew bridges. But, when curvature is introduced, though the pattern changes. For α=12°, maximum torsion occurs at θ=0°; for α=24°, maximum torsion occurs at θ=15° and for α=36°, maximum torsion occurs at θ=45°.

B6N2:

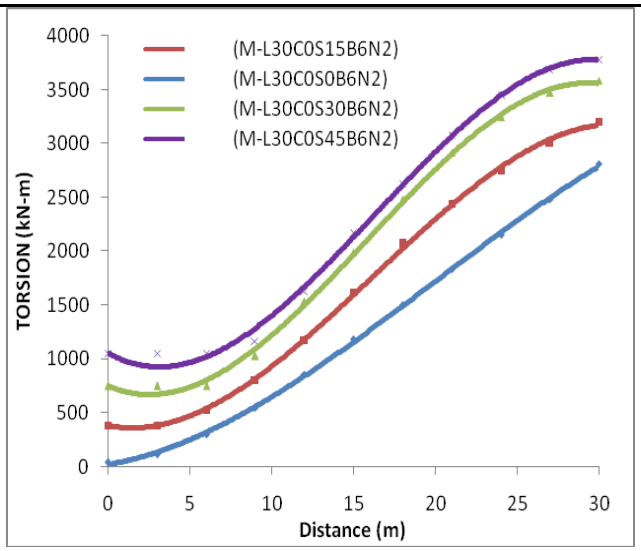

Plot- 13:B=6; N=2; α=0°

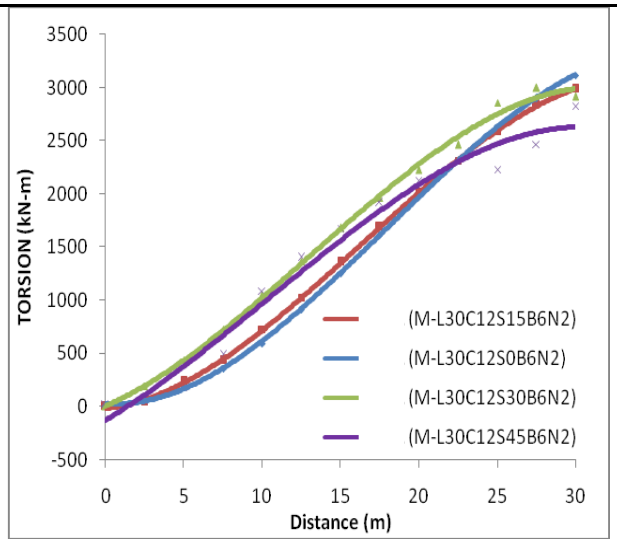

Plot- 14:B=6; N=2; α =12°

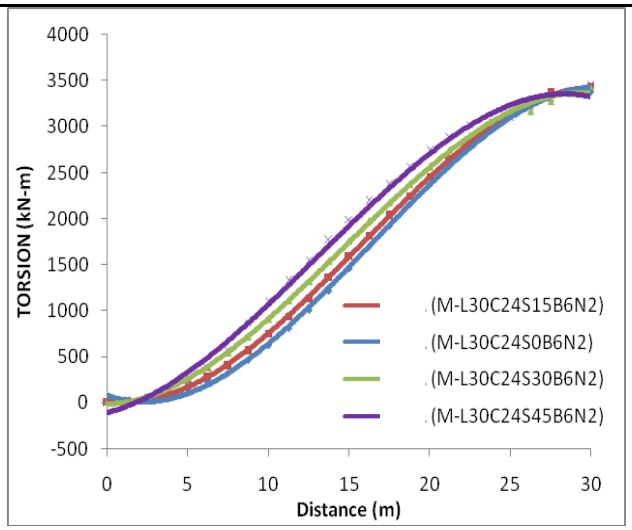

Plot- 15:B=6; N=2; α =24°

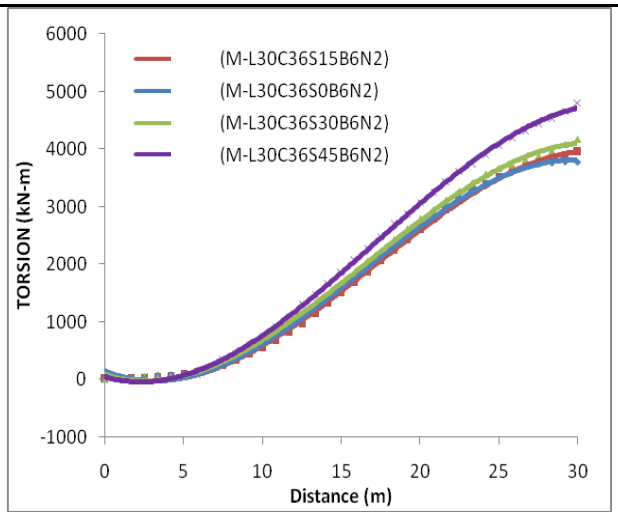

Plot- 16:B=6; N=2; α=36°

Discussion: Above plots shows that unlike dead load case torsional moment has benn obtained for straight model also due to eccentricity of vehicular live load. This torsional moment increases further with skewness for skew bridges. But, when curvature is introduced, though the pattern changes. For α=12°, maximum torsion occurs at θ=0°; for α=24°, maximum torsion occurs at θ=45° and for α=36°, maximum torsion occurs at θ=45°.

6.2.2.2 Variation of Torsional Moment diagram due to Curvature:

Effect on torsional moment diagram for variation in curvature has been plotted and explained graphically for all the four groups as described above.

B5N1:

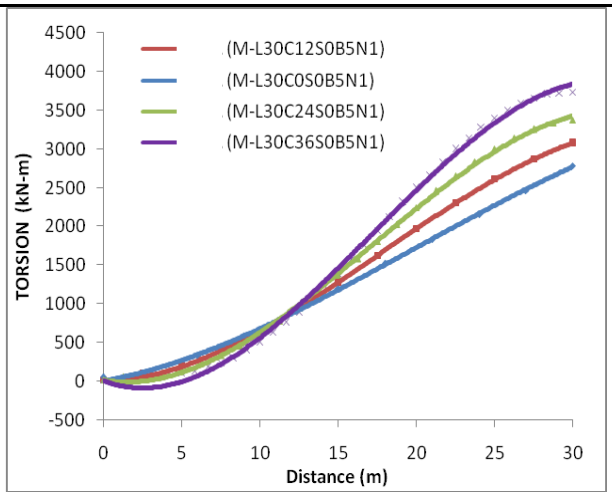

Plot- 17:B=5; N=1; θ=0°

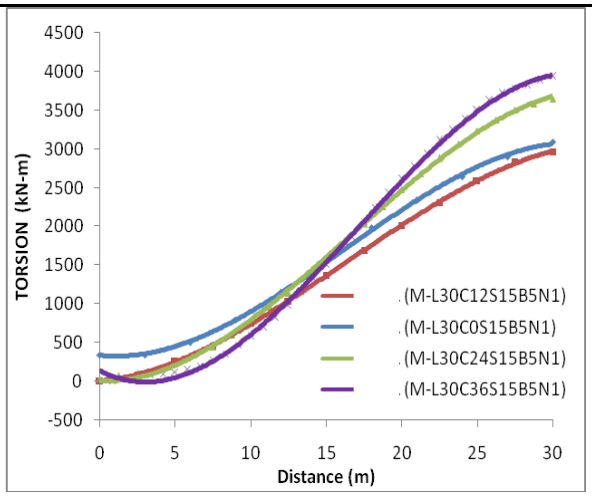

Plot- 18:B=5; N=1; θ =15°

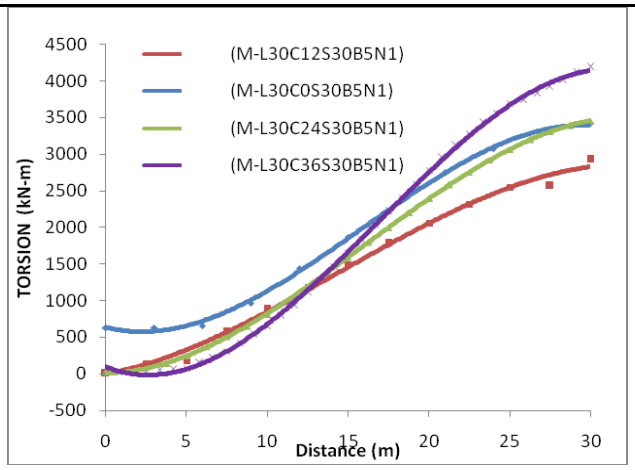

Plot- 19:B=5; N=1; θ =30°

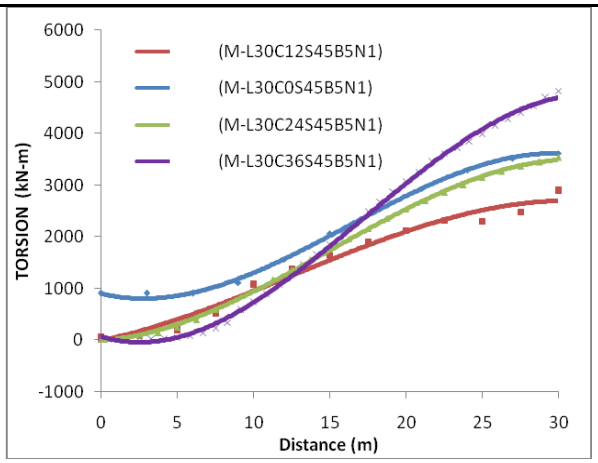

Plot- 20:B=5; N=1; θ=45°

Discussion: It is seen that torsion pattern shows a steeper variation with curvature. The maximum value increases 33% with curvatue (α=0° and 36°). When curvature is introduced, torsion decreases for α=12° and 24° and increases rapidly for α= 36°.

B5N2:

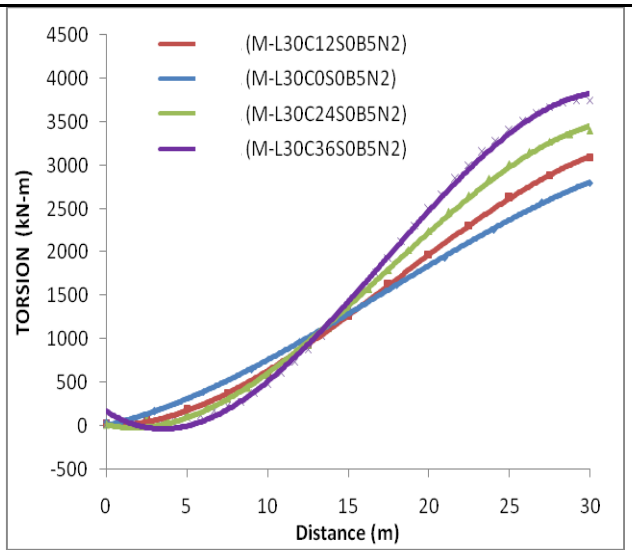

Plot- 21:B=5; N=2; θ=0°

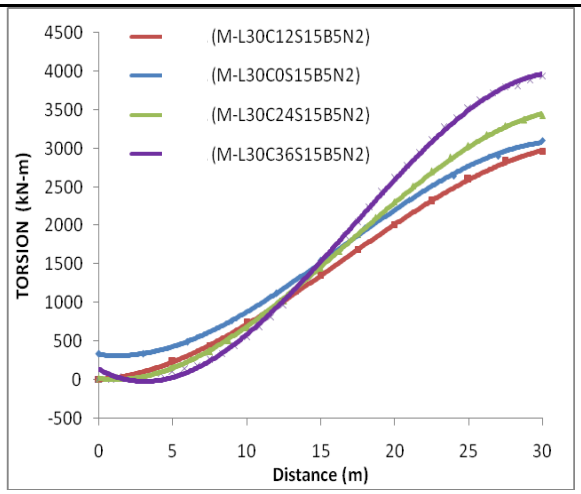

Plot- 22:B=5; N=2; θ =15°

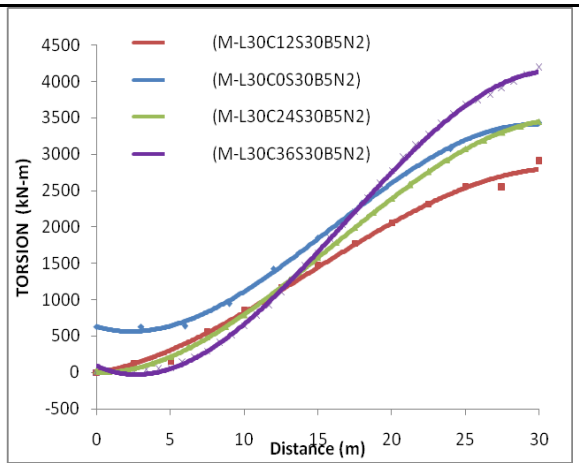

Plot- 23:B=5; N=2; θ =30°

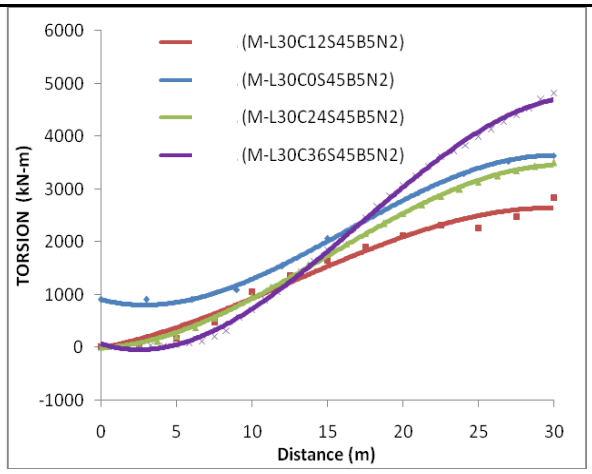

Plot- 24:B=5; N=2; θ=45°

Discussion: It is seen that torsion pattern shows a steeper variation with curvature. The maximum value increases 33% with curvatue (α=0° and 36°). When curvature is introduced, torsion decreases for α=12° and 24° and increases rapidly for α= 36°.

B6N1:

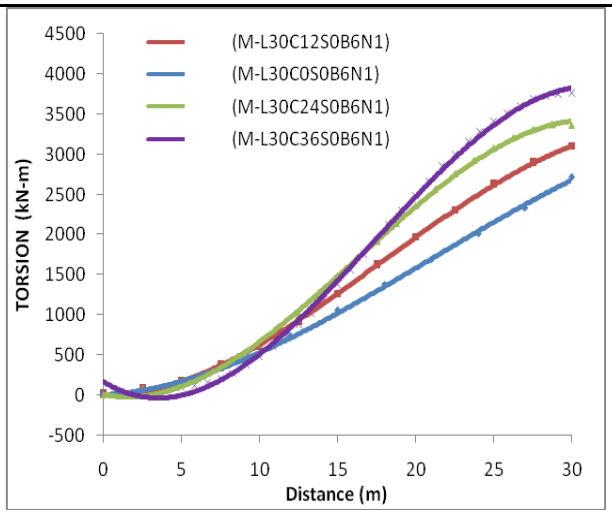

Plot- 25:B=6; N=1; θ=0°

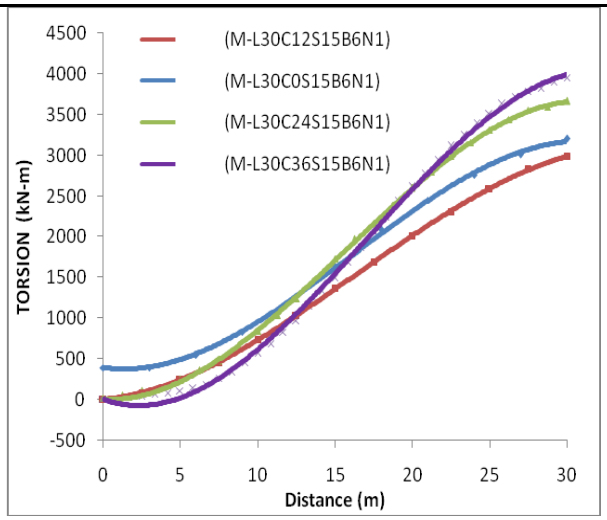

Plot- 26:B=6; N=1; θ =15°

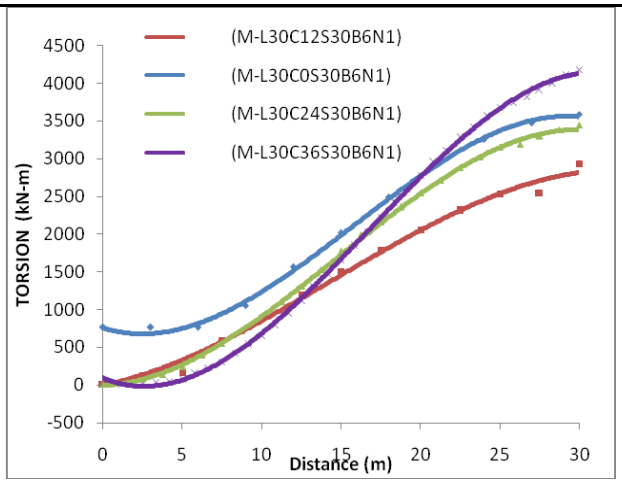

Plot- 27:B=6; N=1; θ =30°

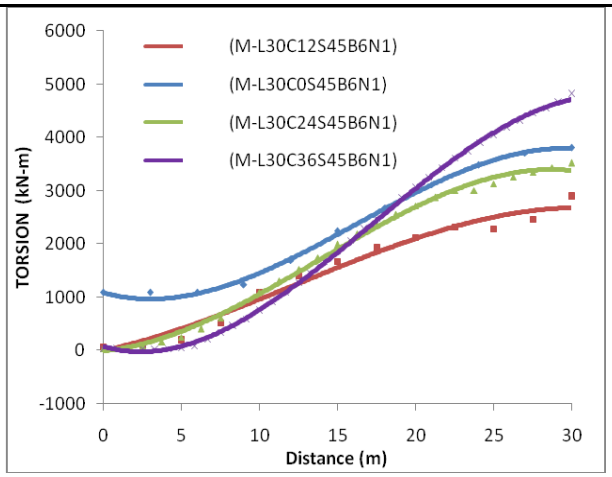

Plot- 28:B=6; N=1; θ=45°

Discussion: It is seen that torsion pattern shows a steeper variation with curvature. When curvature is introduced, torsion decreases for α=12° and 24° and increases rapidly for α= 36°. . The maximum value increases 39% with curvatue (α=0° and 36°) for θ =0° and 27% with curvatue (α=0° and 36°) for θ =45°.

B6N2:

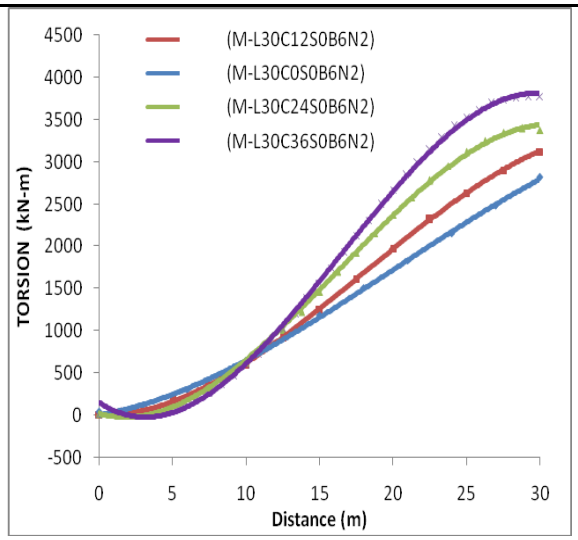

Plot- 29:B=6; N=2; θ=0°

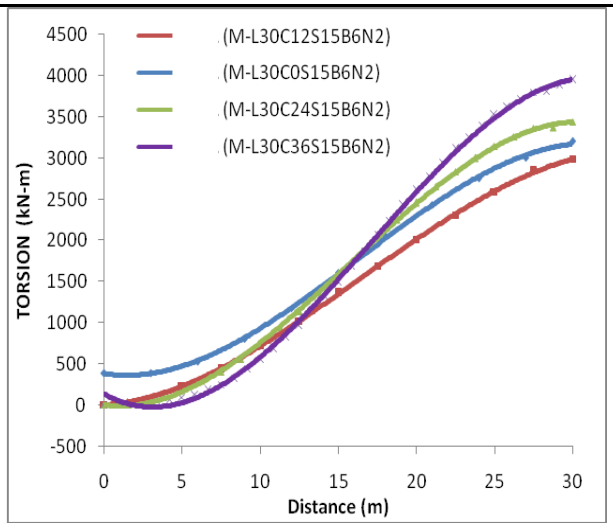

Plot- 30:B=6; N=2; θ =15°

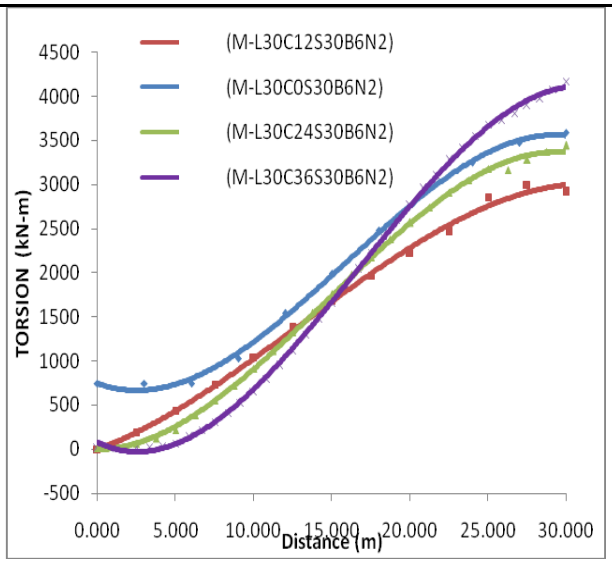

Plot- 31:B=6; N=2; θ =30°

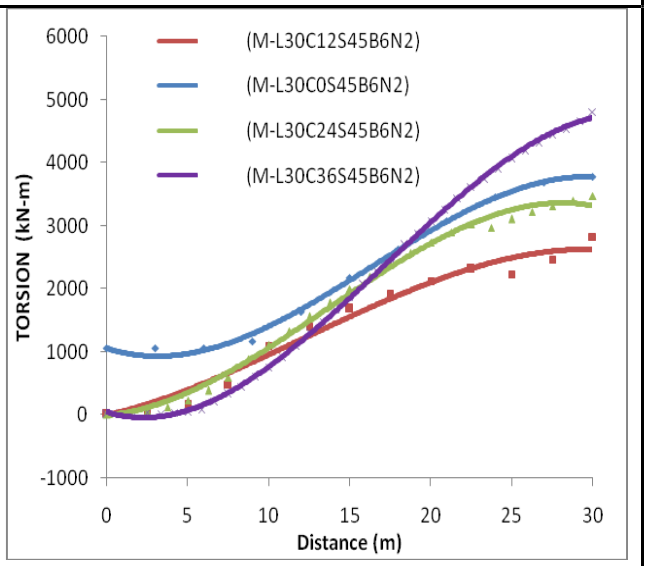

Plot- 32:B=6; N=2; θ=45°

Discussion: It is seen that torsion pattern shows a steeper variation with curvature. When curvature is introduced, torsion decreases for α=12° and 24° and increases rapidly for α= 36°. . The maximum value increases 34% with curvatue (α=0° and 36°) for θ =0° and 27% with curvatue (α=0° and 36°) for θ =45°.

6.2.2.3 Variation of Maximum Torsion:

Variation of maximum torsion has been compared as a ratio to the maximum torsion of the straight model for all the four groups. The comparison has been presented below.

Table 27: Maximum LL Torsion for B5N1

Model ID	Span length (L in m)	Central Angle (α °)	Skew Angle (θ °)	Bottom Width, (B) (m)	Number of Cell (N)	Max. Torsion (KN-m)	As % of straight model	Remarks
M-L30C0S0B5N1	30	0	0	5	1	2784	100%	Increases with Skewness
M-L30C0S15B5N1	30	0	15	5	1	3095	111%	
M-L30C0S30B5N1	30	0	30	5	1	3420	123%	
M-L30C0S45B5N1	30	0	45	5	1	3620	130%	
M-L30C12S0B5N1	30	12	0	5	1	3074	110%	Decreases with Skewness ; Curvature Introduced
M-L30C12S15B5N1	30	12	15	5	1	2984	107%	
M-L30C12S30B5N1	30	12	30	5	1	2980	107%	
M-L30C12S45B5N1	30	12	45	5	1	2908	104%	
M-L30C24S0B5N1	30	24	0	5	1	3377	121%	Shows a variation within 12%
M-L30C24S15B5N1	30	24	15	5	1	3685	132%	
M-L30C24S30B5N1	30	24	30	5	1	3487	125%	
M-L30C24S45B5N1	30	24	45	5	1	3560	128%	
M-L30C36S0B5N1	30	36	0	5	1	3739	134%	Increases with Skewness and Curvature
M-L30C36S15B5N1	30	36	15	5	1	3971	143%	
M-L30C36S30B5N1	30	36	30	5	1	4186	150%	
M-L30C36S45B5N1	30	36	45	5	1	4820	173%	

Table 28: Maximum LL Torsion for B5N2

Model ID	Span length (L in m)	Central Angle (α °)	Skew Angle (θ °)	Bottom Width, (B) (m)	Number of Cell (N)	Max. Torsion (KN-m)	As % of straight model	Remarks
M-L30C0S0B5N2	30	0	0	5	2	2796	100%	Increases with Skewness
M-L30C0S15B5N2	30	0	15	5	2	3108	111%	
M-L30C0S30B5N2	30	0	30	5	2	3430	123%	
M-L30C0S45B5N2	30	0	45	5	2	3635	130%	

Model ID	Span length (L in m)	Central Angle (α °)	Skew Angle (θ °)	Bottom Width, (B) (m)	Number of Cell (N)	Max. Torsion (KN-m)	As % of straight model	Remarks
M-L30C12S0B5N2	30	12	0	5	2	3097	111%	Decreases with Skewness ; Curvature Introduced
M-L30C12S15B5N2	30	12	15	5	2	3010	108%	
M-L30C12S30B5N2	30	12	30	5	2	3026	108%	
M-L30C12S45B5N2	30	12	45	5	2	2973	106%	
M-L30C24S0B5N2	30	24	0	5	2	3403	122%	Shows a variation within 7%
M-L30C24S15B5N2	30	24	15	5	2	3468	124%	
M-L30C24S30B5N2	30	24	30	5	2	3519	126%	
M-L30C24S45B5N2	30	24	45	5	2	3592	128%	
M-L30C36S0B5N2	30	36	0	5	2	3759	134%	Increases with Skewness and Curvature
M-L30C36S15B5N2	30	36	15	5	2	3956	141%	
M-L30C36S30B5N2	30	36	30	5	2	4191	150%	
M-L30C36S45B5N2	30	36	45	5	2	4818	172%	

Table 29: Maximum LL Torsion for B6N1

Model ID	Span length (L in m)	Central Angle (α °)	Skew Angle (θ °)	Bottom Width, (B) (m)	Number of Cell (N)	Max. Torsion (KN-m)	As % of straight model	Remarks
M-L30C0S0B6N1	30	0	0	6	1	2713	100%	Increases with Skewness
M-L30C0S15B6N1	30	0	15	6	1	3200	118%	
M-L30C0S30B6N1	30	0	30	6	1	3587	132%	
M-L30C0S45B6N1	30	0	45	6	1	3803	140%	
M-L30C12S0B6N1	30	12	0	6	1	3102	114%	Decreases with Skewness ; Curvature Introduced
M-L30C12S15B6N1	30	12	15	6	1	3017	111%	
M-L30C12S30B6N1	30	12	30	6	1	2984	110%	
M-L30C12S45B6N1	30	12	45	6	1	2933	108%	
M-L30C24S0B6N1	30	24	0	6	1	3454	127%	Shows a variation within 9%
M-L30C24S15B6N1	30	24	15	6	1	3696	136%	
M-L30C24S30B6N1	30	24	30	6	1	3475	128%	
M-L30C24S45B6N1	30	24	45	6	1	3541	131%	
M-L30C36S0B6N1	30	36	0	6	1	3763	139%	Increases with
M-L30C36S15B6N1	30	36	15	6	1	3972	146%	

Model ID	Span length (L in m)	Central Angle (α °)	Skew Angle (θ °)	Bottom Width, (B) (m)	Number of Cell (N)	Max. Torsion (KN-m)	As % of straight model	Remarks
M-L30C36S30B6N1	30	36	30	6	1	4184	154%	Skewness and Curvature
M-L30C36S45B6N1	30	36	45	6	1	4812	177%	

Table 30: Maximum LL Torsion for B6N2

Model ID	Span length (L in m)	Central Angle (α °)	Skew Angle (θ °)	Bottom Width, (B) (m)	Number of Cell (N)	Max. Torsion (KN-m)	As % of straight model	Remarks
M-L30C0S0B6N2	30	0	0	6	2	2816	100%	Increases with Skewness
M-L30C0S15B6N2	30	0	15	6	2	3203	114%	
M-L30C0S30B6N2	30	0	30	6	2	3587	127%	
M-L30C0S45B6N2	30	0	45	6	2	3779	134%	
M-L30C12S0B6N2	30	12	0	6	2	3119	111%	Decreases with Skewness ; Curvature Introduced
M-L30C12S15B6N2	30	12	15	6	2	3023	107%	
M-L30C12S30B6N2	30	12	30	6	2	2998	106%	
M-L30C12S45B6N2	30	12	45	6	2	2962	105%	
M-L30C24S0B6N2	30	24	0	6	2	3509	125%	Shows a variation within 2%
M-L30C24S15B6N2	30	24	15	6	2	3465	123%	
M-L30C24S30B6N2	30	24	30	6	2	3497	124%	
M-L30C24S45B6N2	30	24	45	6	2	3558	126%	
M-L30C36S0B6N2	30	36	0	6	2	3778	134%	Increases with Skewness and Curvature
M-L30C36S15B6N2	30	36	15	6	2	3982	141%	
M-L30C36S30B6N2	30	36	30	6	2	4171	148%	
M-L30C36S45B6N2	30	36	45	6	2	4798	170%	

It has been seen that, when there is no curvature introduced the torsion varies almost 1.3 to 1.4 times for varying the skew angle (α=0°; θ=0°) to (α=0°; θ=45°). When the curvature

is introduced and it is coupled with skewness, the torsional moment varies up to 1.8 times (α=12°; θ=0° to α=36°; θ=45°).

6.2.2.4 Variation of Maximum Torsion with "B" and "N":

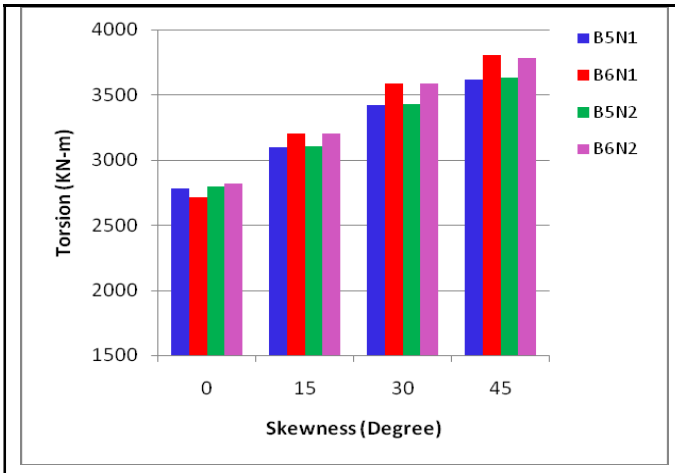

Plot- 1:α=0°

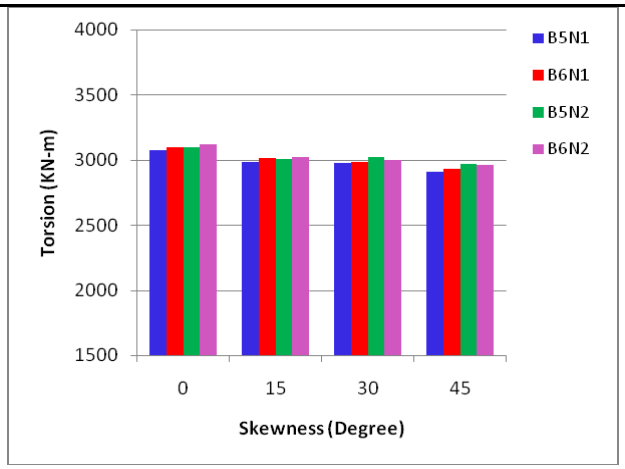

Plot- 2: α=12°

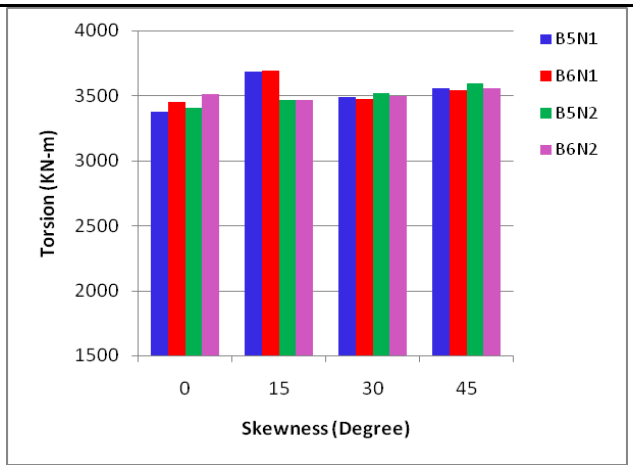

Plot- 3: α=24°

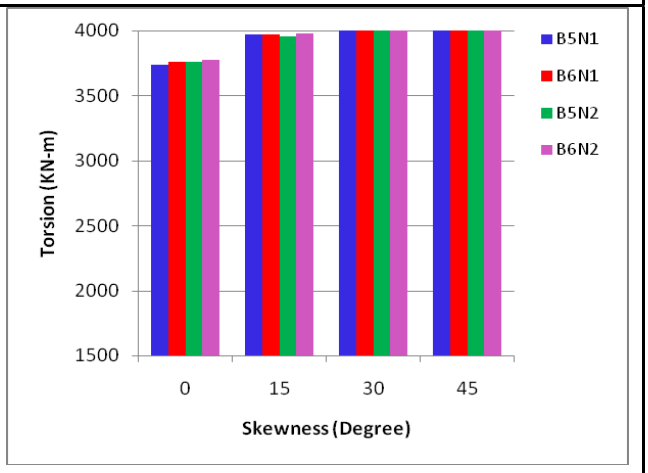

Plot- 4: α=36°

Discussion: It is seen that maximum torsion differs slightly, when no curvature is introduced. But, it shows almost same response when curvature is introduced. However, the value increases with increase in skewness for purely skew bridges but increases with both curvature and skewness for skew-curved bridges. For a particular curvature, variation of maximum torsion is not much with kewness.

6.2.3 Effect on Shear Force:

An important point to note that the bridge is symmetrical; any of the maximum/minimum envelopes for shear will correctly represent the shear force pattern. Hence, maximum shear force has been considered in this study. Minimum envelope is the

anti-symmetric of the maximum envelope. Effect on both the shear force diagram and absolute shear force due to curvature and skewness is presented below.

6.2.3.1 Variation of Shear force diagram due to skewness:

Effect on shear diagram for variation in skewness has been plotted and explained graphically for all the four groups as described above.

B5N1:

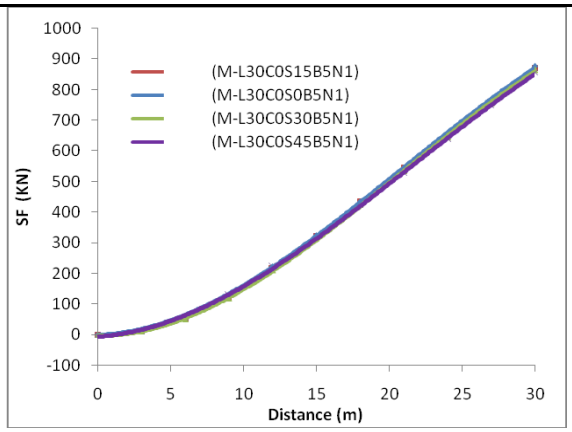

Plot- 1:B=5; N=1; α=0°

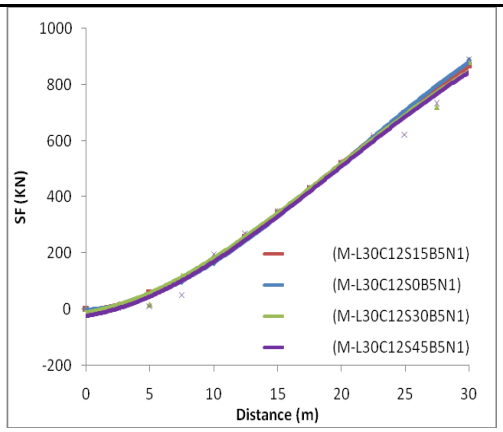

Plot- 2:B=5; N=1; α =12°

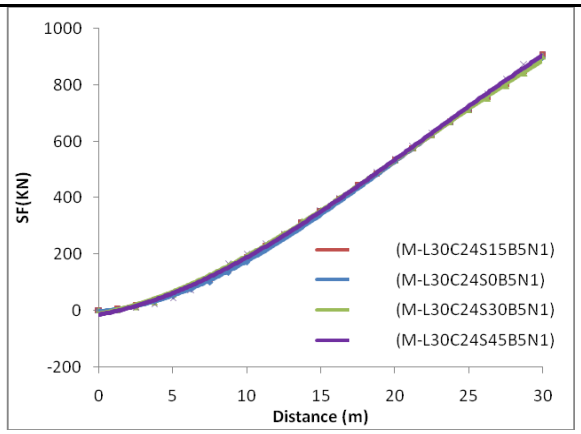

Plot- 3:B=5; N=1; α =24°

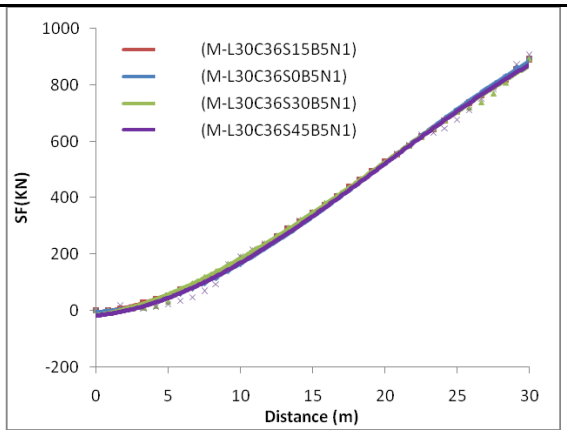

Plot- 4:B=5; N=1; α=36°

Discussion: Variation of shear force is almost same irrespective of curvature and skew. The maximum shear force also does not vary much. Variation of shear force due to curvature and skewness is within ±5%.

B5N2:

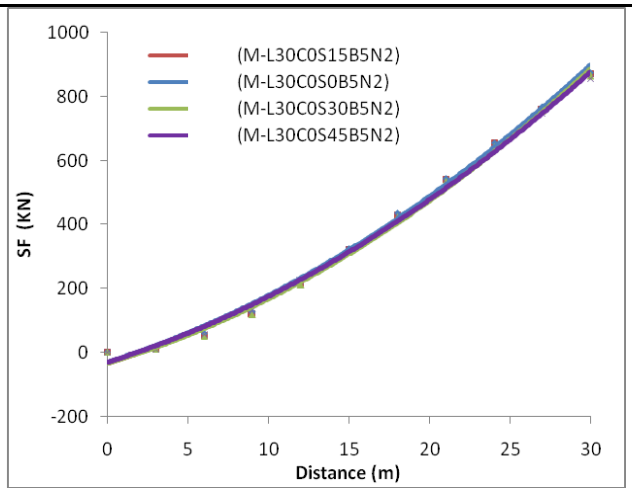

Plot- 5:B=5; N=2; α=0°

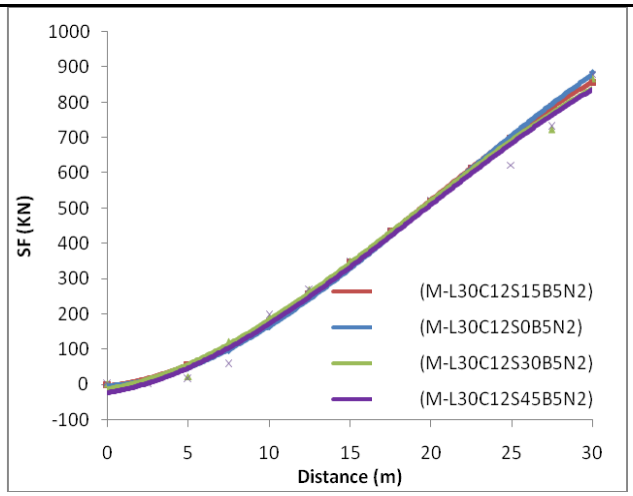

Plot- 6:B=5; N=2; α =12°

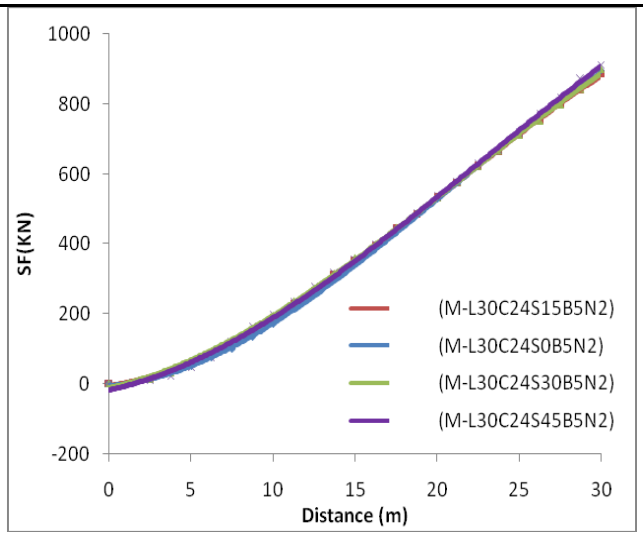

Plot- 7:B=5; N=2; α =24°

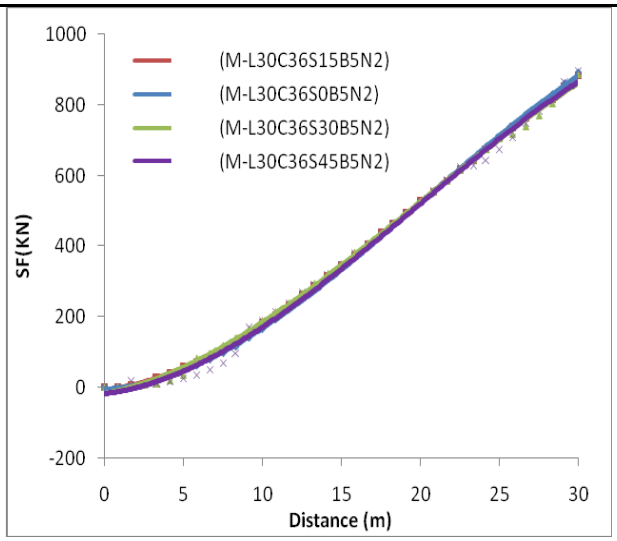

Plot- 8:B=5; N=2; α=36°

Discussion: Variation of shear force is almost same irrespective of curvature and skew. The maximum shear force also does not vary much. Variation of shear force due to curvature and skewness is within ±5%.

B6N1:

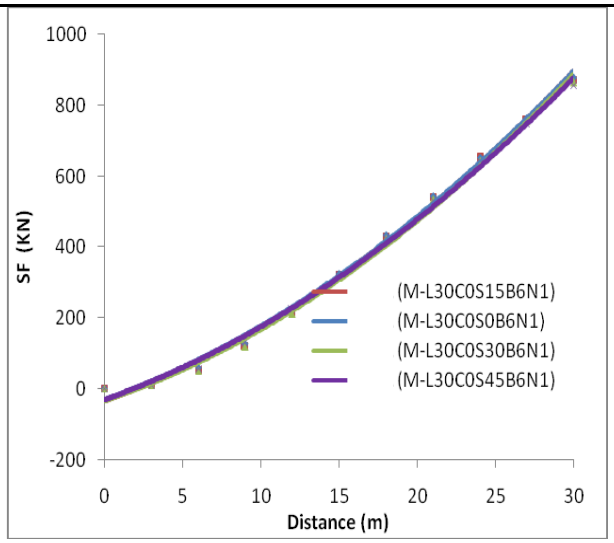

Plot- 9:B=6; N=1; α=0°

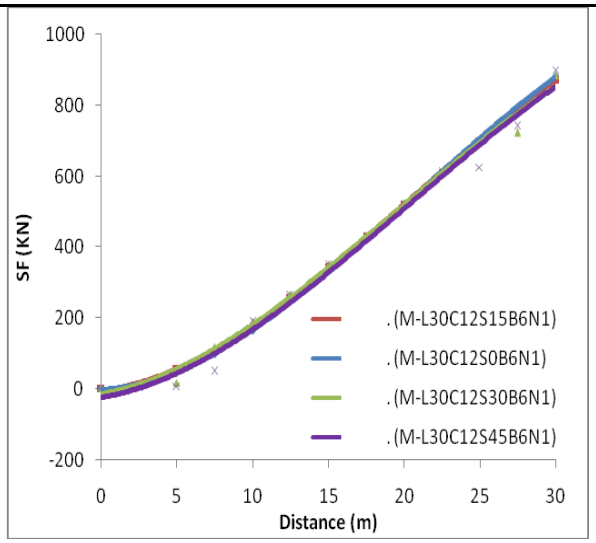

Plot- 10:B=6; N=1; α =12°

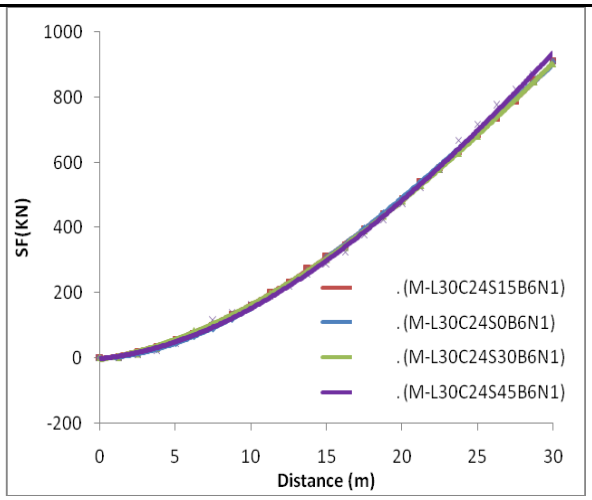

Plot- 11:B=6; N=1; α =24°

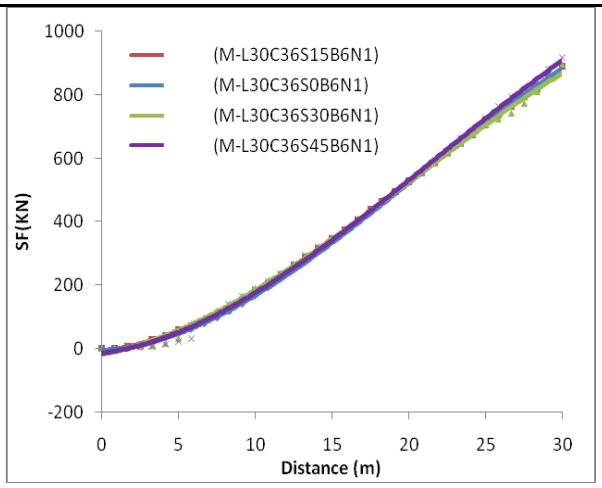

Plot- 12:B=6; N=1; α=36°

Discussion: Variation of shear force is almost same irrespective of curvature and skew. The maximum shear force also does not vary much. Variation of shear force due to curvature and skewness is within ±5%.

B6N2:

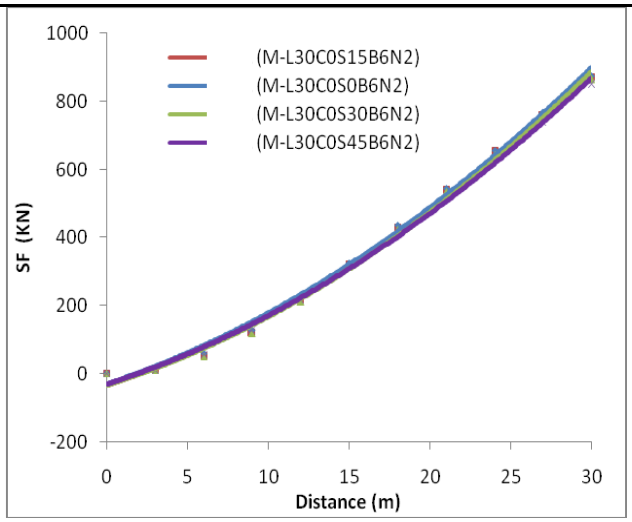

Plot- 13:B=6; N=2; α=0°

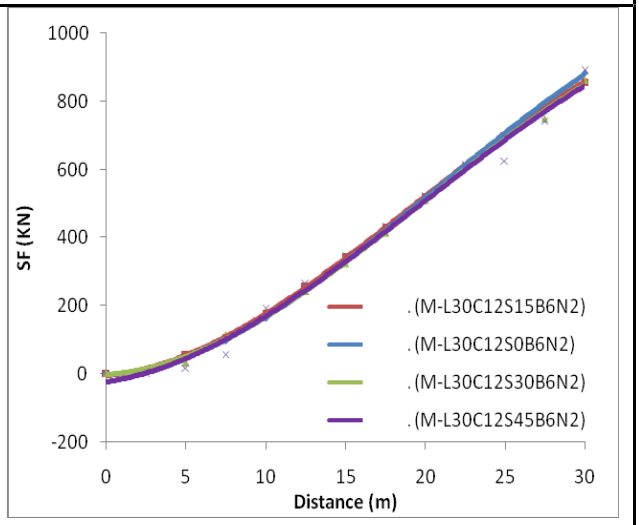

Plot- 14:B=6; N=2; α =12°

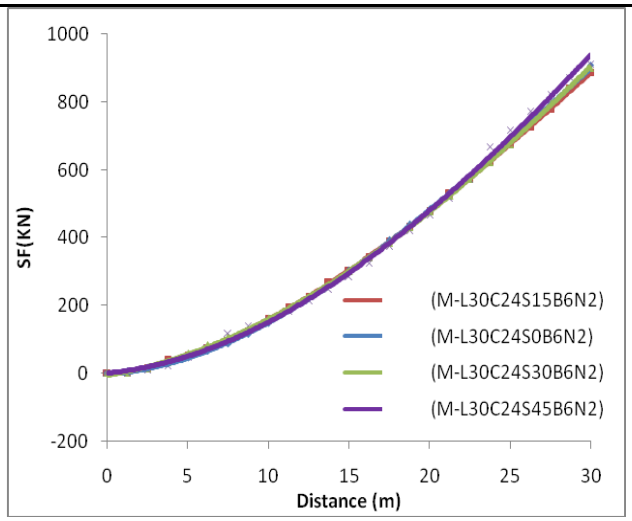

Plot- 15:B=6; N=2; α =24°

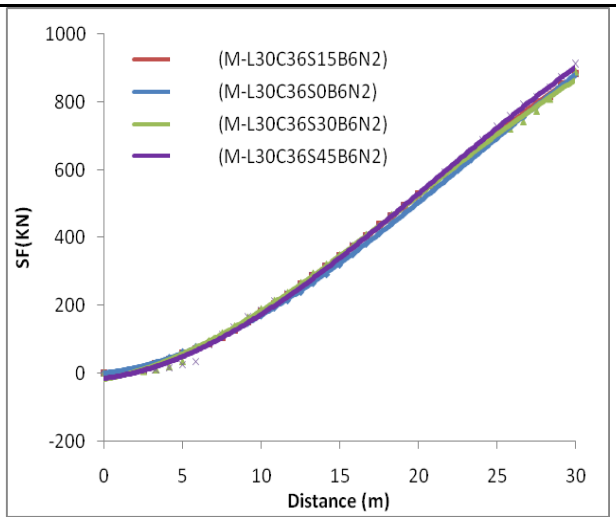

Plot- 16:B=6; N=2; α=36°

Discussion: Variation of shear force is almost same irrespective of curvature and skew. The maximum shear force also does not vary much. Variation of shear force due to curvature and skewness is within ±5%.

6.2.3.2 Variation of Shear force diagram due to Curvature:

Effect on shear force diagram for variation in curvature has been plotted and explained graphically for all the four groups as described above.

B5N1:

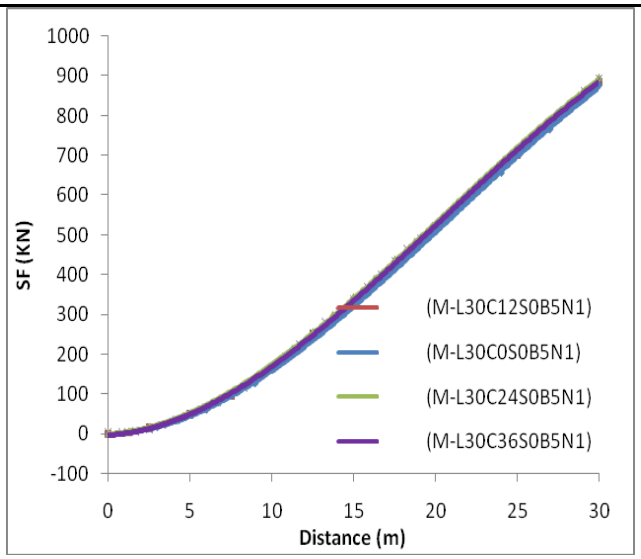

Plot- 17:B=5; N=1; θ=0°

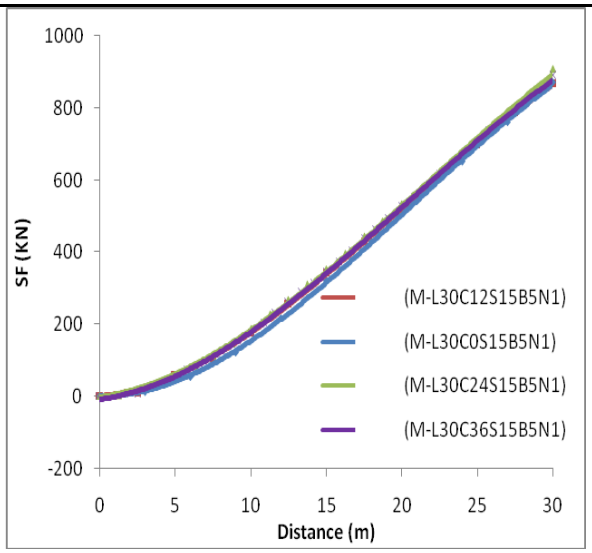

Plot- 18:B=5; N=1; θ =15°

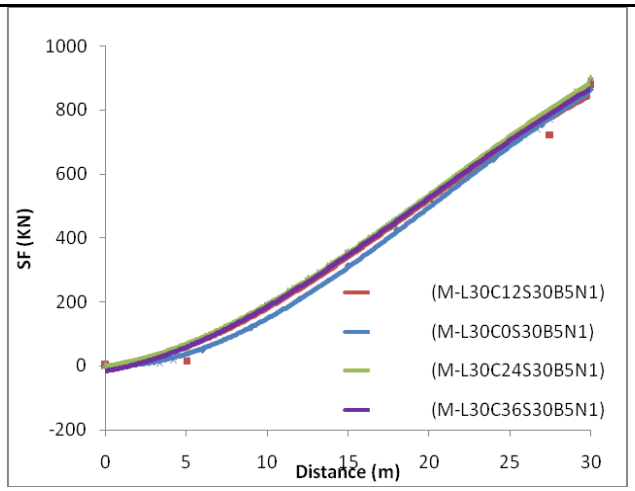

Plot- 19:B=5; N=1; θ =30°

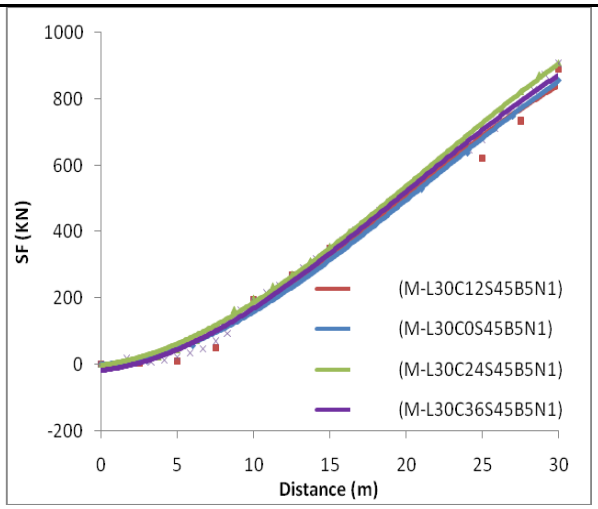

Plot- 20:B=5; N=1; θ=45°

Discussion: Variation of shear force is almost same irrespective of curvature and skew. The maximum shear force also does not vary much. Variation of shear force due to curvature for curved bridges (θ=0°) is 2% and it increases with skewness up to 10% (θ=45°).

B5N2:

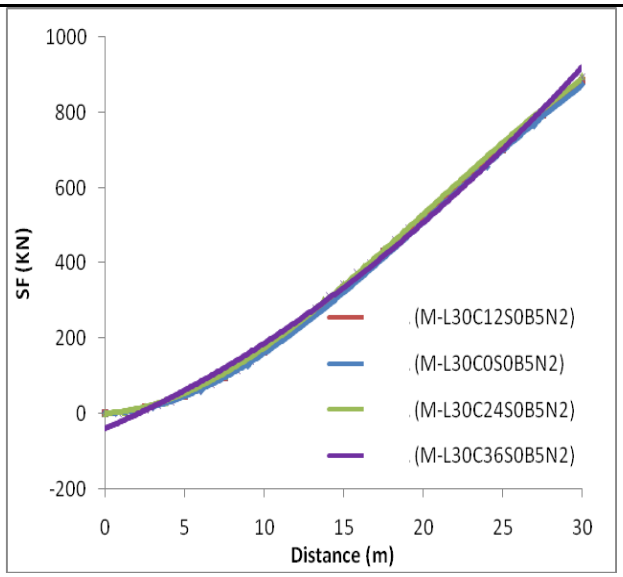

Plot- 21:B=5; N=2; θ=0°

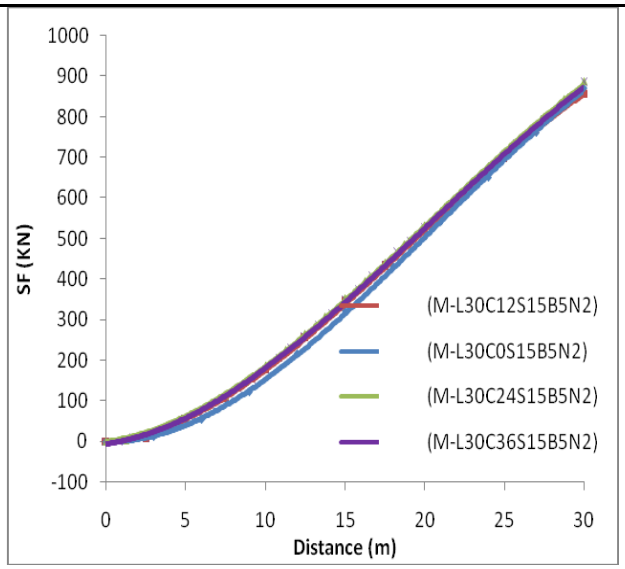

Plot- 22:B=5; N=2; θ =15°

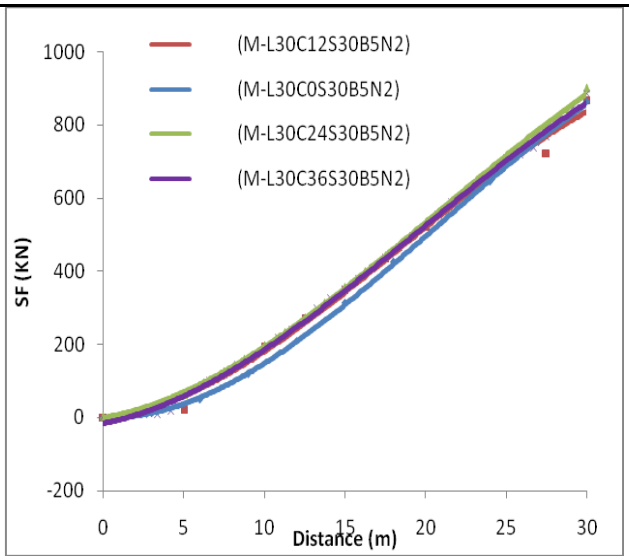

Plot- 23:B=5; N=2; θ =30°

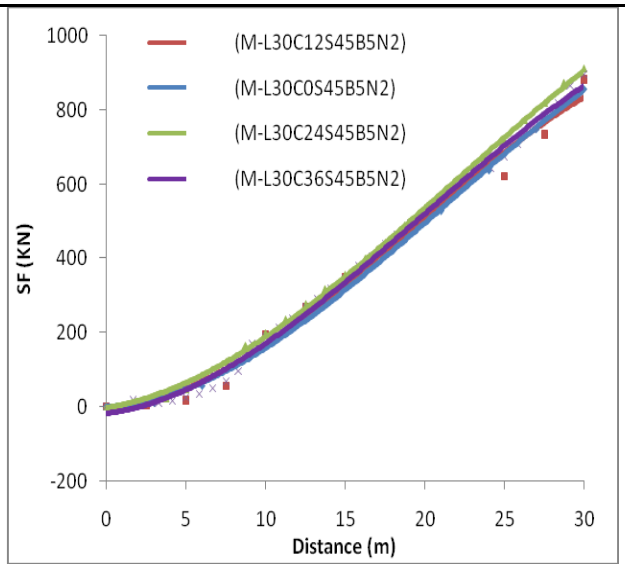

Plot- 24:B=5; N=2; θ=45°

Discussion: Variation of shear force is almost same irrespective of curvature and skew. The maximum shear force also does not vary much. Variation of shear force due to curvature for curved bridges (θ=0°) is 2% and it increases with skewness up to 10% (θ=45°).

B6N1:

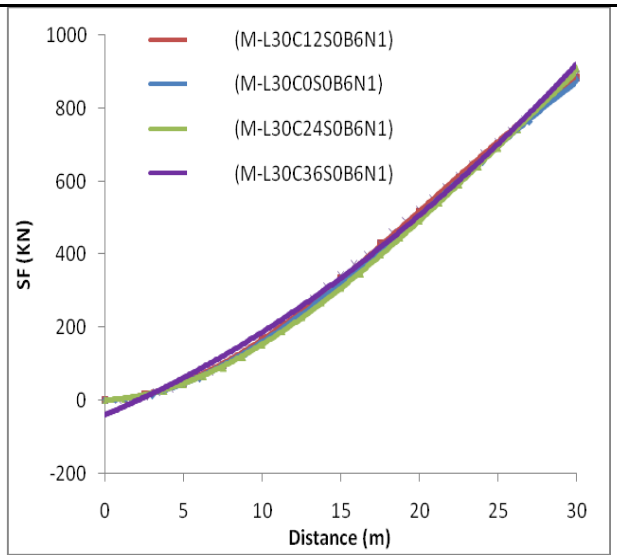

Plot- 25:B=6; N=1; θ=0°

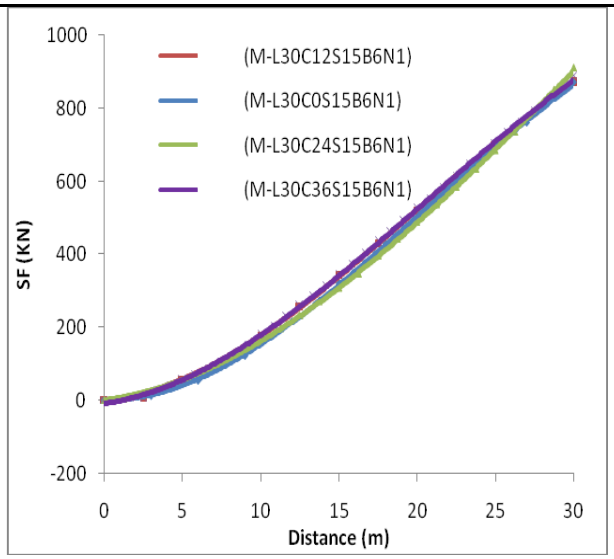

Plot- 26:B=6; N=1; θ =15°

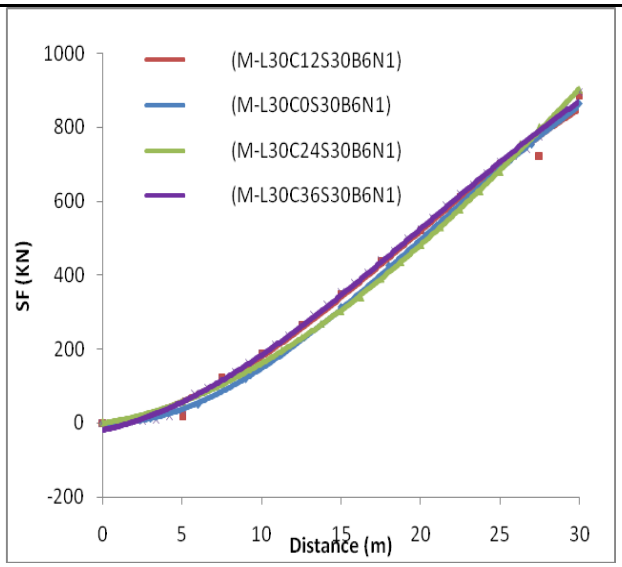

Plot- 27:B=6; N=1; θ =30°

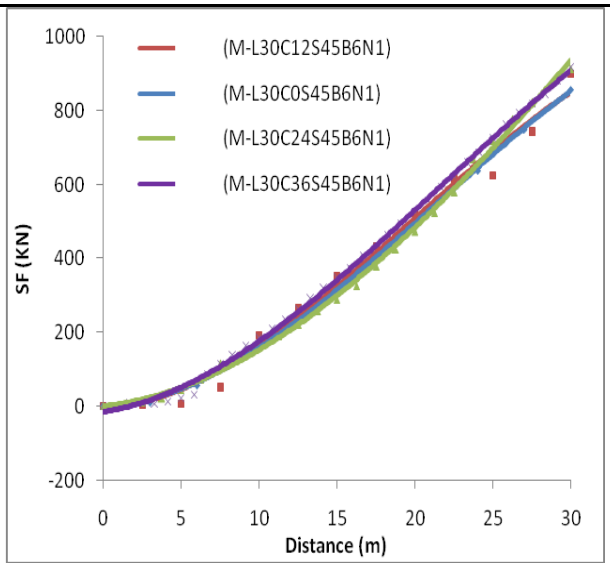

Plot- 28:B=6; N=1; θ=45°

Discussion: Variation of shear force is almost same irrespective of curvature and skew. The maximum shear force also does not vary much. Variation of shear force due to curvature for curved bridges (θ=0°) is 2% and it increases with skewness up to 10% (θ=45°).

B6N2:

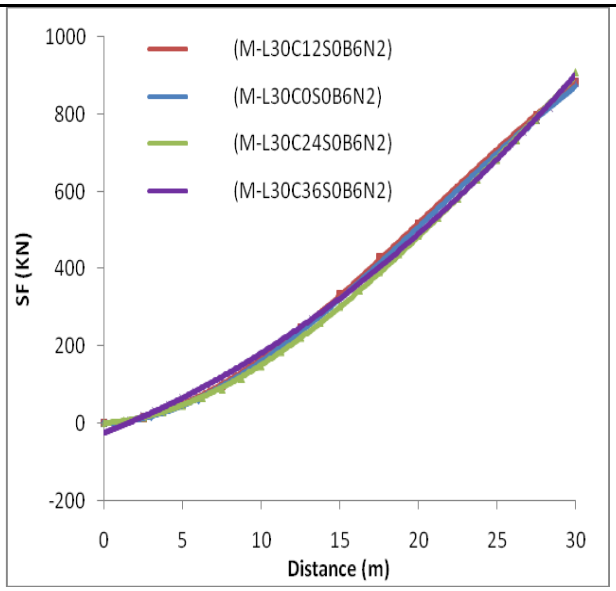

Plot- 29:B=6; N=2; θ=0°

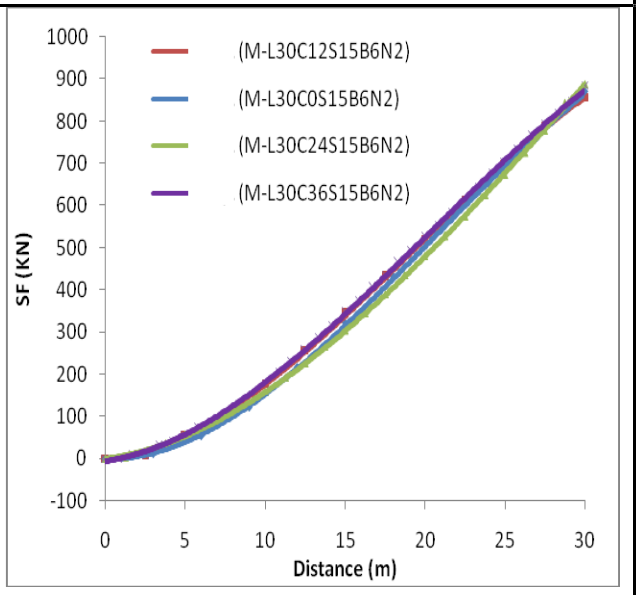

Plot- 30:B=6; N=2; θ =15°

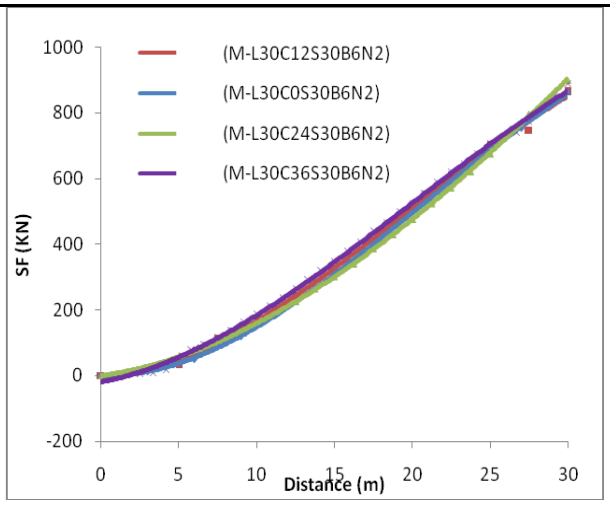

Plot- 31:B=6; N=2; θ =30°

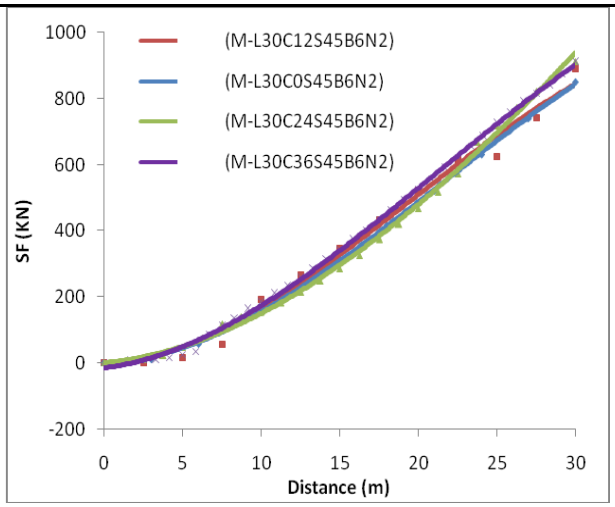

Plot- 32:B=6; N=2; θ=45°

Discussion: Variation of shear force is almost same irrespective of curvature and skew. The maximum shear force also does not vary much. Variation of shear force due to curvature for curved bridges (θ=0°) is 2% and it increases with skewness up to 10% (θ=45°).

6.2.3.3 Variation of Maximum Shear force:

Variation of maximum shear force has been compared as a ratio to the maximum shear force of the straight bridge (α=0° and θ=0°) for all the four groups. The comparison has been presented below.

Table 31: Maximum LL Shear Force for B5N1

Model ID	Span length (L in m)	Central Angle (α °)	Skew Angle, (θ °)	Bottom Width, (B) (m)	Number of Cell (N)	Max. Shear Force (KN)	As % of straight model	Remarks
M-L30C0S0B5N1	30	0	0	5	1	875	100%	Decreases slightly with Skewness
M-L30C0S15B5N1	30	0	15	5	1	871	100%	
M-L30C0S30B5N1	30	0	30	5	1	864	99%	
M-L30C0S45B5N1	30	0	45	5	1	857	98%	
M-L30C12S0B5N1	30	12	0	5	1	886	101%	Varies Up to 8% with Skewness and Curvature
M-L30C12S15B5N1	30	12	15	5	1	869	99%	
M-L30C12S30B5N1	30	12	30	5	1	881	101%	
M-L30C12S45B5N1	30	12	45	5	1	892	102%	
M-L30C24S0B5N1	30	24	0	5	1	898	103%	
M-L30C24S15B5N1	30	24	15	5	1	910	104%	
M-L30C24S30B5N1	30	24	30	5	1	904	103%	
M-L30C24S45B5N1	30	24	45	5	1	914	104%	
M-L30C36S0B5N1	30	36	0	5	1	894	102%	
M-L30C36S15B5N1	30	36	15	5	1	922	105%	
M-L30C36S30B5N1	30	36	30	5	1	930	106%	
M-L30C36S45B5N1	30	36	45	5	1	944	108%	

Table 32: Maximum LL Shear Force for B5N2

Model ID	Span length (L in m)	Central Angle (α °)	Skew Angle (θ °)	Bottom Width, (B) (m)	Number of Cell (N)	Max. Shear Force (KN)	As % of straight model	Remarks
M-L30C0S0B5N2	30	0	0	5	2	876	100%	Decreases slightly with Skewness
M-L30C0S15B5N2	30	0	15	5	2	872	100%	
M-L30C0S30B5N2	30	0	30	5	2	864	99%	
M-L30C0S45B5N2	30	0	45	5	2	857	98%	
M-L30C12S0B5N2	30	12	0	5	2	886	101%	Varies Up to 7% with Skewness and Curvature
M-L30C12S15B5N2	30	12	15	5	2	859	98%	
M-L30C12S30B5N2	30	12	30	5	2	868	99%	
M-L30C12S45B5N2	30	12	45	5	2	881	101%	
M-L30C24S0B5N2	30	24	0	5	2	897	102%	
M-L30C24S15B5N2	30	24	15	5	2	889	101%	
M-L30C24S30B5N2	30	24	30	5	2	902	103%	
M-L30C24S45B5N2	30	24	45	5	2	917	105%	
M-L30C36S0B5N2	30	36	0	5	2	894	102%	
M-L30C36S15B5N2	30	36	15	5	2	921	105%	
M-L30C36S30B5N2	30	36	30	5	2	929	106%	
M-L30C36S45B5N2	30	36	45	5	2	941	107%	

Table 33: Maximum LL Shear Force for B6N1

Model ID	Span length (L in m)	Central Angle (α °)	Skew Angle (θ °)	Bottom Width, (B) (m)	Number of Cell (N)	Max. Shear Force (KN)	As % of straight model	Remarks
M-L30C0S0B6N1	30	0	0	6	1	877	100%	Decreases slightly with Skewness
M-L30C0S15B6N1	30	0	15	6	1	871	99%	
M-L30C0S30B6N1	30	0	30	6	1	864	99%	
M-L30C0S45B6N1	30	0	45	6	1	857	98%	

Model ID	Span length (L in m)	Central Angle (α °)	Skew Angle (θ °)	Bottom Width, (B) (m)	Number of Cell (N)	Max. Shear Force (KN)	As % of straight model	Remarks
M-L30C12S0B6N1	30	12	0	6	1	886	101%	Varies Up to 7% with Skewness and Curvature
M-L30C12S15B6N1	30	12	15	6	1	871	99%	
M-L30C12S30B6N1	30	12	30	6	1	886	101%	
M-L30C12S45B6N1	30	12	45	6	1	901	103%	
M-L30C24S0B6N1	30	24	0	6	1	908	104%	
M-L30C24S15B6N1	30	24	15	6	1	912	104%	
M-L30C24S30B6N1	30	24	30	6	1	904	103%	
M-L30C24S45B6N1	30	24	45	6	1	917	105%	
M-L30C36S0B6N1	30	36	0	6	1	893	102%	
M-L30C36S15B6N1	30	36	15	6	1	916	104%	
M-L30C36S30B6N1	30	36	30	6	1	923	105%	
M-L30C36S45B6N1	30	36	45	6	1	935	107%	

Table 34: Maximum LL Shear Force for B6N2

Model ID	Span length (L in m)	Central Angle (α °)	Skew Angle (θ °)	Bottom Width, (B) (m)	Number of Cell (N)	Max. Shear Force (KN)	As % of straight model	Remarks
M-L30C0S0B6N2	30	0	0	6	2	3348	100%	Decreases slightly with Skewness
M-L30C0S15B6N2	30	0	15	6	2	3350	100%	
M-L30C0S30B6N2	30	0	30	6	2	3356	100%	
M-L30C0S45B6N2	30	0	45	6	2	3369	101%	
M-L30C12S0B6N2	30	12	0	6	2	3348	100%	Varies Up to 7% with Skewness and Curvature
M-L30C12S15B6N2	30	12	15	6	2	3339	100%	
M-L30C12S30B6N2	30	12	30	6	2	3338	100%	
M-L30C12S45B6N2	30	12	45	6	2	3338	100%	

Model ID	Span length (L in m)	Central Angle (α °)	Skew Angle (θ °)	Bottom Width, (B) (m)	Number of Cell (N)	Max. Shear Force (KN)	As % of straight model	Remarks
M-L30C24S0B6N2	30	24	0	6	2	3320	99%	
M-L30C24S15B6N2	30	24	15	6	2	3331	99%	
M-L30C24S30B6N2	30	24	30	6	2	3342	100%	
M-L30C24S45B6N2	30	24	45	6	2	3341	100%	
M-L30C36S0B6N2	30	36	0	6	2	3348	100%	
M-L30C36S15B6N2	30	36	15	6	2	3360	100%	
M-L30C36S30B6N2	30	36	30	6	2	3351	100%	
M-L30C36S45B6N2	30	36	45	6	2	3334	100%	

So, for all the four groups, it is noticed that the shear force due to live load varies maximum up to 10% with curvature and skewness.

6.2.3.4 Variation of Maximum Shear Force with "B: and "N":

Variation of maximum shear force for cross sections having different bottom width and number of cell has also been studied and presented below in bar chart.

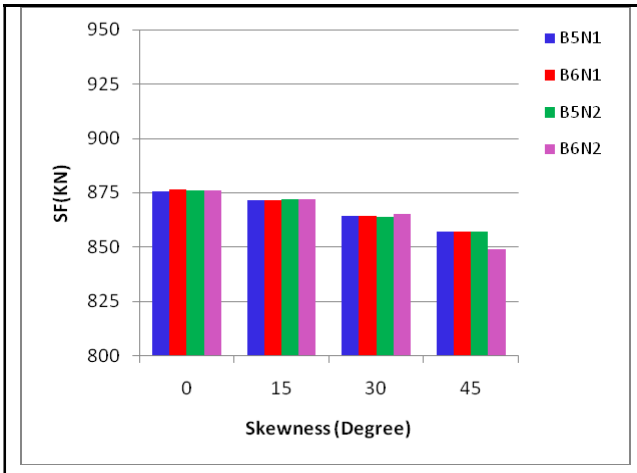

Plot- 1:α=0°

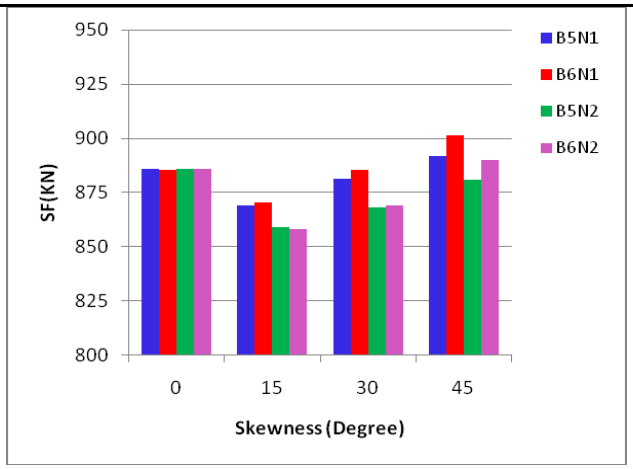

Plot- 2: α=12°

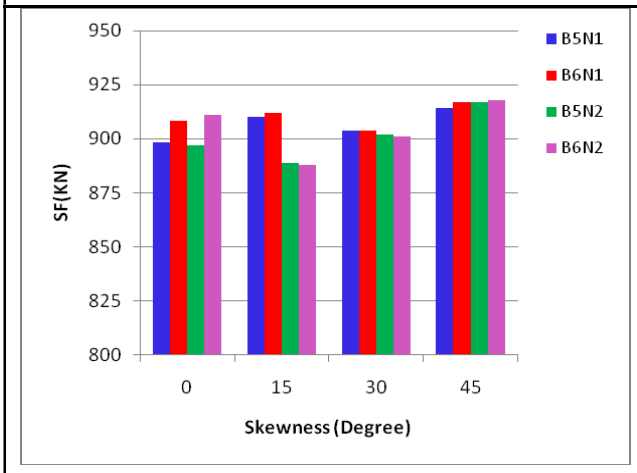

Plot- 3: α=24°

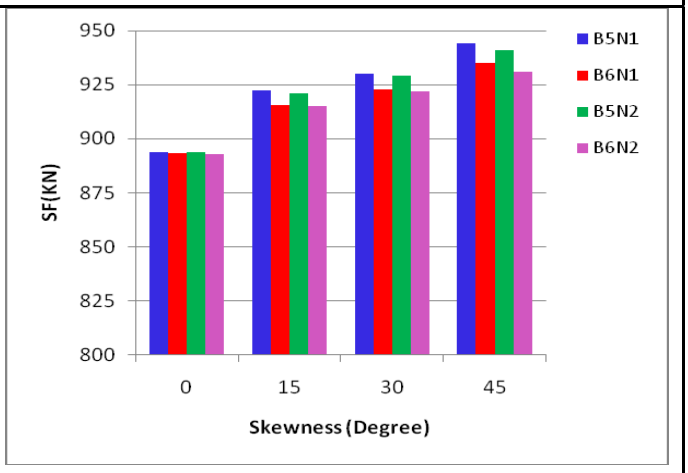

Plot- 4: α=36°

Discussion: It is seen that maximum shear force varies a bit for different types of cross sections having different bottom width and number of cells. This variation is obtained as 3.5% for α=0° and 24° and 5.5% for α=12° and 36°.

6.2.4 Effect on Joint Reaction/Bearing Force:

Bearing is a very complex component of bridge, as it simulates the support condition and negotiates the movement of the bridge due to environmental force. More or less all bearings deteriorate with time. Hence, bearings were always been a major concern for bridge engineers. The scenario becomes worse when skewness or curvature is introduced in a bridge leading to unequal joint reaction. The eccentricity of vehicle load

with bridge centre line also causes inequality in joint reaction. The variation of joint reaction due to curvature and skewness has been studied for all the four groups and presented below in tabular format. R is denoted for Joint Reaction.

Table 35: LL Joint Reaction B5N1

Model ID	Obtuse Corner			Central Joint			Acute Corner		
	R Max (KN)	As % of straight model	Remarks	R (KN)	As % of straight model	Remarks	R Min (KN)	As % of straight model	Remarks
M-L30C0S0B5N1	1033	100%	Increases with Skewness	NA	NA	NA	-179	100%	Increases with Skewness
M-L30C0S15B5N1	1072	104%		NA	NA	NA	-217	121%	
M-L30C0S30B5N1	1118	108%		NA	NA	NA	-313	175%	
M-L30C0S45B5N1	1145	111%		NA	NA	NA	-368	205%	
M-L30C12S0B5N1	1075	104%	Not such increase with Skewness; Curvature Introduced	NA	NA	NA	-202	113%	Increases with Skewness and Curvature
M-L30C12S15B5N1	1079	104%		NA	NA	NA	-207	116%	
M-L30C12S30B5N1	1080	105%		NA	NA	NA	-214	119%	
M-L30C12S45B5N1	1074	104%		NA	NA	NA	-263	147%	
M-L30C24S0B5N1	1129	109%	Increases Slightly with Skewness; Curvature Increased	NA	NA	NA	-273	152%	
M-L30C24S15B5N1	1199	116%		NA	NA	NA	-338	189%	
M-L30C24S30B5N1	1159	112%		NA	NA	NA	-338	189%	
M-L30C24S45B5N1	1175	114%		NA	NA	NA	-346	193%	
M-L30C36S0B5N1	1192	115%	Increases with Skewness and Curvature	NA	NA	NA	-437	244%	
M-L30C36S15B5N1	1225	119%		NA	NA	NA	-373	208%	
M-L30C36S30B5N1	1260	122%		NA	NA	NA	-429	240%	
M-L30C36S45B5N1	1342	130%		NA	NA	NA	-516	288%	

Table 36: LL Joint Reaction B5N2

Model ID	Obtuse Corner			Central Joint			Acute Corner		
	R Max (KN)	As % of straight model	Remarks	R (KN)	As % of straight model	Remarks	R Min (KN)	As % of straight model	Remarks
M-L30C0S0B5N2	930	100%	Increases with Skewness	367	100%	Increases with Skewness	-230	100%	Increases with Skewness
M-L30C0S15B5N2	993	107%		376	102%		-296	129%	
M-L30C0S30B5N2	1076	116%		394	107%		-345	150%	
M-L30C0S45B5N2	1164	125%		444	121%		-334	145%	
M-L30C12S0B5N2	975	105%	Not such increase with Skewness; Curvature Introduced	371	101%	Increases with Skewness and Curvature	-304	132%	Increases with Skewness and Curvature
M-L30C12S15B5N2	962	103%		393	107%		-334	145%	
M-L30C12S30B5N2	930	100%		459	125%		-382	166%	
M-L30C12S45B5N2	865	93%		605	165%		-478	208%	
M-L30C24S0B5N2	1025	110%		376	102%		-393	171%	
M-L30C24S15B5N2	1014	109%		409	111%		-453	197%	
M-L30C24S30B5N2	990	106%		489	133%		-539	234%	
M-L30C24S45B5N2	929	100%		679	185%		-706	307%	
M-L30C36S0B5N2	1090	117%	Increased with Curvature; Not such increase with Skewness	376	102%		-491	213%	
M-L30C36S15B5N2	1100	118%		407	111%		-574	250%	
M-L30C36S30B5N2	1086	117%		502	137%		-720	313%	
M-L30C36S45B5N2	1042	112%		766	209%		-1010	439%	

Table 37: LL Joint Reaction B6N1

Model ID	Obtuse Corner			Central Joint			Acute Corner		
	R Max (KN)	As % of straight model	Remarks	R (KN)	As % of straight model	Remarks	R Min (KN)	As % of straight model	Remarks
M-L30C0S0B6N1	940	100%	Increases with Skewness	NA	NA	NA	-112	100%	Increases with Skewness
M-L30C0S15B6N1	984	105%		NA	NA	NA	-152	135%	
M-L30C0S30B6N1	1030	110%		NA	NA	NA	-244	217%	
M-L30C0S45B6N1	1053	112%		NA	NA	NA	-290	259%	
M-L30C12S0B6N1	975	104%	Not such increase	NA	NA	NA	-133	119%	Increases with

Model ID	Obtuse Corner			Central Joint			Acute Corner		
	R Max (KN)	As % of straight model	Remarks	R (KN)	As % of straight model	Remarks	R Min (KN)	As % of straight model	Remarks
M-L30C12S15B6N1	977	104%	with Skewness; Curvature Introduced	NA	NA	NA	-136	121%	Skewness and Curvature
M-L30C12S30B6N1	976	104%		NA	NA	NA	-147	131%	
M-L30C12S45B6N1	970	103%		NA	NA	NA	-197	175%	
M-L30C24S0B6N1	1022	109%	Increases Slightly with Skewness; Curvature Increased	NA	NA	NA	-179	159%	
M-L30C24S15B6N1	1080	115%		NA	NA	NA	-233	208%	
M-L30C24S30B6N1	1043	111%		NA	NA	NA	-250	223%	
M-L30C24S45B6N1	1057	113%		NA	NA	NA	-334	298%	
M-L30C36S0B6N1	1074	114%	Increases with Skewness and Curvature	NA	NA	NA	-260	232%	
M-L30C36S15B6N1	1099	117%		NA	NA	NA	-310	276%	
M-L30C36S30B6N1	1126	120%		NA	NA	NA	-388	346%	
M-L30C36S45B6N1	1195	127%		NA	NA	NA	-539	480%	

Table 38: LL Joint Reaction B6N2

Model ID	Obtuse Corner			Central Joint			Acute Corner		
	R Max (KN)	As % of straight model	Remarks	R (KN)	As % of straight model	Remarks	R Min (KN)	As % of straight model	Remarks
M-L30C0S0B6N2	836	100%	Increases with Skewness	395	100%	Increases with Skewness	-145	100%	Increases with Skewness
M-L30C0S15B6N2	905	108%		402	102%		-214	148%	
M-L30C0S30B6N2	991	119%		418	106%		-264	182%	
M-L30C0S45B6N2	1061	127%		461	117%		-248	171%	
M-L30C12S0B6N2	873	104%	Not such increase with Skewness; Curvature Introduced	399	101%	Increases with Skewness and Curvature	-208	143%	Increases with Skewness and Curvature
M-L30C12S15B6N2	855	102%		422	107%		-240	166%	
M-L30C12S30B6N2	814	97%		489	124%		-294	203%	
M-L30C12S45B6N2	742	89%		630	159%		-400	276%	
M-L30C24S0B6N2	910	109%		404	102%		-292	201%	
M-L30C24S15B6N2	899	108%		436	110%		-342	236%	
M-L30C24S30B6N2	864	103%		517	131%		-430	297%	

Model ID	Obtuse Corner			Central Joint			Acute Corner		
	R Max (KN)	As % of straight model	Remarks	R (KN)	As % of straight model	Remarks	R Min (KN)	As % of straight model	Remarks
M-L30C24S45B6N2	794	95%		698	177%		-594	410%	
M-L30C36S0B6N2	969	116%	Increased with Curvature; Not such increase with Skewness	405	103%		-369	254%	
M-L30C36S15B6N2	967	116%		440	111%		-449	310%	
M-L30C36S30B6N2	940	112%		535	135%		-588	406%	
M-L30C36S45B6N2	880	105%		781	198%		-859	592%	

Discussion: As vehicular live load is an eccentric load, the vertical reactions obtained are unequal for straight bridges and leads to negative value as minimum reaction. The difference between maximum and minimum vertical reaction increases with introduction of skewness and curvature in bridges. When no curvature is introduced, increase of the maximum vertical reaction is 11% (B5N1) to 12% (B6N1) for a single cell structure while the minimum reaction/negative reaction increases 105% (B5N1) to 159% (B6N1). But, for double cell structure the increase in maximum vertical reaction due to skewness only is observed as 25% (B5N2) and 27% (B6N2) and increase in minimum reaction/negative reaction is observed as 45% (B5N2) to (B6N2) 71%. When, curvature is introduced, the maximum reaction increases only 15% to 30%, while the minimum reaction/negative reaction increases 188% (B5N1) to 492% (B6N2).

The reaction at central joints also increased with skewness up to 20% and increases further when curvature is introduced up to 109%.

An important point to note that, though the rate of increase of maximum reaction with increase in transverse stiffness decreases, the rate of increase of minimum reaction/negative reaction increases further.

6.2.5 Effect on Maximum Deflection:

For the same structure, deflection shows a variation when skewness and curvature is introduced. Maximum deflection near mid span has been considered. The study is presented below in tabular format.

Table 39: LL Deflection for B5N1

Model ID	Span length (L in m)	Central Angle (α °)	Skew Angle, (θ °)	Bottom Width, (B) (m)	Number of Cell (N)	Deflection (mm)	As % of straight model	Remarks
M-L30C0S0B5N1	30	0	0	5	1	2.7	100%	Decreases with Skewness
M-L30C0S15B5N1	30	0	15	5	1	2.6	96%	
M-L30C0S30B5N1	30	0	30	5	1	2.4	89%	
M-L30C0S45B5N1	30	0	45	5	1	2.2	81%	
M-L30C12S0B5N1	30	12	0	5	1	2.9	107%	Increases with curvature and Skewness.
M-L30C12S15B5N1	30	12	15	5	1	3.3	122%	
M-L30C12S30B5N1	30	12	30	5	1	3.8	141%	
M-L30C12S45B5N1	30	12	45	5	1	4.7	174%	
M-L30C24S0B5N1	30	24	0	5	1	3.2	119%	
M-L30C24S15B5N1	30	24	15	5	1	3.9	144%	
M-L30C24S30B5N1	30	24	30	5	1	4.7	174%	
M-L30C24S45B5N1	30	24	45	5	1	6.4	237%	
M-L30C36S0B5N1	30	36	0	5	1	3.7	137%	
M-L30C36S15B5N1	30	36	15	5	1	4.5	167%	
M-L30C36S30B5N1	30	36	30	5	1	6.0	222%	
M-L30C36S45B5N1	30	36	45	5	1	9.4	348%	

Table 40: LL Deflection for B5N2

Model ID	Span length (L in m)	Central Angle (α °)	Skew Angle, (θ °)	Bottom Width, (B) (m)	Number of Cell (N)	Deflection (mm)	As % of straight model	Remarks
M-L30C0S0B5N2	30	0	0	5	2	3.4	100%	Decreases with Skewness
M-L30C0S15B5N2	30	0	15	5	2	3.3	97%	
M-L30C0S30B5N2	30	0	30	5	2	3.1	91%	
M-L30C0S45B5N2	30	0	45	5	2	2.7	79%	

Model ID	Span length (L in m)	Central Angle (α °)	Skew Angle, (θ °)	Bottom Width, (B) (m)	Number of Cell (N)	Deflection (mm)	As % of straight model	Remarks
M-L30C12S0B5N2	30	12	0	5	2	3.8	112%	Increases with curvature and Skewness.
M-L30C12S15B5N2	30	12	15	5	2	4.5	132%	
M-L30C12S30B5N2	30	12	30	5	2	5.5	162%	
M-L30C12S45B5N2	30	12	45	5	2	7.3	215%	
M-L30C24S0B5N2	30	24	0	5	2	4.3	126%	
M-L30C24S15B5N2	30	24	15	5	2	5.3	156%	
M-L30C24S30B5N2	30	24	30	5	2	6.9	203%	
M-L30C24S45B5N2	30	24	45	5	2	10.0	294%	
M-L30C36S0B5N2	30	36	0	5	2	5.0	147%	
M-L30C36S15B5N2	30	36	15	5	2	6.4	188%	
M-L30C36S30B5N2	30	36	30	5	2	8.9	262%	
M-L30C36S45B5N2	30	36	45	5	2	14.7	432%	

Table 41: LL Deflection for B6N1

Model ID	Span length (L in m)	Central Angle (α °)	Skew Angle, (θ °)	Bottom Width, (B) (m)	Number of Cell (N)	Deflection (mm)	As % of straight model	Remarks
M-L30C0S0B6N1	30	0	0	6	1	2.4	100%	Decreases with Skewness
M-L30C0S15B6N1	30	0	15	6	1	2.5	104%	
M-L30C0S30B6N1	30	0	30	6	1	2.2	92%	
M-L30C0S45B6N1	30	0	45	6	1	1.9	79%	
M-L30C12S0B6N1	30	12	0	6	1	2.7	113%	Increases with curvature and Skewness.
M-L30C12S15B6N1	30	12	15	6	1	3.1	129%	
M-L30C12S30B6N1	30	12	30	6	1	3.6	150%	
M-L30C12S45B6N1	30	12	45	6	1	4.5	188%	
M-L30C24S0B6N1	30	24	0	6	1	2.9	121%	
M-L30C24S15B6N1	30	24	15	6	1	3.6	150%	

Model ID	Span length (L in m)	Central Angle (α °)	Skew Angle, (θ °)	Bottom Width, (B) (m)	Number of Cell (N)	Deflection (mm)	As % of straight model	Remarks
M-L30C24S30B6N1	30	24	30	6	1	4.4	183%	
M-L30C24S45B6N1	30	24	45	6	1	6.0	250%	
M-L30C36S0B6N1	30	36	0	6	1	3.4	142%	
M-L30C36S15B6N1	30	36	15	6	1	4.2	175%	
M-L30C36S30B6N1	30	36	30	6	1	5.6	233%	
M-L30C36S45B6N1	30	36	45	6	1	8.7	363%	

Table 42: LL Deflection for B6N2

Model ID	Span length (L in m)	Central Angle (α °)	Skew Angle, (θ °)	Bottom Width, (B) (m)	Number of Cell (N)	Deflection (mm)	As % of straight model	Remarks
M-L30C0S0B6N2	30	0	0	6	2	3.2	100%	Decreases with Skewness
M-L30C0S15B6N2	30	0	15	6	2	3.1	97%	
M-L30C0S30B6N2	30	0	30	6	2	2.9	91%	
M-L30C0S45B6N2	30	0	45	6	2	2.5	78%	
M-L30C12S0B6N2	30	12	0	6	2	3.6	113%	Increases with curvature and Skewness.
M-L30C12S15B6N2	30	12	15	6	2	4.3	134%	
M-L30C12S30B6N2	30	12	30	6	2	5.4	169%	
M-L30C12S45B6N2	30	12	45	6	2	7.2	225%	
M-L30C24S0B6N2	30	24	0	6	2	4.1	128%	
M-L30C24S15B6N2	30	24	15	6	2	5.1	159%	
M-L30C24S30B6N2	30	24	30	6	2	6.6	206%	
M-L30C24S45B6N2	30	24	45	6	2	9.8	306%	
M-L30C36S0B6N2	30	36	0	6	2	4.7	147%	
M-L30C36S15B6N2	30	36	15	6	2	6.1	191%	
M-L30C36S30B6N2	30	36	30	6	2	8.6	269%	
M-L30C36S45B6N2	30	36	45	6	2	14.4	450%	

Discussion: Generally, deflection shows almost a same variation with BM when the bridge is skew, curve or skew curved. It is found that, deflection reduces with skewness for skew bridges (up to 20%). When Curvature comes into picture, deflection increases. For Skew-curved bridges the deflection increases 3.5 to 3.6 times for single cell bridges and 4.3 to 4.5 times for double cell bridges.

6.3 Comparison of maximum responses between 30m and 35m bridges:

A set of 35m bridge having cross section same as B5N1 (30m span) has been modeled also analyzed for the loads as stated in Chapter-5. The maximum responses are obtained and compared with that of the 30m span bridges. The comparison is presented below response wise.

A factor **C** is introduced such that; **C= [Response of Particular Model/Response of straight Model]**. **C** is termed as **Response Coefficient**. C would be expressed as load condition, response type and span length in suffix. For example, C_{DLBM30}=Response Coefficient for DL Bending Moment for 30m span.

As Dead load torsion is zero for straight bridges,

$C_{DLT\ (Span\ Length)}$ = [Response of Particular Model/Response of non-skew Model (θ=0°)]. Response coefficient for Live load torsion is also expressed in same manner.

Rec. prefix is used to express Recommended Response coefficient.

6.3.1 Dead Load Bending Moment:

Table 43: Response Coefficient for Dead Load Bending moment.

Sl No	Central Angle (α°)	Skew Angle, (θ°)	30m Span		35 m Span		Difference in C for two span as % of C_{DLBM30}	Rec. C_{DLBM},
			Max. Bending Moment (KN-m)	C_{DLBM30}	Max. Bending Moment (KN-m)	C_{DLBM35}		
1	0	0	21587	1.00	29265	1.00	0.0%	1.00
2	0	15	20991	0.97	28412	0.97	-0.2%	0.97
3	0	30	19210	0.89	25948	0.89	-0.4%	0.89

Sl No	Central Angle (α°)	Skew Angle, (θ°)	30m Span		35 m Span		Difference in C for two span as % of C_{DLBM30}	Rec. C_{DLBM},
			Max. Bending Moment (KN-m)	C_{DLBM30}	Max. Bending Moment (KN-m)	C_{DLBM35}		
4	0	45	16382	0.76	22047	0.75	-0.7%	0.76
5	12	0	21691	1.00	29429	1.01	0.1%	1.01
6	12	15	22188	1.03	30180	1.03	0.3%	1.03
7	12	30	22920	1.06	31236	1.07	0.5%	1.06
8	12	45	24221	1.12	33046	1.13	0.6%	1.13
9	24	0	22014	1.02	30018	1.03	0.6%	1.02
10	24	15	23023	1.07	31593	1.08	1.2%	1.07
11	24	30	24484	1.13	33854	1.16	2.0%	1.15
12	24	45	27121	1.26	37956	1.30	3.2%	1.28
13	36	0	22569	1.05	31048	1.06	1.5%	1.05
14	36	15	24188	1.12	33655	1.15	2.6%	1.14
15	36	30	26635	1.23	37677	1.29	4.3%	1.26
16	36	45	31447	1.46	46003	1.57	7.9%	1.51

Discussion: The difference of C_{DLBM} between two spans is less than 5% except for the maximum Skew-Curved Bridge. For maximum Skew-Curved Bridge the difference is within 8%, which is very much acceptable for practical engineering problem.

6.3.2 Dead Load Torsion:

Table 44: Response Coefficient for Dead Load Torsion.

Sl No	Central Angle (α°)	Skew Angle, (θ°)	30m Span		35 m Span		Difference in C for two span as % of C_{DLT30}	Rec. C_{DLT},
			Max. Torsion (KN-m)	C_{DLT30}	Max. Torsion (KN-m)	C_{DLT35}		
1	0	0	0	-	0	-	NA	
2	0	15	2324	1.00	3200	1.00	0.0%	1.00
3	0	30	4315	1.86	5932	1.85	-0.2%	1.86
4	0	45	5515	2.37	7552	2.36	-0.6%	2.37
5	12	0	1658	1.00	2567	1.00	0.0%	1.00
6	12	15	1990	1.20	2944	1.15	-4.4%	1.17
7	12	30	2461	1.48	3468	1.35	-9.0%	1.42
8	12	45	3205	1.93	4303	1.68	-13.3%	1.80
9	24	0	3313	1.00	5157	1.00	0.0%	1.00
10	24	15	3818	1.15	5828	1.13	-1.9%	1.14
11	24	30	4527	1.37	6784	1.32	-3.7%	1.34
12	24	45	5621	1.70	8328	1.61	-4.8%	1.66

Sl No	Central Angle (α°)	Skew Angle, (θ°)	30m Span		35 m Span		Difference in C for two span as % of C_{DLT30}	Rec. C_{DLT},
			Max. Torsion (KN-m)	C_{DLT30}	Max. Torsion (KN-m)	C_{DLT35}		
13	36	0	5075	1.00	7979	1.00	0.0%	1.00
14	36	15	5979	1.18	9345	1.17	-0.6%	1.17
15	36	30	7091	1.40	11135	1.40	-0.1%	1.40
16	36	45	9099	1.79	14642	1.84	2.4%	1.81

Discussion: The difference of C_{DLT} between two spans is less than 5% except for two Skew-Curved Bridges (α=12°; θ=30° and 45°). For these Skew-Curved Bridge the difference is 9% (θ=30°) and 13.3% (θ=45°), which can be accepted for practical engineering problem.

6.3.3 Dead Load Shear Force:

Table 45: Response Coefficient for Dead Load Shear Force

Sl No	Central Angle (α°)	Skew Angle, (θ°)	30m Span		35 m Span		Difference in C for two span as % of C_{DLSF30}	Rec. C_{DLSF},
			Max. Shear Force (KN)	C_{DLSF30}	Max. Shear Force (KN)	C_{DLSF35}		
1	0	0	2829	1.00	3293	1.00	0.0%	1.00
2	0	15	2830	1.00	3295	1.00	0.0%	1.00
3	0	30	2836	1.00	3300	1.00	0.0%	1.00
4	0	45	2849	1.01	3313	1.01	-0.1%	1.01
5	12	0	2829	1.00	3293	1.00	0.0%	1.00
6	12	15	2848	1.01	3322	1.01	0.2%	1.01
7	12	30	2841	1.00	3313	1.01	0.2%	1.01
8	12	45	2835	1.00	3306	1.00	0.2%	1.00
9	24	0	2829	1.00	3293	1.00	0.0%	1.00
10	24	15	2828	1.00	3292	1.00	0.0%	1.00
11	24	30	2823	1.00	3287	1.00	0.0%	1.00
12	24	45	2812	0.99	3277	1.00	0.1%	0.99
13	36	0	2829	1.00	3293	1.00	0.0%	1.00
14	36	15	2848	1.01	3322	1.01	0.2%	1.01
15	36	30	2837	1.00	3310	1.01	0.2%	1.00
16	36	45	2818	1.00	3293	1.00	0.4%	1.00

Discussion: As shear force does not vary much, the difference of C_{DLSF} between two spans is less than 0.4%. This is well accepted for engineering studies and practical problem.

6.3.4 Dead Load Maximum Bearing Reaction/Joint Reaction:

Table 46 : Response Coefficient for Dead Load Maximum Bearing reaction

Sl No	Central Angle (α°)	Skew Angle, (θ°)	30m Span		35 m Span		Difference in C for two span as % of $C_{DLRmax30}$	Rec. C_{DLRmax},
			Max. Reaction (KN)	$C_{DLRmax30}$	Max. Reaction (KN)	$C_{DLRmax35}$		
1	0	0	1462	1.00	1726	1.00	0.0%	1.00
2	0	15	1928	1.32	2336	1.35	2.6%	1.34
3	0	30	2334	1.60	2890	1.67	4.9%	1.64
4	0	45	2592	1.77	3231	1.87	5.6%	1.82
5	12	0	1787	1.22	2199	1.27	4.3%	1.25
6	12	15	1869	1.28	2290	1.33	3.8%	1.30
7	12	30	1974	1.35	2405	1.39	3.2%	1.37
8	12	45	2132	1.46	2584	1.50	2.6%	1.48
9	24	0	2123	1.45	2725	1.58	8.7%	1.52
10	24	15	2238	1.53	2875	1.67	8.8%	1.60
11	24	30	2395	1.64	3082	1.79	9.0%	1.71
12	24	45	2648	1.81	3427	1.99	9.6%	1.90
13	36	0	2477	1.69	3290	1.91	12.5%	1.80
14	36	15	2652	1.81	3552	2.06	13.5%	1.94
15	36	30	2903	1.99	3941	2.28	15.0%	2.13
16	36	45	3347	2.29	4682	2.71	18.5%	2.50

Discussion: The difference of C_{DLRmax} between two spans is less than 10% except for Bridges subjected to highest curvature (α=36°). This can be accepted for practical engineering problem. For bridges subjected to highest curvature; C_{DLRmax} varies 12% to 20%.

6.3.5 Dead Load Deflection:

Table 47: Response Coefficient for Dead Load Deflection

Sl No	Central Angle (α°)	Skew Angle, (θ°)	30m Span		35 m Span		Difference in C for two span as % of $C_{DL\delta30}$	Rec. $C_{DL\delta}$,
			Deflection, δ (mm)	$C_{DL\delta30}$	Deflection, δ (mm)	$C_{DL\delta35}$		
1	0	0	9.6	1.00	17.1	1.00	0.0%	1.00
2	0	15	9.3	0.97	16.5	0.96	-0.4%	0.97
3	0	30	8.4	0.88	14.8	0.87	-1.1%	0.87
4	0	45	6.9	0.72	12	0.70	-2.4%	0.71
5	12	0	9.8	1.02	18.3	1.07	4.8%	1.05
6	12	15	10.3	1.07	20.4	1.19	11.2%	1.13

Sl No	Central Angle (α°)	Skew Angle, (θ°)	30m Span		35 m Span		Difference in C for two span as % of $C_{DL\delta30}$	Rec. $C_{DL\delta}$,
			Deflection, δ (mm)	$C_{DL\delta30}$	Deflection, δ (mm)	$C_{DL\delta35}$		
7	12	30	11	1.15	23.6	1.38	20.4%	1.26
8	12	45	12.5	1.30	29.3	1.71	31.6%	1.51
9	24	0	10.4	1.08	20.5	1.20	10.7%	1.14
10	24	15	11.4	1.19	24.3	1.42	19.7%	1.30
11	24	30	13.1	1.36	30.2	1.77	29.4%	1.57
12	24	45	16.5	1.72	42.8	2.50	45.6%	2.11
13	36	0	11.3	1.18	23.8	1.39	18.2%	1.28
14	36	15	13.1	1.36	30	1.75	28.6%	1.56
15	36	30	16.3	1.70	41.2	2.41	41.9%	2.05
16	36	45	23.7	2.47	70.3	4.11	66.5%	3.29

Discussion: The recommended value of $C_{DL\delta}$ varies within 10-15% and is acceptable for practical problem for non-curved bridges and Skew-curved bridges with a limitation of skew angle, θ=15° and curvature of α=24°.

6.3.6 Class 70R Live Load Bending Moment:

Table 48: Response Coefficient for Live Load Maximum Bending Moment

Sl No	Central Angle (α°)	Skew Angle, (θ°)	30m Span		35 m Span		Difference in C for two span as % of C_{LLBM30}	Rec. C_{LLBM},
			Max. Bending Moment (KN-m)	C_{LLBM30}	Max. Bending Moment (KN-m)	C_{LLBM35}		
1	0	0	6466	1.00	7842	1.00	0.0%	1.00
2	0	15	6409	0.99	7750	0.99	-0.3%	0.99
3	0	30	6097	0.94	7336	0.94	-0.8%	0.94
4	0	45	5866	0.91	6914	0.88	-2.8%	0.89
5	12	0	6674	1.03	8100	1.03	0.1%	1.03
6	12	15	7300	1.13	8774	1.12	-0.9%	1.12
7	12	30	8069	1.25	9613	1.23	-1.8%	1.24
8	12	45	9210	1.42	10876	1.39	-2.6%	1.41
9	24	0	6946	1.07	8461	1.08	0.4%	1.08
10	24	15	7790	1.20	9426	1.20	-0.2%	1.20
11	24	30	8765	1.36	10577	1.35	-0.5%	1.35
12	24	45	10456	1.62	12640	1.61	-0.3%	1.61
13	36	0	7287	1.13	8939	1.14	1.1%	1.13
14	36	15	8273	1.28	10138	1.29	1.0%	1.29
15	36	30	9675	1.50	11916	1.52	1.5%	1.51
16	36	45	12265	1.90	15454	1.97	3.9%	1.93

Discussion: The difference of C_{LLBM} between two spans is less than 5%, which is very much acceptable for practical engineering problem.

6.3.7 Class 70R Live Load Torsion:

Table 49: Response Coefficient for Live Load Maximum Torsion

Sl No	Central Angle (α°)	Skew Angle, (θ°)	30m Span		35 m Span		Difference in C for two span as % of C_{LLT30}	Rec. C_{LLT},
			Max. Torsion (KN-m)	C_{LLT30}	Max. Torsion (KN-m)	C_{LLT35}		
1	0	0	2784	1.00	2899	1.00	0.0%	1.00
2	0	15	3095	1.11	3257	1.12	1.1%	1.12
3	0	30	3420	1.23	3630	1.25	1.9%	1.24
4	0	45	3620	1.30	3881	1.34	3.0%	1.32
5	12	0	3074	1.00	3267	1.00	0.0%	1.00
6	12	15	2984	0.97	3199	0.98	0.9%	0.98
7	12	30	2980	0.97	3169	0.97	0.1%	0.97
8	12	45	2908	0.95	3107	0.95	0.5%	0.95
9	24	0	3377	1.00	3654	1.00	0.0%	1.00
10	24	15	3685	1.09	3979	1.09	-0.2%	1.09
11	24	30	3487	1.03	3821	1.05	1.3%	1.04
12	24	45	3560	1.05	4118	1.13	6.9%	1.09
13	36	0	3739	1.00	4228	1.00	0.0%	1.00
14	36	15	3971	1.06	4553	1.08	1.4%	1.07
15	36	30	4186	1.12	5008	1.18	5.8%	1.15
16	36	45	4820	1.29	6143	1.45	12.7%	1.37

Discussion: The difference of C_{LLT} between two spans is less than 5%, except skew curved bridges having (α=36°; θ=30° and 45°) which is very much acceptable for practical engineering problem.

6.3.8 Class 70R Live Load Shear Force:

Table 50: Response Coefficient for Live Load Shear Force

Sl No	Central Angle (α°)	Skew Angle, (θ°)	30m Span		35 m Span		Difference in C for two span as % of C_{LLSF30}	Rec. C_{LLSF},
			Max. Shear Force (KN)	C_{LLSF30}	Max. Shear Force (KN)	C_{LLSF35}		
1	0	0	875	1.00	909	1.00	0.0%	1.00
2	0	15	871	1.00	904	0.99	-0.1%	0.99

Sl No	Central Angle (α°)	Skew Angle, (θ°)	30m Span		35 m Span		Difference in C for two span as % of C_{LLSF30}	Rec. C_{LLSF},
			Max. Shear Force (KN)	C_{LLSF30}	Max. Shear Force (KN)	C_{LLSF35}		
3	0	30	864	0.99	897	0.99	-0.1%	0.99
4	0	45	857	0.98	889	0.98	-0.1%	0.98
5	12	0	886	1.01	917	1.01	-0.3%	1.01
6	12	15	869	0.99	905	1.00	0.3%	0.99
7	12	30	881	1.01	913	1.00	-0.2%	1.01
8	12	45	892	1.02	925	1.02	-0.1%	1.02
9	24	0	898	1.03	928	1.02	-0.5%	1.02
10	24	15	910	1.04	937	1.03	-0.8%	1.04
11	24	30	904	1.03	927	1.02	-1.2%	1.03
12	24	45	914	1.04	937	1.03	-1.3%	1.04
13	36	0	894	1.02	924	1.02	-0.4%	1.02
14	36	15	922	1.05	952	1.05	-0.6%	1.05
15	36	30	930	1.06	958	1.05	-0.8%	1.06
16	36	45	944	1.08	969	1.07	-1.2%	1.07

Discussion: As shear force does not vary much, the difference of C_{LLSF} between two spans is less than 0.4%. This is well accepted for engineering studies and practical problem.

6.3.9 Class 70R Live Load Bearing Reaction/Joint Reaction:

Table 51: Response Coefficient for Live Load Maximum Bearing Reaction

Sl No	Central Angle (α°)	Skew Angle, (θ°)	30m Span		35 m Span		Difference in C for two span as % of $C_{LLRmax30}$	Rec. C_{LLRmax},
			Max. Reaction (KN)	$C_{LLRmax30}$	Max. Reaction (KN)	$C_{LLRmax35}$		
1	0	0	1033	1.00	1067	1.00	0.0%	1.00
2	0	15	1072	1.04	1117	1.05	0.9%	1.04
3	0	30	1118	1.08	1173	1.10	1.6%	1.09
4	0	45	1145	1.11	1208	1.13	2.2%	1.12
5	12	0	1075	1.04	1110	1.04	0.0%	1.04
6	12	15	1079	1.04	1122	1.05	0.7%	1.05
7	12	30	1080	1.05	1118	1.05	0.2%	1.05
8	12	45	1074	1.04	1107	1.04	-0.2%	1.04
9	24	0	1129	1.09	1190	1.12	2.0%	1.10
10	24	15	1199	1.16	1261	1.18	1.8%	1.17
11	24	30	1159	1.12	1216	1.14	1.6%	1.13
12	24	45	1175	1.14	1242	1.16	2.3%	1.15
13	36	0	1192	1.15	1276	1.20	3.6%	1.17

Sl No	Central Angle (α°)	Skew Angle, (θ°)	30m Span		35 m Span		Difference in C for two span as % of $C_{LLRmax30}$	Rec. C_{LLRmax},
			Max. Reaction (KN)	$C_{LLRmax30}$	Max. Reaction (KN)	$C_{LLRmax35}$		
14	36	15	1225	1.19	1315	1.23	4.0%	1.21
15	36	30	1260	1.22	1380	1.29	6.0%	1.26
16	36	45	1342	1.30	1560	1.46	12.5%	1.38

Discussion: The difference of C_{LLRmax} between two spans is less than 5%, except skew curved bridges having (α=36°; θ=30° and 45°) which is very much acceptable for practical engineering problem.

6.3.10 Class 70R Live Load Deflection:

Table 52: Response Coefficient for Live Load Deflection

Sl No	Central Angle (α°)	Skew Angle, (θ°)	30m Span		35 m Span		Difference in C for two span as % of $C_{LL\delta30}$	Rec. $C_{LL\delta30}$,
			Deflection, δ (mm)	$C_{LL\delta30}$	Deflection, δ (mm)	$C_{LL\delta35}$		
1	0	0	2.7	1.00	4.7	1.00	0.0%	1.00
2	0	15	2.6	0.96	4.6	0.98	1.6%	0.97
3	0	30	2.4	0.89	4.2	0.89	0.5%	0.89
4	0	45	2.2	0.81	3.7	0.79	-3.4%	0.80
5	12	0	2.9	1.07	5.3	1.13	5.0%	1.10
6	12	15	3.3	1.22	6.2	1.32	7.9%	1.27
7	12	30	3.8	1.41	7.5	1.60	13.4%	1.50
8	12	45	4.7	1.74	9.9	2.11	21.0%	1.92
9	24	0	3.2	1.19	6.1	1.30	9.5%	1.24
10	24	15	3.9	1.44	7.6	1.62	11.9%	1.53
11	24	30	4.7	1.74	9.8	2.09	19.8%	1.91
12	24	45	6.4	2.37	14.6	3.11	31.1%	2.74
13	36	0	3.7	1.37	7.2	1.53	11.8%	1.45
14	36	15	4.5	1.67	9.5	2.02	21.3%	1.84
15	36	30	6.0	2.22	10.2	2.17	-2.3%	2.20
16	36	45	9.4	3.48	24	5.11	46.7%	4.29

Discussion: The recommended value of $C_{LL\delta}$, varies within 10-15% and is acceptable for practical problem for non-curved bridges and Skew-curved bridges with a limitation of skew angle, θ=15° and curvature of α=24°.

Capter-7: Conclusions

7.0 General:

Five types of bridge responses e.g. bending moment, torsion, shear force, support reaction and deflection has been studied in the present thesis. The major point wise conclusion has been presented in Section 7.1; while Section 7.2 indicates the future scope.

7.1 Conclusions:

An exhaustive parametric study has been carried out to examine the effect of curvature and skewness on various bridge responses of simply supported concrete box girder bridge. The three dimensional modeling and finite element analyses of the concrete box girder bridges for various combination of curvature, skewness, cross section and span has been carried out using SAP 2000 software package. The study shows that the bridge responses vary significantly with curvature and skewness.

7.1.1 Bending Moment:

It has been found that bending moment decreases up to 25% and 10% in dead load and live load cases, respectively, for skew bridges (curvature is zero). For curved bridges (skew angle is zero) the bending moment enhances up to 5% and 13% for dead load and live load cases respectively. When the bridge is subjected to both skew angle and curvature the bending moment enhances to 45% to 50% and 90% to 100% for dead load and live load respectively. It is also examined that critical section for live load shifts up to 33% with skewness.

The response coefficients for dead load and live load bending moment as obtained for 30m span is in good agreement with those of 35m span also. The maximum variation in bending moment response coefficient is 7.9% and 3.9% for dead load and live load respectively. This may be acceptable for all practical purpose.

7.1.2 Torsion:

No dead load torsion is obtained for straight bridges. It has been found that torsion under dead load cases increases up to 130% for skew bridges (curvature is zero). The dead load torsion decreases up to 30% (with respect to torsion for θ=15°; α=0°) when curvature is just introduced (α=12°). When curvature effect is coupled with skewness the dead load torsion increases very rapidly.

It is noted that unlike dead load case, torsion is obtained for straight bridge in live load cases due to live load eccentricity. Live load torsion enhances with skewness (curvature is zero), decreases with skewness when mild curvature is introduced (α=12°), shows a mild increment of 2% to 12% for α=24° and increases very rapidly for α=36°. The live load torsion slightly decreases with increase in torsional stiffness.

The response coefficients for dead load and live load torsion as obtained for 30m span is in good agreement with those of 35m span also. The variation in torsion response coefficient is within 10% for both dead load and live load in most of the cases. Maximum variation is obtained as 13%. This may be acceptable for all practical purpose.

7.1.3 Shear Force:

Shear force does not vary much with curvature and skewness. The maximum variation of dead load and live load shear force is obtained as 2% and 8% respectively.

The response coefficients for shear force are also in very close for both the span in dead load and live load case as the maximum difference obtained as 0.4% for dead load and 1.3% for live load. This may be acceptable for all engineering purpose.

7.1.4 Bearing reaction/Joint Reaction:

It is observed that the vertical reaction becomes unequal with introduction of curvature and skewness. When no curvature is introduced, increase/decrease of the vertical reaction is 72% to 75% for a single cell structure. But, for double cell structure the increase in reaction due to skewness only is observed as 128% to 138% and decrease in reaction is observed as 93% to 99%. When, curvature is introduced, the difference in

reactions increases further; causing uplift at one acute corner and 2 to 2.4 time reactions at adjacent obtuse corner. The reaction at central joints also decreased with skewness up to 30% and increases further when skewness is coupled with curvature.

As vehicular live load is an eccentric load, the vertical reactions, obtained in live load case, are unequal for straight bridges and leads to negative value as minimum reaction. The difference between maximum and minimum vertical reaction increases with introduction of skewness and curvature in bridges. Maximum vertical reaction increases up to 11%-12%, while the minimum reaction/negative reaction enhances up to 105%-159% for a single cell structure when no curvature is introduced. But, for double cell structure the increase in maximum vertical reaction is observed as 25%-27% and increase in minimum reaction/negative reaction is observed as 45%-71%. When, curvature is introduced, the maximum reaction shows an upward variation of 15% to 30% only, while the minimum reaction/negative reaction shows a rapid variation188%-492%. The reaction at central joints also increased with skewness up to 20% and increases further up to 109%, when curvature is introduced. It is also noted that, though the rate of increase of maximum reaction with increase in transverse stiffness decreases, the rate of increase of minimum reaction/negative reaction increases further.

Bearings are very important component of bridge as it simulates the support condition transfers the loads to substructure. As noted the difference in joint reaction in skew curved bridges varies manifold, special care should be take in design and placing of bearings. Special type of bearing (spherical bearing/knuckle bearing) may be provided at acute corners of the skew bridges or at inner ends of curved/skew-curved bridges to resist the uplift force, if required.

The difference between response coefficients for maximum dead load reaction between two span is obtained within 10% for all models except for the models in highest curvature i.e $\alpha=36°$. For highest curvature the maximum difference is obtained as 18.5%. The response coefficient for maximum live load reaction differs within 10% for all cases except for the model subjected to highest curvature and skewness. For that case the

difference is obtained as 12.5%. It is proposed to follow the recommended response coefficients for all practical engineering problems.

7.1.5 Deflection:

In both the dead load and live load deflection reduces with skewness up to 25% and 20% respectively. As the bridge is coupled with curvature and skewness deflection due to dead load and live load increases 2.5times and 2.5-3.5 times respectively.

The response coefficients for dead and live load deflection in both the span differs around 20% for models subjected to central angle up to $\alpha=24°$ coupled with skewness up to $\theta=15°$. Only the difference in response coefficients of dead load deflection for $\alpha=12°$ and $\theta=45°$ is beyond this limit. It is proposed to follow the recommended response coefficients for all practical engineering problems up to this limit.

7.2 Future Scope:

The critical discussion of the review of the accumulated literature, mentioned in Chapter 3, highlights the different areas which needs attention, from researches of concrete box girder bridge. The primary five responses for skew-curved simply supported box girder bridge has been studied under this thesis. There is vast area remaining unexplored; may be studied in future. For example, same parametric study can be carried out for principal stresses. The same parametric study can be carried out for different spans, to increase the accuracy of the response coefficients further. There may be four types of geometric variation of skew-curved bridge. In this thesis only one type of bridge geometry, which is most common in practice, has been studied. Other three geometry of skew-curve bridge can be explored. Also, skew-curved concrete box girder bridge having two or more span and continuous and integral over supports needs to be explored. Effect of prestress and secondary forces i.e. creep, shrinkage, temperature is to be studied. Dynamic analysis for all of the above cases may also be carried out.

REFERENCE:

I. AASTHO LRFD Bridge design specification-2012

II. Rakshit KS, Design and Construction of Highway Bridges

III. Sisodiya RG, Cheung YK, Ghali A, "Finite Element Analysis of Skew, Curved Box-Girder Bridge", Publication of Kajima institute of Construction Technology, Japan, Vol. 30, pp. 191-199, 1970.

IV. Brown TG, Ghali A, "Semi-Analytic Solution of Skew Box Girder Bridges", Proc. Of Institution of Civil Engineers Part 2, Vol. 59, No. 3, pp. 487-500, 1975

V. Mark R. Wallace (1976), Studies of Skewed Concrete Box Girder Bridge by, Division of Structures, California Department of Transportation

VI. Bouwkamp JG, Scordelis AC, Wasti ST, "Failure Study of a Skew Box Girder Bridge Model", IABSE Congress Report, Vol. 11, pp. 855-860, 1980.

VII. Scordelis AC, Bouwkamp JG, Wasti ST, Seible F, "Ultimate Strength of Skew RC Box Girder Bridge", Journal of the Structural Division ASCE, Vol. 108, No. 1, pp. 105-121 and pp. 89-104, 1982

VIII. Wasti ST, Scordelis AC, "Comparative Structural Behavior of Straight, Curved and Skew Reinforced Concrete Box Girder Bridge Models". Analysis and Design of Bridges Springer Netherlands, Vol. 74, pp. 191-211, 1984.

IX. Paavola J, "A Finite Element Technique for Thin-Walled Girders", Computers & Structures, Vol. 44, No. 1, pp. 159-175, 1992.

X. Shushkewich KW. (July-1998), Approximate Analysis of Concrete Box Girder Bridges, ASCE, Journal of Bridge Engineering, Vol.114, No.7, Pg. 1644-1657

XI. Jun-Tao K, Jun-Jie Z, Guo-Ding W, Qin-Han F, Rui D, "A New Method on Resolving the Rotation in the Plane of Skew Bridges", Wuhan University Journal of Natural Sciences, Vol. 10, No. 6, pp. 1081-1084, 2005.

XII. Ashebo DB, Chan TH, Yu L, "Evaluation of Dynamic Loads on a Skew Box Girder Continuous Bridge Part I: Field Test and Model Analysis" Engineering Structures Vol. 29, No. 6, pp. 1052-1063, 2007.

XIII. Grace NF, Patki KD, Soliman EM, Hanson JQ, "Flexural Behavior of Side -By-Side Box-Beam Bridges: A Comparative Study", PCI Journal, Vol. 56, No. 3, pp. 94-112, 2011.

XIV. Hodson DJ, Barr PJ, Halling MW, "Live-Load Analysis of Post tensioned Box-Girder Bridges", Journal of Bridge Engineering ASCE, Vol. 17, No. 4, pp. 644-651, 2011 and "Live Load Test and Finite Element Analysis of a Box Girder Bridge for the Long Term Bridge Performance Program", MS Dissertation in Utah State University, 2011.

XV. Mohseni Iman, Rashid A. Khalim, (2011) ,"Transverse load distribution of skew cast-in-place concrete multicell box - girder bridges subjected to traffic condition", Department of Civil Engineering, University Kebangsaan Malaysia (National University of Malaysia)

XVI. Reddy P, Karuna S, "Comparative study on normal and skew bridge of PSC box girder", International Journal of Research in Engineering and Technology", Vol-04, Issue-06, June-2015.

XVII. Gupta T, Kumar M, "Structural Response of Concrete Skew Box-Girder Bridges-A State-of-the-Art Review", International Journal of Bridge Engineering (IJBE), Vol. 5, No. 1, (2017), pp. 37-59

XVIII. Sennah Khaled M., Kennedy John B., "State-of-The-Art in Design of Curved Box-Girder Bridges", May-June, 2001, Journal of Bridge Engineering

XIX. Sarode Asish B, Vesmawala G.R, "Torsional Behavior and Constancy of Curved Box Girder Superstructures", TARCE - Vol.1, No.2, July-December, 2012

XX. Miner L, Zokaie T, Fell Ben, "Effect of Curved Alignment and Skewed Support on Bridge Response"

XXI. Raj B, Jivani D, "Parametric Study on Effect of Curvature and Skew on Box Type Bridge", May 2016, IJSDR, Volume 1, Issue 5

XXII. Gupta Tanmoy, Kumar Manoj, "Flexural response of skew-curved concrete box-girder bridges", ELSEVIER, Engineering Structures 163 (2018), pp- 358–372

XXIII. Computers & Structures, Inc., Introduction to SAP2000/Bridge, Version 14, April 2009

XXIV. Computers & Structures, Inc., CSI Analysis Reference Manual, July 2016

XXV. Computers & Structures, Inc., SAP 2000 Basic Analysis Reference Manual, Version 14, April 2009

XXVI. IRC-6:2017: Standard Specification and code of Practice for Road Bridges, Section-II: Loads and Stresses.

XXVII. IRC-112: 2011: Code of Practice for Concrete Road Bridges